

NASA CR-159,297



3 1176 00169 0578

NASA-CR-159297

1981 0010572

NASA CONTRACTOR REPORT 159297

**SCI**

CVT

**AERONAUTICAL & MARINE SYSTEMS**  
DIVISION

SYSTEMS CONTROL, INC. (CVT) ■ 1801 PAGE MILL ROAD ■ PALO ALTO, CA 94304 ■ TELEX 348-433 ■ (415) 494-1165

DEVELOPMENT OF ADVANCED TECHNIQUES FOR ROTORCRAFT  
STATE ESTIMATION AND PARAMETER IDENTIFICATION

W.E. Hall, Jr.  
J.G. Bohn  
J.H. Vincent

SYSTEMS CONTROL, INC. (Vt)  
Palo Alto, CA 94304

Contract NAS-14549  
August 1980

**NASA**

National Aeronautics and  
Space Administration

Langley Research Center  
Hampton, Virginia 23665

**LIBRARY COPY**

**MAR 31 1981**

LANGLEY RESEARCH CENTER  
LIBRARY, NASA  
HAMPTON, VIRGINIA



NF01095

1. Report No. NASA CR 159297		2. Government Accession No.		3. Recipient's Catalog No.	
4. Title and Subtitle DEVELOPMENT OF ADVANCED TECHNIQUES FOR ROTORCRAFT STATE ESTIMATION AND PARAMETER IDENTIFICATION			5. Report Date NOVEMBER 1980		
			6. Performing Organization Code		
7. Author(s) W.E. Hall, Jr., J.G. Bohn, J.H. Vincent			8. Performing Organization Report No.		
9. Performing Organization Name and Address SYSTEMS CONTROL, INC. (Vt) 1801 Page Mill Road Palo Alto, Ca. 94304			10. Work Unit No. (TRAIS)		
			11. Contract or Grant No. NASI - 14549		
12. Sponsoring Agency Name and Address NATIONAL AERONAUTICS AND SPACE ADMINISTRATION Washington, D.C. 20546			13. Type of Report and Period Covered CONTRACTOR REPORT		
			14. Sponsoring Agency Code		
15. Supplementary Notes Contract Monitors: Robert Chen, NASA Ames Research Center Robert L. Tomaine, NASA Langley Research Center					
16. Abstract An integrated methodology for rotorcraft system identification has been described. This methodology consists of rotorcraft mathematical modeling, three distinct data processing steps, and a technique for designing inputs to improve the identifiability of the data. These elements are as follows:  <ul style="list-style-type: none"> <li>(1) A Kalman Filter/Smoother Algorithm which estimates states and sensor errors from error-corrupted data. Gust time histories and statistics may also be estimated.</li> <li>(2) A Model Structure Estimation Algorithm for isolating a model which adequately explains the data.</li> <li>(3) A Maximum Likelihood Algorithm for estimating the parameters and estimates for the variance of these estimates.</li> <li>(4) An Input Design Algorithm, based on a maximum likelihood approach, which provides inputs to improve the accuracy of parameter estimates.</li> </ul> <p>A discussion of each step is presented, with examples to both flight and simulated data cases.</p>					
17. Key Words Helicopter Math Model Parameter Identification Model Structure Determination			18. Distribution Statement UNCLASSIFIED-UNLIMITED		
19. Security Classif. (of this report)		20. Security Classif. (of this page)		21. No. of Pages	22. Price



## TABLE OF CONTENTS

	Page
Foreword . . . . .	v
Nomenclature . . . . .	vii
Definitions of Inertial Constants . . . . .	xiii
I. INTRODUCTION . . . . .	1
Organization of Report . . . . .	5
II. ROTORCRAFT MATHEMATICAL MODELS FOR SYSTEM IDENTIFICATION . . . . .	7
Specification of Rotorcraft Model Criteria . . . . .	7
Math Model Selection . . . . .	8
Linear and Nonlinear Math Model Description . . . . .	10
III. ROTORCRAFT STATE ESTIMATION . . . . .	39
Requirements for Rotorcraft State Estimation . . . . .	39
Review of State Estimation Algorithms . . . . .	40
Rotorcraft State Estimation Algorithm . . . . .	44
IV. MODEL STRUCTURE ESTIMATION . . . . .	71
Requirements . . . . .	71
Model Structure Estimation Approaches . . . . .	72
Rotorcraft Model Structure Estimation Method . . . . .	87
Description of a Model Structure Estimation Algorithm . . . . .	89
V. ROTORCRAFT PARAMETER ESTIMATION . . . . .	99
Introduction . . . . .	99
Rotorcraft Parameter Estimation Approaches . . . . .	99
Rotorcraft Parameter Identification Method . . . . .	105
VI. INPUT DESIGN . . . . .	119
Requirements for Input Design . . . . .	119
Input Design Methods . . . . .	120
VII. DATA PROCESSING RESULTS . . . . .	131
CH-53A Results . . . . .	131
Bell 609 Rotorcraft Results . . . . .	202
RSRA Results . . . . .	206
UH-1H Results . . . . .	210

TABLE OF CONTENTS (Continued)

	Page
VIII. CONCLUSIONS . . . . .	235
REFERENCES . . . . .	237
APPENDICES . . . . .	243

## FOREWORD

This report describes the work performed by Systems Control, Inc. (Vt) for the National Aeronautics and Space Administration and the United States Army Research and Technology Laboratories (AVRADCOM). The contract research effort which has led to the results in this report was financially supported by the AVRADCOM. Technical monitors for this project were Dr. Robert Chen and Mr. Robert L. Tomaine. At Systems Control, Inc. (Vt), Dr. W. Earl Hall, Jr. was the principal investigator and Dr. N.K. Gupta, Mr. R.S. Hansen, and Mr. J.G. Bohn were the project engineers. Programming support was provided by Ms. S. DuHamel and Mr. B. Bird. Report preparation efforts were directed by Ms. C. Walker.

## NOMENCLATURE

<u>Symbol</u>	<u>Definition</u>
a	Blade airfoil section lift curve slope, $\partial C_{\ell} / \partial \alpha$
$a_1$	Longitudinal rotor tilt
$\left. \begin{array}{l} a_x \\ a_y \\ a_z \end{array} \right\}$	Body axis acceleration, $m/sec^2$
B	(1) Blade flapping motion coefficient; (2) Covariance of innovation vector
$b_1$	Lateral rotor tilt
$\left. \begin{array}{l} C_{\ell} \\ C_M \\ C_N \end{array} \right\}$	Fuselage aerodynamic X,Y, and Z-axis moment coefficients
$\left. \begin{array}{l} C_{m_x} \\ C_{m_y} \\ C_Q \end{array} \right\}$	Hub X,Y, and Z-axis moment coefficients in rotor axes
$\left. \begin{array}{l} C_H \\ C_R \\ C_Y \\ C_T \end{array} \right\}$	Hub X,Y, and Z-axis force coefficients in rotor axes
c	Blade reference chord length, m (ft)
E	Expected value operator
F	(1) System dynamics matrix; (2) Statistical test function
G	System noise or control matrix
g	Acceleration due to gravity, $9.8 m/sec^2$ (32.174 $ft/sec^2$ )
$g_s$	Structural damping coefficient

<u>Symbol</u>	<u>Definition</u>
H	(1) Rotor hub inplane force, along rotor X axis, N (lb); (2) System observation matrix
$I_o$	Blade moment of inertia $\int_0^R r^2 m dr$ ; Kg-m <sup>2</sup> (slug-ft <sup>2</sup> )
$I_b$	Reference blade moment of inertia, Kg-m <sup>2</sup> (slug ft <sup>2</sup> )
$I_x, I_y, I_z$	Fuselage moment of inertia about X, Y, Z body axes Kg-m <sup>2</sup> (slug ft- <sup>2</sup> )
$I_\beta, I_\zeta$	Blade flap and lag moments of inertia, nondimensional
K	Kalman gain matrix
L	Body-axis rolling (X-axis) moment, N-m (ft-lb)
$\bar{L}$	Hub rolling moment, rotor axis, N-m (ft-lb)
m	(1) Total helicopter mass, Kg (slugs) (2) Blade mass per unit span, Kg/m (slug/ft)
M	(1) Body-axis pitching (Y-axis) moment, N-m (ft-lb) (2) Information matrix
$\bar{M}$	Hub pitching moment, rotor axis, N-m (ft-lb)
$\mathcal{M}$	Angular momentum, N-m-sec (lb-ft-sec)
$M_x$	Rotor aerodynamic rolling (X-axis) moment, rotor axes, N-m (ft-lb)
$M_y$	Rotor aerodynamic pitching (Y-axis) moment, rotor axes, N-m (ft-lb)
$N_b$	Number of blades on the rotor
N	Body-axis yawing (Z-axis) moment, N-m (ft-lb)
P	State error covariance matrix
$P_B$	Body-axis roll (X-axis) rate, rad/sec
$Q_B$	Body-axis pitch (Y-axis) rate, rad/sec
Q	(1) Rotor aerodynamic torque, rotor axes, N-m (ft-lb) (2) Process noise statistics matrix



<u>Symbol</u>	<u>Definition</u>
$\bar{Q}$	Rotor hub yawing moment, rotor axes, N-m (ft-lb)
$R_B$	Body-axis yaw (Z-axis) rate, rad/sec
R	(1) Reference rotor radius, m (ft); (2) Measurement noise statistics matrix; (3) Correlation coefficient
r	Position along blade radius, m (ft)
$r_{FA}$	Blade pitch bearing radial offset, m (ft)
S	Standard estimation error
T	Rotor thrust (Z-axis) force, rotor axes, N (lb)
$U_B$	Fuselage X-axis translational velocity, body axes, m/sec (ft/sec)
$V_B$	Fuselage Y-axis translational velocity, body axes, m/sec (ft/sec)
v	System measurement noise vector
$W_B$	Fuselage Z-axis translational velocity, body axes, m/sec (ft/sec)
w	System noise vector
X	Longitudinal axis designation
$X_B$	Body-axis X force, N (lb)
$X_{HUB}$	Rotor hub longitudinal location relative to vehicle reference center, positive forward, m (ft)
$X_{FA}$	Rotor blade torque offset, m (ft)
$X_O$	Blade chordwise bending deflection, m (ft)
$X_I$	Distance of blade c.g. aft of blade elastic axis, m (ft)
x	System state vector
Y	(1) Lateral axis designation; (2) Set of system measurements

<u>System</u>	<u>Definition</u>
$Y_B$	Body-axis Y force, N (lb)
$Y^R$	Rotor hub lateral force, rotor axes, N (lb)
$y$	System measurement vector
$Z$	(1) Vertical axis designation; (2) Blade lagging
$Z_B$	Body-axis Z force, N (lb)
$Z_{HUB}$	Rotor hub vertical location relative to vehicle reference center, positive downward, m (ft)
$Z_{FA}$	Gimbal undersling, m (ft)
$Z_o$	Blade vertical bending displacement, m (ft)

#### NOMENCLATURE (GREEK)

<u>Symbol</u>	<u>Definition</u>
$\alpha$	(1) Aircraft angle of attack, rad; (2) Angular displacements about rotor axes, rad
$\beta$	(1) Blade flapping degree of freedom or flap angle, rad; (2) Aircraft sideslip angle, rad
$\Gamma$	Discrete system noise matrix
$\gamma$	Lock number, $\rho a c R^4 / I_b$
$\delta$	Kroneker delta function
$\delta_e, \delta_r, \delta_a$	Elevator, rudder, and aileron deflection, rad
$\delta_F$	Flaperon deflection, rad
$\delta_{TR}$	Tail rotor collective pitch, rad
$\delta_1$	Hub precone angle, rad
$\delta_2$	Blade droop, outboard of pitch bearing, rad
$\delta_3$	Blade sweep, outboard of pitch bearing, rad
$\epsilon$	Estimate error
$\zeta$	Blade lagging degree of freedom or lag angle, rad

<u>Symbol</u>	<u>Definition</u>
$\delta_{LO}$	General longitudinal control deflection, rad
$\delta_{LA}$	General lateral control deflection, rad
$\theta$	(1) Blade pitch angle, rad; (2) Set of parameter values
$\theta_B$	Vehicle pitch angle, about Y body axis, rad
$\theta_R$	Rotor shaft tilt relative to Z rotor axis, positive forward, rad
$\mu$	Vehicle density parameter, $m/\rho R^3$
$v$	Innovation vector
$v_\beta, v_\zeta$	Blade flap and lag rotating natural frequencies, rad/sec
$\rho$	Air density, $Kg/m^3$ (slug/ft <sup>3</sup> )
$\sigma$	(1) Rotor solidity, $N_b c/\pi r$ ; (2) Standard deviation
$\psi_s$	Rotor azimuth angle, rotor axes, rad
$\Omega$	Rotor angular rate, rad/sec

#### NOMENCLATURE (SUPERSCRIPTS)

<u>Symbol</u>	<u>Definition</u>
$(\dot{\quad})$	Time derivative, d/dt
$(\hat{\quad})$	Estimated value
$(\sim)^{o,1C,1S}$	Rotor coning, longitudinal cyclic, lateral cyclic degree of freedom, respectively, shaft-fixed axes
$(\quad)^*$	Normalized on $I_b$
$(\quad)'$	Geometric derivation, d/dr
A	Aerodynamic
W	Wing

<u>Symbol</u>	<u>Definition</u>
H	Horizontal stabilizer
V	Vertical stabilizer
FUS	Fuselage
TR	Tail Rotor
T	Matrix transpose

NOMENCLATURE (SUBSCRIPTS)

<u>Symbol</u>	<u>Definition</u>
( ) <sub>o,1C,1S</sub>	Rotor coning, longitudinal cyclic, lateral cyclic degree of freedom respectively, shaft-fixed axes
b	Rotor blade
c	Collective pitch
o	Trim or steady-state condition

DEFINITIONS OF INERTIAL CONSTANTS [3]

$$S_{q_i}^* = \int_0^1 \bar{\eta}_i m dr / I_b$$

$$I_0^* = \int_0^1 r^2 m dr / I_b$$

$$I_{\dot{q}_i \alpha}^* = \int_0^1 \bar{\eta}_i r m dr / I_b$$

$$I_{\dot{q}_i \alpha} = \frac{1}{I_b} \int_0^1 \bar{k}_B \cdot \bar{\eta}_i \left( -Z_{FA} + r\delta_1 - (r-r_{FA})\delta_2 \right. \\ \left. + \bar{L}_B \dot{\bar{i}}_B \cdot (Z_0 \bar{i} - x_0 \bar{k} - x_I \bar{K}) \right) m dr$$

$$I_{\dot{q}_i \psi}^* = \frac{1}{I_b} \left\{ \int_0^1 r m \int_0^r \bar{\eta}_i^1 \cdot (Z_0 \bar{i} - x_0 \bar{k} - x_I \bar{K}) \cdot d\rho dr \right. \\ \left. - \int_0^1 \bar{L}_B \cdot \eta_i \left( -r\delta_1 + (r-r_{FA})\delta_2 \right) m dr \right. \\ \left. - \int_0^1 \bar{k}_B \cdot \bar{\eta}_i \left( x_{FA} + r_{FA} \delta_3 + \bar{k}_B \cdot (Z_0 \bar{i} - x_0 \bar{k} - x_I \bar{K}) \right) m dr \right\}$$

$$I_{q_k \dot{q}_i}^* = \frac{1}{I_b} \left[ - \int_0^1 \vec{\eta}_k \cdot \vec{k}_B m \int_0^r \vec{\eta}_i \cdot (z_0 \vec{i} - x_0 \vec{k} - x_I \vec{K}) \cdot d\rho dr \right. \\ \left. + \int_0^1 \vec{\eta}_i \cdot \vec{k}_B m \int_0^r \vec{\eta}_k \cdot (z_0 \vec{i} - x_0 \vec{k} - x_C \vec{K}) \cdot d\rho dr \right. \\ \left. - \int_0^1 \vec{\eta}_k \cdot \left\{ [(x_C - x_I) \vec{k} m \vec{k}_B \cdot \vec{\eta}_i] \cdot \right. \right.$$

(continued)

$$\begin{aligned}
& - m(\delta_{FA_1} - \delta_{FA_2} + \beta_G) \vec{j} \times \vec{n}_i \} dr \\
& + \vec{n}_k(r_{FA}) \cdot (\delta_{FA_2} \vec{i}_B + \delta_{FA_3} \vec{k}_B \int_{r_{FA}}^1 \vec{k}_B \cdot \vec{n}_i m dr) ]
\end{aligned}$$

UNIT CONVERSION\*

$$1 \text{ ft/sec} = 0.3048 \text{ m/sec}$$

$$1 \text{ m/sec} = 3.2808 \text{ ft/sec}$$

$$1 \text{ "g"} = 32.2 \text{ ft/sec}^2 = 9.81 \text{ m/sec}^2$$

$$1 \text{ lb/in}^2 = 703.1 \text{ Kg/m}^2 \quad 6897.41 \text{ N/m}^2$$

\* This report supports the computer programs previously installed at NASA-LaRC and NASA-Ames. These programs utilize English units in order to be consistent with the engineering units outputted by the type of data provided to SCI (Vt) by the government. In order to directly compare results with the output of these codes, English units have been retained herein.

## INTRODUCTION

The rotorcraft has presented a formidable design challenge to the engineering profession throughout the development of these unique vehicles. As the significant breakthroughs in the state of the art have been achieved, there has been a growing need for validated analytical methods in continuing to guide engineering decisions. Indeed, the expansion of computer-aided analytical methods for predicting rotorcraft aerodynamic performance, vibrations, loads, stability, control, and handling quality characteristics has affected, to varying degrees, all phases of rotorcraft engineering. As the vehicles have become more complex, and the analytical methods more sophisticated, the problem of validating these analytical methods has itself become a significant issue. In particular, the validation of analytical predictions of rotorcraft stability, control, and handling qualities must address a multitude of problems associated with vehicle test, instrumentation, and data processing. These validation methods must further interface with a wide spectrum of analytical models, from highly sophisticated digital simulations (e.g. C-81 and GENHEL) to simple transfer functions (e.g., rotorcraft handling quality specifications).

Clearly, the establishment of a systematic methodology for using test data to validate, and upgrade, a variety of analytical models is an evolutionary task. Significant advances to achieving such a methodology have been accomplished for fixed-wing aircraft [refs. 1,2] and are generically categorized as parameter identification methods. Applications of such techniques to rotorcraft have not been extensive, but two notable efforts have been reported using two different approaches. Molusis [ref. 3] performed an extensive development of the Kalman filter concept to six-degree-of-freedom vehicle models, and reemphasized the need to include rotor degrees of freedom. Gould and Hindson [ref. 4] developed a least squares quasi-linearization procedure which recognized the difficulties of the sensor bias problem. These efforts represent significant steps toward a comprehensive rotorcraft model validation methodology, primarily addressing the quantification of estimates from a given model.

Applications of these methods, as well as results from fixed-wing applications, indicated that the parameter estimation solution, though an essential part of the required

methodology, must be integrated with other requirements. These include:

(1) Data quality improvement must be achieved by assuring the completeness and minimum accuracy level of onboard and off-board sensors (e.g., air data, gyros, accelerometers, force and moment transducers, radar, optics). Data filtering options, such as Fourier transform methods, must be used judiciously to avoid loss of desired information. Multivariable data filtering methods, such as Kalman filtering, should be available to calibrate multi-component measurements.

(2) Size of the identifiable (validatable) model is inherently limited by the information content of the data and the computational resources available (e.g., algorithms and computers). The goal is not to obtain time history matches of the estimated model output with the actual data (which is generally possible if enough parameters are included in the model), but rather to derive the most accurate estimates of the model parameters which can be obtained from the data. Even if a large number of parameters is identified, reasonable computational limits must be observed.

(3) Test design considerations, which include specific maneuvers to improve the quality of data, should be integral parts of an overall test objective. Test design also requires specification of the data processing integration to diagnose and resolve particular model or instrumentation problems.

These are the principal issues which form the background of the methodology presented in this report. The overall methodology has implications beyond stability and control (see Johnson and Gupta, [ref. 5], but only the stability and control issues will be treated here.

System identification is a generic classification for the methodology of integrating simulation, wind tunnel tests, and flight tests in order to improve or validate predictive models of vehicles. This classification is a significant extension of the process of parameter identification, which is but one step in the overall process, as will be introduced in this section.

The following more formal definition of system identification has been found useful [ref. 6]:

"System identification determines, from a given input/output data record of vehicle test response, an estimate of the physical model which relates the observed data."



This definition implies that system identification involves the following:

(1) A mathematical model: Though the governing equations for vehicles may be known, it is frequently found that other equations (e.g., effects) are present, and the data must be analyzed to isolate what the actual model is.

(2) Parameters of the model: This is the parameter identification requirement, where the coefficients of the model are quantified from the data.

(3) Random errors: Random errors must be isolated and removed from the model effects.

Figure 1.1 shows a representation of how the system identification procedure is used with vehicle input and output data to produce estimates of linear and nonlinear coefficients.

Conceptually, the mathematical principles of system identification process are directly related to curve fitting of data to a model, and statistical analysis of the resulting errors. Indeed, for simple models and perfect data, elementary least squares methods will meet most requirements for model quantification. The problem, particularly for rotorcraft applications, is that the models are not simple and the instrumentation is both costly and complex. The model complexity presents two difficulties, one obvious, the other more subtle. The first difficulty is the computer algorithmic requirements imposed by processing large amounts of flight data and correlating these data to high order, multivariable models. Both feasibility and cost considerations limit the extent to which brute numerical force can be applied to such objectives. The second, and more subtle difficulty, is the avoidance of overparameterization of the model relative to the quantity and quality of data available. A frequent criterion of "excellence" of curve fitting techniques is the fit between the data and the estimated model output. In fact, it is now recognized that such fit can always be improved by adding more model parameters, even though the parameters do not reflect any actual physical effect (i.e., overparameterization). While it is necessary then to obtain a reasonable fit to the data, it must be realized that such is not the explicit objective of identification. The objective of the identification is to achieve a validated predictive model which can be subsequently used for design evaluations.

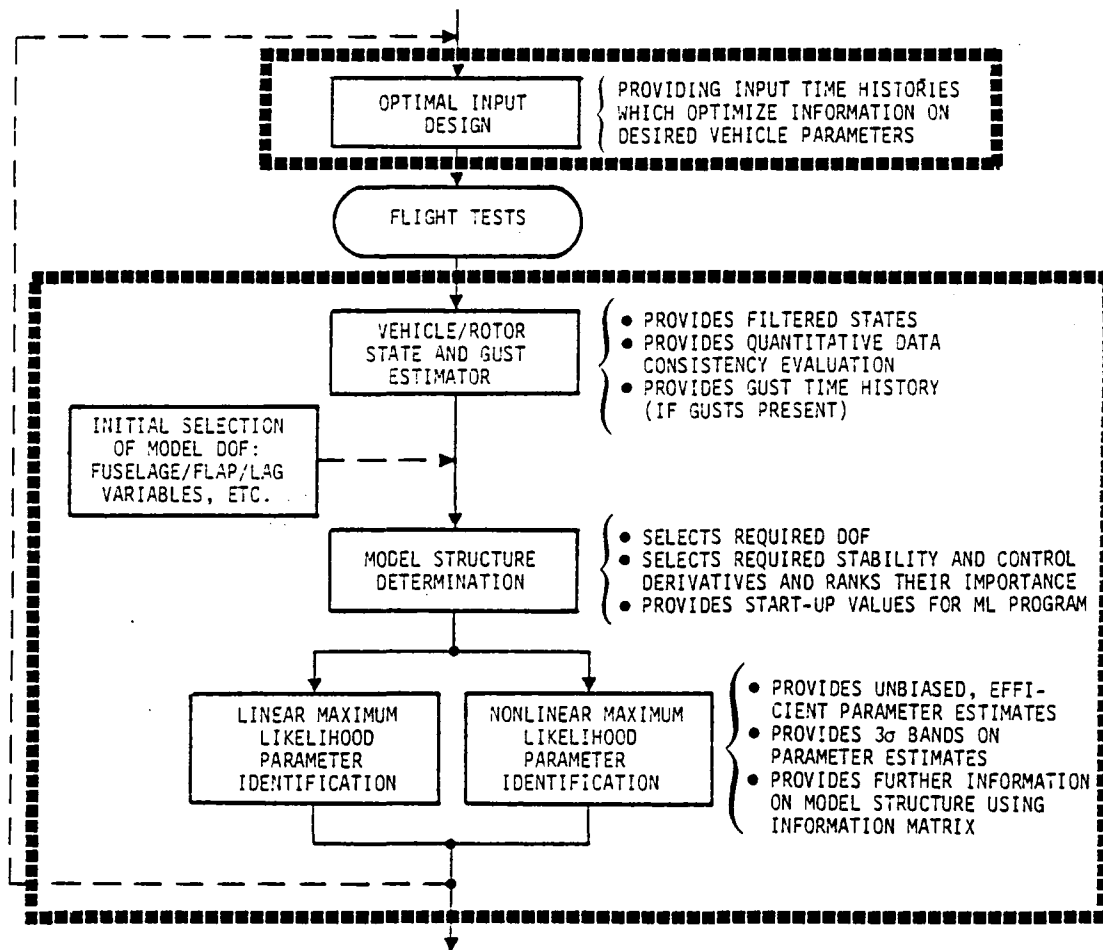


FIGURE 1.1.- INTEGRATED ROTORCRAFT SYSTEM IDENTIFICATION PROCEDURE

The objective of the rotorcraft identification methodology discussed here is to successively treat the problems of data quality, model structure estimation, and parameter estimation in a systematic fashion, iterating with the test maneuvers specifications to improve the identifiability of the stability and control coefficients from data. Each subdivision of the rotorcraft estimation problem has specific requirements for data from analysis, wind tunnel tests, or previous tests. The overall flow of this procedure is shown in Figure 1.1.

The key elements depicted in Figure 1.1 are integrated to sequentially perform the steps of:

State estimation.— Satisfies the requirement for estimating the actual states and controls from data containing biases, scale factors, and random noise.

Model structure estimation.— Satisfies the requirement for isolating that part of a model which can realistically be determined for a given set of data. The estimated model is the equations for the linear or nonlinear system.

Parameter identification.— Satisfies the requirement of accurately estimating the parameters of the model isolated by the model structure estimation step. Two algorithms are noted, one for linear models, the other for nonlinear models. (This approach is taken for a computational requirements reduction which is realized by optimizing a program by linear model computations not possible with nonlinear models.)

Input design.— Satisfies the requirement for having a method of specifying tests to improve the accuracy of parameters and estimated models.

In theory, all aspects of this data processing could be performed with one single algorithmic method. This "procedural ambiguity" is admittedly present. The resolution shown in Figure 1.1 incorporates the desire to utilize various types and qualities of a priori data to optimize a particular step within minimum cost/maximum accuracy constraints.

## Organization of Report

Chapter 2 summarizes the rotorcraft mathematical models which are the basic identification models of the algorithms discussed in the following chapters. Chapter 3 presents the background, requirements and selected state estimation algorithms. Chapter 4 discusses the general model structure estimation problem, and details the algorithm for rotorcraft estimation. Chapter 5 reviews the parameter identification algorithms and Chapter 6, the input design requirements and algorithms. Chapter 7 reviews specific numerical results from each step of the algorithm. Chapter 8 presents conclusions of this effort.

## CHAPTER II

### ROTORCRAFT MATHEMATICAL MODELS FOR SYSTEM IDENTIFICATION

#### Specification of Rotorcraft Model Criteria

Overview. - This section considers the analytical models selected for implementing the rotorcraft parameter identification methods employed in this study. As is well known, detailed dynamic models of rotorcraft tend to be of great complexity due to the large number of degrees of freedom and time-varying nonlinear characteristics of parameters that must be considered. Given that the principal objective of this work is the identification of parameters relating to fuselage and rotor dynamics, and not a study of the modeling task per se, the basic model requirements were fixed by questions of system identifiability rather than model generality.

The principal guidelines for model selection are summarized in the following criteria.

Math model criteria. - The objectives of the parameter identification work planned in this effort governed the determination of applicability on the part of several alternative model formulations. It was established that model selection should be made relative to the following criteria:

- (1) The model must contain all degrees of freedom of importance to rotorcraft handling qualities analyses. Rotor modes must be explicitly shown and not reduced to quasi-static form by inclusion in fuselage equations of motion. The rotor modes required are the first harmonics of longitudinal and lateral flapping and lagging blade motion, plus coning.
- (2) Explicit representations must be given to both fuselage and rotor aerodynamics. Fuselage effects must be shown as component build-up so that component effects may be determined if suitable instrumentation is present.
- (3) The model must be usable with minor modifications for both linear and nonlinear analyses as would be required in this effort, in order to provide the consistency needed to isolate the effects of particular system nonlinearities.
- (4) The model must be general enough to treat different types of rotors and different numbers of blades.
- (5) The model should relate to a known theoretical treatment of the rotorcraft dynamics problem, in order to

give insight into the origins and assumptions implicit in the parameters identified. That is, a general-purpose identification model with arbitrary parameters should not be used; state selection should be in accordance with previous analytical work.

- (6) The model should utilize both dimensional and non-dimensional parameters in a manner that provides the simplest and most meaningful representation of rotorcraft inertial and aerodynamic characteristics from the point of view of the handling qualities analyst.

The characteristics of various methods of rotorcraft modeling are examined in light of these requirements in the following subsection.

### Math Model Selection

Math model types.— There exist three basic types of rotorcraft models that have found wide applicability in analytical studies and have been used by many researchers: In order of generally increasing complexity, they are:

- (1) Quasi-static, 6 DOF models in which rotor dynamic effects are assumed negligible (by setting rotor state rates equal to zero) and rotor aerodynamic performance effects are combined with fuselage effects. Rotor forces and moments may be represented in terms of the classical rotor parameters inflow ratio ( $\lambda$ ), advance ratio ( $\mu$ ), and blade pitch ( $\theta$ ). The equations may be linearized and analyzed in a manner analogous to fixed-wing aircraft methods [ref. 7].
- (2) Rotor blade dynamics models, in which the rotor degrees of freedom are represented explicitly and rotor forces and moments are coupled to the fuselage through constraints at the rotor hub, and in which rotor blade aerodynamic characteristics are determined using one of several azimuthal averaging techniques [ref. 8].
- (3) Rotor blade dynamic models such as in (2), except that rotor blade aerodynamic characteristics are determined exactly at a large number of azimuthal stations and accelerations and rates are integrated numerically from one station to the next to determine blade motion in time-history form. This method, implemented on a digital computer, is powerful in terms of high accuracy and nonlinear capability. No averaging assumptions are required, and the accuracy is limited only by integration errors and computer truncation errors.

The first model type is very useful for vehicle handling qualities studies in which blade dynamic modes may not be of concern, as it is of low order (8 states) and contains easily-determined parameters. It is useful either in a nonlinear, time-history output form or in a linearized, small-perturbation, eigenvalue and eigenvector analysis form. However, the absence of explicit rotor blade dynamics which leads to this simplicity makes the model inappropriate for studying blade aerodynamics effects, which is one of the principal objectives of modern rotorcraft research.

The third type of model contains a very high level of detail in its time history calculations, and represents in fact a simulation of rotor dynamics that may include as many parameter nonlinearities as desired due to the flexibility of digital computers in integrating the equations of motion with variable coefficients. The capability to perform modal analyses is lost with this type of model, however, due to its numerical nature. Modal analyses require a model expressed in linear mathematical form. The maximum of analytical flexibility comes with a linear model derived from the nonlinear simulation, at a given flight condition. In this linear model, the coefficients of the differential equations represent averages of nonlinear parameters around the rotor azimuth.

This comprises the second type of model. Several efforts have led to analytically-determined, linear models that show the origins of the nonlinear coefficients that must be arranged, and then impose averaging techniques to arrive at a linear, closed-form system of equations. Outstanding among these approaches is that of Johnson [ref. 8].

In the case of linear parameter identification, a linear, state-space model is employed in the identification program. For identification of nonlinear parameters, the same basic linear model is used but additional, nonlinear effects are accounted for through the introduction of functions to represent equation coefficients and the inclusion of nonlinear terms in the forcing function and inertia models. The basic method of determining the parameters is unchanged, though the numerical operations are more involved. This flexibility suggested the selection of a model that was linear at given flight points, but that could be modified by additive constants and nonlinear coefficient functionals for successive flight conditions or nonlinear parameter estimation.

The type two math model selected is based on the general work of Johnson [ref. 8] specialized to the single-rotor helicopter case. This model, derived by rigorous aeroelastic analysis, contains all of the required characteristics for the present purpose and provides a sound framework to serve as a basis for

both linear and nonlinear parameter identification. The following subsection reviews the background of this model and its application to the present parameter identification effort.

### Linear and Nonlinear Math Model Description

Overview.— This section contains a review of the formulation of the set of equations used as the basis for parameter identification work in this study. Many of the features of the model developed in ref. 8 were neglected as not appropriate to experimental handling qualities studies, particularly the provision for higher-harmonic blade bending mode shapes. Rotor dynamics are determined from rotor inertial and aerodynamic characteristics, transformed to hub forces and moments, and added to fuselage inertial and aerodynamic forces and moments, from which accelerations of and about the vehicle center of mass are then computed. A schematic of the flow of computations in this process is shown in Figure 2.1. In the following, the particular elements shown in this figure are discussed.

#### Formulation of equations of motion.—

(1) Coordinate Systems and Transformations. Rotor blade inertial and aerodynamic characteristics are calculated in a coordinate system fixed with the blade (i.e., rotating with rotor angular velocity), then Fourier-transformed into a non-rotating, shaft-fixed coordinate system. This transformation is well-discussed in ref. 9. The rotor may then be viewed as a cone whose semivertex angle and inclination relative to the shaft change in accordance with blade motions, transformed. Vehicle reference axes are fixed in the rotorcraft fuselage, and the relationship between rotor and vehicle degrees of freedom, forces, and moments is illustrated in Figure 2.2. Transformations between the two orthogonal, right-handed coordinate systems are shown in Figures 2.3 and 2.4, and are summarized in equation form in Figure 2.5. In the equations used in this study, and presented below, axis transformations were expanded and written out in equation form.

(2) Nondimensionalization. Particular care was given to the use of dimensional and nondimensional parameters in the equations of motion. The generality and conciseness of using nondimensional coefficients introduces computational problems if points of singularity (e.g., zero airspeed in hover) occur and when operating conditions depart substantially from reference conditions. Dimensional parameters, on the other hand, relate more directly to flight measurement data but are scale- and flight condition-dependent. In this study, both types of parameters were used. As will be seen below, the basic nonlinear

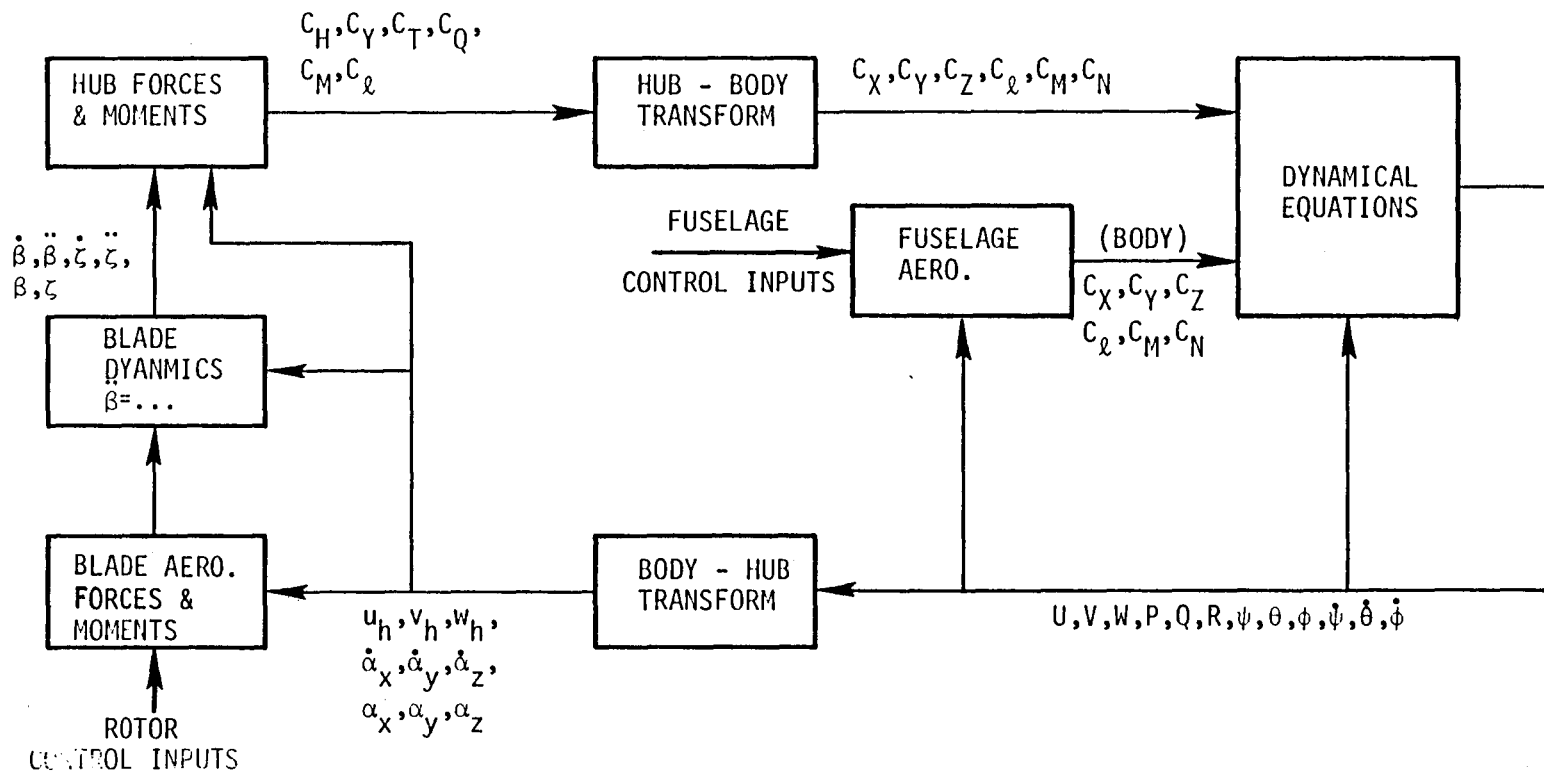


FIGURE 2.1.- SCHEMATIC OF EQUATIONS OF MOTION



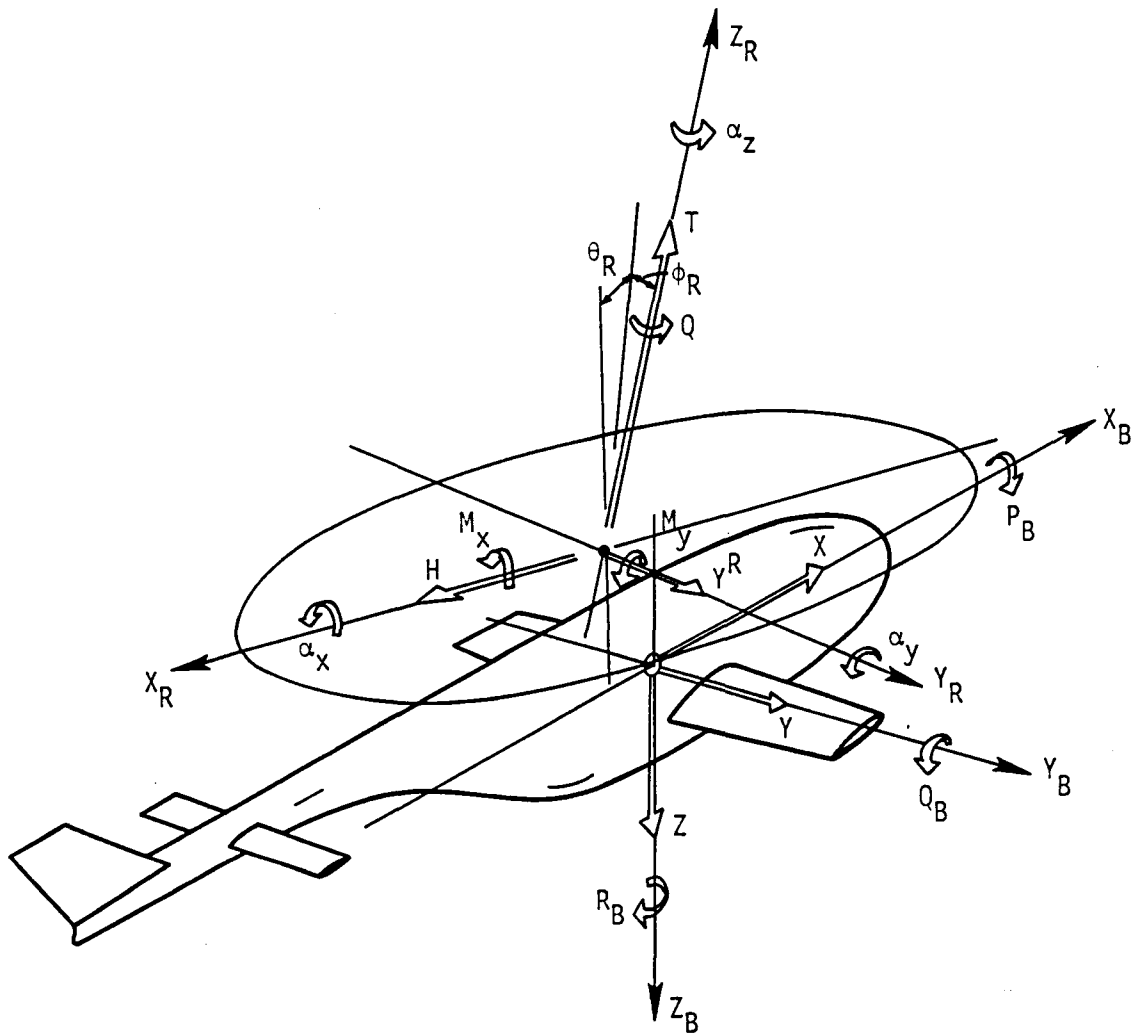


FIGURE 2.2.- BODY AND ROTOR AXIS SYSTEMS

General Transformation from Shaft Axes to Body Axes:

$$\begin{bmatrix} T_{S \rightarrow B} \end{bmatrix} = \begin{bmatrix} -\cos \theta_R & -\sin \phi_R \sin \theta_R & \cos \phi_R \sin \theta_R \\ 0 & \cos \phi_R & \sin \phi_R \\ -\sin \theta_R & \sin \phi_R \cos \theta_R & -\cos \phi_R \cos \theta_R \end{bmatrix}$$

$$\begin{bmatrix} X_B \\ Y_B \\ Z_B \end{bmatrix} = \begin{bmatrix} T_{S \rightarrow B} \end{bmatrix} \begin{bmatrix} X_S \\ Y_S \\ Z_S \end{bmatrix}$$

FORCE COEFFICIENTS:

$$\begin{bmatrix} C_X^R \\ C_Y^R \\ C_Z^R \end{bmatrix} = \begin{bmatrix} T_{S \rightarrow B} \end{bmatrix} \cdot \begin{bmatrix} C_H \\ C_{Y_h} \\ C_T \end{bmatrix}$$

Rotor Forces  
in Rotor Axes

$$\begin{bmatrix} C_X^R \\ C_Y^R \\ C_Z^R \end{bmatrix} = \begin{bmatrix} -C_H \cos \theta_R - C_{Y_h} \sin \phi_R \sin \theta_R & + C_T \cos \phi_R \sin \theta_R \\ C_{Y_h} \cos \phi_R & + C_T \sin \phi_R \\ -C_H \sin \theta_R + C_{Y_h} \sin \phi_R \cos \theta_R & - C_T \cos \phi_R \cos \theta_R \end{bmatrix}$$

MOMENT COEFFICIENTS

$$\bar{C}_m = \bar{C}_{m_0} + \bar{r}_{hub} \times \bar{C}_F$$

$$\begin{bmatrix} C_n^R \\ C_m^R \\ C_q^R \end{bmatrix} = \begin{bmatrix} T_{S \rightarrow B} \end{bmatrix} \begin{bmatrix} C_m^R \\ C_{m_y}^R \\ C_q^R \end{bmatrix} ; \quad \bar{r}_{HUB} \times \bar{C}_F = \begin{bmatrix} \bar{i} & \bar{j} & \bar{k} \\ X_{HUB} & 0 & Z_{HUB} \\ C_X^R & C_Y^R & C_Z^R \\ -C_Y^R & Z_{HUB} & \\ C_X^R & Z_{HUB} & -C_Z^R \\ C_Y^R & X_{HUB} & \end{bmatrix} \begin{bmatrix} X_{HUB} \\ Z_{HUB} \\ X_{HUB} \end{bmatrix}$$

Rotor Moments in Body Axes     Rotor Moments in Rotor Axes

FIGURE 2.3. — TRANSFORMATION OF ROTOR FORCES AND MOMENTS TO BODY AXES

Required:  $X_h, Y_h, Z_h, \alpha_x, \alpha_y, \alpha_z$  : Translational and Rotational Displacements due to Body axis motion,  $x, y, z, \phi, \theta, \psi$ .

$$\begin{bmatrix} X_h \\ Y_h \\ Z_h \end{bmatrix}_{\text{Rotor}} = \underbrace{\begin{bmatrix} T_{B \rightarrow S} \end{bmatrix}}_{\text{Conversion from body to rotor axes.}} \underbrace{\begin{bmatrix} -T_{HUB}^X \end{bmatrix}}_{\text{Conversion of angular to translational displacement}} \underbrace{\begin{bmatrix} T_{E \rightarrow B} \end{bmatrix}}_{\text{Euler Angle to body axis rotation}} \begin{bmatrix} \phi \\ \theta \\ \psi \end{bmatrix}_{\text{Body}} + \begin{bmatrix} T_{B \rightarrow S} \end{bmatrix} \begin{bmatrix} X \\ Y \\ Z \end{bmatrix}_{\text{Body}}$$

Matrices (in order of use):

$$\begin{bmatrix} T_{E \rightarrow B} \end{bmatrix} = \begin{bmatrix} 1 & 0 & -\sin\theta_0 \\ 0 & \cos\phi_0 & \sin\phi_0 \cos\theta_0 \\ 0 & -\sin\phi_0 & \cos\phi_0 \sin\theta_0 \end{bmatrix} \quad (\text{initial attitude } \phi_0, \theta_0, \psi_0)$$

$$\begin{bmatrix} -T_{HUB}^X \end{bmatrix} = \begin{bmatrix} 0 & Z_{HUB} & -Y_{HUB} \\ 0 & Z_{HUB} & -Y_{HUB} \\ 0 & Y_{HUB} & -X_{HUB} \end{bmatrix} \quad (\text{Hub coordinates are } \begin{matrix} X_{HUB} & Y_{HUB} \\ J+Z_{HUB} & k \end{matrix} \text{ in body axes})$$

$$\begin{bmatrix} T_{B \rightarrow S} \end{bmatrix} = \begin{bmatrix} -\cos\theta_R & 0 & -\sin\theta_R \\ -\sin\phi_R \sin\theta_R & \cos\phi_R & \sin\phi_R \cos\theta_R \\ \cos\phi_R \sin\theta_R & \sin\phi_R & -\cos\phi_R \cos\theta_R \end{bmatrix}$$

and,

$$\begin{bmatrix} \alpha_x \\ \alpha_y \\ \alpha_z \end{bmatrix}_{\text{Rotor}} = \begin{bmatrix} T_{B \rightarrow S} \end{bmatrix} \begin{bmatrix} T_{E \rightarrow B} \end{bmatrix} \begin{bmatrix} \phi \\ \theta \\ \psi \end{bmatrix}_{\text{Body}}$$

FIGURE 2.4. — TRANSFORMATION OF BODY AXIS MOTION INTO ROTOR AXES

BODY AXES (REFERENCE)	FORCES				MOMENTS			
	AXIS	BODY	ROTOR	BODY	ROTOR			
	X	$C_X$	$-C_H \cos \theta_R + C_T \sin \theta_R$	$C_\ell$	$-C_{m_x} \cos \theta_R + C_Q \sin \theta_R - C_Y^R \tilde{z}_{HUB}$			
Y	$C_Y$	$C_Y^R$	$C_m$	$C_{m_y} + \tilde{z}_{HUB} (-C_H \cos \theta_R + C_T \sin \theta_R) - \tilde{x}_{HUB} (-C_H \sin \theta_R - C_T \cos \theta_R)$				
Z	$C_Z$	$-C_H \sin \theta_R - C_T \cos \theta_R$	$C_n$	$-C_{m_x} \sin \theta_R - C_Q \cos \theta_R + C_Y^R \tilde{x}_{HUB}$				
$X_R$	-	$C_H$	-	$C_{m_x}$				
$Y_R$	-	$C_Y^R$	-	$C_{m_y}$				
$Z_R$	-	$C_T$	-	$C_Q$				

FIGURE 2.5. — FORCE AND MOMENT COEFFICIENTS — TRANSFORMATION SUMMARY

equations are dimensional, with physical units of force and moment, though fuselage aerodynamic contributions are expressed as nondimensional coefficients multiplied by the reference nondimensionalizing terms. All nondimensionalizing was done on rotor characteristics:  $\rho\Omega^2 R^4 \pi$  for forces,  $\rho\Omega^2 R^5 \pi$  for moments. Conversion from conventional, fixed-wing coefficient definitions for components (such as horizontal and vertical tail) must be made where required.

The linear equations are nondimensional, on rotor characteristics. The nonlinear equations are dimensional but feature nondimensional rotor equations which are dimensionalized prior to the parameter identification step. This approach was taken to avoid complete dimensionalization of the complex inertial and aerodynamic constants in the basic rotor equations. An added factor in the equations of reference is that they are also normalized on rotor blade inertia; this was not retained in the present equations, resulting in additional scaling changes between the two sets.

A summary of the final nondimensionalization definitions is given in Table 2.1.

(3) Fuselage Aerodynamics. Fuselage aerodynamics are expressed in coefficient form based on rotor characteristics. A component buildup method is used, in which the force and moment contribution of each component (in the presence of all the others) is added to yield net total fuselage forces and moments. A typical buildup is shown in Table 2.2. It is important to note that the contributions of individual components cannot be separated unless the appropriate load-cell instrumentation is installed on the components; otherwise, the sum of all components will be identified as a parameter varying with, say,  $w$ , another parameter varying with  $q$ , and so on. This is shown by the arrangement of terms in Table 2.2 and the equations below. Groups of these terms are parameters to be identified.

Note that flap and control deflections are included, as are tail rotor force and moment. And, in the complete moment equations (below), the effects of rotation of the tail rotor (and engine) angular momentum vectors are included.

(4) Rotor Equations of Motion. The rotor equations of motion describe, in shaft axes, the motion of the rotor disk in response to aerodynamic and inertial forces and moments. The rotor forces and moments determined by these equations are transferred to the fuselage as hub forces and moments, and are discussed in the following paragraphs. The rotor

TABLE 2.1. — NONDIMENSIONALIZING FACTORS FOR EQUATIONS OF MOTION

<u>Parameter</u>	<u>Units</u>	<u>Factor</u>
1. Length	m (ft)	R
2. Linear velocity	m/sec (ft/sec)	$\Omega R$
3. Angular velocity	rad/sec	$\Omega$
4. Mass	Kg (slugs)	$\rho R^3$
5. Force	newton (lb)	$\rho \Omega^2 R^4 \pi$
6. Moment	nt-m (ft-lb)	$\rho \Omega^2 R^5 \pi$
7. Moment of inertia	$\text{kg-m}^2$ (slug-ft <sup>2</sup> )	$\rho R^5 \pi$
8. Angular Momentum	$\text{kg-m}^2/\text{sec}$ (slug-ft <sup>2</sup> /sec)	$\rho \Omega R^5 \pi$

Examples:  $C_x = X(\text{lb}) / (\rho \Omega^2 R^4 \pi)$  (Force)

$C_m = M(\text{ft-lb}) / (\rho \Omega^2 R^5 \pi)$  (Moment)

$I_{b_{nd}} = I_{b_{dim}} / \rho R^5 \pi$  (Moment of inertia)

TABLE 2.2. - FUSELAGE AERODYNAMICS

X-Force

$$C_X^A = C_X^W + C_X^H + C_X^V + C_X^{FUS} + C_X^{TR} = \sum_K C_X^K$$

where:  $C_X^W = C_{X_0}^W + C_{X_\alpha}^W \alpha + C_{X_{\alpha^2}}^W \alpha^2 + C_{X_u}^W u + C_{X_\beta}^W \beta + C_{X_{\delta_F}}^W \delta_F$

$$C_X^H = C_{X_0}^H + C_{X_\alpha}^H \alpha$$

$$C_X^V = C_{X_0}^V + C_{X_\beta}^V \beta$$

$$C_X^{FUS} = C_{X_0}^{FUS} + C_{X_\alpha}^{FUS} \alpha + C_{X_\beta}^{FUS} \beta + C_{X_{\alpha^2}}^{FUS} \alpha^2 + C_{X_u}^{FUS} u$$

$$C_X^{TR} = C_{X_0}^{TR} + C_{X_\beta}^{TR} \beta$$

Hence,

$$\begin{aligned} C_X^A &= C_{X_0}^W + C_{X_\alpha}^W \alpha + C_{X_{\alpha^2}}^W \alpha^2 + C_{X_u}^W u + C_{X_\beta}^W \beta + C_{X_{\delta_F}}^W \delta_F + C_{X_0}^H + C_{X_\alpha}^H \alpha^H \\ &+ C_{X_0}^V + C_{X_\beta}^V \beta + C_{X_0}^{FUS} + C_{X_\alpha}^{FUS} \alpha + C_{X_{\alpha^2}}^{FUS} \alpha^2 + C_{X_\beta}^{FUS} \beta + C_{X_u}^{FUS} u \\ &+ C_{X_0}^{TR} + C_{X_\beta}^{TR} \beta \\ &= (C_{X_0}^W + C_{X_0}^H + C_{X_0}^V + C_{X_0}^{FUS} + C_{X_0}^{TR}) + (C_{X_\alpha}^W + C_{X_\alpha}^H + C_{X_\alpha}^{FUS}) \alpha \\ &+ (C_{X_{\alpha^2}}^W + C_{X_{\alpha^2}}^{FUS}) \alpha^2 + (C_{X_u}^W + C_{X_u}^{FUS}) u + (C_{X_\beta}^W + C_{X_\beta}^V + C_{X_\beta}^{FUS} + C_{X_\beta}^{TR}) \beta \\ &+ C_{X_{\delta_F}}^W \delta_F \end{aligned}$$

TABLE 2.2 - CONTINUED

Y-Force

$$C_Y^A = C_Y^W + C_Y^H + C_Y^V + C_Y^{FUS} + C_Y^{TR}$$

where:  $C_Y^W = C_{Y_0}^W + C_{Y_B}^W$

$$C_Y^V = C_{Y_0}^V + C_{Y_B}^V$$

$$C_Y^{FUS} = C_{Y_0}^{FUS} + C_{Y_B}^{FUS} + C_{Y_B}^{FUS} \beta^2$$

$$C_Y^{TR} = C_{Y_0}^{TR} + C_{Y_B}^{TR} + C_{Y_\alpha}^{TR}$$

Hence,

$$\begin{aligned} C_Y^A &= C_{Y_0}^W + C_{Y_B}^W + C_{Y_0}^H + C_{Y_B}^H + C_{Y_0}^V + C_{Y_B}^V + C_{Y_0}^{FUS} + C_{Y_B}^{FUS} + C_{Y_B}^{FUS} \beta^2 \\ &\quad + C_{Y_0}^{TR} + C_{Y_B}^{TR} + C_{Y_\alpha}^{TR} \\ &= (C_{Y_0}^W + C_{Y_0}^H + C_{Y_0}^V + C_{Y_0}^{FUS} + C_{Y_0}^{TR}) + (C_{Y_B}^W + C_{Y_B}^H + C_{Y_B}^V + C_{Y_B}^{FUS} + C_{Y_B}^{TR}) \\ &\quad + C_{Y_B}^{FUS} \beta^2 + C_{Y_\alpha}^{TR} \end{aligned}$$



TABLE 2.2. - CONTINUED

Z-Force

$$C_Z^A = C_Z^W + C_Z^H + C_Z^V + C_Z^{FUS} + C_Z^{TR}$$

where:  $C_Z^W = C_{Z_0}^W + C_{Z_\alpha}^W + C_{Z_\alpha}^W 2\alpha^2 + C_{Z_u}^W + C_{Z_{\delta_F}}^W \delta_F$

$$C_Z^H = C_{Z_0}^H + C_{Z_\alpha}^H \alpha + C_{Z_\beta}^H \beta$$

$$C_Z^V = C_{Z_0}^V + C_{Z_\alpha}^V \alpha + C_{Z_\beta}^V \beta$$

$$C_Z^{FUS} = C_{Z_0}^{FUS} + C_{Z_\alpha}^{FUS} \alpha + C_{Z_\beta}^{FUS} \beta$$

$$C_Z^{TR} = C_{Z_0}^{TR} + C_{Z_\alpha}^{TR} \alpha + C_{Z_\beta}^{TR} \beta$$

Hence,

$$\begin{aligned} C_Z^A &= C_{Z_0}^W + C_{Z_\alpha}^W + C_{Z_\alpha}^W 2\alpha^2 + C_{Z_u}^W + C_{Z_{\delta_F}}^W \delta_F + C_{Z_0}^H + C_{Z_\alpha}^H \alpha + C_{Z_\beta}^H \beta \\ &\quad + C_{Z_0}^V + C_{Z_\alpha}^V \alpha + C_{Z_\beta}^V \beta + C_{Z_0}^{FUS} + C_{Z_\alpha}^{FUS} \alpha + C_{Z_\beta}^{FUS} \beta + C_{Z_0}^{TR} + C_{Z_\alpha}^{TR} \alpha + C_{Z_\beta}^{TR} \beta \\ &= (C_{Z_0}^W + C_{Z_0}^H + C_{Z_0}^V + C_{Z_0}^{FUS} + C_{Z_0}^{TR}) + (C_{Z_\alpha}^W + C_{Z_\alpha}^H + C_{Z_\alpha}^V + C_{Z_\alpha}^{TR} + C_{Z_\alpha}^{FUS}) \alpha \\ &\quad + (C_{Z_\beta}^W + C_{Z_\beta}^H + C_{Z_\beta}^V + C_{Z_\beta}^{FUS} + C_{Z_\beta}^{TR}) \beta + C_{Z_\alpha}^W 2\alpha^2 + C_{Z_{\delta_F}}^W \delta_F \end{aligned}$$

TABLE 2.2. - CONTINUED

Rolling Moment

$$C_l^A = C_l^W + C_l^H + C_l^V + C_l^{FUS} + C_l^{TR}$$

where:  $C_l^W = C_{l_0}^W + C_{l_\beta}^W + C_{l_\alpha}^W$

$$C_l^H = C_{l_0}^H + C_{l_\beta}^H + C_{l_\alpha}^H$$

$$C_l^V = C_{l_0}^V + C_{l_\beta}^V + C_{l_\alpha}^V$$

$$C_l^{FUS} = C_{l_0}^{FUS} + C_{l_\beta}^{FUS} + C_{l_\alpha}^{FUS}$$

$$C_l^{TR} = C_{l_0}^{TR} + C_{l_\beta}^{TR} + C_{l_\alpha}^{TR}$$

Hence,

$$\begin{aligned} C_l^A &= C_{l_0}^W + C_{l_\beta}^W + C_{l_\alpha}^W + C_{l_\beta}^H + C_{l_0}^H + C_{l_\alpha}^H + C_{l_0}^V + C_{l_\alpha}^V + C_{l_\beta}^V \\ &\quad + C_{l_0}^{FUS} + C_{l_\beta}^{FUS} + C_{l_\alpha}^{FUS} + C_{l_0}^{TR} + C_{l_\beta}^{TR} + C_{l_\alpha}^{TR} \\ &= (C_{l_0}^W + C_{l_0}^H + C_{l_0}^V + C_{l_0}^{FUS} + C_{l_0}^{TR}) + (C_{l_\alpha}^W + C_{l_\alpha}^V + C_{l_\alpha}^H + C_{l_\alpha}^{FUS} + C_{l_\alpha}^{TR}) \\ &\quad + (C_{l_\beta}^W + C_{l_\beta}^H + C_{l_\beta}^V + C_{l_\beta}^{FUS} + C_{l_\beta}^{TR}) \end{aligned}$$

TABLE 2.2. - CONTINUED

Pitching Moment

$$C_M^A = C_M^W + C_M^H + C_M^V + C_M^{FUS} + C_M^{TR}$$

where:  $C_M^W = C_{M_0}^W + C_{M_\alpha}^W + C_{M_{\alpha^2}}^W + C_{M_u}^W + C_{M_{\delta F}}^W$

$$C_M^H = C_{M_0}^H + C_{M_\alpha}^H + C_{M_u}^H + C_{M_\beta}^H$$

$$C_M^V = C_{M_0}^V + C_{M_\alpha}^V + C_{M_\beta}^V$$

$$C_M^{FUS} = C_{M_0}^{FUS} + C_{M_\alpha}^{FUS} + C_{M_\beta}^{FUS}$$

$$C_M^{TR} = C_{M_0}^{TR} + C_{M_\alpha}^{TR} + C_{M_\beta}^{TR}$$

Hence,

$$C_M^A = C_{M_0}^W + C_{M_\alpha}^W + C_{M_{\alpha^2}}^W + C_{M_u}^W + C_{M_{\delta F}}^W + C_{M_0}^H + C_{M_\alpha}^H$$

$$+ C_{M_u}^H + C_{M_\beta}^H + C_{M_0}^V + C_{M_\alpha}^V + C_{M_\beta}^V + C_{M_0}^{FUS}$$

$$+ C_{M_\alpha}^{FUS} + C_{M_\beta}^{FUS} + C_{M_0}^{TR} + C_{M_\alpha}^{TR} + C_{M_\beta}^{TR}$$

$$= (C_{M_0}^W + C_{M_0}^H + C_{M_0}^V + C_{M_0}^{FUS} + C_{M_0}^{TR}) + (C_{M_\alpha}^W + C_{M_\alpha}^H + C_{M_\alpha}^V +$$

$$C_{M_\alpha}^{FUS} + C_{M_\alpha}^{TR}) + (C_{M_\beta}^H + C_{M_\beta}^V + C_{M_\beta}^{FUS} + C_{M_\beta}^{TR}) + (C_{M_{\delta F}}^W) \delta_F + (C_{M_u}^W + C_{M_u}^H) u$$

TABLE 2.2. - CONCLUDED

Table 2.2 (cont'd)

Yawing Moment

$$C_N^A = C_N^W + C_N^H + C_N^V + C_N^{FUS} + C_N^{TR}$$

where:  $C_N^W = C_{N_o}^W + C_{N_\beta}^W$

$$C_N^H = C_{N_o}^H + C_{N_\beta}^H + C_{N_\alpha}^H$$

$$C_N^V = C_{N_o}^V + C_{N_\beta}^V + C_{N_\alpha}^V$$

$$C_N^{FUS} = C_{N_o}^{FUS} + C_{N_\beta}^{FUS} + C_{N_\alpha}^{FUS}$$

$$C_N^{TR} = C_{N_o}^{TR} + C_{N_\beta}^{TR} + C_{N_\alpha}^{TR}$$

Hence,

$$C_N^A = C_{N_o}^W + C_{N_\beta}^W + C_{N_o}^H + C_{N_\beta}^H + C_{N_\alpha}^H + C_{N_o}^V + C_{N_\beta}^V + C_{N_\alpha}^V$$

$$+ C_{N_o}^{FUS} + C_{N_\beta}^{FUS} + C_{N_\alpha}^{FUS} + C_{N_o}^{TR} + C_{N_\beta}^{TR} + C_{N_\alpha}^{TR}$$

$$= (C_{N_o}^W + C_{N_o}^H + C_{N_o}^V + C_{N_o}^{FUS} + C_{N_o}^{TR}) + (C_{N_\beta}^W + C_{N_\beta}^H + C_{N_\beta}^V + C_{N_\beta}^{FUS} + C_{N_\beta}^{TR})_\beta$$

$$+ (C_{N_\alpha}^H + C_{N_\alpha}^V + C_{N_\alpha}^{FUS} + C_{N_\alpha}^{TR})_\alpha$$

equations used in this study, derived from reference 2 and retaining only first-order blade flap and lag modes, are shown in Table 2.3. It will be noted that single parameters, either constant or nonlinear functionals, are used in these equations to represent the complex, theoretically derived coefficients of reference 2. By referring to these theoretical expressions, the content and derivation of identified parameters may be determined. It will also be noted that fuselage rates and accelerations have been transformed into the rotor (shaft) axes.

(5) Rotor Hub Forces and Moments. Rotor dynamics are determined completely by the rotor equations discussed above. As the result of these motions, forces and moments are imposed on the rotor hub; and in this way, rotor forces and moments are both aerodynamic and inertial in origin. Table 2.4 shows the equations for the hub forces and moments, in rotor axes. The aerodynamic parameters in these equations must be identified, along with those relating to rotor and fuselage aerodynamics.

Time-varying rotor forces and moments have been modeled in this study using the averaging method of Johnson [ref. 8], which replaces periodic rotor force and moment coefficients with constant, Fourier-averaged values of the coefficients to obtain a set of constant-coefficient ordinary differential equations amenable to rigorous mathematical analysis. All of the effects of the rotor on the airframe have been modeled, in the present study, by computing rotor-related hub forces and moments under this constant-coefficient approximation and resolving them into body axes for the usual force and moment summation.

General, nonlinear vehicle equations of motion.— Using the coordinate system definitions, nondimensionalization technique, and analyses of vehicle component aerodynamics and rotor dynamics, a general set of complete vehicle equations of motion may be written. The basis for the general equations is Euler's equations referenced to a set of body-fixed axes; these equations are shown in Table 2.5. They are shown here as dimensional equations, and the degrees of freedom appear as their true values, not as perturbation quantities.

The nonlinear vehicle equations for use in this study are shown in Table 2.6. They are obtained by introducing the expressions developed in the previous subsection for fuselage aerodynamics and hub reactions due to the rotor. While the rotor equations given in the preceding subsection are for small-perturbation motion from trim, their use to compute actual hub forces and moments is valid, as biases due to steady state (trim) conditions are included in all of the equations and are identified along with the aerodynamic parameters.

TABLE 2.3. — ROTOR DYNAMICAL EQUATIONS OF MOTION

Rotor Dynamics

Coning ( $\beta_0$ )

$$\begin{aligned}
 I_{\beta}^* \ddot{\beta} + I_{\beta\alpha}^* \ddot{\psi}_s + (I_{\beta}^* g_s v_{\beta} + 2I_{\beta\beta}^*) \dot{\beta} + & M_{\beta}^0 + M_{\beta_0}^0 \beta_0 + M_{\beta_{1c}}^0 \beta_{1c} + M_{\beta_{1s}}^0 \beta_{1s} + M_{\beta_0}^0 \dot{\beta}_0 + \\
 2I_{\beta\psi}^* \dot{\psi}_s + I_{\beta}^* v_{\beta}^2 \beta_0 + S_{\beta}^* [U_B \sin\theta_R - \dot{W}_B \cos\theta_R - & = M_{\beta_{1c}}^0 \dot{\beta}_{1c} + M_{\beta_{1s}}^0 \dot{\beta}_{1s} + M_{\zeta_0}^0 \zeta_0 + M_{\zeta_{1c}}^0 \zeta_{1c} + M_{\zeta_{1s}}^0 \zeta_{1s} + \\
 \dot{Q}_B (\tilde{Z}_{HUB} \sin\theta_R - \tilde{X}_{HUB} \cos\theta_R)] + I_{\beta\alpha}^* (-\tilde{P}_B \cos\theta_R - & M_{\zeta_0}^0 \dot{\zeta}_0 + M_{\zeta_{1c}}^0 \dot{\zeta}_{1c} + M_{\zeta_{1s}}^0 \dot{\zeta}_{1s} + M_{\psi_s}^0 \dot{\psi}_s + M_{\psi_s}^0 \dot{\psi}_s + \\
 \tilde{R}_B \sin\theta_R) & M_U^0 \tilde{U}_B + M_V^0 \tilde{V}_B + M_W^0 \tilde{W}_B + M_P^0 \tilde{P}_B + M_Q^0 \tilde{Q}_B + \\
 & M_R^0 \tilde{R}_B + 2I_{\beta\psi}^* (\tilde{P}_B \sin\theta_R - \tilde{R}_B \cos\theta_R) + \\
 & M_{\theta_0}^0 \theta_0 + M_{\theta_{1c}}^0 \theta_{1s} + M_{\theta_{1s}}^0 \theta_{1s}
 \end{aligned}$$

Longitudinal Flapping ( $\beta_{1c}$ )

$$\begin{aligned}
 I_{\beta}^* \ddot{\beta}_c + (I_{\beta}^* g_s v_{\beta} + 2I_{\beta\beta}^*) \dot{\beta} + & M_{\beta_{1c}}^{1c} + M_{\beta_0}^{1c} \beta_0 + M_{\beta_{1c}}^{1c} \beta_{1c} + M_{\beta_{1s}}^{1c} \beta_{1s} + M_{\beta_0}^{1c} \dot{\beta}_0 + M_{\beta_{1c}}^{1c} \dot{\beta}_{1c} + M_{\beta_{1s}}^{1c} \dot{\beta}_{1s} + \\
 2I_{\beta_{1s}}^* \dot{\beta}_{1s} - I_{\beta\alpha}^* \dot{Q}_B + S_{\beta}^* [\dot{V}_B - & = M_{\zeta_0}^{1c} \zeta_0 + M_{\zeta_{1c}}^{1c} \zeta_{1c} + M_{\zeta_{1s}}^{1c} \zeta_{1s} + M_{\zeta_0}^{1c} \dot{\zeta}_0 + M_{\zeta_{1c}}^{1c} \dot{\zeta}_{1c} + M_{\zeta_{1s}}^{1c} \dot{\zeta}_{1s} + \\
 \tilde{P}_B \tilde{Z}_{HUB} + \tilde{R}_B \tilde{X}_{HUB}] & M_{\psi_s}^{1c} \dot{\psi}_s + M_{\psi_s}^{1c} \dot{\psi}_s + M_U^{1c} \tilde{U}_B + M_V^{1c} \tilde{V}_B + M_W^{1c} \tilde{W}_B + M_P^{1c} \tilde{P}_B + \\
 & M_Q^{1c} \tilde{Q}_B + M_R^{1c} \tilde{R}_B + I_{\beta}^* (v_{\beta}^2 - 1) \beta_{1c} + (I_{\beta}^* g_s v_{\beta} + 2I_{\beta\beta}^*) \beta_{1s} + \\
 & 2I_{\beta\alpha}^* (-\tilde{P}_B \cos\theta_R - \tilde{R}_B \sin\theta_R) + M_{\theta_0}^{1c} \theta_0 + M_{\theta_{1c}}^{1c} \theta_{1c} - M_{\theta_{1s}}^{1c} \theta_{1s}
 \end{aligned}$$

TABLE 2.3. - CONCLUDED

## Rotor Dynamics (Continued)

Lateral Flapping ( $\beta_{1s}$ )

$$\begin{aligned}
 I_{\beta}^* \ddot{\beta}_{1s} - 2I_{\beta}^* \dot{\beta}_{1c} + (I_{\beta}^* g_s v + 2I_{\beta\beta}^*) \dot{\beta}_{1s} + & M_{01s} + M_{\beta_0} \beta_0 + M_{\beta_{1c}} \beta_{1c} + M_{\beta_{1s}} \beta_{1s} + M_{\beta_0} \dot{\beta}_0 \\
 I_{\beta\alpha}^* (-\ddot{P}_B \cos\theta_R - \ddot{R}_B \sin\theta_R) - S_{\beta}^* [-\ddot{U}_B \cos\theta_R - & M_{\beta_{1c}}^{1s} \dot{\beta}_{1c} + M_{\beta_{1s}}^{1s} \dot{\beta}_{1s} + M_{\zeta_0}^{1s} \dot{\zeta}_0 + M_{\zeta_{1c}}^{1s} \dot{\zeta}_{1c} + M_{\zeta_{1s}}^{1s} \dot{\zeta}_{1s} + \\
 \ddot{W}_B \sin\theta_R - \ddot{Q}_B (\ddot{Z}_{HUB} \cos\theta_R - \ddot{X}_{HUB} \sin\theta_R)] & M_{\zeta_0}^{1s} \dot{\zeta}_0 + M_{\zeta_{1c}}^{1s} \dot{\zeta}_{1c} + M_{\zeta_{1s}}^{1s} \dot{\zeta}_{1s} + M_{\psi_s}^{1s} \dot{\psi}_s + \\
 & M_{\psi_s}^{1s} \psi_s + M_u^{1s} \ddot{U}_B + M_v^{1s} \ddot{V}_B + M_w^{1s} \ddot{W}_B + M_p^{1s} \ddot{P}_B + \\
 & M_Q^{1s} \ddot{Q}_B + M_R^{1s} \ddot{R}_{B\rho} - I_{\beta}^* (v_{\beta}^2 - 1) \beta_{1s} - 2I_{\beta\alpha}^* \ddot{Q}_B + \\
 & M_{\theta_0}^{1s} \ddot{\theta}_0 + M_{\theta_{1c}}^{1s} \ddot{\theta}_{1c} + M_{\theta_{1s}}^{1s} \ddot{\theta}_{1s}
 \end{aligned}$$

Lagging Modes ( $\zeta_0, \zeta_{1c}, \zeta_{1s}$ )

Substitute in the above three equations, "z" for "β"

"Q" for "M"

TABLE 2.4. — HUB FORCES AND MOMENTS

$$\begin{aligned}
 C_H &= (\sigma a/2\gamma)(S_{\beta}^* \ddot{\beta}_{1s} + S_{\zeta}^* \ddot{\zeta}_{1s}) + (H_0 + H_{\beta_0} \beta_0 + H_{\beta_{1c}} \beta_{1c} + \dots) + \\
 &\quad + (H_{\theta_0} \theta_0 + H_{\theta_{1c}} \theta_{1c} + H_{\theta_{1s}} \theta_{1s}) \quad C_H^{AERO} \\
 &\quad \underbrace{\hspace{10em}}_{\Delta C_H^{CONTROL}} \\
 C_T &= (ca/\gamma)(-S_{\beta}^* \ddot{\beta}_0 - S_{\zeta}^* \ddot{\zeta}_0) + (T_0 + T_{\beta_0} \beta_0 + T_{\beta_{1c}} \beta_{1c} + \dots) + \\
 &\quad + (T_{\theta_0} \theta_0 + T_{\theta_{1c}} \theta_{1c} + T_{\theta_{1s}} \theta_{1s}) \quad C_T^{AERO} \\
 &\quad \underbrace{\hspace{10em}}_{\Delta C_T^{CONTROL}} \\
 C_Y^R &= (-ca/2\gamma)(S_{\beta}^* \ddot{\beta}_{1c} + S_{\zeta}^* \ddot{\zeta}_{1c}) + (Y_0 + Y_{\beta_0} \beta_0 + Y_{\beta_{1c}} \beta_{1c} + \dots) + \\
 &\quad + (Y_{\theta_0} \theta_0 + Y_{\theta_{1c}} \theta_{1c} + Y_{\theta_{1s}} \theta_{1s}) \quad C_Y^{R,AERO} \\
 &\quad \underbrace{\hspace{10em}}_{\Delta C_Y^R^{CONTROL}} \\
 C_{m_x} &= (-\sigma a/2\gamma)(I_{\beta\alpha}^* \ddot{\beta}_{1s} - 2I_{\beta\alpha}^* \dot{\beta}_{1c} + 2I_{\beta\alpha}^* \dot{\beta}_{1s} - 2I_{\beta\alpha}^* \beta_{1c} + \\
 &\quad 2I_{\alpha\gamma}^* \alpha_{\gamma} + I_{\gamma\alpha}^* \ddot{\zeta}_{1s} - 2I_{\gamma\alpha}^* \dot{\zeta}_{1c} + 2I_{\gamma\alpha}^* \dot{\zeta}_{1s} - 2I_{\gamma\alpha}^* \zeta_{1c}) + \\
 &\quad (\bar{L}_0 + \bar{L}_{\beta_0} \beta_0 + \bar{L}_{\beta_{1c}} \beta_{1c} + \dots) + (\bar{L}_{\theta_0} \theta_0 + \bar{L}_{\theta_{1c}} \theta_{1c} + \bar{L}_{\theta_{1s}} \theta_{1s}) \\
 &\quad \underbrace{\hspace{10em}}_{C_{m_x}^{AERO}} \quad \underbrace{\hspace{10em}}_{\Delta C_{m_x}^{CONTROL}} \\
 C_{m_y} &= (ca/2\gamma)(I_{\beta\alpha}^* \ddot{\beta}_{1c} + I_{\gamma\alpha}^* \ddot{\zeta}_{1c} + 2I_{\beta\alpha}^* \dot{\beta}_{1c} + 2I_{\beta\alpha}^* \dot{\beta}_{1s} + \\
 &\quad 2I_{\beta\alpha}^* \beta_{1s} + 2I_{\alpha x}^* \alpha_x + 2I_{\gamma\alpha}^* \dot{\zeta}_{1s} + 2I_{\gamma\alpha}^* \dot{\zeta}_{1c} + 2I_{\gamma\alpha}^* \zeta_{1s}) + \\
 &\quad (\bar{M}_0 + \bar{M}_{\beta_0} \beta_0 + \bar{M}_{\beta_{1c}} \beta_{1c} + \dots) + (\bar{M}_{\theta_0} \theta_0 + \bar{M}_{\theta_{1c}} \theta_{1c} + \bar{M}_{\theta_{1s}} \theta_{1s}) \\
 &\quad \underbrace{\hspace{10em}}_{C_{m_y}^{AERO}} \quad \underbrace{\hspace{10em}}_{\Delta C_{m_y}^{CONTROL}} \\
 C_Q &= (ca/\gamma)(I_{\beta\alpha}^* \ddot{\beta}_0 + I_{\gamma\alpha}^* \ddot{\zeta}_0 + I_0^* \ddot{\psi}_s - I_{\beta\psi}^* \dot{\beta}_0 - 2I_{\gamma\phi}^* \dot{\zeta}_0) + \\
 &\quad (\bar{Q}_0 + \bar{Q}_{\beta_0} \beta_0 + \bar{Q}_{\beta_{1c}} \beta_{1c} + \dots) + (\bar{Q}_{\theta_0} \theta_0 + \bar{Q}_{\theta_{1c}} \theta_{1c} + \bar{Q}_{\theta_{1s}} \theta_{1s}) \\
 &\quad \underbrace{\hspace{10em}}_{C_Q^{AERO}} \quad \underbrace{\hspace{10em}}_{\Delta C_Q^{CONTROL}}
 \end{aligned}$$



TABLE 2.5 — GENERAL NONLINEAR EQUATIONS OF MOTION

General Nonlinear Equations of Motion

In Body-Fixed Axes,

- Translational:  $\dot{\bar{V}} + \bar{\Omega} \times \bar{V} = \frac{1}{m} \Sigma \bar{F}$  (Aero, Rotor, Gravity)
- Rotational:  $\dot{\bar{M}} + \bar{\Omega} \times \bar{M} = \Sigma \text{Moments}$  (Aero, Rotor)

$\bar{M}_0 = \text{Angular Momentum of Airplane} = \bar{I} \cdot \bar{\Omega}$

$$\bar{I} = \begin{bmatrix} I_{xx} & -I_{xy} & -I_{xz} \\ -I_{yx} & I_{yy} & -I_{yz} \\ -I_{zx} & -I_{zy} & I_{zz} \end{bmatrix}, \quad \bar{\Omega} = \begin{bmatrix} P \\ Q \\ R \end{bmatrix},$$

$$\text{Moments} = \begin{bmatrix} L \\ M \\ N \end{bmatrix} \begin{matrix} \text{(Roll)} \\ \text{(Pitch)} \\ \text{(Yaw)} \end{matrix}$$

$\bar{M} = \underbrace{\bar{M}_0}_{\text{Angular Momentum of Tail Rotor, Engines, Etc.}} + \Delta \bar{M}$

Expanding the translational equations, obtain

$$\begin{bmatrix} \dot{U} \\ \dot{V} \\ \dot{W} \end{bmatrix} = \frac{1}{m} \begin{bmatrix} \Sigma F_x \text{ (Aero+Rotor)} \\ \Sigma F_y \text{ (Aero+Rotor)} \\ \Sigma F_z \text{ (Aero+Rotor)} \end{bmatrix} + \begin{bmatrix} RV - QW \\ PW - RU \\ QU - PV \end{bmatrix} + g \begin{bmatrix} -\sin\theta \\ \cos\theta \sin\phi \\ \cos\theta \cos\phi \end{bmatrix}$$

Expanding the rotational equations, obtain

$$\begin{bmatrix} I_{xx} \dot{P} \\ I_{yy} \dot{Q} \\ I_{zz} \dot{R} \end{bmatrix} = \begin{bmatrix} \Sigma L \text{ (Aero+Rotor)} \\ \Sigma M \text{ (Aero+Rotor)} \\ \Sigma N \text{ (Aero+Rotor)} \end{bmatrix} - \begin{bmatrix} \Delta \bar{M}_x + Q\Delta M_z - R\Delta M_y \\ \Delta \bar{M}_y + R\Delta M_x - P\Delta M_z \\ \Delta \bar{M}_z + P\Delta M_y - Q\Delta M_x \end{bmatrix}$$

$$- \begin{bmatrix} R^2 I_{yz} - Q^2 I_{zy} + PR I_{yz} + QR(I_{zz} - I_{yy}) - PQ I_{xz} - \dot{Q} I_{xy} - \dot{R} I_{xz} \\ P^2 I_{zx} - R^2 I_{xz} + PQ I_{zy} + PR(I_{xx} - I_{zz}) - QR I_{xy} - \dot{P} I_{yx} - \dot{R} I_{yz} \\ -P^2 I_{yx} + Q^2 I_{xy} - PR I_{yz} + PQ(I_{yy} - I_{xx}) + QR I_{xz} - \dot{Q} I_{zy} - \dot{P} I_{xz} \end{bmatrix}$$

TABLE 2.6. — TRANSLATIONAL EQUATIONS OF MOTION

$$\begin{aligned}
 \dot{U}_B - \frac{1}{m}(\rho\Omega^2 R^4 \pi) [-(\sigma a/2\gamma)(S_{\beta\beta 1s}^{**} + S_{\zeta\zeta 1s}^{**})\cos \theta_R + (\sigma a/\gamma)(-S_{\beta\beta 0}^{**} - S_{\zeta\zeta 0}^{**})\sin \theta_R] &= R_B V_B - Q_B W_B - g \sin \theta + \frac{1}{m}(\rho\Omega^2 R^4 \pi)[C_x^W + C_x^H + C_x^V + C_x^{FUS} + C_x^{TR}) - C_H^{AERO} \cos \theta_R + C_T^{AERO} \sin \theta_R + (C_{x\delta_e} \delta_e + C_{x\delta_a} \delta_a + C_{x\delta_r} \delta_r + C_{x\delta_{TR}}) + \Delta C_{TCONTROL} \sin \theta_R - \Delta C_{HCONTROL} \cos \theta_R] \\
 \dot{V}_B - \frac{1}{m}(\rho\Omega^2 R^4 \pi)[(-\sigma a/2\gamma)(S_{\beta\beta 1c}^{**} + S_{\zeta\zeta 1c}^{**})] &= P_V W_V - R_B U_B + g \cos \theta \sin \phi + \frac{1}{m}(\rho\Omega^2 R^4 \pi). [(C_Y^W + C_Y^H + C_Y^V + C_Y^{FUS} + C_Y^{TR}) + C_Y^{R,AERO} + (C_{Y\delta_a} \delta_a + C_{Y\delta_r} \delta_r + C_{Y\delta_e} \delta_e + C_{Y\delta_{TR}}) + \Delta C_{YCONTROL}^R] \\
 \dot{W}_B - \frac{1}{m}(\rho\Omega^2 R^4 \pi)[(-\sigma a/2\gamma)(S_{\beta\beta 1s}^{**} + S_{\zeta\zeta 1s}^{**})\sin \theta_R + (\sigma a/\gamma)(S_{\beta\beta 0}^{**} + S_{\zeta\zeta 0}^{**})\cos \theta_R] &= Q_B U_B - P_B V_B - g \cos \theta \cos \phi + \frac{1}{m}(\rho\Omega^2 R^4 \pi). [(C_Z^W + C_Z^H + C_Z^V + C_Z^{FUS} + C_Z^{TR}) - C_H^{AERO} \sin \theta_R - C_T^{AERO} \cos \theta_R + (C_{Z\delta_e} \delta_e + C_{Z\delta_r} \delta_r + C_{Z\delta_A} \delta_A + C_{Z\delta_{TR}} \delta_{TR}) - \Delta C_{HCONTROL} \sin \theta_R - \Delta C_{TCONTROL} \cos \theta_R]
 \end{aligned}$$

TABLE 2.6. - CONTINUED

Roll

$$\begin{aligned}
 I_X \dot{P}_B - I_{wy} \dot{Q}_B - I_{xz} \dot{R}_B + (\rho \Omega^2 R^5 \pi) (\sigma a / 2 \gamma) &= - \dot{\Delta M}_x - Q_B \Delta M_z + R_B^2 \Delta M_y - R_V I_{yz} + Q_B^2 I_{zy} - \\
 [(-I_{\beta\alpha}^* \ddot{\beta}_{1s} - I_{\zeta\alpha}^* \ddot{\zeta}_{1s}) \cos \theta_R - 2(I_{\beta\alpha}^* \ddot{\beta}_0 + &= P_B R_B I_{yx} - W_B R_B (I_z - I_y) + P_B Q_B I_{xz} + (\rho \Omega^2 R^5 \pi) \cdot \\
 I_{\zeta\alpha}^* \ddot{\zeta}_0 + I_0^* \ddot{\psi}_s) \sin \theta_R + \tilde{z}_{HUB} (S_{\beta 1c}^* + &[(C_{\ell}^W + C_{\ell}^H + C_{\ell}^V + C_{\ell}^{FUS} + C_{\ell}^{TR}) + (\sigma a / 2 \gamma) \cdot \\
 S_{\zeta 1c}^{**})] &\cos \theta_R (-2I_{\beta\alpha}^* \dot{\beta}_{1c} + I_{\beta\alpha}^* \beta_{1c} - 2I_{\beta\alpha}^* \beta_{1c} + \\
 &2I_0 \tilde{Q}_B) - C_{m_x}^{AERO} \cos \theta_R + (\sigma a / \gamma) \sin \theta_R \cdot \\
 (-2I_{\beta\psi}^* \dot{\beta}_0 - 2I_{\zeta\psi}^* \dot{\zeta}_0) + C_Q^{AERO} \sin \theta_R - & \\
 C_Y^{R,AERO} \tilde{z}_{HUB} + (C_{\ell_{\delta_a}} \delta_a + C_{\ell_{\delta_r}} \delta_r + & \\
 C_{\ell_{\delta_{TR}}} \delta_{TR}) - \Delta C_{m_x}^{CONTROL} \cos \theta_R + \Delta C_{Q}^{CONTROL} \sin \theta_R - & \\
 \Delta C_Y^{CONTROL} \dot{\tilde{z}}_{HUB} &]
 \end{aligned}$$

TABLE 2.6. - CONTINUED

Pitch

$$\begin{aligned}
 I_y \dot{Q}_B - I_{yx} \dot{P}_B - I_{yz} \dot{R}_B - (\rho \Omega^2 R^5 \pi) (\sigma a / 2\gamma) (I_{\beta\alpha}^* \ddot{\beta}_{1c} + & - \Delta \dot{M}_y - R_B \Delta M_x + P_B \Delta M_z - P_B^Z I_{zx} + \\
 I_{\zeta\alpha}^* \ddot{\zeta}_{1c}) + (\sigma a / 2\gamma) [-\bar{z}_{HUB} \cos \theta_R (S_{\beta\beta}^* \ddot{\beta}_{1s} + & = R_B^Z I_{xz} - P_B R_B (I_x - I_z) + Q_B R_B I_{xy} + \\
 S_{\zeta\zeta}^* \ddot{\zeta}_{1s}) + 2 \bar{z}_{HUB} \sin \theta_R (-S_{\beta\beta}^* \ddot{\beta}_o - S_{\zeta\zeta}^* \ddot{\zeta}_o) + & (\rho \Omega^2 R^5 \pi) [(C_m^W + C_m^H + C_m^V + C_m^{FUS} + C_m^{TR}) \triangleright + \\
 \bar{x}_{HUB} \sin \theta_R (S_{\beta\beta}^* \ddot{\beta}_{1s} + S_{\zeta\zeta}^* \ddot{\zeta}_o) + 2 \bar{x}_{HUB} \cos \theta_R & (\sigma a / 2\gamma) (2I_{\beta\alpha}^* \dot{\beta}_{1c} + 2I_{\beta\alpha}^* \dot{\beta}_{1s} + 2I_{\beta\alpha}^* \beta_{1s} + \\
 (-S_{\beta\beta}^* \ddot{\beta}_o - S_{\zeta\zeta}^* \ddot{\zeta}_o))] & 2I_o^* (-\bar{p}_B \cos \theta_R - \bar{r}_B \sin \theta_R) + 2I_{\zeta\alpha}^* \dot{\zeta}_{1s} + \\
 & 2I_{\zeta\alpha}^* \dot{\zeta}_{1c} + 2I_{\zeta\alpha}^* \zeta_{1s}) + C_{m_y}^{AERO} + \bar{z} \quad \triangleright \\
 & (-C_H^{AERO} \cos \theta_R + C_T^{AERO} \sin \theta_R) + \bar{x}_{HUB} \cdot \\
 & (C_H^{AERO} \sin \theta_R + C_T^{AERO} \cos \theta_R) + \\
 & (C_{m_{\delta_e}} + C_{m_{\delta_r}} + C_{m_{\delta_{TR}}}) + \Delta C_{m_y}^{CONTROL} + \\
 & \bar{z}_{HUB} (-\Delta C_{H_{CONTROL}} \cos \theta_R + \Delta C_{T_{CONTROL}} \sin \theta_R) \\
 & \bar{x}_{HUB} (\Delta C_{H_{CONTROL}} \sin \theta_R + \Delta C_{T_{CONTROL}} \cos \theta_R)
 \end{aligned}$$

$\triangleright$  Typical Parameter Expansion -

$$\begin{aligned}
 C_m^W + C_m^H + C_m^V + C_m^{FUS} + C_m^{TR} = C_m^{AERO} \text{ (Exc. Rotor)} = (C_{m_o}^W + C_{m_o}^H + C_{m_o}^V + C_{m_o}^{FUS} + C_{m_o}^{TR}) + (C_{m_\alpha}^W + C_{m_\alpha}^H + C_{m_\alpha}^{FUS} + C_{m_\alpha}^{TR}) \alpha + \\
 (C_{m_u}^W + C_{m_u}^H + C_{m_u}^{TR}) u + (C_{m_q}^H + C_{m_q}^{FUS} + C_{m_q}^{TR}) Q_B
 \end{aligned}$$

$\triangleright$  Hub aero forces and moments in terms of parameters, as shown in "hub forces and moments," Table 2.4.

TABLE 2.6. - CONCLUDED

<u>Yaw</u>	
$I_{ZB} \dot{R}_B - I_{ZX} \dot{P}_B - I_{ZY} \dot{Q}_B + (\rho \Omega^2 R^5 \pi) (\sigma / 2\gamma).$ $[-I_{\beta\alpha}^* \ddot{\beta}_{1s} \sin \theta_R - 2(I_{\beta\alpha}^* \ddot{\beta}_0 + I_{\zeta\alpha}^* \ddot{\zeta}_0 +$ $I_{\psi_s}^* \ddot{\psi}_s) \cos \theta_R + \tilde{X}_{HUB} (S_{\beta}^* \ddot{\beta}_{1c} + S_{\zeta}^* \ddot{\zeta}_{1c})]$	$- \Delta \dot{M}_Z - P_B \Delta M_y + Q_B \Delta M_x + P_B I_{yx} - Q_B I_{xy} +$ $P_B R_B I_{yz} - P_B Q_B (I_y - I_x) - Q_B R_B I_{xz} +$ $(\rho \Omega^2 R^5 \pi) [(C_n^W + C_n^H + C_n^H + C_n^V + C_n^{FUS} + C_n^{TR}) +$ $(\sigma / 2\gamma) (\sin \theta_R) (-2I_{\beta\alpha}^* \dot{\beta}_{1c} + I_{\beta\alpha}^* \dot{\beta}_{1s} -$ $2I_{\beta\alpha}^* \beta_{1c} + 2I_{\psi_0}^* \dot{Q}_B) - C_{m_x}^{AERO} \sin \theta_R -$ $(\sigma / \gamma) (\cos \theta_R) (-2I_{\beta\psi}^* \dot{\beta}_0 - 2I_{\zeta\psi}^* \dot{\zeta}_0) -$ $C_Q^{AERO} \cos \theta_R + C_Y^{R,AERO} \cdot \tilde{X}_{HUB} +$ $(C_{n_{\delta_r}} \delta_r + C_{n_{\delta_a}} \delta_a + C_{n_{\delta_{TR}}} \delta_{TR}) - C_{m_x}^{CONTROL} \sin \theta_R -$ $\Delta C_{Q_{CONTROL}} \cos \theta_R + \Delta C_{Y_{CONTROL}}^R \cdot \tilde{X}_{HUB}]$

This model is employed for nonlinear simulation and parameter identification work, for which time histories are the principal output required.

Linear vehicle equations of motion.— The linear equations of motion for the rotorcraft, shown in Table 2.7, are a special set which are derived from the nonlinear equations by the well known linearization technique using a first-term Taylor expansion of all parameters and states. Note that the effects of gravity and controls are also linearized. This model is used for linear parameter identification and general model analysis studies, and adds the last of the modeling capabilities desired in this study.

Modeling the Two-Bladed Rotor.— The modeling aspects of a two-bladed rotor differ from those of a rotor with three or more blades because the two-bladed rotor is not axisymmetric and its inertial properties, as well as its aerodynamics, possess periodically-varying characteristics. The modeling of this rotor is again based on the method employed by Johnson [ref. 8], in his analysis of the general rotor dynamics problem. This method substitutes constant, average values of the coefficients for this time periodically-varying values, and in so doing, achieves simplicity and clarity in the dynamic formulation. As noted in reference 8, it introduces some errors because the periodic and nonaxisymmetric properties of the testing rotor are pronounced. Nevertheless, the method, appropriate to rotor dynamics studies, is certainly also appropriate to rotorcraft handling qualities studies, and provides for continuity of method in the present model formulation. The constant coefficient method is particularly well suited to the sophisticated system identification methods employed in the present study because periodic effects will be distributed throughout the identified model in such a way that maximum dynamic fidelity is obtained. In this way, the results of system identification analysis of the two-bladed rotor will guide future modeling effort toward useful model structures for handling qualities and flight dynamics studies.

Identification and State Estimation in the Two-Bladed Rotor.— For the purpose of system identification, a linear time-invariant model of the two-bladed rotor gives a high level of modeling error at 2 per rev. This modeling error occurs because the two-bladed rotor possesses a plane of symmetry which rotates with the blades and crosses a reference point twice in each rotation. In a steady state, this error term can be filtered out. The filtering is most effective when low frequency characteristics are desired.

TABLE 2.7 — SCIDNT LINEAR MODEL

$$\dot{x} = Fx + Gu$$

$$y = Hx + Du$$

Example:

$\frac{d}{dt}$	u	$X_u X_v X_w X_p$	$X_q - W_0$	$X_r$	0	$-gc_0$	0	$X_{\beta_0}$	$X_{\beta_{1c}}$	$X_{\beta_{1s}}$	$X_{\zeta_0}$	$X_{\zeta_{1c}}$	$X_{\zeta_{1s}}$	$X_{\beta_0}$	$X_{\beta_{1c}}$	$X_{\beta_{1s}}$	$X_{\zeta_0}$	$X_{\zeta_{1c}}$	$X_{\zeta_{1s}}$	u	
	v	$Y_u Y_v Y_w Y_p + W_0$	$Y_q$	$Y_r - U_0$	$gc\phi_0 c\theta_0$	$-gs\phi_0 \theta_0$	0	$Y_{\beta_0}$	$Y_{\beta_{1c}}$	$Y_{\beta_{1s}}$	$Y_{\zeta_0}$	$Y_{\zeta_{1c}}$	$Y_{\zeta_{1s}}$	$Y_{\beta_0}$	$Y_{\beta_{1c}}$	$Y_{\beta_{1s}}$	$Y_{\zeta_0}$	$Y_{\zeta_{1c}}$	$Y_{\zeta_{1s}}$	v	
	w	$Z_u Z_v Z_w Z_p$	$Z_q + U_0$	$Z_r$	$-gs\phi_0 c\theta_0$	$-gc\phi_0 s\theta_0$	0	$Z_{\beta_0}$	$Z_{\beta_{1c}}$	$Z_{\beta_{1s}}$	$Z_{\zeta_0}$	$Z_{\zeta_{1c}}$	$Z_{\zeta_{1s}}$	$Z_{\beta_0}$	$Z_{\beta_{1c}}$	$Z_{\beta_{1s}}$	$Z_{\zeta_0}$	$Z_{\zeta_{1c}}$	$Z_{\zeta_{1s}}$	w	
	p	$L_u^* L_v^* L_w^* L_p^*$	$L_q^*$	$L_r^*$	0	0	0	$L_{\beta_0}^*$	$L_{\beta_{1c}}^*$	$L_{\beta_{1s}}^*$	$L_{\zeta_0}^*$	$L_{\zeta_{1c}}^*$	$L_{\zeta_{1s}}^*$	$L_{\beta_0}^*$	$L_{\beta_{1c}}^*$	$L_{\beta_{1s}}^*$	$L_{\zeta_0}^*$	$L_{\zeta_{1c}}^*$	$L_{\zeta_{1s}}^*$	p	
	q	$M_u M_v M_w M_p$	$M_q$	$M_r$	0	0	0	$M_{\beta_0}$	$M_{\beta_{1c}}$	$M_{\beta_{1s}}$	$M_{\zeta_0}$	$M_{\zeta_{1c}}$	$M_{\zeta_{1s}}$	$M_{\beta_0}$	$M_{\beta_{1c}}$	$M_{\beta_{1s}}$	$M_{\zeta_0}$	$M_{\zeta_{1c}}$	$M_{\zeta_{1s}}$	q	
	r	$N_u^* N_v^* N_w^* N_p^*$	$N_q^*$	$N_r^*$	0	0	0	$N_{\beta_0}^*$	$N_{\beta_{1c}}^*$	$N_{\beta_{1s}}^*$	$N_{\zeta_0}^*$	$N_{\zeta_{1c}}^*$	$N_{\zeta_{1s}}^*$	$N_{\beta_0}^*$	$N_{\beta_{1c}}^*$	$N_{\beta_{1s}}^*$	$N_{\zeta_0}^*$	$N_{\zeta_{1c}}^*$	$N_{\zeta_{1s}}^*$	r	
	$\phi$	0 0 0 1	$s\phi_0 t\theta_0$	$c\phi_0 t\theta_0$	0	0	0	0	0	0	0	0	0	0	0	0	0	0	0	0	$\phi$
	$\theta$	0 0 0 0	$c\phi_0$	$-s\phi_0$	0	0	0	0	0	0	0	0	0	0	0	0	0	0	0	0	$\theta$
	$\psi$	0 0 0 0	$s\phi_0/c\theta_0$	$c\phi_0/c\theta_0$	0	0	0	0	0	0	0	0	0	0	0	0	0	0	0	0	$\psi$
	$\beta_0$	0 0 0 0	0	0	0	0	0	0	0	0	0	0	0	0	1	0	0	0	0	0	$\beta_0$
	$\beta_{1c}$	0 0 0 0	0	0	0	0	0	0	0	0	0	0	0	0	0	1	0	0	0	0	$\beta_{1c}$
	$\beta_{1s}$	0 0 0 0	0	0	0	0	0	0	0	0	0	0	0	0	0	0	1	0	0	0	$\beta_{1s}$
	$\zeta_0$	0 0 0 0	0	0	0	0	0	0	0	0	0	0	0	0	0	0	0	1	0	0	$\zeta_0$
	$\zeta_{1c}$	0 0 0 0	0	0	0	0	0	0	0	0	0	0	0	0	0	0	0	0	1	0	$\zeta_{1c}$
	$\zeta_{1s}$	0 0 0 0	0	0	0	0	0	0	0	0	0	0	0	0	0	0	0	0	0	1	$\zeta_{1s}$
$\beta_0^0$	$B_u^0 B_v^0 B_w^0 B_p^0$	$B_q^0$	$B_r^0$	0	0	0	$B_{\beta_0}^0$	$B_{\beta_{1c}}^0$	$B_{\beta_{1s}}^0$	$B_{\zeta_0}^0$	$B_{\zeta_{1c}}^0$	$B_{\zeta_{1s}}^0$	$B_{\beta_0}^0$	$B_{\beta_{1c}}^0$	$B_{\beta_{1s}}^0$	$B_{\zeta_0}^0$	$B_{\zeta_{1c}}^0$	$B_{\zeta_{1s}}^0$	$\beta_0^0$		
$\beta_{1c}^0$	$B_u^c B_v^c B_w^c B_p^c$	$B_q^c$	$B_r^c$	0	0	0	$B_{\beta_0}^c$	$B_{\beta_{1c}}^c$	$B_{\beta_{1s}}^c$	$B_{\zeta_0}^c$	$B_{\zeta_{1c}}^c$	$B_{\zeta_{1s}}^c$	$B_{\beta_0}^c$	$B_{\beta_{1c}}^c$	$B_{\beta_{1s}}^c$	$B_{\zeta_0}^c$	$B_{\zeta_{1c}}^c$	$B_{\zeta_{1s}}^c$	$\beta_{1c}^0$		
$\beta_{1s}^0$	$B_u^s B_v^s B_w^s B_p^s$	$B_q^s$	$B_r^s$	0	0	0	$B_{\beta_0}^s$	$B_{\beta_{1c}}^s$	$B_{\beta_{1s}}^s$	$B_{\zeta_0}^s$	$B_{\zeta_{1c}}^s$	$B_{\zeta_{1s}}^s$	$B_{\beta_0}^s$	$B_{\beta_{1c}}^s$	$B_{\beta_{1s}}^s$	$B_{\zeta_0}^s$	$B_{\zeta_{1c}}^s$	$B_{\zeta_{1s}}^s$	$\beta_{1s}^0$		
$\zeta_0^0$	$Z_u^0 Z_v^0 Z_w^0 Z_p^0$	$Z_q^0$	$Z_r^0$	0	0	0	$Z_{\beta_0}^0$	$Z_{\beta_{1c}}^0$	$Z_{\beta_{1s}}^0$	$Z_{\zeta_0}^0$	$Z_{\zeta_{1c}}^0$	$Z_{\zeta_{1s}}^0$	$Z_{\beta_0}^0$	$Z_{\beta_{1c}}^0$	$Z_{\beta_{1s}}^0$	$Z_{\zeta_0}^0$	$Z_{\zeta_{1c}}^0$	$Z_{\zeta_{1s}}^0$	$\zeta_0^0$		
$\zeta_{1c}^0$	$Z_u^c Z_v^c Z_w^c Z_p^c$	$Z_q^c$	$Z_r^c$	0	0	0	$Z_{\beta_0}^c$	$Z_{\beta_{1c}}^c$	$Z_{\beta_{1s}}^c$	$Z_{\zeta_0}^c$	$Z_{\zeta_{1c}}^c$	$Z_{\zeta_{1s}}^c$	$Z_{\beta_0}^c$	$Z_{\beta_{1c}}^c$	$Z_{\beta_{1s}}^c$	$Z_{\zeta_0}^c$	$Z_{\zeta_{1c}}^c$	$Z_{\zeta_{1s}}^c$	$\zeta_{1c}^0$		
$\zeta_{1s}^0$	$Z_u^s Z_v^s Z_w^s Z_p^s$	$Z_q^s$	$Z_r^s$	0	0	0	$Z_{\beta_0}^s$	$Z_{\beta_{1c}}^s$	$Z_{\beta_{1s}}^s$	$Z_{\zeta_0}^s$	$Z_{\zeta_{1c}}^s$	$Z_{\zeta_{1s}}^s$	$Z_{\beta_0}^s$	$Z_{\beta_{1c}}^s$	$Z_{\beta_{1s}}^s$	$Z_{\zeta_0}^s$	$Z_{\zeta_{1c}}^s$	$Z_{\zeta_{1s}}^s$	$\zeta_{1s}^0$		

TABLE 2.7. - CONTINUED

$$\begin{array}{cccc}
 X_{\delta_c} & X_{\delta_{LO}} & X_{\delta_{LA}} & X_{\delta_r} \\
 Y_{\delta_c} & Y_{\delta_{LO}} & Y_{\delta_{LA}} & Y_{\delta_r} \\
 Z_{\delta_c} & Z_{\delta_{LO}} & Z_{\delta_{LA}} & Z_{\delta_r} \\
 L_{\delta_c}^* & L_{\delta_{LO}}^* & L_{\delta_{LA}}^* & L_{\delta_r}^* \\
 M_{\delta_c} & M_{\delta_{LO}} & M_{\delta_{LA}} & M_{\delta_r} \\
 N_{\delta_c} & N_{\delta_{LO}} & N_{\delta_{LA}} & N_{\delta_r} \\
 0 & 0 & 0 & 0 \\
 0 & 0 & 0 & 0 \\
 0 & 0 & 0 & 0 \\
 0 & 0 & 0 & 0 \\
 0 & 0 & 0 & 0 \\
 0 & 0 & 0 & 0 \\
 0 & 0 & 0 & 0 \\
 0 & 0 & 0 & 0 \\
 0 & 0 & 0 & 0 \\
 B_{\delta_c}^O & B_{\delta_{LO}}^O & B_{\delta_{LA}}^O & 0 \\
 B_{\delta_c}^C & B_{\delta_{LO}}^C & B_{\delta_{LA}}^C & 0 \\
 B_{\delta_c}^S & B_{\delta_{LO}}^S & B_{\delta_{LA}}^S & 0 \\
 Z_{\delta_c}^O & Z_{\delta_{LO}}^O & Z_{\delta_{LA}}^O & 0 \\
 Z_{\delta_c}^C & Z_{\delta_{LO}}^C & Z_{\delta_{LA}}^C & 0 \\
 Z_{\delta_c}^S & Z_{\delta_{LO}}^S & Z_{\delta_{LA}}^S & 0
 \end{array}
 + \begin{array}{c}
 \delta_c \\
 \delta_{LO} \\
 \delta_{LA} \\
 \delta_r
 \end{array}$$

Where

$$\begin{bmatrix} L^* \\ N^* \end{bmatrix} = \begin{bmatrix} I_x & -I_{xz} \\ -I_{xz} & I_z \end{bmatrix}^{-1} \begin{bmatrix} L \\ N \end{bmatrix}$$



Thus, accurate estimates of stability and control parameters may be obtained from models given previously.

The problem is made more complicated because of the changing level of the 2 per rev error in a transient. A continuously tracking filter is required to minimize the error. This is particularly significant for system identification where most information about parameter values is available in a transient. The computer programs based on the models presented in this chapter may incorporate such tracking filters.

When rotor-blade measurements are available, difficulties are caused in transformations from the rotating system to the fixed system. In three or more bladed rotors, the positions of the blade tips at any time define the instantaneous position of the tip-path-plane (TPP). For a two-bladed rotor, two points on the blade cannot define an instantaneous plane. The following procedure may be used, however, for the transformation.

$$\begin{aligned}\beta_1 &= \beta_0 + \beta_{1c} \cos(\Omega t) + \beta_{1s} \sin(\Omega t) \\ \beta_2 &= \beta_0 + \beta_{1c} \cos(\Omega t + \pi) + \beta_{1s} \sin(\Omega t + \pi) \\ &= \beta_0 - \beta_{1c} \cos(\Omega t) - \beta_{1s} \sin(\Omega t)\end{aligned}$$

In the matrix notation, these equations are

$$\begin{bmatrix} \beta_1 \\ \beta_2 \end{bmatrix} = T \begin{bmatrix} \beta_0 \\ \beta_{1c} \\ \beta_{1s} \end{bmatrix}$$

where

$$T = \begin{bmatrix} 1 & \cos \Omega t & \sin \Omega t \\ 1 & -\cos \Omega t & -\sin \Omega t \end{bmatrix}$$

Differentiating the above equation once and then twice, we get

$$\begin{bmatrix} \dot{\beta}_1 \\ \dot{\beta}_2 \end{bmatrix} = \dot{T} \begin{bmatrix} \beta_0 \\ \beta_{1c} \\ \beta_{1s} \end{bmatrix} + T \begin{bmatrix} \dot{\beta}_0 \\ \dot{\beta}_{1c} \\ \dot{\beta}_{1s} \end{bmatrix}$$

$$\begin{pmatrix} \ddot{\beta}_0 \\ \ddot{\beta}_1 \\ \ddot{\beta}_2 \end{pmatrix} = \ddot{T} \begin{bmatrix} \beta_0 \\ \beta_{1c} \\ \beta_{1s} \end{bmatrix} + 2\dot{T} \begin{bmatrix} \dot{\beta}_0 \\ \dot{\beta}_{1c} \\ \dot{\beta}_{1s} \end{bmatrix} + T \begin{bmatrix} \ddot{\beta}_0 \\ \ddot{\beta}_{1c} \\ \ddot{\beta}_{1s} \end{bmatrix}$$

since the dynamic system of equations defines the relationship between the tip-path-plane acceleration and the corresponding velocity and position, we have

$$\begin{bmatrix} \ddot{\beta}_0 \\ \ddot{\beta}_{1c} \\ \ddot{\beta}_{1s} \end{bmatrix} = F_R(\theta) \begin{bmatrix} \beta_0 \\ \beta_{1c} \\ \beta_{1s} \end{bmatrix} + F'_R(\theta) \begin{bmatrix} \dot{\beta}_0 \\ \dot{\beta}_{1c} \\ \dot{\beta}_{1s} \end{bmatrix} + G_R(\theta) \begin{bmatrix} \delta_c \\ \delta_{L0} \\ \delta_{LA} \end{bmatrix}$$

We have six equations and six unknowns  $\beta_0, \beta_{1c}, \beta_{1s}, \dot{\beta}_0, \dot{\beta}_{1c}, \dot{\beta}_{1s}$ . We can determine these unknowns in terms of  $\beta_1, \beta_2$ , and their first- and second-order derivatives and rotor inputs. The transformation is both time varying and parameter dependent. In addition, both flapping rate and flapping acceleration measurements are required.

The problem may be simplified somewhat by taking the sum and difference of  $\beta_1$  and  $\beta_2$  before time derivatives are derived. Equations for  $\beta_{1c}$  and  $\beta_{1s}$  are still complex.

A more direct approach is based on using the blade-flapping measurements without transformations to the fixed axis system. Periodic gains with 1 per rev periodicity are then obtained. The implementation is more difficult because of the need to store a time history of Kalman filter gains.

## CHAPTER III

### ROTORCRAFT STATE ESTIMATION

State estimation is the process of quantifying the time histories of significant vehicle response variables, based on measurements which themselves are susceptible to errors. The input data to the state estimation process are the measurements and the desired outputs are best estimates of the vehicle states and of the measurement errors (e.g., biases, scale factors, etc.).

The first section reviews the specific requirements for rotorcraft state estimation. The second section then summarizes the fundamentals of state estimation, followed by the third section which presents the basis of a rotorcraft state estimation algorithm. The fourth section discusses the structure of the computer program DEKFIS (for Discrete Extended Kalman Filter and Smoother).

#### Requirements for Rotorcraft State Estimation

Rotorcraft flight testing for handling qualities, stability and control, and simulation validation objectives requires the measurement of a multitude of variables. Examples of such measurements are on-board variables such as accelerations, velocity, position, attitude, angular rates, and control inputs. Off-board measurements may also be required. Radar tracking is an example. These measurements are, in general, subject to instrumentation errors due to random noise, bias, scale factor, channel cross-talk, and dynamic lags. Further errors are introduced with instrumentation data conditioning and transfer due to sampling effects and word length limitations. The determination of the best estimate of required vehicle states from these measurements is therefore non-trivial.

The systematic methodology for estimating the vehicle states and for estimating the errors in the measurements is denoted as state estimation. This methodology has evolved very rapidly in the past 15 years as digital computers have become more widespread as a flight test data processing tool. Parallel to the use of these digital computers has been the development of algorithms for minimizing the error of the estimated time histories relative to the actual responses. The number of measurements required for rotorcraft dynamic state description presents a formidable state estimation requirement for these algorithms.

The general requirements for rotorcraft state estimation are to provide the following improvements over raw flight data:

- (1) data consistency for related attitude, rate and acceleration measurements (e.g., between radar and integrated linear accelerometer measurement position);
- (2) the capability to handle redundant instrumentation at different locations;
- (3) corrections for instrumentation errors such as scale factor and bias errors, instrumentation dynamic lag, cross-talk and random noise;
- (4) estimates for gusts and other unmeasured states; and
- (5) estimates for all states.

The specific requirements for rotorcraft state estimation are as follows:

- (1) estimation of fuselage states in presence of gusts, and estimates of gusts and gust statistics;
- (2) estimation of rotor states; and
- (3) estimates of component forces and moments.

These general and specific requirements pose a significant computational task because of the large number of vehicle, instrumentation, and statistical parameters which must be estimated.

Resolution of these requirements involves three principal issues. These issues are:

- (1) the state estimation algorithm;
- (2) the specific models to be estimated; and
- (3) the algorithm implementation.

These issues are addressed in the following subsections.

#### Review of State Estimation Algorithms

There is now an extensive body of experience and documentation which provides extensive background to the science and art of modern applied state estimation [10]. This section is a summary of the principal aspects of this technology which are necessary for understanding the rotorcraft estimation approaches discussed in subsequent sections.

Linear continuous and discrete system models.- The general problem of state estimation is based on a formulation of the linearized system dynamics and measurement equations, viz

$$\dot{x} = Fx + Gw \quad , \quad x(0) \text{ given} \quad (3.1)$$

$$y = Hx + v \quad (3.2)$$

where

$x \triangleq$  system state

$w \triangleq$  system noise (random, white process with power spectral density,  $Q$ )

$y \triangleq$  system measurements

$v \triangleq$  system measurement noise (random, white process with power spectral density,  $R$ )

$F \triangleq$  system dynamics matrix (assumed constant)

$G \triangleq$  system noise matrix (assumed constant)

$H \triangleq$  system observation matrix (assumed constant)

(Explicit vectors and matrices for rotorcraft application are given in the next section.)

Equations (3.1) and (3.2) are a continuous model for the system. The corresponding discrete model, describing system characteristics at discrete times  $i$  and  $i+1$  ( $0 \triangleq i \triangleq N$ ), is

$$x_{k+1} = \phi x_k + \Gamma w_k \quad , \quad x_0 \text{ given} \quad (3.3)$$

$$y_k = H_k x_k + v_k \quad (3.4)$$

where  $x_k$ ,  $y_k$ ,  $w_k$  and  $v_k$  are the sampled values at time  $k$  of the corresponding terms in Eqs. (3.1) and (3.2), and the matrices  $\phi$ ,  $\Gamma$ , and  $H$  are the discrete equivalents of  $F$ ,  $G$ , and  $H$ .

State estimation algorithms.- The state estimation problem is the determination of the continuous estimate of  $x$ ,  $\hat{x}$ , or the sequence of estimates of  $x_k$ ,  $\hat{x}_k$ , from measurements  $y$  or  $y_k$ , respectively. The estimate  $\hat{x}$  is obtained from Eqs. (3.1) and (3.2) as

$$\dot{\hat{x}} = F\hat{x} + PH^T R^{-1}(y - H\hat{x}) \quad , \quad \hat{x}(0) = \bar{x} \text{ given} \quad (3.5)$$

$$\dot{P} = FP + PF^T - PH^T R^{-1}HP + \Gamma Q \Gamma^T, \quad P(0) \text{ assumed} \quad (3.6)$$

and the estimate  $\hat{x}_k$  from Eqs. (3.3) and (3.4) as

$$\hat{x}_k = \phi \hat{x}_{k-1} + P_k H_k^T R^{-1} (y_k - H \phi \hat{x}_{k-1}),$$

$$\hat{x}_0 = \bar{x}_0, \text{ given} \quad (3.7)$$

$$P_k = [(\phi P_{k-1} \phi^T + \Gamma Q \Gamma^T)^{-1} + H_k^T R^{-1} H_k]^{-1},$$

$$P(0) \text{ assumed} \quad (3.8)$$

The following characteristics are apparent from these equations:

- (1) The filter is initialized with estimates of the initial state  $\hat{x}(0)$  and state error covariance,  $P(0)$ . In general, these initializations must be assumed.
- (2) Estimates of the process and measurement noise statistics,  $Q$  and  $R$ , must be provided to the algorithm. These statistics must be estimated a priori (or at least by a modification of the algorithms described by Eqs. (3.1)-(3.4)).

The quantity  $PH^T R^{-1}$  is denoted as the Kalman gain,  $K$ ,

$$K = PH^T R^{-1} \quad (3.9)$$

and is explicitly dependent on  $R$  and on  $Q$  (Eqs. (3.6), (3.8)).

- (3) The following special cases may be identified from the discrete algorithm equations, (3.7) and (3.8).

(a)  $\phi$  known,  $Q$  is finite

This corresponds to the case shown in Eqs. (3.7) and (3.8).

(b)  $\phi$  is unity,  $Q$  is finite

Equations (7) and (8) become

$$\hat{x}_k = \hat{x}_{k-1} + K_k (y_k - H_k \hat{x}_{k-1}) \quad (3.10)$$

$$P_k = [(P_{k-1} + \Gamma Q \Gamma^T)^{-1} + H^T R^{-1} H]^{-1} \quad (3.11)$$

which represents a fitting process for a process where the value of the state at time,  $K$ ,  $x_k$ , is related to the value at time  $k-1$ ,  $x_{k-1}$ , within the standard deviation associated with  $Q$ . Note that this implies no knowledge of the deterministic dependence of  $x_k$  on  $x_{k-1}$ . As  $Q$  increases, the information provided to  $x_k$  by knowledge of  $x_{k-1}$  decreases. This type of representation is denoted as a random walk model.

(c)  $\phi$  is unity,  $Q$  approaches infinity (e.g., large)

Equations (3.10) and (3.11) become

$$\hat{x}_k = (H^T R^{-1} H)^{-1} H^T R^{-1} y_k \quad (3.12)$$

$$P_k = (H^T R^{-1} H)^{-1} \quad (3.13)$$

which corresponds to the well known least square single point estimate of  $x_k$  given the measurement  $y_k$ , and is independent of estimates  $\hat{x}_{k-1}$ , etc.

These considerations are relevant to selection of the a priori assumptions on  $Q$ . Similar conclusions are appropriate for the continuous equations (3.3)-(3.4).

Smoothing.- The estimation algorithms of the last subsection yield an estimate, at any time  $t$ , of the state,  $x(t)$ , based on measurements  $y(t)$ , up to and including time  $t$ . One would expect, however, that the accuracy of such point estimates could be increased if, in addition to the past data up to  $t$ , future data from  $t$  to  $T$  could also be incorporated. In the context of sequential estimation approaches (as opposed to a batch estimation wherein all data are simultaneously processed), smoothing is the generic

operation for using future data to improve intermediate time estimate accuracy. The Kalman filter estimation algorithm can achieve this by processing the data forward until the last data point. The filter and smoother estimates are then identical because they have the same information available. Reverse smoothing then consists of stepping back from the last measurement and forming the smoothed estimate by adding a correction term to the forward filter estimates.

The process of stepping back through the data can be shown [10] to not only reduce the uncertainty in the state estimate, but also provide an estimate of the uncertainty in the state (e.g., process noise). These characteristics then lead to specific modes of smoother operation denoted as fixed point smoothing and fixed interval smoothing. Fixed point smoothing is the mode in which the accuracy of a specific point estimate is improved. In particular, the initial condition estimate of state and its error covariance are improved based on all the data. Fixed interval smoothing is the use of data over an interval to provide improvements to the estimates of the measurement noise statistics and the process noise statistics.

It should be noted that smoothing type of iterations can be performed over any span of data. Hence, local, iterated smoothing is frequently used for improving estimates of states whose actual transition dynamics are nonlinear.

The smoothing operation on data in a nontrivial computational problem; the filter requires the storage of estimates and covariances of, at most, two successive data points. The smoothing solution requires that these estimates and covariances be retained for all data points. Further, the backward propagation of the filter may, for a system whose transition matrix is stable, become unstable (depending on data rate). Such a combination of high computer storage requirements and possible numerical instabilities has resulted in few examples of useful filter/smoother implementations.

### Rotorcraft State Estimation Algorithm

The high dimensionality of rotorcraft state estimation requires a highly systematic integration of the filter/smoother characteristics discussed in the last section. The DEKFIS program utilizes a Friedland-Duffy extended Kalman filter with a locally iterated smoothing algorithm to provide the filter estimates. An additional fixed interval



smoothing algorithm can be used to estimate the gusts (i.e., process noise) and provide smoothed estimates. This section details the specific organization of the rotorcraft state estimation algorithms.

Structure of model and filter/smoothener.- The fundamental rotorcraft sensor model consists of two types of elements in the filter state vector. These are the time-varying states of the vehicle dynamic model and "constant states" associated with sensor biases. (These constant states will therefore be referenced as biases.) The general filter model will therefore be of the form

$$\dot{x}_1(t) = f(x_1, x_2, u, t) + \Gamma(t)w(t) \quad , \quad x_1(0) = x_{1_0} \quad (3.14)$$

$$\dot{x}_2(t) = 0 \quad , \quad x_2(0) = b_0 \quad (3.15)$$

with measurements

$$y(t) = h(x_1, x_2, u, t) + v(t) \quad (3.16)$$

where  $x_{1_0}$  is the dynamic state initial condition and  $b_0$  is the a priori estimate of bias, and noise statistics

$$E\{w(t)\} = \bar{w}(t)$$

$$E\{[w(t) - \bar{w}(t)][w(\tau) - \bar{w}(\tau)]^T\} = Q(t)\delta(t - \tau)$$

$$E\{v(t)\} = \bar{v}(t)$$

$$E\{[v(t) - \bar{v}(t)][v(\tau) - \bar{v}(\tau)]^T\} = R(t)\delta(t - \tau)$$

Equations (3.14) and (3.16) are nonlinear and must be linearized in order to satisfy the linearity requirement of the Kalman filter solution. These linearized equations are of the form

$$\dot{x}_1 = Fx_1 + Bx_2 + Gu + \Gamma w \quad (3.17)$$

$$\dot{x}_2 = 0 \quad (3.18)$$

$$y = Hx_1 + Cx_2 + Du + v \quad (3.19)$$

where

$$F \triangleq \frac{\partial f}{\partial x_1}$$

$$B \triangleq \frac{\partial f}{\partial x_2}$$

$$G \triangleq \frac{\partial f}{\partial u}$$

$$H \triangleq \frac{\partial h}{\partial x_1}$$

$$C \triangleq \frac{\partial h}{\partial x_2}$$

$$D \triangleq \frac{\partial h}{\partial u}$$

Using the Friedland-Duffy approach, the filter equations can be written as sets of bias-free filter equations for the primary states and bias filter equations for the bias states.

Bias-Free Filter Equations:

$$\tilde{M}_i = (\tilde{\Phi} \tilde{P} \tilde{\Phi}^T + \Gamma_D Q \Gamma_D^T)_{i-1} \quad (3.20)$$

$$\bar{x}_i = \int_{t_{i-1}}^{t_i} f(\hat{x}_{i-1}, b_{i-1}, u_{i-1}, t_{i-1}) dt + \hat{x}_{i-1} \quad (3.21)$$

$$\tilde{W}_i = (H \tilde{M}_i H^T + R)_i \quad (3.22)$$

$$K_{x_i} = (\tilde{M}_i H^T \tilde{W}_i^{-1})_i \quad (3.23)$$

$$\tilde{P}_i = [I - K_{x_i} H]_i \tilde{M}_i \quad (3.24)$$

$$v_i = y_i - h(\bar{x}_i, 0, u_i, t_i) \quad (3.25)$$

$$\hat{x}_i = \bar{x}_i + K_{x_i} v_i \quad (3.26)$$

where  $\Phi = \exp\{F\Delta T\}$

$$\Gamma_D = F^{-1}(\Phi - I)\Gamma$$

Bias Filter Equations:

$$U_i = \phi_{i-1} V_{i-1} + F_{i-1}^{-1} \{ \phi_{i-1} - I \} B_{i-1} \quad (3.27)$$

$$S_i = H_i U_i + C_i \quad (3.28)$$

$$V_i = U_i - K_{X_i} S_i \quad (3.29)$$

$$\hat{W}_i = \tilde{W}_i + S_i P_{b_{i-1}} S_i^T \quad (3.30)$$

$$K_{b_i} = P_{b_{i-1}} S_i^T \hat{W}_i^{-1} \quad (3.31)$$

$$P_{b_i} = [I - K_b \ S_i] P_{b_{i-1}} \quad (3.32)$$

$$\hat{b}_i = \hat{b}_{i-1} + K_{b_i} (v_i - S_i \hat{b}_{i-1}) \quad (3.33)$$

Note that the primary state estimate at the  $i^{\text{th}}$  time point is denoted by  $\hat{x}_i$  and the secondary state (or bias) estimate is denoted by  $\hat{b}_i$ . The bias filter also utilizes  $K_{X_i}$ ,  $\hat{W}_i$  and  $v_i$  which are computed in the bias-free filter. These two sets are fully coupled by the composite state update which corrects the bias-free state estimate for the effects of the bias.

Composite State and Covariance Update:

$$\hat{x}_i^C = \begin{bmatrix} I & V_i \\ 0 & I \end{bmatrix} \begin{bmatrix} \hat{x}_i \\ \hat{b}_i \end{bmatrix} \quad (3.34)$$

$$P_i^C = \begin{bmatrix} P_x & P_{xb} \\ P_{xb}^T & P_b \end{bmatrix}_i \quad (3.35)$$

$$P_x = \tilde{P}_i + V_i P_{b_i} V_i^T \quad (3.36)$$

$$P_{xb_i} = V_i P_{b_i} \quad (3.37)$$

For the local smoothing options, it is possible to iterate on either the bias-free state estimates and/or the composite state filter estimates.

Bias-Free Local Smoothing:

$$\hat{x}_{i-1|i} = \hat{x}_{i-1} + \tilde{P}_{i-1} \phi_{i-1}^T [I - K_X H]_i^T H_i^T R^{-1} v_i \quad (3.38)$$

Composite State Local Smoothing:

$$\hat{x}_{i-1|i}^C = \hat{x}_{i-1}^C + P_{i-1}^C \phi_{i-1}^C \left\{ I - \begin{bmatrix} K_X \\ - \\ K_b \end{bmatrix} [H \ C] \right\}_i^T \begin{bmatrix} H^T \\ C^T \end{bmatrix}_i R^{-1} v_i \quad (3.39)$$

where

$$\phi^C = \begin{bmatrix} \phi & F^{-1}\{\phi - I\}B \\ 0 & I \end{bmatrix} \quad (3.40)$$

The fixed interval smoothing equations are used when the filter estimates are inadequate. These equations are necessary when some states are driven by process noise (i.e., gust states) and it is necessary to estimate this process noise. A further benefit of fixed interval smoothing is that smoothing estimates are computed for all the primary states. These equations are shown below.

Fixed Interval Smoothing:

$$(1) \hat{x}_i|N = \hat{x}_i - P_i \phi_i^T \lambda_i \quad (3.41)$$

$$(2) \hat{w}_i|N = \bar{w}_i - Q_i \Gamma_i^T \lambda_i \quad (3.42)$$

$$\lambda_{i-1} = (I - P_i H_i^T R_i^{-1} H_i)^T [\phi_i^T \lambda_i - H_i^T R_i^{-1} (z_i - H_i \bar{x}_i)], \lambda_N = 0 \quad (3.43)$$

Note that  $\bar{x}_i$  is the estimate from the bias-free (forward) filter. Using the above equations, it is possible to estimate the process and measurement noise covariance by:

$$\hat{R} = \frac{1}{N-1} \sum_{i=1}^N v_i v_i^T \quad (3.44)$$

These equations are implemented in the filter/smoothing algorithm, which is initialized with a priori estimates of  $x_0$ ,  $P_0$ ,  $Q$  and  $R$ . Figure 3.1 depicts the overall structure of the filter/smoothing, indicating the basic sequence of filtering, fixed-point smoothing, and fixed interval smoothing.

Rotorcraft State Estimation Program. The filter/smoothing algorithm of Figure 3.1 is used with different rotorcraft models. The reason for some decomposition of the rotorcraft model is basically computational; simultaneous quantification of all vehicle dynamic and measurement system equations with a Kalman filter is simply beyond the memory capability of existing computers (for a given finite execution time limitation). The model decomposition is based on the principal objectives of an overall rotorcraft filtering approach.

For this effort, the objective is to provide state estimates and sensor error coefficient estimates for use by subsequent parameter identification software. The specific models (to be included in the filter) which result to achieve this objective are as follows:

- (1) Fuselage/gust estimation to estimate the rigid body translational and rotational states, errors of the associated on-board and off-board sensor model, and gust statistics.
- (2) Rotor state estimator to estimate the rotor flapping and lead-lag states.
- (3) Force and moment static estimator to estimate the distribution of forces and moments from load cell sensors. (This estimator is denoted as the RSRA estimator because its principal application is to the Rotor Systems Research Aircraft.)

Table 3.1 summarizes the resulting filter/smoothing options, and their applications.

Figure 3.2 illustrates the basic integration logic for the three filter models in order to meet the application requirements of Table 3.1. Detailed models for each of these options will now be presented.

Fuselage/gust estimator equations.- The state and measurement vectors for the fuselage/gust estimator are shown in Table 3.2. The user of DEKFIS has the option of choosing which states (and, hence, which equations are to be

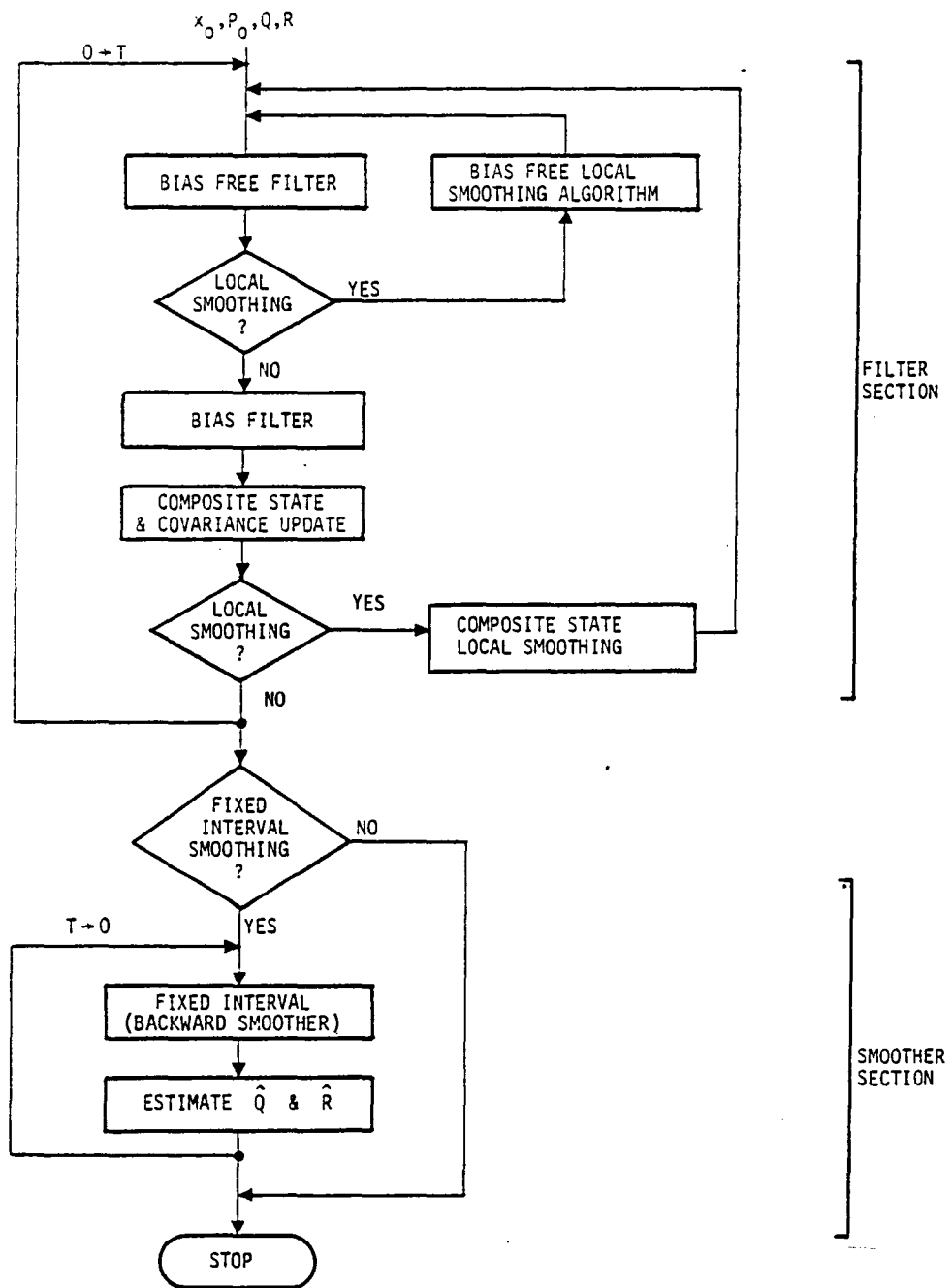


FIGURE 3.1. - STRUCTURE OF DEKFIS.

TABLE 3.1. - FILTER/SMOOTHER EQUATION OF MOTION OPTIONS

	FUSELAGE/GUST ESTIMATOR	ROTOR STATE ESTIMATOR	RSRA ESTIMATOR
Single Rotor Helicopter	✓	✓	
Multi-rotor Helicopter	✓	Repeat for each rotor	
RSRA-Fixed Wing Configuration	✓		✓
RSRA-Compound Configuration	✓	✓	✓
Whirl Stand Data		✓	

integrated), which measurements and which process noise sources are to be used for a particular problem.

The  $\underline{x}_1$  vector is of size  $25 \times 1$  and contains the primary states for the fuselage/gust estimator. These are: the aircraft attitudes - Euler angles  $\phi$ ,  $\theta$ ,  $\psi$ ; the aircraft inertial velocities in the aircraft body axis -  $v_x$ ,  $v_y$ ,  $v_z$ ; the fuselage angular rates -  $p$ ,  $q$ ,  $r$ ; the linear accelerometer indicated acceleration -  $a_{x_I}$ ,  $a_{y_I}$ ,  $a_{z_I}$  (this differs from the actual linear acceleration by a first order lag associated with measuring that acceleration); the angular accelerometer indicated acceleration -  $\dot{p}_I$ ,  $\dot{q}_I$ ,  $\dot{r}_I$  (likewise lagged); gust velocities in an inertial north, east, vertical frame -  $V_{g_N}$ ,  $V_{g_E}$ ,  $V_{g_V}$ ; and the aircraft position in an inertial north, east, vertical frame -  $X_N$ ,  $Y_E$ ,  $Z_V$

The  $\underline{y}$  vector is of size  $24 \times 1$  and contains the measurements for the fuselage/gust estimator. These are: the aircraft attitudes -  $\phi_m$ ,  $\theta_m$ ,  $\psi_m$ ; the airspeed in the aircraft body axis -  $v_{x_m}$ ,  $v_{y_m}$ ,  $v_{z_m}$  (or either alternately or redundantly as  $V_m$ ,  $\beta_m$ ,  $\alpha_m$  measurements); the aircraft angular

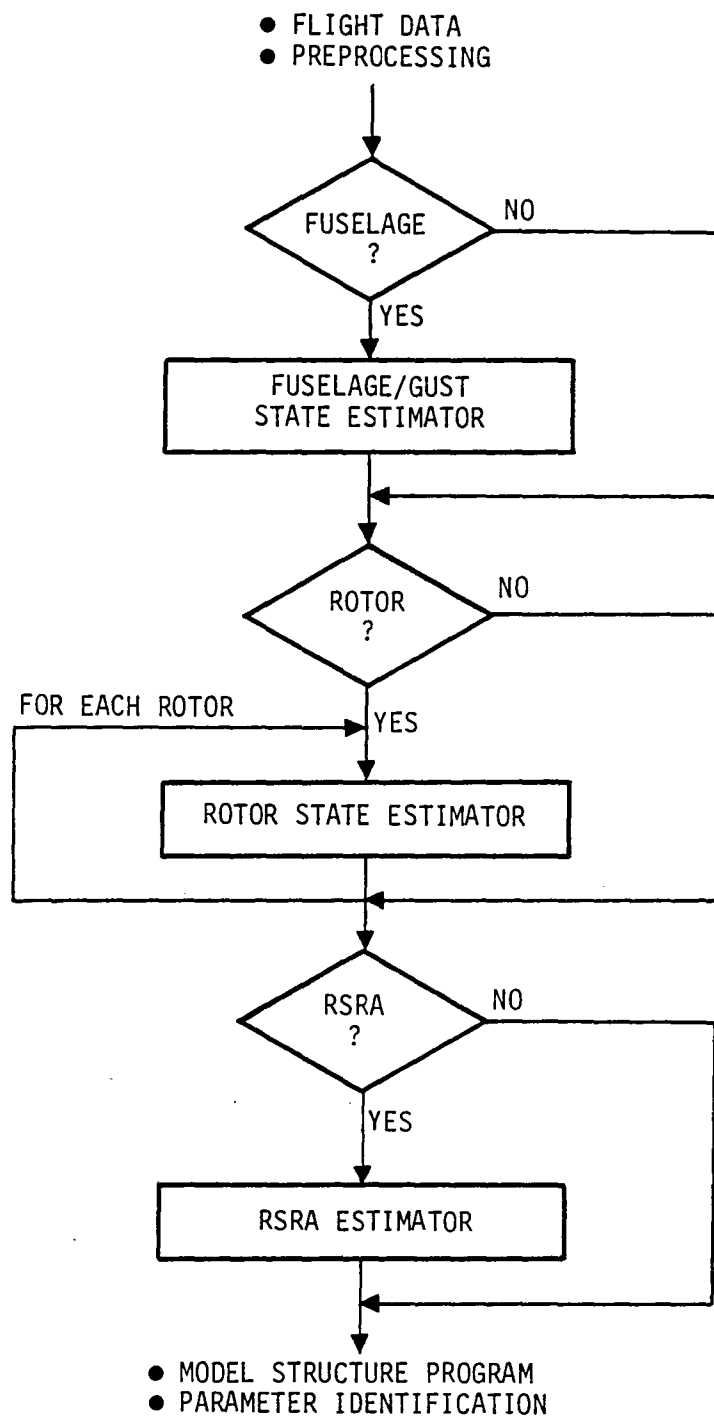


FIGURE 3.2. — FLOWCHART AND OPTIONS OF STATE ESTIMATOR



TABLE 3.2.—FUSELAGE/GUST ESTIMATOR VECTOR DEFINITIONS

		cont'd				
$\underline{x}_1 =$ 25x1	$\begin{bmatrix} \phi \\ \theta \\ \psi \\ v_x \\ v_y \\ v_z \\ p \\ q \\ r \\ a_{xI} \\ a_{yI} \\ a_{zI} \\ \dot{p}_I \\ \dot{q}_I \\ \dot{r}_I \\ v_{GN} \\ v_{GE} \\ v_{GV} \\ x_N \\ y_E \\ z_V \\ \text{dummy} \\ \text{dummy} \\ \text{dummy} \\ \text{dummy} \end{bmatrix}$	$\underline{x}_2 =$ 50x1	$\begin{bmatrix} b_\phi \\ b_\theta \\ b_\psi \\ b_{vx} \\ b_{vy} \\ b_{vz} \\ b_p \\ b_q \\ b_r \\ b_{axI} \\ b_{ayI} \\ b_{azI} \\ b_{\dot{p}I} \\ b_{\dot{q}I} \\ b_{\dot{r}I} \\ b_{xN} \\ b_{yE} \\ b_{zV} \\ b_v \\ b_\beta \\ b_\alpha \\ b_R \\ b_{\beta R} \\ b_{\alpha R} \\ k_\phi \end{bmatrix}$	$\begin{bmatrix} k_\theta \\ k_\psi \\ k_{vx} \\ k_{vy} \\ k_{vz} \\ k_p \\ k_q \\ k_r \\ k_{axI} \\ k_{ayI} \\ k_{azI} \\ k_{\dot{p}I} \\ k_{\dot{q}I} \\ k_{\dot{r}I} \\ k_{xN} \\ k_{yE} \\ k_{zV} \\ k_v \\ k_\beta \\ k_\alpha \\ k_R \\ k_{\beta R} \\ k_{\alpha R} \\ \text{dummy} \\ \text{dummy} \end{bmatrix}$	$\underline{z} =$ 24x1	$\begin{bmatrix} \phi_m \\ \theta_m \\ \psi_m \\ v_{xm} \\ v_{ym} \\ v_{zm} \\ p_m \\ q_m \\ r_m \\ a_{xIm} \\ a_{yIm} \\ a_{zIm} \\ \dot{p}_{Im} \\ \dot{q}_{Im} \\ \dot{r}_{Im} \\ x_{Nm} \\ y_{Em} \\ z_{Vm} \\ v_m \\ \beta_m \\ \alpha_m \\ R_m \\ \beta_{Rm} \\ \alpha_{Rm} \end{bmatrix}$
$\underline{w} =$ 9x1	$\begin{bmatrix} w_1 \\ w_2 \\ w_3 \\ w_4 \\ w_5 \\ w_6 \\ w_7 \\ w_8 \\ w_9 \end{bmatrix}$			$\underline{v} =$ 24x1	$\begin{bmatrix} v_1 \\ v_2 \\ \cdot \\ v_{24} \end{bmatrix}$	

rates -  $p_m, q_m, r_m$ ; the linear accelerometer measurements -  $a_{x_{I_m}}, a_{y_{I_m}}, a_{z_{I_m}}$ ; the angular accelerometer measurements -  $\dot{p}_{I_m}, \dot{q}_{I_m}, \dot{r}_{I_m}$ ; and radar position measurements in an inertial north, east, vertical frame -  $X_{N_m}, Y_{E_m}, Z_{V_m}$  (or alternately  $R_m, \beta_{R_m}, \alpha_{R_m}$ ).

The  $x_2$  vector is of size  $50 \times 1$  and contains the biases (i.e.,  $b_i$ 's) and scale factors (i.e.,  $k_i$ 's) for each of the measurements.

The  $w$  vector is a  $9 \times 1$  process noise vector. This process noise drives the linear accelerations -  $w_1, w_2, w_3$ ; the angular accelerations -  $w_4, w_5, w_6$ ; and the gusts -  $w_1, w_2, w_3$ .

The  $v$  vector is a  $24 \times 1$  measurement noise vector each element of which corrupts one of the aforementioned measurements.

The nonlinear fuselage/gust equations are presented below.

Primary State Equations:

$$\dot{\phi} = p + (r \cos\phi + q \sin\phi) \tan\theta$$

$$\dot{\theta} = q \cos\phi - r \sin\phi$$

$$\dot{\psi} = (r \cos\phi + q \sin\phi) / \cos\theta$$

$$\begin{aligned} \dot{v}_x = & v_y r - v_z q - g \sin\theta + g \sin\theta(o) + w_1 - w_5 l_{z_1} + w_6 l_{y_1} \\ & + (q^2 + r^2) l_{x_1} - q p l_{y_1} - r p l_{z_1} \end{aligned}$$

$$\begin{aligned} \dot{v}_y = & v_z p - v_x r + g \sin\phi \cos\theta - g \sin\phi(o) \cos\theta(o) + w_2 - w_6 l_{x_2} \\ & + w_4 l_{z_2} - p q l_{x_2} + (p^2 + r^2) l_{y_2} - r q l_{z_2} \end{aligned}$$

$$\begin{aligned} \dot{v}_z = & v_x q - v_y p + g \cos\phi \cos\theta - g \cos\phi(o) \cos\theta(o) \\ & + w_3 - w_4 l_{y_3} + w_5 l_{x_3} - p r l_{x_3} - q r l_{y_3} + (p^2 + r^2) l_{z_3} \end{aligned}$$

$$\dot{p} = w_4$$

$$\dot{q} = w_5$$

$$\dot{r} = w_6$$

$$\dot{a}_{x_I} = \alpha_1 a_{x_I} - \alpha_1 w_1$$

$$\dot{a}_{y_I} = \alpha_2 a_{y_I} - \alpha_2 w_2$$

$$\dot{a}_{z_I} = \alpha_3 a_{z_I} - \alpha_3 w_3$$

$$\ddot{p}_I = \alpha_4 \dot{p}_I - \alpha_4 w_4$$

$$\ddot{q}_I = \alpha_5 \dot{q}_I - \alpha_5 w_5$$

$$\ddot{r}_I = \alpha_6 \dot{r}_I - \alpha_6 w_6$$

$$\dot{V}_{g_N} = \alpha_7 V_{g_N} - \alpha_7 w_7$$

$$\dot{V}_{g_E} = \alpha_8 V_{g_E} - \alpha_8 w_8$$

$$\dot{V}_{g_V} = \alpha_9 V_{g_V} - \alpha_9 w_9$$

$$\begin{aligned} \dot{X}_N &= v_x \cos\theta \cos\psi + v_y \sin\theta \sin\phi \cos\psi - v_y \cos\phi \sin\psi \\ &\quad + v_z \sin\theta \cos\phi \cos\psi + v_z \sin\phi \sin\psi \end{aligned}$$

$$\begin{aligned} \dot{Y}_E &= v_x \cos\theta \sin\psi + v_y \sin\theta \sin\phi \sin\psi + v_y \cos\phi \cos\psi \\ &\quad + v_z \sin\theta \cos\phi \sin\psi - v_z \sin\phi \cos\psi \end{aligned}$$

$$\dot{Z}_V = -v_x \sin\theta + v_y \cos\theta \sin\phi + v_z \cos\theta \cos\phi$$

Secondary State Equations:

$$\dot{\underline{x}}_2 = \underline{0}$$

Measurement Equations:

$$\phi_m = k_\phi \phi + b_\phi + n_1$$

$$\theta_m = k_\theta \theta + b_\theta + n_2$$

$$\psi_m = k_\psi \psi + b_\psi + n_z$$

$$v_{x_m} = k_{v_x} (v_x + v_{x_g}) + b_{v_x} + n_4$$

$$v_{y_m} = k_{v_y} (v_y + v_{y_g}) + b_{v_y} + n_5$$

$$v_{z_m} = k_{v_z} (v_z + v_{z_g}) + b_{v_z} + n_6$$

$$p_m = k_p p + b_p + n_7$$

$$q_m = k_q q + b_q + n_8$$

$$r_m = k_r r + b_r + n_9$$

$$a_{x_{I_m}} = k_{a_{x_I}} (a_{x_I} + g \sin\theta(o)) + b_{a_{x_I}} + n_{10}$$

$$a_{y_{I_m}} = k_{a_{y_I}} (a_{y_I} - g \sin\phi(o) \cos\theta(o)) + b_{a_{y_I}} + n_{11}$$

$$a_{z_{I_m}} = k_{a_{z_I}} (a_{z_I} - g \cos\phi(o) \cos\theta(o)) + b_{a_{z_I}} + n_{12}$$

$$(\dot{p}_I)_m = k_{\dot{p}_I} \dot{p}_I + b_{\dot{p}_I} + n_{13}$$

$$(\dot{q}_I)_m = k_{\dot{q}_I} \dot{q}_I + b_{\dot{q}_I} + n_{14}$$

$$(\dot{r}_I)_m = k_{\dot{r}_I} \dot{r}_I + b_{\dot{r}_I} + n_{15}$$

$$X_{N_m} = k_{X_N} X_N + b_{X_N} + n_{16}$$

$$Y_{E_m} = k_{Y_E} Y_E + b_{Y_E} + n_{17}$$

$$Z_{V_m} = k_{Z_V} Z_V + b_{Z_V} + n_{18}$$

$$V_m = k_V \left( (v_x + v_{x_g} + q \ell_{z_4} - r \ell_{y_4})^2 + (v_y + v_{y_g} + r \ell_{x_4} - p \ell_{z_4})^2 + (v_z + v_{z_g} + p \ell_{y_4} - q \ell_{x_4})^2 \right)^{\frac{1}{2}} + b_V + n_{19}$$

$$\beta_m = k_\beta \tan^{-1} \left( (v_y + v_{y_g} + r \ell_{x_5} - p \ell_{z_5}) / (v_x + v_{x_g} + q \ell_{z_5} - r \ell_{y_5}) \right) + b_\beta + n_{20}$$

$$\alpha_m = k_\alpha \tan^{-1} \left( (v_z + v_{z_g} + p \ell_{y_6} - q \ell_{x_6}) / (v_x + v_{x_g} + q \ell_{z_6} - r \ell_{y_6}) \right) + b_\alpha + n_{21}$$

$$R_m = k_R (X_N^2 + Y_E^2 + Z_V^2)^{\frac{1}{2}} + b_R + n_{22}$$

$$\beta_{R_m} = k_{\beta_R} \tan^{-1} \left( -Z_V / (X_N^2 + Y_E^2)^{\frac{1}{2}} \right) + b_{\beta_R} + n_{23}$$

$$\alpha_{R_m} = k_{\alpha_R} \tan^{-1} (-Y_E / X_N) + b_{\alpha_R} + n_{24}$$

where,

$$v_{x_g} = (V_{g_N} + V_{w_N}) \cos \theta \cos \psi + (V_{g_E} + V_{w_E}) \cos \theta \sin \psi - (V_{g_V} + V_{w_V}) \sin \theta$$

$$v_{y_g} = (V_{g_N} + V_{w_N}) \sin \theta \sin \phi \cos \psi - (V_{g_N} + V_{w_N}) \cos \phi \sin \psi + (V_{g_E} + V_{w_E}) \sin \theta \sin \phi \sin \psi + (V_{g_E} + V_{w_E}) \cos \phi \cos \psi + (V_{g_V} + V_{w_V}) \cos \theta \sin \phi$$

$$v_{z_g} = (V_{g_N} + V_{w_N}) \sin \theta \cos \phi \cos \psi + (V_{g_N} + V_{w_N}) \sin \phi \sin \psi + (V_{g_E} + V_{w_E}) \sin \theta \cos \phi \sin \psi - (V_{g_E} + V_{w_E}) \sin \phi \cos \psi + (V_{g_V} + V_{w_V}) \cos \theta \cos \phi$$

The parameters used in these equations are defined in the fuselage/gust estimator parameter list shown in Table 3.3.

TABLE 3.3. - FUSELAGE/GUST ESTIMATOR-PARAMETER LIST

PARAMETER INDEX	PARAMETER DESCRIPTION
1-25	$x_1$ ic's (use uncompressed vector)
26-75	$x_2$ ic's (use uncompressed vector)
76	$l_{x1}$ } $a_x$ accelerometer location, ft (relative to c.g.)
77	$l_{y1}$ }
78	$l_{z1}$ }
79	$l_{x2}$ } $a_y$ accelerometer location, ft
80	$l_{y2}$ }
81	$l_{z2}$ }
82	$l_{x3}$ } $a_z$ accelerometer location, ft
83	$l_{y3}$ }
84	$l_{z3}$ }
85	$l_{x4}$ } V probe location, ft
86	$l_{y4}$ }
87	$l_{z4}$ }
88	$l_{x5}$ } $\beta$ vane location, ft
89	$l_{y5}$ }
90	$l_{z5}$ }
91	$l_{x6}$ } $\alpha$ vane location, ft
92	$l_{y6}$ }
93	$l_{z6}$ }
94	$\alpha_1$ } accelerometer time constants
95	$\alpha_2$ }
96	$\alpha_3$ }
97	$\alpha_4$ }
98	$\alpha_5$ }
99	$\alpha_6$ }
100	$\alpha_7$ } gust power spectral time constants
101	$\alpha_8$ }
102	$\alpha_9$ }
103	$V_{WN}$ } steady gust components (wind)
104	$V_{WE}$ }
105	$V_{WV}$ }

Rotor state estimator equations.- The state and measurement equations for the rotor state estimator are shown in Table 3.4. As in the previous estimator, the user has the option to flag which states, measurements and process noise sources he wants to use.

The  $\underline{x}_1$  vector is a 14x1 vector of primary states used in the rotor state estimator. These are: rotor coning angle -  $\beta_0$ ; rotor longitudinal flapping -  $\beta_{1C}$ ; rotor lateral flapping -  $\beta_{1S}$ ; similar fixed system coordinates for the rotor lagging motion -  $\zeta_0$ ,  $\zeta_{1C}$ ,  $\zeta_{1S}$ ; rotor azimuth angle -  $\psi_R$ ; and the time derivatives of each of these -  $\dot{\beta}_0$ ,  $\dot{\beta}_{1C}$ ,  $\dot{\beta}_{1S}$ ,  $\dot{\zeta}_0$ ,  $\dot{\zeta}_{1C}$ ,  $\dot{\zeta}_{1S}$ , and  $\dot{\psi}_R$ .

The  $\underline{y}$  vector is 13x1 vector of measurements for the rotor state estimator. These are: the individual blade flapping angles  $\beta_{i_m}$ ,  $i=1,6$ ; the individual blade lagging angles  $\zeta_{i_m}$ ,  $i=1,6$ ; and the cosine of rotor azimuth -  $\cos\psi_{R_m}$ .

The  $\underline{x}_2$  vector is a 26x1 vector of biases and scale factors for each of the aforementioned measurements.

The  $\underline{w}$  vector is a 7x1 vector of process noise sources each driving one of the seven rotor degrees of freedom modeled.

The  $\underline{v}$  vector is a 13x1 vector of measurement noises each corrupting one of the 13 measurements.

The state and measurement equations for the rotor state estimator are presented below.

Primary State Equations:

$$\dot{\underline{x}}_1 = \underline{F} \underline{x}_1 + \underline{\Gamma} \underline{w}$$

TABLE 3.4— ROTOR STATE ESTIMATOR VECTOR DEFINITIONS

$\underline{x}_1 =$ 14x1	$\begin{bmatrix} \beta_0 \\ \beta_1c \\ \beta_1s \\ 0 \\ \zeta_1c \\ \zeta_1s \\ \psi_R \\ 0 \\ 0 \\ 0 \\ 0 \\ 0 \\ 0 \\ 0 \\ \psi_R \end{bmatrix}$	$\underline{x}_2 =$ 26x1	$\begin{bmatrix} b\beta_1 \\ b\beta_2 \\ b\beta_3 \\ b\beta_4 \\ b\beta_5 \\ b\beta_6 \\ b\zeta_1 \\ b\zeta_2 \\ b\zeta_3 \\ b\zeta_4 \\ b\zeta_5 \\ b\zeta_6 \\ b\cos\psi_R \\ k\beta_1 \\ k\beta_2 \\ k\beta_3 \\ k\beta_4 \\ k\beta_5 \\ k\beta_6 \\ k\zeta_1 \\ k\zeta_2 \\ k\zeta_3 \\ k\zeta_4 \\ k\zeta_5 \\ k\zeta_6 \\ k\cos\psi_R \end{bmatrix}$	$\underline{y} =$ 13x1	$\begin{bmatrix} \beta_{1m} \\ \beta_{2m} \\ \beta_{3m} \\ \beta_{4m} \\ \beta_{5m} \\ \beta_{6m} \\ \zeta_{1m} \\ \zeta_{2m} \\ \zeta_{3m} \\ \zeta_{4m} \\ \zeta_{5m} \\ \zeta_{6m} \\ \cos \psi_{Rm} \end{bmatrix}$
				$\underline{v} =$ 13x1	$\begin{bmatrix} n_1 \\ n_2 \\ n_{13} \\ \vdots \\ \vdots \\ n_{13} \end{bmatrix}$
$\underline{w} =$ 7x1	$\begin{bmatrix} w_1 \\ w_2 \\ w_3 \\ w_4 \\ w_5 \\ w_6 \\ w_7 \end{bmatrix}$				



where

$$\underline{\underline{F}} = \begin{array}{c} \begin{array}{cccccc} & & 1.0 & & & \\ & & & 1.0 & & \\ & & & & 1.0 & \\ & & & & & 1.0 \\ & & & & & & 1.0 \\ & & & & & & & 1.0 \\ \underline{\underline{0}} & & & & & & & \end{array} \\ \hline \begin{array}{cccccc} & & & & & \\ & & & & & \\ & & & & & \\ & & & & & \\ & & & & & \\ & & & & & \\ \underline{\underline{0}} & & & & & \underline{\underline{0}} \end{array} \end{array}, \underline{\underline{\Gamma}} = \begin{array}{c} \begin{array}{cccccc} & & & & & \\ & & & & & \\ & & & & & \\ & & & & & \\ & & & & & \\ & & & & & \\ \underline{\underline{0}} & & & & & \end{array} \\ \hline \begin{array}{cccccc} 1.0 & & & & & \\ & 1.0 & & & & \\ & & 1.0 & & & \\ & & & 1.0 & & \\ & & & & 1.0 & \\ & & & & & 1.0 \\ & & & & & & 1.0 \\ & & & & & & & 1.0 \end{array} \end{array}$$

Secondary State Equations:

$$\dot{\underline{x}}_2 = \underline{0}$$

Measurement Equations:

$$\begin{aligned} \beta_{1_m} &= k_{\beta_1} (\beta_o - \beta_{1C} \cos(\psi_R + \phi_1) - \beta_{1S} \sin(\psi_R + \phi_1)) + b_{\beta_1} + n_1 \\ \vdots \\ \beta_{i_m} &= k_{\beta_i} (\beta_o - \beta_{1C} \cos(\psi_R + \phi_i) - \beta_{1S} \sin(\psi_R + \phi_i)) + b_{\beta_i} + n_i \\ \vdots \\ \beta_{6_m} &= k_{\beta_6} (\beta_o - \beta_{1C} \cos(\psi_R + \phi_6) - \beta_{1S} \sin(\psi_R + \phi_6)) + b_{\beta_6} + n_6 \\ \zeta_{1_m} &= k_{\zeta_1} (\zeta_o - \zeta_{1C} \cos(\psi_R + \theta_1) - \zeta_{1S} \sin(\psi_R + \theta_1)) + b_{\zeta_1} + n_7 \\ \vdots \\ \zeta_{i_m} &= k_{\zeta_i} (\zeta_o - \zeta_{1C} \cos(\psi_R + \theta_i) - \zeta_{1S} \sin(\psi_R + \theta_i)) + b_{\zeta_i} + n_{i+6} \\ \vdots \\ \zeta_{6_m} &= k_{\zeta_6} (\zeta_o - \zeta_{1C} \cos(\psi_R + \theta_6) - \zeta_{1S} \sin(\psi_R + \theta_6)) + b_{\zeta_6} + n_{12} \\ \cos \psi_{R_m} &= k_{\cos \psi_R} \cos(\psi_R) + b_{\cos \psi_R} + n_{13} \end{aligned}$$

The parameters used in these equations are defined in the rotor state estimator parameter list shown in Table 3.5.

TABLE 3.5. - ROTOR STATE ESTIMATOR PARAMETER LIST

Parameter	Description
$\phi_1$ $\phi_2$ $\phi_3$ $\phi_4$ $\phi_5$ $\phi_6$	Blade flapping measurement phase angles, rad.
$\theta_1$ $\theta_2$ $\theta_3$ $\theta_4$ $\theta_5$ $\theta_6$	Blade lagging measurement phase angles, rad.

RSRA estimator equations.- The state and measurement equations for the RSRA state estimator are shown in Table 3.6.

The  $\underline{x}_1$  vector is a 10x1 vector of primary states for the RSRA estimator. These states are: the rotor forces at the hub in the aircraft body axis system -  $X_R, Y_R, Z_R$ ; the rotor moments at the hub -  $L_R, M_R, N_R$ ; the inertial accelerations of the transmission in the body axis system -  $a_{t_x}, a_{t_y}, a_{t_z}$ ; and the sum of the engine and tail rotor drive shaft torques -  $Q_t$ .

The  $\underline{y}$  vector is a 10x1 vector of measurements consisting of: the transmission load cell reactive forces - A, B, C, D, E, and F; transmission accelerations -  $a_{t_{x_m}}, a_{t_{y_m}}, a_{t_{z_m}}$ ; and total drive shaft torques -  $Q_t$ .

The  $\underline{x}_2$  vector is a 20x1 vector of biases and scale factors for each of the 10 measurements.

TABLE 3.6.— RSRA STATE ESTIMATOR VECTOR DEFINITIONS

$\underline{x}_1 = \begin{bmatrix} X_R \\ Y_R \\ Z_R \\ L_R \\ M_R \\ N_R \\ at_x \\ at_y \\ at_z \\ Q_t \end{bmatrix}$ <p>10x1</p>	$\underline{x}_2 = \begin{bmatrix} b_A \\ b_B \\ b_C \\ b_D \\ b_E \\ b_F \\ bat_x \\ bat_y \\ bat_z \\ bQT \\ k_A \\ k_B \\ k_C \\ k_D \\ k_E \\ k_F \\ kat_x \\ kat_y \\ kat_z \\ kQT \end{bmatrix}$ <p>20x1</p>	$\underline{y} = \begin{bmatrix} A \\ B \\ C \\ D \\ E \\ F \\ at_{xm} \\ at_{ym} \\ at_{zm} \\ Q_{tm} \end{bmatrix}$ <p>10x1</p>
$\underline{w} = \begin{bmatrix} w_1 \\ w_2 \\ w_3 \\ w_4 \\ w_5 \\ w_6 \\ w_7 \\ w_8 \\ w_9 \\ w_{10} \end{bmatrix}$ <p>10x1</p>	$\underline{u} = \begin{bmatrix} \dot{p} \\ \dot{q} \\ \dot{r} \\ p \\ q \\ r \end{bmatrix}$ <p>6x1</p>	$\underline{v} = \begin{bmatrix} n_1 \\ n_2 \\ \vdots \\ n_{10} \end{bmatrix}$

The  $\underline{u}$  vector is a  $6 \times 1$  control vector of body angular accelerations -  $\dot{p}$ ,  $\dot{q}$ ,  $\dot{r}$ ; and body angular rates -  $p$ ,  $q$ ,  $r$  that are treated as deterministic inputs. These six quantities should be obtained from a prior fuselage/gust estimator run.

The  $\underline{w}$  vector is a  $10 \times 1$  vector of process noise sources that drives each of the states.

The  $\underline{v}$  vector is a  $10 \times 1$  measurement noise vector.

The state and measurement equations for the RSRA state estimator are presented below. These equations are based on Reference (11).

Primary State Equations:

$$\dot{\underline{x}}_1 = \underline{w}$$

Secondary State Equations:

$$\dot{\underline{x}}_2 = \underline{0}$$

Measurement Equations:

$$\begin{aligned} A = & h_{11}X_R + h_{12}Y_R + h_{13}Z_R + h_{14}L_R + h_{15}M_R + h_{16}N_R - h_{11}m_t a_{t_x} \\ & - h_{12}m_t a_{t_y} - h_{13}m_t a_{t_z} - h_{14}I_{t_{xx}}\dot{p} - h_{14}(I_{t_{zz}} - I_{t_{yy}})r p \\ & + h_{14}f_6 m_t a_{t_y} - h_{14}Q_t - h_{15}I_{t_{rr}}\dot{q} - h_{15}(I_{t_{xx}} - I_{t_{zz}})q r \\ & + h_{15}f_5 m_t a_{t_z} - h_{15}f_6 m_t a_{t_x} - h_{16}I_{t_{zz}} \dot{r} \\ & - h_{16}f_5 m_t a_{t_y} - h_{16}(I_{t_{yy}} - I_{t_{xx}})pq + n_1 \end{aligned}$$

$$\begin{aligned} B = & h_{21}X_R + h_{22}Y_R + h_{23}Z_R + h_{24}L_R + h_{25}M_R + h_{26}N_R - h_{21}m_t a_{t_x} \\ & - h_{22}m_t a_{t_y} - h_{23}m_t a_{t_z} - h_{24}I_{t_{xx}}\dot{p} - h_{24}(I_{t_{zz}} - I_{t_{yy}})r p \\ & + h_{24}f_6 m_t a_{t_y} - h_{24}Q_t - h_{25}I_{t_{rr}}\dot{q} - h_{25}(I_{t_{xx}} - I_{t_{zz}})q r \end{aligned}$$

$$+h_{25}f_5m_t a_{t_z} - h_{25}f_6m_t a_{t_x} - h_{26}I_{t_{zz}} \dot{r}$$

$$-h_{26}f_5m_t a_{t_y} - h_{26}(I_{t_{yy}} - I_{t_{xx}})pq + n_2$$

$$C = \frac{f_3}{(f_1+f_2)}X_R - \frac{f_1}{(f_1+f_2)}Z_R - \frac{1}{(f_1+f_2)}M_R - \frac{f_3}{(f_1+f_2)}m_t a_{t_x}$$

$$+ \frac{f_1}{(f_1+f_2)}m_t a_{t_z} + \frac{I_{t_{yy}}}{(f_1+f_2)}\dot{q} + \frac{(I_{t_{xx}} - I_{t_{zz}})}{(f_1+f_2)}qr - \frac{f_5 m_t}{(f_1+f_2)}a_{t_z}$$

$$+ \frac{f_6 m_t}{(f_1+f_2)}a_{t_x} + n_3$$

$$D = \frac{f_2}{(f_1+f_3)}Y_R - \frac{1}{(f_1+f_3)}N_R + \frac{f_2}{(f_1+f_3)}m_t a_{t_y} + \frac{I_{t_{zz}}}{(f_1+f_3)} +$$

$$+ \frac{(I_{t_{yy}} - I_{t_{xx}})}{(f_1+f_3)}pq + \frac{f_5 m_t}{(f_1+f_3)}a_{t_y} + n_4$$

$$E = \frac{f_1+f_3-f_2}{f_1+f_3}Y_R - \frac{1}{(f_1+f_3)}N_R - \frac{f_1+f_3-f_2}{f_1+f_3}m_t a_{t_y} + \frac{I_{t_{zz}}}{(f_1+f_3)} \dot{r}$$

$$+ \frac{(I_{t_{yy}} - I_{t_{xx}})}{(f_1+f_3)}pq + \frac{f_5 m_t}{(f_1+f_3)}a_{t_y} + n_5$$

$$F = X_R - m_t a_{t_x} + n_6$$

$$a_{t_{x_m}} = a_{t_x} + n_7$$

$$a_{t_{y_m}} = a_{t_y} + n_8$$

$$a_{t_{z_m}} = a_{t_z} + n_9$$

$$Q_{t_m} = Q_t + n_{10}$$

where,

$$h_{11} = h_{21} = -\frac{1}{2} \frac{f_3}{(f_1+f_2)}$$

$$h_{12} = -h_{22} = \frac{-f_3}{y_t} + \frac{(f_4-f_3)f_2}{y_t(f_1+f_3)}$$

$$h_{13} = h_{23} = -\frac{1}{2} \frac{f_2}{(f_1+f_2)}$$

$$h_{14} = -h_{24} = \frac{1}{y_t}$$

$$h_{15} = h_{25} = \frac{1}{2(f_1+f_2)}$$

$$h_{16} = -h_{26} = \frac{(f_4-f_3)}{y_t(f_1+f_3)}$$

The parameters used in these equations are defined in Table 3.7. Figure 3.3 shows the RSRA transmission orientation on the airframe and the location of the six load cells (A-F). Figure 3.4 shows the physical description of the parameters. The most basic parameters are  $x_t$ ,  $y_t$ ,  $z_t$ ,  $z_R$  and  $i_t$  where:  $x_t$ ,  $y_t$ ,  $z_t$  are the rotor mounting geometry dimensions in the transmission principle axis system;  $z_R$  is the distance from the rotor hub to the transmission center of gravity along the shaft; and  $i_t$  is the transmission incidence with respect to the longitudinal body axis.

TABLE 3.7. - RSRA STATE ESTIMATOR PARAMETER LIST

Parameter	Description
$y_T$	See Text
$f_1$	$f_1 = \frac{x_t}{2} \cos i_t + (z_R + z_t) \sin i_t$
$f_2$	$f_2 = \frac{x_t}{2} \cos i_t - (z_R + z_t) \sin i_t$
$f_3$	$f_3 = (z_R + z_t) \cos i_t + \frac{x_t}{2} \sin i_t$
$f_4$	$f_4 = (z_R + z_t) \cos i_t - \frac{x_t}{2} \sin i_t$
$f_5$	$f_5 = z_R \sin i_t$
$f_6$	$f_6 = z_R \cos i_t$
$M_t$	Transmission mass, slugs
$I_{txx}$	} Transmission principle moments of inertia, slug - ft <sup>2</sup> .
$I_{tyy}$	
$I_{tzz}$	

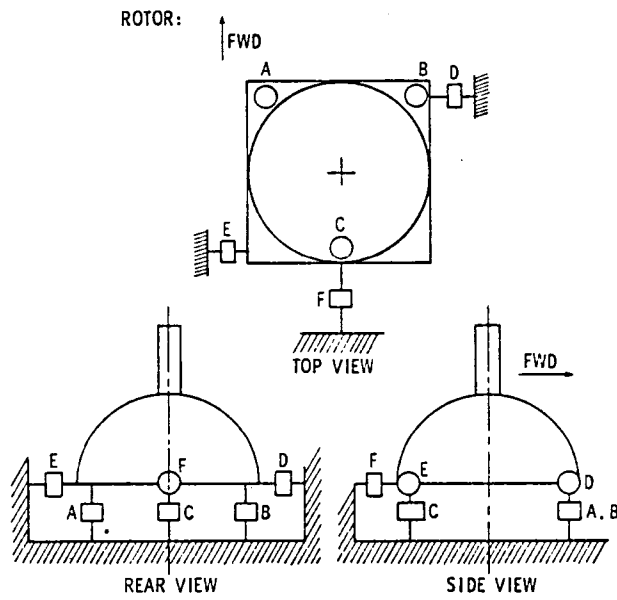


FIGURE 3.3.— RSRA HUB FORCE/MOMENT MEASUREMENT SYSTEM CONFIGURATION



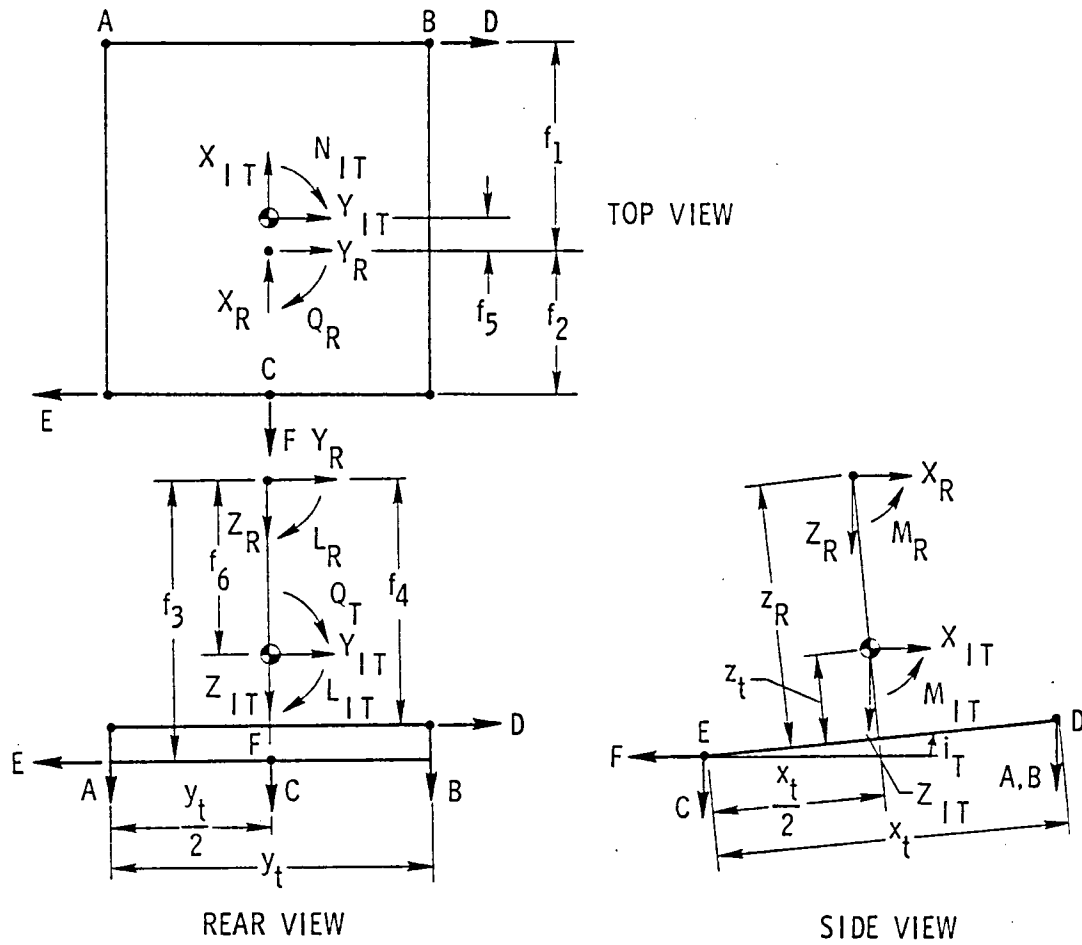


FIGURE 3.4.— RSRA ROTOR HUB FORCE/MOMENT MEASURE-  
MENT SYSTEM PARAMETER DEFINITIONS

## CHAPTER IV

### MODEL STRUCTURE ESTIMATION

#### Requirements

System identification methodology has been used successfully in many applications. This wide scope of application has focussed attention to one particular phase of the system identification methodology--the model structure determination phase--as an essential step. This step consists of processing the input/output data to determine the significant linear and nonlinear equations and associated parameters which are necessary to represent an observed system response. The significance of model structure determination in the overall system identification procedure is illustrated in Figure 4.1. A number of techniques must be used in the data processing stage, particularly for nonlinear operation regimes, to obtain the maximum information from the data for any particular rotorcraft. In the first stage, unmeasured or failed channels of data are reconstructed based on available measurements. This also gives preliminary force and moment coefficient time histories of interest. In the model

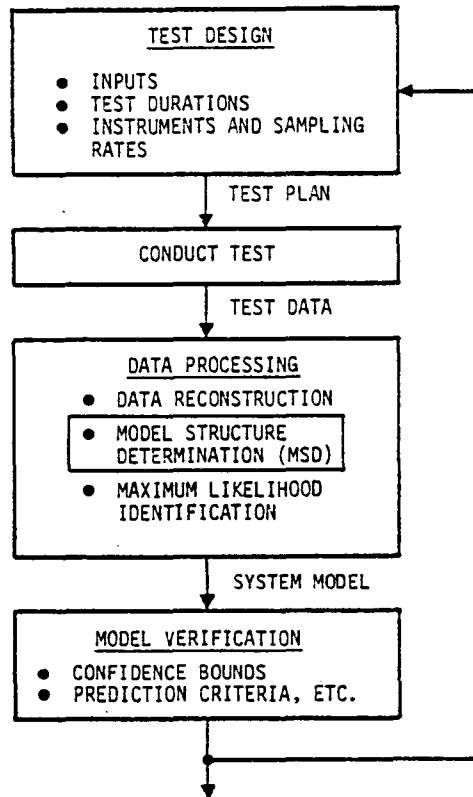


FIGURE 4.1.-- ROLE OF MODEL STRUCTURE DETERMINATION IN ROTORCRAFT SYSTEM IDENTIFICATION PROCEDURE.

structure determination (MSD) stage, the dependent forces and moments are related to the independent variables (e.g., angle-of-attack, Mach no., etc.) to provide the model with the most useful predictive capability. The maximum likelihood method is used in the third stage to refine the parameters of the model structure selected in the previous stage, as well as to validate the model structure.

It must be noted that this procedure will produce a mathematical model from the data which represents the particular data characteristics. No one set of data can completely define a unique model for all possible conditions. Additional dynamic tests (with specified input designs), scale model tests, or analytical correlation are always required to arrive at such a unique model. These additional requirements are discussed in detail in this chapter.

This step is particularly important in rotorcraft model identification because: (1) general rotorcraft models tend to be of high order with many dynamic effects, (2) rotor dynamics may or may not be important in any maneuver, (3) longitudinal and lateral motions may be coupled, and (4) there are significant nonlinearities in aerodynamic behavior particularly near hover and in transition.

Clearly the model structure determination is an extremely important step in rotorcraft identification work. Yet, the authors think that this is the first attempt at MSD for rotorcraft. The basic rotorcraft characteristics add new complexities to the problem. This chapter will also discuss how some techniques previously used for fixed-wing airplanes are specialized to rotorcraft applications. Numerical approaches are also described because the number of models to be tested may be very large.

The second section discusses the general model structure estimation method. Specializations required for rotorcraft applications are given in the third section. Finally, the fourth section describes the basis of a specific algorithm on which the computer program developed in this effort is based.

### Model Structure Estimation Approaches

Though the fundamental problem of model structure estimation has been recognized since the origin of physical science, the utilization of statistical methods to systematically determine significant characteristics in nonlinear dynamic systems was first presented in 1974 [12,13]. Such

methods have been applied to static systems [14] (e.g., in econometrics and biometrics) and to linear systems [15]. From a more fundamental approach, however, the work of Akaike [16] and Kullback [17] provided the significant theoretical formulation concepts for both linear and nonlinear systems. The theoretical basis of the methods discussed in this chapter is found in the cited work of Thiel, Akaike and Kullback. The application to aerospace systems can be traced to the work of Gerlach [18] in the Netherlands who demonstrated the use of a linear technique on actual test data.

The model structural determination process for rotorcraft has been isolated into three significant issues:

- (1) Specification of classes of a priori models.
- (2) Criteria for hypothesis testing of data against models.
- (3) Numerical procedures.

Specification of classes of a priori models.- The first major step in the model structure estimation process is the selection of mathematical forms to be correlated and tested against data. The specification of these models must be sufficiently broad to include the most probable relationship without attempting to consider all models. In order to form a tractable a priori model base, the following general considerations have been found to be relevant:

- (1) It is useful to recognize two aspects of mathematical models of physical systems. Basic models are derived from fundamental physical laws. Useful engineering models are, to some extent, empirical, wherein many of the system interrelationships are defined by tests and appropriate interpretation of the results. This obviously means that the role of physical engineering analysis in the model structure estimation process is essential. In particular, it is important to keep in mind that rotorcraft may have faster and slower modes.
- (2) The ultimate validation criteria, which include ability to explain existing data, consistency of empirical results with phenomenological considerations and ability to predict data, dictate model form.

- (3) The objective for which the model is to be used will indicate the levels of complexity required and the regime over which the model should be valid. This means that there may not be a unique model to describe a particular vehicle. In fact, model selection depends mainly on the use to which the model is put.

Selection of Functional Forms.- In order to optimize the initial model for computational speed and numerical accuracy, it must include elements of known phenomenological behavior supplemented by various classes of functional forms, depending on the particular problem. In the absence of strong phenomenological evidence to the contrary, polynomials are well known as simple and versatile choices for mathematical models. Indeed, polynomials serve exceedingly well in modeling lift, drag, and moment coefficients for helicopters. If, however, it is known that the process is susceptible to a growth phenomenon, such as vortex buildup from aircraft control deflections, exponential or logarithmic functions are desirable. The use of polynomials should therefore be undertaken with a reasonably clear understanding of the limitations. This fact was emphasized in the second chapter. Factors which affect the particular polynomial form including the following:

- (1) A priori phenomenological information about the process.
- (2) Range of variation of the dependent variables (and possibility of differences in physical phenomena over that range).
- (3) Specification of whether the polynomial is to be differentiated (requiring valid slope representation) or integrated (requiring high reliability in the initial value).
- (4) Computational resources available to use the model (in terms of speed and memory).

To meet these requirements, two basic polynomial formulations have been used, as shown in Table 4.1:

- (1) A regular polynomial is used to represent a simple continuous phenomenon. This polynomial is usually linear in the unknown parameters  $C_i$  (though many cases arise in which the polynomial is nonlinear in the unknown parameters). For improved numerical conditioning, orthogonal polynomials are desired. The classical orthogonal polynomials of

TABLE 4.1.— SELECTION OF FUNCTIONAL FORMS FOR MODEL STRUCTURE DETERMINATION

TYPE OF PHENOMENON	BASIC FORM	IMPROVED NUMERICAL CONDITIONING
Homogeneous	<p style="text-align: center;">POLYNOMIAL</p> $y = \sum_{i=0}^m C_i x^i$	<p style="text-align: center;">ORTHOGONAL POLYNOMIAL</p> $y = \sum_{i=0}^m c_i p_i(x) \quad 0 \leq x \leq 1$ <p style="text-align: center;">where <math>\int_a^b p_m p_n dx = \delta_{mn}</math></p>
Heterogeneous	<p style="text-align: center;">SPLINE</p> $y = \sum_{i=0}^m C_i x^i + \sum_{j=1}^n \sum_{i=v+1}^m C_{ij} (x-x_j)^i$ <p style="text-align: center;">where <math>(x-x_j)^i = \begin{cases} 0 &amp; x &lt; x_j \\ (x-x_j)^i &amp; x \geq x_j \end{cases}</math></p>	<p style="text-align: center;">B-SPLINE</p> $y_j = \sum_{i=0}^{m+1} \frac{(m+1)(x-x_{i+1})^q}{w_j(x_{i+j})}$ <p style="text-align: center;"><math>v = m-1</math></p> $w_j(x) = (x-x_j)(x-x_{j+1}) \dots (x-x_{j+q+1})$

Legendre, Laguerre, and Hermite may be generated by three term recurrence relations which are easily programmed. The Tschebycheff polynomial is known to demonstrate the properties of both the Fourier series and the orthogonal polynomials [19].

- (2) A spline of order  $n$  and continuity  $\nu$  is used to represent a simple heterogeneous phenomenon. The spline function consists of piecewise polynomials wherein the derivatives are continuous. Hence, the spline preserves the continuity of lower order derivatives across function discontinuities. There are  $n+1$  regions defined by  $x < x_1, x_1 \leq x < x_2, \dots, x_n \leq x$ . At each of the transition points,  $x_i$ , which are called knots, the first derivatives of the function  $y$  are continuous. The independent variable  $y$  is a linear function of parameters,  $C_i$ , but is a non-linear function of knot locations. B-splines are used for improved numerical conditioning (see Table 4.1).

The representations for a single independent variable can be generalized to many independent variables in several ways. Straightforward generalizations of the polynomial and spline forms for two variables are given in Table 4.2. Such an approach is useful for cases where the number of independent variables and/or terms in approximating polynomials is small. For several independent variables, a more organized procedure has been found necessary. The method which has been implemented to achieve this is an extension of Ivakhnenko's group concept [20]. Table 4.2 shows the typical equations which are used to evaluate large levels of subsets of model terms. For example, the equation of Table 4.2 (for regular polynomials) is written in terms of the second variable for all the unknown variables in the first equation.

The models specified using the above procedure will in general be too complex. The next section discusses statistical criteria which are used to simplify the above representations such that useful models are obtained from a limited set of data.

Quantitative criteria for comparison of competitive models against test data.- The representations of the previous sections are quite flexible and allow for a very large number of model structures. In certain applications, several competing representations based on different independent

TABLE 4.2.— GENERAL POLYNOMIALS FOR FUNCTION OF SEVERAL VARIABLES

TYPE OF PHENOMENON	BASIC FORM	HIERARCHICAL FORM
Homogeneous	$y = \sum_{i=0}^{m_1} \sum_{j=0}^{m_2} C_{ij} x^i(1) x^j(2)$	<p>MULTIPLE SUBSET POLYNOMIALS</p> $y = \sum_{i=0}^{m_1} C_i x^i(1)$ $C_i = \sum_{j=1}^{m_2} C_{ij} x^j(2)$
Heterogeneous	<p>POLYNOMIAL SPLINE</p> $y = \sum_{i_1=0}^{m_1} \sum_{i_2=0}^{m_2} C_{i_1 i_2} x^{i_1}(1) x^{i_2}(2)$ $\sum_{j_1=1}^{n_1} \sum_{j_2=1}^{n_2} \sum_{i_1=v_1+1}^{m_1} \sum_{i_2=v_2+1}^{m_2} C_{i_1 j_1 i_2 j_2} [x(1) - x_{j_1}(1)]^{i_1} [x(2) - x_{j_2}(2)]^{i_2} + \dots$	<p>MULTIPLE SUBSET SPLINE</p> $y = \sum_{i=0}^{m_1} C_i x^i(1) + \sum_{j=0}^{m_1} \sum_{i=v+1}^{m_1} C_{ij} [x(1) - x_j(2)]_+^i$ $C = \sum_{i=0}^{m_2} d_i x^i(2) + \sum_{j=1}^{m_2} \sum_{i=v_2+1}^{m_2} d_{ij} [x(2) - x_j(2)]_+^i$



variables may be hypothesized leading to a further increase in the number of plausible model structures. The use of measured data isolates the most likely model and indicates model adequacy in explaining the observed behavior. This section discusses several classes of criteria used for this purpose. The tradeoffs to be considered in the particular selection of the criteria are:

- (1) The distribution function of the noise. Certain criteria are applicable when the noise is white Gaussian while others are more general;
- (2) A priori knowledge about noise distribution function; and
- (3) Number of models to be compared.

Let there be  $N$  sets of measurements (or reconstructed values) represented by  $y_i$  and  $x_i(1), x_i(2), \dots, x_i(p)$ ,  $i=1,2,\dots,N$ . Quantitative criteria used for model substantiation based on this data may be divided into four broad categories, shown in Table 4.3. Note that all these criteria can be used with both the equation error and the dynamic model formulations.

Fit error statistics. Fit error is a measure of the difference between the measured response and its estimate based on the model. Suppose two models  $M_1$  (with  $m_1$  parameters,  $\theta_1$ ) and  $M_2$  (with  $m_2$  parameters,  $\theta_2$ ) are to be compared. Let  $\hat{y}_i(M_1, \hat{\theta}_1)$  and  $\hat{y}_i(M_2, \hat{\theta}_2)$  be the estimated values of  $y_i$  based on models  $M_1$  and  $M_2$ , respectively ( $\hat{\theta}_1$  and  $\hat{\theta}_2$  are the corresponding parameter estimates). Then the fit error leads to the following criterion

$$\left. \begin{array}{l} \frac{1}{N} \sum_{i=1}^N [y_i - \hat{y}_i(M_1, \hat{\theta}_1)]^2 \\ \frac{1}{N} \sum_{i=1}^N [y_i - \hat{y}_i(M_2, \hat{\theta}_2)]^2 \end{array} \right\} \begin{array}{l} < 1 \text{ Select Model } M_1 \\ > 1 \text{ Select Model } M_2 \end{array} \quad (4.1)$$

Improved results are obtained if the fit error is corrected for the number of unknown parameters in the model. The adjusted fit error for model  $M_1$  is

TABLE 4.3.— COMPARISON OF CRITERIA FOR VALIDATION OF MODELS AGAINST TEST DATA

CLASS	EQUATION	COMMENTS
<u>FIT ERROR</u> <ul style="list-style-type: none"> <li>• Error Covariance</li> <li>• Whiteness Test</li> <li>• Fit Error Corrected for Degrees of Freedom</li> </ul>	$\frac{1}{N} \sum (y_i - \hat{y}_i)^2$ $\frac{1}{N} \sum (y_i - \hat{y}_i)(y_{i+1} - \hat{y}_{i+1}) \text{ etc.}$ $\frac{1}{N-m_1} \sum (y_i - \hat{y}_i)^2$	<ul style="list-style-type: none"> <li>• Since fit error always increases with number of parameters, subjective termination criteria required.</li> </ul>
<u>LIKELIHOOD APPROACH</u> <ul style="list-style-type: none"> <li>• Likelihood Ratio</li> <li>• Log Likelihood Ratio Corrected for Degrees of Freedom</li> </ul>	$p(Y M_1, \hat{\theta}_1) / p(Y M_2, \hat{\theta}_2)$ $\log \{ p(Y M_1, \hat{\theta}_1) / p(Y M_2, \hat{\theta}_2) \}$ $-2m_1 + 2m_2$	<ul style="list-style-type: none"> <li>• Equations given for two models--see text for generalizations</li> <li>• Requires knowledge of probability distributions, a priori</li> <li>• Works with any noise distribution</li> </ul>
<u>PREDICTION ERROR</u> <ul style="list-style-type: none"> <li>• Direct Determination over an Independent Data Set</li> <li>• Estimate Over Same Region as Data</li> <li>• Estimate Over a New Region</li> </ul>	$\frac{1}{N_p} \sum_{i=1}^{N_p} (y_i - y_{ip})^2$ $\frac{N+m_1}{N-m_1} \cdot \frac{1}{N} \cdot \sum_{i=1}^N (y_i - \hat{y}_i)^2$ $\frac{1}{N_p} \sum_{i=1}^{N_p} [\sigma_i^2 + \hat{\sigma}_i^2(M_1)]$	<ul style="list-style-type: none"> <li>• Excellent when model is used for prediction</li> <li>• Automatically incorporates degrees of freedom</li> </ul>
<u>F-RATIO</u> <ul style="list-style-type: none"> <li>• Equation F-Ratio</li> <li>• Parameter F-Ratio</li> <li>• Parzen's Test</li> </ul>	$\frac{R^2/m}{(1-R^2)/(N-m)}$ $\frac{(R_2^2 - R_1^2)/m_2}{(1-R_2^2)/(N-m_1-m_2)}$ <p>See Ref. 13</p>	<ul style="list-style-type: none"> <li>• Most used test in econometrics and biometrics</li> <li>• Easy to implement</li> <li>• Excellent for a first cut</li> </ul>

$$\frac{1}{(N - m_1)} \sum_{i=1}^N [y_i - \hat{y}_i(M_1, \hat{\theta}_1)]^2 \quad (4.2)$$

The fit error should be rarely used directly for comparison of models. It is, however, very useful in establishing the validity of the model selected by other approaches.

**Likelihood ratio statistics.** The likelihood approach has been used extensively for both parameter estimation and comparison of competitive models based on test data. The central concept is the likelihood function, which defines the probability that the measured data were generated by any specific model or any set of parameter values. The likelihood function for model  $M_1$  is  $p(Y|M_1, \hat{\theta}_1)$  where  $Y$  is the set of measurements  $y_1, y_2, \dots, y_N$  and  $\hat{\theta}_1$  is the maximum likelihood estimate of  $\theta_1$  assuming model  $M_1$  holds. The model selection criterion is the ratio of the likelihood functions for models  $M_1$  and  $M_2$ . The likelihood ratio must, however, be corrected for the degrees of freedom. Otherwise the results will always favor more complex models. When there are  $p$  competitive models to be compared, the following procedure may be used.

Step 1: Compute  $J_i, i = 1, 2, \dots, p$

$$J_i = \ln \{p(Y|M_i, \hat{\theta}_i)\} - 2m_i$$

Step 2: Let  $J_j$  be such that

$$J_j > J_i, \quad i \neq j$$

Then  $J_j$  is the "most likely" model.

For two candidate models the method simplifies to

$$\ln \left\{ \frac{p(Y|M_1, \hat{\theta}_1)}{p(Y|M_2, \hat{\theta}_2)} \right\} - 2m_1 + 2m_2 \left. \begin{array}{l} > 0, \text{ Select } M_1 \\ < 0, \text{ Select } M_2 \end{array} \right\} \quad (4.3)$$

Important generalizations of the likelihood ratio result when one model is the subset of the other model, or in general, all models considered are subsets of the same maximum

model. Let the maximal model be characterized by parameters  $\theta$ . When certain parameters are zero, a lower order subset is obtained. (Note that this may be used to model a wide variety of situations.) The log likelihood function may then be expanded in a multidimensional Taylor series about our best estimate  $\hat{\theta}$  of  $\theta$ .

$$\begin{aligned} \ln p(Y|\theta) = \ln p(Y|\hat{\theta}) + \frac{\partial \ln p(Y|\hat{\theta})}{\partial \hat{\theta}} (\theta - \hat{\theta}) \quad (4.4) \\ + \frac{1}{2} (\theta - \hat{\theta})^T M(\theta - \hat{\theta}) + \dots \end{aligned}$$

where  $M$  is the information matrix. Since  $\hat{\theta}$  is the best estimate of  $\theta$ , the first gradient of the likelihood has mean zero and covariance  $M^{-1}$ . To test the hypothesis that a lower order model is valid, the estimated  $\hat{\theta}$  equal to zero will decrease the likelihood function significantly. A model structure determination principle based on this concept was detailed by Gupta [21].

The likelihood method is optimal under a variety of circumstances. Its rigorous applicability is limited by the theoretical requirement to know the probability density of the measurements for each model.

Prediction error statistic.- The capability of a model to predict system responses for a class of inputs is a desirable quality. Therefore, prediction error of models may be used as the quantitative criteria to select the model which best substantiates the measured data. There are two methods to determine the prediction error of a model. In the first method the measured data is divided into two parts. The first part of the data is used to estimate unknown parameters in each model. The estimated models are then used to predict the response for the second data set. The model which predicts the response most accurately is the desired model. The second method is indirect where the prediction error is estimated statistically. The prediction error is either based on the same input as the one used to estimate the models or covers a different region (the choice depends on the ultimate application of the model). A good estimate of prediction error for a model  $M_1$  with  $m_1$  parameters over the data region may be shown to be [16]

$$\frac{N+m_1}{N-m_1} \left\{ \frac{1}{N} \sum_{i=1}^N [y_i - \hat{y}_i(M_1, \hat{\theta}_1)]^2 \right\} \quad (4.5)$$

The prediction over a data region  $y_{pi}$ ,  $i = 1, 2, \dots, N_p$  is computed as follows. Let  $\hat{y}_{pi}(M_1, \hat{\theta}_1)$  be the estimated value for  $y_{pi}$  with mean square error  $\hat{\sigma}_i^2(M_1)$  for model  $M_1$ . If  $\sigma_i^2$  is the variance of noise in  $y_{pi}$ , the prediction error is

$$\frac{1}{N_p} \sum_{i=1}^{N_p} [\sigma_i^2 + \hat{\sigma}_i^2(M_1)] \quad (4.6)$$

Prediction error criteria are most useful when the estimated model is to be used for simulation. They automatically incorporate the degree of freedom correction for number of unknown parameters in the model.

F-ratio statistic.- The F-ratio is perhaps the most widely used statistic for model hypothesis testing in econometrics and biometrics. The test is based on the assumption of normally distributed random disturbances and requires a priori specification of acceptance-rejection boundary.

These assumptions are restrictive, and as noted in Ref. 12, F-tests should not be used as the only criterion for the adequacy of a model. On the other hand, they do have compensating attributes which include the following:

- (1) Standard algorithms have been optimized for computer implementation of F-ratio statistical hypothesis testing. They allow the consideration of an extremely large number of models.
- (2) A relative maximum of the F-ratio with the number of parameters is often found in practice. This maximum is cited in Ref. 12 as an experimental result, which to the authors' knowledge, has not yet been investigated by other researchers.
- (3) For many practical cases, it gives the same result as more sophisticated approaches.

The desirable performance of the F-ratio, in spite of the assumptions, is presumably due to the robustness of the statistic and the particular self-check features used in the implementation. In particular, application of the F-test criterion on properly prefiltered data has been found to improve the utility of the statistics. Three approaches

have been used based on: (1) equation F-ratio, (2) parameter F-ratio, and (3) Parzen's test. The equation F-ratio tests the validity of the entire model. It is given by

$$F = \frac{R^2/m}{(1 - R^2)/(N-m)} \quad (4.7)$$

where  $R$  is the equation multiple correlation coefficient,  $N$  is the number of data points, and  $m$  is the number of parameters in the equation.

The parameter F-ratio statistic is applied as follows. Suppose that the complete set of parameters  $\theta$  is divided into two subsets of  $\theta_1$  and  $\theta_2$  of size  $m_1$  and  $m_2$ . An F-test can be used to test the hypothesis that  $\theta_2$  is equal to any specific value (usually zero) while parameters  $\theta_1$  are chosen to minimize fit error. The F-ratio of parameters  $\theta_2$  is

$$F(\theta_2) = \frac{(R_2^2 - R_1^2)/m_2}{(1 - R_2^2)/(N - m_1 - m_2)} \quad (4.8)$$

where

$R_1$  is multiple correlation coefficient with parameters  $\theta_1$

$R_2$  is multiple correlation coefficient with parameters  $\theta_1$  and  $\theta_2$

If the F-ratio is small compared to a threshold, parameters  $\theta_2$  may be set to zero. F-ratio for parameters in the equation is computed in a similar manner. In practice, the F-test is performed on single parameters rather than on sets of parameters.

Parzen [22] devised a unique method based on the F-statistic to develop models for physical systems. The method assumes that the "true" model is very complex and has several degrees of freedom. Since the measured data contains noise and does not encompass the entire operation regime, the estimated model must be a simplified version of the true model. Each simplified model is then compared with a high order model using an F-statistic.

Summary.- Quantitative criteria presented in this section look at model structure optimality from different viewpoints. Extensive experience has indicated that for well-behaved systems, all the tests (except fit error) give similar model structures if the noise has a normal distribution and the specified a priori minimal model includes all the effects observed in the data. If the distribution of the noise is significantly different from normal or if the noise is not white, the likelihood ratio test gives the best results.

Numerical procedures.- Implementation of methods to develop models from test data must consider the following factors:

- (1) The number of hypothesized models may be very large (number in billions or more is common).
- (2) All models contain some level of modeling error (i.e., no model of a physical system is perfect). The models are "good" or "poor," not "right" or "wrong."
- (3) Many physical systems are dynamic. The modeling of system dynamics may improve the model structure estimates.
- (4) Distribution functions are usually not known and must be approximated.
- (5) It should be possible to incorporate the analyst's opinion.
- (6) Computation time should be reasonable.

These factors indicate that proper implementation is a key part of the successful model structure determination process.

Three formulations have been successfully used:

- (1) Equation error.
- (2) Kalman filter (or Extended Kalman filter).
- (3) Maximum likelihood (or its special case, output error).

Equation error formulation.- In the equation error formulation, measurements of dependent and independent variables are related by

$$\bar{y}_i = f(\bar{X}_i, \theta) + \epsilon_i, \quad i = 1, 2, \dots, N \quad (4.9)$$

$\bar{X}_i$  is the set of  $p$  independent variables at the  $i$ th point and  $\theta$  is the  $k \times 1$  vector of unknown parameters.  $\bar{y}_i$  and  $\bar{X}_i$  are obtained by reconstruction from available measurements. For example  $\bar{y}_i$  may represent angular accelerations obtained by differentiating measurements of angular rates. Such reconstruction is often necessary in equation error formulations. The results shown here are for uncorrelated and Gaussian noise, though extension to other cases is straightforward. The above equation is linearized about the nominal value  $\theta_0$  of the parameter vector

$$\bar{y}_i - f(\bar{X}_i, \theta_0) \approx \frac{\partial f(\bar{X}_i, \theta_0)}{\partial \theta} (\theta - \theta_0) + \epsilon_i \quad (4.10)$$

$$i = 1, 2, \dots, N$$

which may be written as

$$\Delta Y = A \Delta \theta + \epsilon \quad (4.11)$$

$\Delta Y$  is an  $N \times 1$  vector and  $A$  is an  $N \times k$  matrix. Note that Eq. (4.1) will usually be an overdetermined system ( $N > k$ ).  $\Delta \theta$  is chosen to minimize  $\|\Delta Y - A \Delta \theta\|^2$ .

Nominal parameter values  $\theta_0$  are obtained either from a priori estimates or from a previous iteration. Equation (4.11) must be solved a number of times until convergence occurs. Most nonlinear equations of engineering significance can be solved by iteratively forming and solving a series of linear equations (4.11).

A straightforward way to evaluate all of the possible models is to solve the complete least square problem for each of the parameter subsets. This is unpractical even for systems with 25 unknown parameters (34 million models). One method to make the procedure feasible is to use the stepwise regression procedure [12]. By considering one parameter at a time, only a small fraction of all the subsets is tested. This allows the analysis of models having up to 400 candidate parameters. One disadvantage of the method is that it usually finds only one subset of each size, unlike the complete search methods.



Kalman filter.- The Kalman filter and extended Kalman filter have been applied to many problems in state estimation, parameter identification and fault detection. Like the least squares method, the parameter estimates resulting from a Kalman filter are biased. To use this approach for model structure estimation, one set of dynamic equations is written for each model proposed, i.e., for the ith model

$$\dot{x}_i = f(M_i, x_i) + w(t) \quad , \quad 0 \leq t \leq T \quad (4.12)$$

$$y(k) = h(M_i, x_i, k) + v(k) \quad , \quad k = 1, 2, \dots, N \quad (4.13)$$

The states  $x_i$ , of course, include the unknown parameters in each model. An extended Kalman filter is developed for these equations. One or more of the following quantities is then used to compare the models:

- (1) Innovations: The innovation for model  $i$  is  $y(k) - \hat{y}(k, k-1, M_i)$ . Its bias and covariance is a good measure of one-step-ahead prediction error. It could also be used to compute certain likelihood ratios by making suitable assumptions. The problem with innovation is that while the parameters are being adjusted in the initial portion of data, innovations are large and more complex models may be unnecessarily penalized.
- (2) Fit Error: The fit error for model  $i$  is  $y(k) - \hat{y}(k, N, M_i)$  and can be used like innovations to compare models. Residuals may also be used.
- (3) Parameter Estimates and Covariances: This is a poor basis of a test because predicted covariances are often grossly in error when determined using a Kalman filter.

Problems with using a Kalman filter for model structure determination are: (1) choice of measurement and process noise covariance have a strong influence on model; in general, increasing process noise covariance will result in less complex models, (2) filter divergence because of poor starting values may invalidate an otherwise good model, and (3) since one extended Kalman filter is required for each model (34 million Kalman filters for a problem with 25 parameters, each of which could be zero), the method often requires unacceptable computation time in practical systems.

Maximum likelihood method.- Several of the problems associated with extended Kalman filter may be solved by using the maximum likelihood method. This method has been described extensively [12,13] in the literature. It gives accurate estimates of parameters as well as associated error covariances. Though all of the quantities used for model comparison with Kalman filter may be applied, the likelihood ratio and prediction error tests are most appropriate. In certain cases, log likelihood ratio expansions of the kind shown in the likelihood statistic test section can simplify the implementation significantly.

The maximum likelihood procedure is very general and includes equation error and Kalman filter procedure as special cases. A major problem with a direct application of the procedure for model structure estimation is the excessive computation time requirement. This technique is best applied when the equation error has substantially reduced the number of plausible models.

Summary.- A comprehensive advanced model structure determination for dynamic systems is an essential aspect of system identification for rotorcraft. The critical elements of such a procedure are:

- (1) Specification of functional forms for useful models.
- (2) Criteria for selecting an adequate model against competing models.
- (3) Efficient numerical algorithms for integrating the conflicting requirements of adequate functional forms and accurate criteria.

The next section will show how these choices are made for rotorcraft model structure determination problem.

#### Rotorcraft Model Structure Estimation Method

The previous section discussed a fairly comprehensive model structure determination method for a wide variety of rotorcraft. Conceptually, any combination of functional form, model evaluation criteria and numerical procedure may be used in developing mathematical models of rotorcraft from real time data. Practically, the choice of an acceptable combination is dictated by the following considerations:

- (1) Rotorcraft models are usually of high order with complex interactions, both mechanical and aerodynamic between rotor(s) and fuselage.
- (2) There are many different classes of rotorcraft and very little experience exists in processing rotorcraft data.
- (3) There is poor wind tunnel data base for many helicopter types and analytical simulations (like C-81) though useful for simulations are not as good for determination of model form.
- (4) The characteristics of typical rotorcraft change significantly from hover to transition and cruise. In addition, functional relationships between forms of aerodynamic coefficients at various speeds is not thoroughly understood.
- (5) Because of model complexities, certain important interactions are likely to be unidentifiable for any maneuver.
- (6) In the face of the above problems, the computation time should be reasonable even for complex and long maneuvers in which several control inputs are applied sequentially or simultaneously.

These considerations suggest the following selections:

- (1) A model based on dynamic equations of motions, in which all unknown functional forms (aerodynamic coefficients, interaction coefficients, unknown torques, moments and forces) are written as multi-dimensional polynomials in corresponding independent variables.
- (2) F-ratio, equation F-ratio or prediction error criteria are used in model selection.
- (3) The equation error method is used in the model. This is partly justified because the MSD step is followed by a parameter identification step based on the maximum likelihood technique.

We now describe an algorithm based on the above selections in detail.

Description of a Model  
Structure Estimation Algorithm

The use of the state estimation approach as the first step on the data, and the selections of the polynomial function forms and equation error approach lead to a model structure problem in the following general form

$$y = X\theta + \varepsilon \quad (4.14)$$

where  $y$  is an  $(m \times 1)$  vector of observations,  $X$  is an  $m \times p$  matrix of known coefficients ( $m > p$ ) and  $\theta$  is a  $p \times 1$  vector of parameters.  $\varepsilon$  is an  $(n \times 1)$  vector of disturbance or error random variables with  $\mathcal{E}(\varepsilon) = 0$  (zero mean) and variance  $\mathcal{E}(\varepsilon\varepsilon^T) = \sigma^2 I$  (components of  $\varepsilon$  are uncorrelated with the same variance  $\sigma^2$ ).

Basic principles.- Minimization of  $J$  with respect to  $\theta$  yields the well-known least squares estimator

$$\hat{\theta} = (X^T X)^{-1} X^T y$$

where  $(X^T X)$  is nonsingular. Substituting Eq. (4.14) into Eq. (4.15), it is easily shown that

$$\mathcal{E}(\hat{\theta}) = \theta \quad (4.16)$$

$$\mathcal{E}[(\hat{\theta} - \theta)(\hat{\theta} - \theta)^T] = \sigma^2 (X^T X)^{-1} \quad (4.17)$$

where  $X$  is fixed in repeated samples and assuming  $\mathcal{E}(X^T \varepsilon) = 0$ .

In actual experimentation,  $\sigma^2$  is not known and must be estimated. This is due to the fact that  $\varepsilon = y - X\theta$ , the error, is a nonobservable, stochastic variable. However, estimates of the variance of  $\hat{\varepsilon} = y - X\hat{\theta}$  (Fig. 4.2),  $s^2$ , may be determined which estimate  $\sigma^2$ . The sum of squares of the residuals is found by solving Eqs. (4.11) and (4.14) for  $\hat{\varepsilon}^T \hat{\varepsilon}$ , i.e.,

$$\begin{aligned} \hat{\varepsilon}^T \hat{\varepsilon} &= (y - X\hat{\theta})^T (y - X\hat{\theta}) = \varepsilon^T M \varepsilon \\ &= y^T M y \end{aligned}$$

where  $M = (I_m - XOX^T X)^{-1} X^T$ . Note that  $M^2 = M = M^T$ . Since  $M$  is thus idempotent and  $\text{tr} M = m - p$ ,\* taking the expectation of Eq. (4.18) yields

$$s^2 = \frac{1}{m-p} (y - X\hat{\theta})^T (y - X\hat{\theta}) = \frac{\hat{\varepsilon}^T \hat{\varepsilon}}{m-p} \quad (4.19)$$

which estimates  $\sigma^2$ . Equation (4.19) in Eq. (4.17) gives the sample estimate of the covariance of  $\hat{\theta}$

$$(\hat{\theta} - \theta)(\hat{\theta} - \theta)^T = s^2 (X^T X)^{-1} \quad (4.20)$$

Note that Eq. (4.15) produces unbiased estimates of  $\hat{\theta}$  only if the model is correct.

Decomposition of variance.- Substituting the estimate into  $J$ , it is found that

$$\hat{J} = \hat{\varepsilon}^T \hat{\varepsilon} = y^T y - \hat{y}^T \hat{y} \quad (4.21)$$

where

$$\hat{y} = E(y|X) = X\hat{\theta} \quad (4.22)$$

Equation (4.21), a consequence of orthogonality theorem of least squares, decomposes the sum of squares of the data variation  $(y^T y)$  into the contribution from the sum of squares of the regression equation  $(\hat{y}^T \hat{y})$  and sum of squares of the residuals  $(\hat{\varepsilon}^T \hat{\varepsilon})$ , i.e.,

$$y^T y = \hat{y}^T \hat{y} + \hat{\varepsilon}^T \hat{\varepsilon} \quad (4.23)$$

The basic idea of subset regression is to compute the reduction in error sum of squares  $(\hat{\varepsilon}^T \hat{\varepsilon})$  relative to the increase in regression sum of squares  $(\hat{y}^T \hat{y})$  which is

---

\*The rank of  $I - M = X(X^T X)^{-1} X^T$  is  $p$ , and the rank of  $I_m$  is  $m$ . If the observations are not centered, then  $p$  is replaced by  $p+1$ .

caused by adding (or subtracting) new variables  $\theta_i$  in the regression. Ratios based on these incremental sum of squares may then be used to determine the significance of these added parameters. These ratios may be formulated as test statistics for which, under the assumption of normally distributed errors,  $\epsilon$ , standard significance testing may be performed. That the errors are, in fact, normally distributed, is justified by the central limit theorem on the normality of the distribution of a large number of random disturbances.

Significance of the regression equation.— The solution  $\hat{\theta}$ , Eq. (4.15), to the minimization of error sum of squares is unique when  $X$  has full column rank. Any coefficient vector which differs from the least squares vector  $\hat{\theta}$  must lead to a larger sum of squares. That is, for any other coefficient vector,  $\theta$ ,

$$(y - X\theta) = (y - X\hat{\theta}) - X(\theta - \hat{\theta}) \quad (4.24)$$

has an error sum of squares

$$(y - X\theta)^T (y - X\theta) = y^T y + (\theta - \hat{\theta})^T X^T X (\theta - \hat{\theta}) . \quad (4.25)$$

The quantity  $(\theta - \hat{\theta})$  is the "sampling error" of the regression.

Assume that it is desired to test the hypothesis that  $\theta$  is some specific numerical value, say  $\theta_0$  (e.g.,  $\theta_0 = 0$  if there is not dependence of the data on  $\theta$ ). Then, if  $\theta_0$  is the true value of  $\theta$ ,

$$\hat{\theta} - \theta_0 = \hat{\theta} - \theta = (X^T X)^{-1} X^T (X\theta + \epsilon) - \theta = (X^T X)^{-1} X^T \epsilon. \quad (4.26)$$

Using Eqs. (4.18) and (4.16), Eq. (4.23) then becomes

$$(y - X\theta_0)^T (y - X\theta_0) = \epsilon^T \epsilon + \epsilon^T (I - M) \epsilon . \quad (4.27)$$

In order to fulfill the requirements for using statistical tests based on the sum of squares of Eq. (4.27), it is necessary to recall the fact that an idempotent quadratic form in independent standardized normal variates is a chi-squared variate with degrees of freedom given by the rank of

the quadratic form\* (Sec. 15.11, Ref. 23). Furthermore, if the two normalized sum of squares  $S_i/\sigma^2$  and  $S_j/\sigma^2$  are  $\chi^2(v_i)$  and  $\chi^2(v_j)$  distributed, and  $S_i$  and  $S_j$  are independent, then

$$F = \frac{S_i/v_i}{S_j/v_j} \quad (4.28)$$

is a Fisher F-ratio distributed with  $v_i$  and  $v_j$  degrees of freedom.

As discussed after Eq. (4.18), the rank of  $\mathcal{M}$  is  $m-p$  and that of  $I - \mathcal{M}$  is  $p$ . Thus, the ratio

$$\frac{\varepsilon^T (I - \mathcal{M}) \varepsilon / p}{\varepsilon^T \varepsilon / m-p} \quad (4.29)$$

is distributed as  $F(p, m-p)$ , if  $\theta = \theta_0$ . But from Eqs. (4.18) and (4.19),  $\varepsilon^T \varepsilon = (m-p)s^2$  and it is easily shown that  $\varepsilon^T (I - \mathcal{M}) \varepsilon = (\hat{\theta} - \theta_0)^T X^T X (\hat{\theta} - \theta_0)$ , if  $\theta = \theta_0$ . Hence,

$$\frac{(\hat{\theta} - \theta_0)^T X^T X (\hat{\theta} - \theta_0)}{ps^2} \sim F(p, m-p) \quad (4.30a)$$

Examination of Eq. (4.24) shows that the numerator of Eq. (4.26) is the difference between the sum of squares regression on  $\theta_0$  and the sum of squares of the actual parameters  $\theta$ .

High values of  $F(p, m-p)$  correspond to rejection of the hypothesis that  $\theta = \theta_0$ . In particular, to test whether the data depends on a specific parameter,  $\theta_i$  of  $\theta$ , the  $F(p, m-p)$  ratio is evaluated for  $\theta_0 = 0$ .

---

\* A sum of squares  $S_i$  can be written as  $y^T A y$  where  $y$  is vector,  $A$  is a matrix of known constants. Then the number of degrees of freedom of  $S_i$  is defined to be the rank of  $A$ .

A recursive form of Eq. (4.30a) is

$$F(q, m-p) = \frac{(\hat{\theta} - \theta_0)^T X^T X (\hat{\theta} - \theta_0)}{qs^2} \quad (4.30b)$$

where  $q$  is the number of parameters in the regression at any stage in adding (or deleting) parameters to improve fit.

The F-ratio tests are based on quotients of regression "fit" to error "fit." The quantity,

$$\begin{aligned} R^2 &= \frac{(X\hat{\theta})^T (X\hat{\theta})}{y^T y} \\ &= \hat{y}^T \hat{y} / y^T y \end{aligned} \quad (4.31)$$

measures the regression sum of squares to observation sum of squares. The positive square root of Eq. (4.31),  $R$ , is the multiple correlation coefficient. The closer  $R$  is to unity, the better the performance of the subset of regression variables. Note that  $R$  is the cosine of the angle between the data vector and the  $p$  dimensional subspace spanned by the included subset of regression variables.

From the sum of squares decomposition (4.20), and Eq. (4.31), it may be shown that

$$F = \frac{R^2/p-1}{(1-R^2)/(m-p)} \quad (4.32)$$

which expresses the F-ratio in terms of  $R^2$ .

The closer  $R$  is to unity, the stronger the dependence of the data on the regression parameters and the higher the F-value. If there is little dependence,  $R$  is "small," the hypothesis  $\theta_i = 0$  is "correct," and  $F$  is "small."

This test is dependent on choosing a critical value of  $F$  which specifies the cutoff levels. This critical  $F$  is chosen as a function of  $m$  (number of observations) and  $p$  (number of parameters) from tables of  $F$  statistical tables for a desired confidence level. The confidence level can be selected on the basis of a priori knowledge about level of noise in data.



Significance of individual conditions to the regression equations.- The multiple correlation coefficient measures the dependence of the data on the complete set of regression variables. If several sets of parameters are to be evaluated with respect to their respective explanations of the data, the R coefficient would serve as one measure of relative performance. Unfortunately, it follows from the definition of R that increasing the number of explanatory variables always increases R, unless the added variables are linearly related to other included variables. Beyond a certain point, the added variables start fitting the random noise  $\epsilon$ . For example, if the number of variables is increased to m, a perfect fit can be obtained and R is one. In order to eliminate parameters not significant, only the most linearly independent variables are desired.

Stated in terms of the sum of squares principal, it is desired to incorporate those new variables into the regression which most reduce the error, given that the other variables are included in the regression. If the increase in regression sum of squares due to adding a new variable, say  $x_j$ , after variables  $x_i$  have been included in the regression, is denoted as  $\Delta ||\hat{y}||$ , then the ratio

$$R_{yx_j \cdot x_1, x_2, \dots, x_{j-1}, x_{j+1}, \dots, x_p}^2 = \frac{\Delta ||\hat{y}||}{\hat{\epsilon}^T \hat{\epsilon} + \Delta ||\hat{y}||} \quad (4.33)$$

measures the partial contribution of  $x_j$  to the regression. The square root of  $R_{yx_j \cdot x_1, \dots, x_p}^2$  is the partial correlation coefficient. Several forms of this definition may be written. One is defined by letting  $\tilde{y}$  be the residuals from the regression of  $x_j$  on the same variables. It may then be shown

$$R_{\tilde{y}\tilde{x}_j}^2 = \frac{(\sum \tilde{y}\tilde{x}_j)^2}{(\sum \tilde{x}_j^2)(\sum \tilde{y}^2)} \quad (4.34)$$

Note that, in general,  $\sum_j R_{\tilde{y}\tilde{x}_j}^2 \neq R^2$ .

Now, let the regression equation  $y = X\theta + \epsilon$  be partitioned as

$$y = X_1\theta_1 + X_2\theta_2 + \epsilon \quad (4.35)$$

where  $X_1$  includes  $q$  variables and  $X_2$  contains  $p-q$  variables. Then

$$y - X_1\theta_1 = X_2\theta_2 + \epsilon \quad (4.36)$$

which shows that an estimate of  $\theta_2$  could be obtained by regressing the residuals from the regression of  $y$  on  $X_1$  (i.e., which estimates  $\theta_1$ ). Then the vector  $y - X_1\theta_1$  is regressed as a new observation, say  $y^{(1)}$ , which may be regressed on  $X_2$  to estimate  $\theta_2$ . This decomposition can be applied to each possible subset of variables,  $X_i$ , "bringing in" new variables from the right to left hand side of Eq. (4.36). The requirement on "bringing in" new variables may be satisfied by examining the significance of each variable.

The  $F$  test may be used to determine the significance of a single parameter by noting the estimate of the variance  $\sigma^2$ ,  $s^2$ , is distributed as  $\sigma^2 \chi_{m-p}^2$ . Hence,  $s^2/\sigma^2 \sim (\chi_{m-p}^2)/(m-p)$  from Eq. (4.19). Then for the parameter  $\theta_i$ ,

$$\frac{\hat{\theta}_i - \theta_i}{s_{\theta_i}} = \frac{(\hat{\theta}_i - \theta_i)/\sigma_{\theta_i}}{s_{\theta_i}/\sigma_{\theta_i}} \quad (4.37)$$

where  $s_{\theta_i}$  is the standard error of  $\theta_i$ , which, from Eq. (4.20) is

$$s_{\theta_i} = s \sqrt{s_{ii}} \quad (4.38)$$

where  $s_{ii}$  is the square root of the  $i$ th diagonal term of  $(X^T X)^{-1}$ .

Since  $(\hat{\theta}_i - \theta_i)/\sigma_{\theta_i} \sim n(0,1)$ , it follows that, by definition of Student's  $t$  distribution that

$$\frac{\hat{\theta}_i - \theta_i}{s_i} \sim t_{m-p} \quad (4.39)$$

In particular, if it is desired to test the hypothesis  $\theta_i = 0$  (i.e.,  $y$  does not depend on  $\theta$ ), the statistic  $t = \theta_i/s_{\theta_i}$  is used. It is shown [23] that the F distribution with 1 and  $(m-p)$  degrees of freedom is equivalent to the  $t^2$  distribution with  $m-p$  degrees of freedom. Hence, the significance of individual regression coefficients,  $\theta$ , is determined from F-ratios

$$F = \theta_i^2/s_i^2 \quad (4.40)$$

If the ratio (4.40) indicates a variable is not significant, then the variable is deleted. To bring in another variable, the partial correlation coefficients of all other parameters are examined. To form the F-ratio for these coefficients, Eq. (4.33) (with Eq. (4.38)) may be manipulated to show

$$R_{\tilde{y}\tilde{x}_j}^2 = \frac{(\theta_j/s_{\theta_j})}{(\theta_j/s_{\theta_i})^2 + (m-q)} \quad (4.41)$$

where  $q$  is the number of variables already in the regression. The corresponding F-test is

$$F_j = \frac{r_{\tilde{y}\tilde{x}_j}^2 (m-q)}{1 - r_{\tilde{y}\tilde{x}_j}^2} \quad (4.42)$$

The variable (F-ratio with 1 and  $m-q$  degrees of freedom), is calculated for each of the remaining variables. The variable with the highest value is then brought into the regression.

Summary.- The variables  $x_1, x_2, \dots, x_p$  are postulated as possible causative factors in determining the observed data,  $y$  (Eq. (4.35)). The variables  $x_1, x_2, \dots, x_p$  are ranked according to the magnitude of their individual partial

correlation coefficients with  $y$ . The variables with the highest significance ( $F$  to enter) is added to the regression. The significance of the added parameter is then tested to determine if it is above the critical  $F$  value for deletion (Eq. (4.40)). As variables are entered, new  $F$ -ratios are computed from the remaining variables not in the regression since the degrees of freedom have been reduced. This process is terminated when no new variables satisfy the  $F$ -ratio required to enter and when one is to be removed.

At each variable incorporation, the multiple correlation coefficient ( $R$ , Eq. (4.31)), the equation  $F$ -ratio (Eq. (4.32)), and the standard error of the entered parameter (Eq. (4.38)) are all included.

It is noted that, in general, the particular variables finally selected are not unique. Use of orthogonal variables would result in uniqueness.

Numerical methods.- The previous sections have demonstrated that both classical and subset regression parameters are obtainable from steps in the solution of a set of linear equations (ref. Eq. (4.15)). In order to reinforce this connection, consider the augmented data-coefficient matrix (with rank  $p+1$ )

$$A = \begin{bmatrix} X^T X & X^T y \\ y^T X & y^T y \end{bmatrix}$$

Using the inversion of Eq. (4.15), it is found that the final element of  $A^{-1}$ ,  $a^f$ , is

$$\begin{aligned} a^f &= \frac{1}{y^T y - y^T X (X^T X)^{-1} X^T y} = \frac{1}{y^T y - \theta^T X^T X} \\ &= \frac{1}{(1 - R^2) y^T y} \end{aligned}$$

i.e., the multiple correlation coefficient (and the sum of squares  $||\hat{\epsilon}||$ ) are directly obtainable. Similarly, it is found that the diagonal element of  $(X^T X)^{-1}$  corresponding to the  $i$ th coefficient of  $x$ , is

$$(X^T X)_{ii}^{-1} = \frac{1}{(1 - P_i^2) \bar{x}_i^T \bar{x}_i}$$

where  $P_i^2$  is the multiple correlation coefficient of the regression of  $x_k$  on  $x_1, x_2, \dots, x_{i-1}, x_{i+1}, \dots, x_p$ . It may be further shown that the variance of  $\hat{\theta}_i$  is

$$\text{var } \hat{\theta}_i = \sigma^2 (X^T X)_{ii}^{-1} = \frac{\sigma^2}{(1 - P_i^2) \bar{x}_i^T \bar{x}_i}.$$

Computationally, the inversion of  $A$  is based on the Gauss-Jordan pivot algorithm. Let the  $k$ th diagonal element of  $A$  be nonzero. Applying a Gauss-Jordan pivot on this element is a new matrix whose  $ij$ th element is  $\tilde{a}_{ij}$ , i.e.,

$$\tilde{a}_{ij} = \begin{cases} a_{ij} - a_{ik} a_{kj} / a_{kk} & i \neq k, j \neq k \\ -a_{ik} / a_{kk} & i \neq k, j = k \\ a_{kj} / a_{kk} & i = k, j \neq k \\ 1 / a_{kk} & i = k, j = k \end{cases}$$

The final result of this inversion is the matrix  $B$ ,

$$B = \begin{bmatrix} (X^T X)^{-1} & \hat{\theta} \\ -\hat{\theta}^T & ||\hat{\epsilon}|| \end{bmatrix}$$

The recursive algorithm of the Gauss-Jordan pivot sweeps through the  $A$  matrix, generating statistical parameters which guide the deletion and addition of new variables. Details of this selection for the Gauss-Jordan pivot are found in Ref. 24. One further parameter of this method is the tolerance. This is a parameter of the computation algorithm itself and is a measure of the accuracy of the calculations and computer. If  $\bar{a}_{ii}$  is the value of the  $i$ th diagonal element of the non-negative matrix  $(a_{ij})$  after pivoting on several elements, then  $\bar{a}_{ii} / a_{ii}$  is the tolerance.

## CHAPTER V

### ROTORCRAFT PARAMETER ESTIMATION

#### Introduction

Rotorcraft parameter identification is the process of extracting the stability and control derivatives for a given mathematical model structure using a set of flight test or simulated data. In the past, aircraft identification has been carried out as an ancillary part of experimental flight test work. The principal source of stability and control derivatives has always been wind tunnel results and theoretical calculations. However, as the result of what is often gross disagreement between wind tunnel and flight test derivatives, and the known difficulties of obtaining wind tunnel values, as well as extrapolating these values to full scale, there is an increasing emphasis on obtaining these parameters from actual flight data.

In the field of system identification, most of the effort had been, for a number of years, confined to the solution of low order linear problems. However, during the past few years, powerful digital techniques have been developed which are capable of solving the more difficult nonlinear aircraft problems. The problem of extracting aerodynamic coefficients for rotorcraft is one of the most difficult identification problems.

The development of accurate parameter estimation is a logical step following model structure determination. This is because the model structure estimation step (described in the previous chapter) gives a reasonable model of rotorcraft forces, moments and other dynamic parameters, but the estimates of parameters resulting from the least square approach may be of questionable accuracy. Several procedures have been used for estimating nonlinear system parameter in the past. Because of the complexity of rotorcraft dynamics, the selection of an appropriate identification method is extremely important. This chapter discusses various identification methods pointing out the advantages and disadvantages of each. Finally, one method is selected for further investigation.

#### Rotorcraft Parameter Estimation Approaches

General discussion.- Most identification methods that have been or are currently being applied to rotorcraft problems can be classified as either:

- (1) equation error methods,
- (2) output error methods, or
- (3) advanced methods.

These methods differ by: (1) the performance criterion that they are developed from, (2) the kind of estimates they produce, and (3) the problems to which they can be applied.

Equation error methods [25] assume a performance criterion that minimizes the equation error squared (the process noise). All of these methods are basically least squares techniques. In general, it is necessary to measure the response variables and their time derivatives to apply these methods. This results in  $n$  or more linear equations in  $n$  unknowns. For the case where the time derivatives are not measured, various "method functions" are used to operate on the equations (e.g., time derivatives, Laplace or Fourier transforms, etc.), to obtain equations that are linear in the unknowns. Since these methods do not allow for measurement errors (sensor noise, etc.) they result in biased estimates when this type of error does exist. The principal use of these methods are as start-up techniques for the output error and advanced methods. The equation error methods have been used or are being used by Calspan Corp. [25], Air Force Flight Test Center [26], and by Gerlach [27].

Output error methods [28-33] minimize the square of the error between the actual system output and the output of a model. These methods assume measurement noise but no process noise. Typical output error methods include Newton-Raphson; Gradient methods; the Kalman filter (without process noise); and modified Newton-Raphson, differential correction, and quasilinearization (all three of which are the same method).

It should be noted that analog matching is basically a manual form of the output error methods (it attempts to match the simulated response to the actual response). This method has been used by the Air Force Flight Test Center [26], the Naval Air Test Center [34], and the NASA-Dryden Flight Research Center [35] for the F-104, X-15, B-70, HL-10, M2/Fe, X-24, and PA-30 aircraft. The modified Newton-Raphson method has been used extensively in flight test applications for the past several years. It is the one method that has been used on an operational basis and for which the most experience exists. It is known that this method has been or is being used by: (1) the NASA Dryden Flight Research Center [35] on lifting bodies (X-24, F-3, X-14, SB-70, 990, HL-10, M2/F3), Jet Star

and PA-30 aircraft, (2) the NASA Ames Research Center [36] on the Learjet, XV-5, 990, and C-8 aircraft, and (3) the NASA Langley Research Center [37] on the XC-142, Navion and F-4 aircraft.

The principal disadvantage of output error methods is that, because they do not include process noise in their performance criterion, the results degrade when process noise (gusts, modeling errors) exists. This may result in the program not converging or in estimates that have large variances or poor estimates [38]. However, as long as these methods are applied to linear flight regions, or where the form of the equations are known, and where gusts are not significant, they work very well.

There are two advanced methods which have been applied to flight data with both process and measurement noise. These are:

- (1) The Kalman filter and smoother [39-41]
- (2) The maximum likelihood method [42-47]

Because of the advanced nature of these algorithms, they are discussed in some detail in the following subsections.

Extended Kalman filter/smoothing parameter identification methods.- In 1961-1962, R.E. Kalman published a sequence of papers in which he proposed a filter with the capability of estimating randomly disturbed states of a system from noisy measurements. The Kalman filter has, since then, been the object of intense research and development. It is significant to note that the Kalman filter for state estimation is a particular solution to a more general problem of estimating both unknown states and parameters of a dynamical system. Kalman, himself, suggested in this early work that the filter could be adapted for estimation of the parameters as well as the states by simply augmenting the parameters to the state and estimating both simultaneously. This is still the first approach that is usually tried in developing parameter identification algorithms, because it does have a strong intuitive and simple implementation. Unfortunately, the approach is found to suffer from certain inherent problems in actual implementation, particularly for high order systems perturbed by both process and measurement noise.

There is a simple reason for the difficulties encountered by this approach. The Kalman filter is strictly a state estimator derived on the assumption of known parameters. Assuming a filter of the Kalman type for also estimating the parameters is an "after-the-fact" adjustment. Practically, the result is that to apply the Kalman filter to even a



linear system requires that the linear system be converted into a nonlinear system. Although this transformation does not, in itself, degrade the algorithm effectiveness, it does cause other problems which can. Other problems which are reported are;

- (1) The Kalman filter approach, even with the algorithm modifications such as smoothing, produces biased estimates of the parameters [41]. Hence, the parameter estimates may be in error.
- (2) Any Kalman filter algorithm requires initial guesses for both states and parameters, as well as their respective state and parameter variances [39,41]. The necessity for providing good state variances is not a severe limitation. However, parameter variances are usually much harder to guess than state variances. Unfortunately, the Kalman filter approach does require accurate parameter variance initiation to obtain good estimates. A common technique is to use initial guesses and variance obtained from a least squares regression on the data. These results are biased, however, and in order to account for bad guesses, arbitrary variance multiplication "factors" must be used to ensure even algorithm convergence [41]. Such "guesses" for each type of case run require highly skilled personnel.
- (3) The Kalman filter approach is often claimed to estimate parameters in the presence of process noise, even though there is no theoretical justification for its ability to do so. What is done is actually to either filter the data by some smoothing technique or simply adjust the process noise covariance terms of the filter until convergence is achieved. Molusis [39] uses the smoothing approach to filter the data. The problem with this approach is that the resulting data may contain less information about the parameters of interest, again causing errors in the estimates. The iterating smoothing approach suggested by Chen, et al. [41] is probably the best implementation of extended Kalman filter for parameter estimation.

Maximum likelihood methods.- The previous section alluded to the fact that the Kalman filter for state estimation is a particular solution of the more general problem of simultaneous state and parameter estimation. Realizing the difficulties of trying to use the Kalman filter approach in practical application, a return to the original formulation of the simultaneous state and parameter estimation problem leads to a more general estimator. This formulation--a maximum likelihood approach--is one of the ways a Kalman filter state estimator is derived. The maximum likelihood method is illustrated in Figure 5.1. Conceptually, this technique can be summarized as follows:

"Find the probability density functions of the observations for all possible combinations of unknown parameter values. Select the density function whose value is highest among all density functions at the measured values of the observations. The corresponding parameter values are the maximum likelihood estimates."

The method is a combination of three steps:

- (1) A Kalman filter to estimate the states.
- (2) A Levenberg-Marquardt optimization technique for the parameter estimates.
- (3) An algorithm to estimate the noise statistics (mean and variance of the measurement and process noise).

The method has the following important features:

- (1) Parameter Estimate Variances. In estimating parameters from flight data, it is essential to predict the error in these estimates, that is, the confidence level associated with the estimates. The maximum likelihood method automatically computes the lower bounds on the variances of the parameter estimates. Since the maximum likelihood estimate is asymptotically efficient, the actual variances in the parameter estimates approach these bounds for long data records. The method does not require initial parameter variances to initialize the algorithm.

FLIGHT TEST DATA, WIND TUNNEL VALUES OF  
AERODYNAMIC PARAMETERS

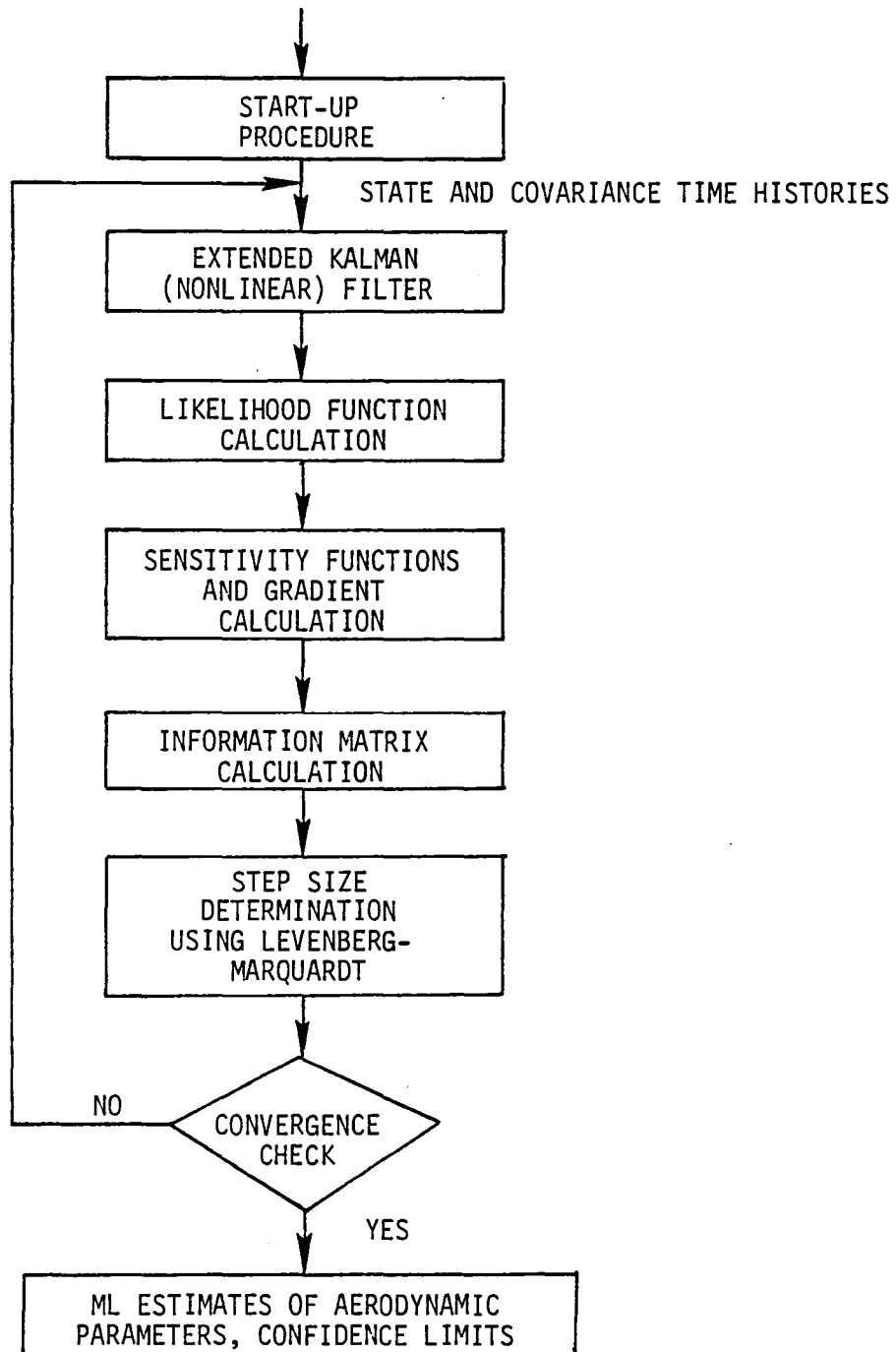


FIGURE 5.1.— FLOWCHART OF MAXIMUM LIKELIHOOD IDENTIFICATION PROGRAM

- (2) Noise Statistics. Many identification algorithms assume that the means and variances of the process and measurement noise are known. In fact, these quantities are generally not known and should be identified. Typical noise parameters that should be identified include sensor biases, c.g. offsets, the variance of the random measurement noise, and the mean and variance of the  
  
require a priori knowledge of the process or measurement noise covariances but determines them as part of the identification procedure.
- (3) State Estimates. In addition to estimating the parameters of the aircraft models (stability and control derivatives), it is also necessary to estimate the airplane response variables (state variables). The maximum likelihood method obtains the best mean square state estimates as part of the parameter identification process.

In addition, the generality of the maximum likelihood method has important operational features:

- (1) In the absence of process noise, the method is equivalent to the output error method which many flight test agencies already use.
- (2) In the absence of measurement noise, the maximum likelihood method reduces to a least squares approach.
- (3) The method requires no "fine tuning" or "fiddling" to provide estimates for new cases.

#### Rotorcraft Parameter Identification Method

It is clear from the discussions of the previous section that the maximum likelihood provides an optimal blend of optimality and flexibility in rotorcraft identification problems. It is for this reason that the maximum likelihood method has been selected for investigation in rotorcraft applications. The maximum likelihood method is one of the most flexible techniques in statistics for identification of parameters from input-output data. Suppose it is possible

to make a set of observations on a system, whose model has  $p$  unknown parameters  $\theta$ . For any given set of values of the parameters  $\theta$  from the feasible set  $\Theta$ , we can assign a probability  $p(Z|\theta)$  to each outcome  $Z$ . If the outcome of an actual experiment is  $z$ , it is of interest to know which sets of values of  $\theta$  might have led to these observations. This concept is embedded in the likelihood function  $\mathcal{L}(\theta|z)$ . This function is of fundamental importance in estimation theory because of the likelihood principle of Fisher and others [48-50] which states that if the system model is correct, all information about unknown parameters is contained in the likelihood function. The maximum likelihood method finds a set of parameters  $\hat{\theta}$  to maximize this likelihood function

$$\hat{\theta} = \max_{\theta \in \Theta} \mathcal{L}(\theta|z) \quad (5.1)$$

In other words, the probability of the outcome of  $z$  is higher with parameters  $\hat{\theta}$  in the model than with any other values of parameters from the feasible set. Usually it is more convenient to work with the logarithm of the likelihood function (it is possible to do so because the logarithm is a strictly monotonic function).

Consider a nonlinear rotorcraft of the following form

$$\dot{x} = f(x,u,\theta,t) + \Gamma(\theta,t)w \quad 0 \leq t \leq T$$

$$E[x(0)] = x_0(\theta)$$

$$E\{[x(0) - x_0(\theta)][x(0) - x_0(\theta)]^T\} = P_0(\theta)$$

where

$x(t)$  is  $n \times 1$  state vector

$u(t)$  is  $l \times 1$  input vector

$\theta$  is  $p \times 1$  vector of unknown parameters

$\Gamma$  is  $n \times q$  process noise distribution matrix

$w(t)$  is  $q \times 1$  random process noise vector

Let there be  $m$  measurements  $y(t_k)$  taken at discrete times  $t_k$

$$y(t_k) = h(x(t_k), u(t_k), \theta, t_k) + v(t_k)$$

$$k = 1, 2, 3, \dots, N$$

$w(t)$  and  $v(t_k)$  are Gaussian random noises with the following properties

$$E[w(t)] = 0 \quad E[v(t_k)] = 0 \quad E[w(t) v^T(t_k)] = 0$$

$$E[w(t) w^T(\tau)] = Q(\theta, t) \delta(t - \tau),$$

$$E[v(t_j) v^T(t_k)] = R(\theta, t_j) \delta_{jk}$$

The log-likelihood function for this mathematical model can be shown to be of the form

$$\log[\mathcal{L}(\theta|z)] = -\frac{1}{2} \sum_{i=1}^N \{v^T(i) B^{-1}(i) v(i) + \log|B(i)|\}$$

where  $v(i)$  is the innovations vector at sample point  $t_i$  and  $B(i)$  is its covariance. An estimate of the unknown parameters is obtained by maximizing the likelihood function or the log-likelihood function from the feasible set of parameter values

$$\hat{\theta} = \max_{\theta \in \Theta} \log [\mathcal{L}(\theta|z)] \quad (5.2)$$

$$= \max \left[ -\frac{1}{2} \sum_{i=1}^N \{v^T(i) B^{-1}(i) v(i) + \log|B(i)|\} \right] \quad (5.3)$$

The log-likelihood function depends on the innovations and their covariance. To optimize the likelihood function, a

way must be found for determining these quantities. Both innovations and their covariance are outputs of an extended Kalman filter. The developments of the required Kalman filter is discussed in subsequent paragraphs.

The extended Kalman filter is conventionally divided into two parts. In the first part, called the prediction equations, the state equations and state estimate covariance equations are propagated in time from one measurement point to the next. In the second part, called the measurement update equations, the measurements and associated measurement noise covariances are used to improve state estimates. The covariance matrix is also updated at this point to reflect the additional information obtained from the measurements.

Prediction equations.— The state prediction is done using the equations of motion. Starting at time  $t_{i-1}$  with current estimate  $\hat{x}(i-1|i-1)$  of the state  $x(t_i)$  and the covariance  $P(i-1|i-1)$ , the following equations are used to find the predicted state  $\hat{x}(i|i-1)$  and the associated covariance  $P(i|i-1)$ ; see Bryson and Ho (Ref. 10).

$$\frac{d}{dt} \hat{x}(t|t_{i-1}) = f(\hat{x}(t|t_{i-1}), u(t), \theta, t) \quad (5.4)$$

$$\dot{P}(t|t_{i-1}) = F(t) P(t|t_{i-1}) + P(t|t_{i-1}) F^T(t) + \Gamma Q \Gamma^T \quad (5.5)$$

$$t_{i-1} \leq t \leq t_i$$

The  $n \times n$  matrix  $F$  is obtained by linearizing  $f$  about the best current estimate

$$F(t) = \frac{\partial f(\hat{x}(t|t_{i-1}), u(t), \theta, t)}{\partial \hat{x}(t|t_{i-1})} \quad (5.6)$$

Using (5.4) to (5.6), we can obtain

$$\hat{x}(t_i|t_{i-1}) \triangleq \hat{x}(i|i-1) \quad (5.7)$$

$$P(t_i|t_{i-1}) \triangleq P(i|i-1) \quad (5.8)$$

Thereafter, the measurement update equations are used.

Measurement update equations.— The covariance and state estimate are updated using the measurements. The necessary relations are derived by Bryson and Ho (ref. 10) and are presented here without proof. The innovation and its covariance are

$$v(i) = y(i) - h(\hat{x}(i|i-1), u(t_i), \theta, t_i) \quad (5.9)$$

$$B(i) = H(i) P(i|i-1) H^T(i) + R \quad (5.10)$$

where H is obtained by linearizing h,

$$H(i) = \frac{\partial h(\hat{x}(i|i-1), u(t_i), \theta, t_i)}{\partial \hat{x}(i|i-1)} \quad (5.11)$$

The Kalman gain and the state update equations are

$$K(i) = P(i|i-1) H^T(i) B^{-1}(i) \quad (5.12)$$

$$\hat{x}(i|i) = \hat{x}(i|i-1) + K(i) v(i) \quad (5.13)$$

Finally,  $P(i|i)$ , the covariance of error in updated state, is obtained by

$$P(i|i) = (I - K(i) H(i)) P(i|i-1) \quad (5.14)$$

The maximum likelihood method can be shown to reduce to output error in the absence of process noise. If there is no measurement noise, it reduces to the equation error method. These simplifications are discussed in Appendix A.

Optimization procedure.— It is possible to use any one of several numerical procedures for this optimization problem. The authors have found by experience that the Levenberg-Marquardt optimization technique provides the most rapid convergence. This technique has both the Newton-Raphson and the steepest descent algorithms as special cases. The general Levenberg-Marquardt approach is discussed in references [51 and 52]. The algorithm requires computation of the first and second order partials of the log-likelihood function.



$$\begin{aligned}
\frac{\partial \log (\mathcal{L}(\theta|z))}{\partial \theta_j} &= - \sum_{i=1}^N \left\{ v^T(i) B^{-1}(i) \frac{\partial v(i)}{\partial \theta_j} \right. \\
&\quad - \frac{1}{2} v^T(i) B^{-1}(i) \frac{\partial B(i)}{\partial \theta_j} B^{-1}(i) v(i) \\
&\quad \left. + \frac{1}{2} \text{Tr} \left( B^{-1}(i) \frac{\partial B(i)}{\partial \theta_j} \right) \right\}
\end{aligned} \tag{5.15}$$

Also

$$\begin{aligned}
\frac{\partial^2 \log (\mathcal{L}(\theta|z))}{\partial \theta_j \partial \theta_k} &= - \sum_{i=1}^N \left\{ \frac{\partial v^T(i)}{\partial \theta_k} B^{-1}(i) \frac{\partial v(i)}{\partial \theta_j} \right. \\
&\quad - \frac{\partial v^T(i)}{\partial \theta_j} B^{-1}(i) \frac{\partial B(i)}{\partial \theta_k} B^{-1}(i) v(i) \\
&\quad - \frac{\partial v(i)}{\partial \theta_j} B^{-1}(i) \frac{\partial B(i)}{\partial \theta_k} B^{-1}(i) v(i) \\
&\quad + v^T(i) B^{-1}(i) \frac{\partial B(i)}{\partial \theta_j} B^{-1}(i) \frac{\partial B(i)}{\partial \theta_k} B^{-1}(i) v(i) \\
&\quad - \frac{1}{2} \text{Tr} \left[ B^{-1}(i) \frac{\partial B(i)}{\partial \theta_j} B^{-1}(i) \frac{\partial B(i)}{\partial \theta_k} \right] \\
&\quad + \frac{\partial^2 v(i)}{\partial \theta_j \partial \theta_k} B^{-1}(i) v(i) \\
&\quad - v^T(i) B^{-1}(i) \frac{\partial^2 B(i)}{\partial \theta_j \partial \theta_k} B^{-1}(i) v(i) \\
&\quad \left. + \frac{1}{2} \text{Tr} \left( B^{-1}(i) \frac{\partial^2 B(i)}{\partial \theta_j \partial \theta_k} \right) \right\} \quad j, k = 1, 2, \dots, p
\end{aligned}$$

The last three terms in the equation for second partial of the the log-likelihood function involve second partials of innovation and its covariance. Those terms are usually dropped. So, the second partial is approximated by

$$\begin{aligned}
\frac{\partial^2 \log(\mathcal{L}(\theta|z))}{\partial\theta_j \partial\theta_k} \cong & - \sum_{i=1}^N \left\{ \frac{\partial v^T(i)}{\partial\theta_j} B^{-1}(i) \frac{\partial v(i)}{\partial\theta_k} \right. \\
& - \frac{\partial v^T(i)}{\partial\theta_k} B^{-1}(i) \frac{\partial B(i)}{\partial\theta_j} B^{-1}(i) v(i) \\
& - \frac{\partial v(i)}{\partial\theta_j} B^{-1}(i) \frac{\partial B(i)}{\partial\theta_k} B^{-1}(i) v(i) \\
& + v^T(i) B^{-1}(i) \frac{\partial B(i)}{\partial\theta_j} B^{-1}(i) \frac{\partial B(i)}{\partial\theta_k} B^{-1}(i) v(i) \\
& \left. - \frac{1}{2} \text{Tr} \left[ B^{-1}(i) \frac{\partial B(i)}{\partial\theta_j} B^{-1}(i) \frac{\partial B(i)}{\partial\theta_k} \right] \right\}
\end{aligned} \tag{5.16}$$

The gradients of innovation and its covariance for parameter  $\theta_j$  are:

$$\frac{\partial v(i)}{\partial\theta_j} = - \frac{\partial h}{\partial x} \Big|_{x=\hat{x}(i|i-1)} \frac{\partial \hat{x}(i|i-1)}{\partial\theta} - \frac{\partial h}{\partial\theta} \tag{5.17}$$

$$j = 1, 2, \dots, p; \quad i = 1, 2, \dots, N$$

$$\begin{aligned}
\frac{\partial B(i)}{\partial\theta_j} = & \frac{\partial H(i)}{\partial\theta_j} P(i|i-1) H^T(i) + H(i) \frac{\partial P(i|i-1)}{\partial\theta_j} H^T(i) \\
& + H(i) P(i|i-1) \frac{\partial H^T(i)}{\partial\theta_j} + \frac{\partial R}{\partial\theta_j}
\end{aligned} \tag{5.18}$$

$$j = 1, 2, \dots, p; \quad i = 1, 2, \dots, N$$

Recursive equations can be obtained for gradients of the predicted state and its covariance. This is done in stages by using the prediction and measurement update equations of Kalman filter. Differentiating (5.4) to (5.6) with respect to  $\theta_j$

$$\begin{aligned} \frac{d}{dt} \frac{\partial \hat{x}(t|t_{i-1})}{\partial \theta_j} &= \frac{\partial f(\hat{x}(t|t_{i-1}), u(t), t, \theta)}{\partial \theta_j} \\ &+ \frac{\partial f(\hat{x}(t|t_{i-1}), u(t), t, \theta)}{\partial \hat{x}(t|t_{i-1})} \times \frac{\partial \hat{x}(t|t_{i-1})}{\partial \theta_j} \end{aligned} \quad (5.19)$$

$$\frac{\partial \hat{x}(0|0)}{\partial \theta_j} = \frac{\partial x_0(\theta)}{\partial \theta_j}$$

$$\begin{aligned} \frac{d}{dt} \frac{\partial P(t|t_{i-1})}{\partial \theta_j} &= \frac{\partial F(t)}{\partial \theta_j} P(t|t_{i-1}) + F(t) \frac{\partial P(t|t_{i-1})}{\partial \theta_j} \\ &+ \frac{\partial P(t|t_{i-1})}{\partial \theta_j} F^T(t) + P(t|t_{i-1}) \frac{\partial F^T(t)}{\partial \theta_j} + \frac{\partial \Gamma}{\partial \theta_j} Q \Gamma^T \\ &+ \Gamma \frac{\partial Q}{\partial \theta_j} \Gamma^T + \Gamma Q \frac{\partial \Gamma^T}{\partial \theta_j} \end{aligned} \quad (5.20)$$

$$\frac{\partial P(0|0)}{\partial \theta_j} = \frac{\partial P_0(\theta)}{\partial \theta_j} \quad t_{i-1} \leq t \leq t \quad (5.21)$$

$$\frac{\partial F(t)}{\partial \theta} = \frac{\partial^2 f(\hat{x}(t|t_{i-1}), u(t), \theta, t)}{\partial \theta_j \partial \hat{x}(t|t_{i-1})} \quad j = 1, 2, \dots, p$$

The sensitivity functions are updated at measurement points by differentiating (5.11) to (5.14) with respect to  $\theta_j$ .

$$\frac{\partial H(i)}{\partial \theta_j} = \frac{\partial^2 h(\hat{x}(i|i-1), u(t_i), \theta, t_i)}{\partial \theta_j \partial \hat{x}(i|i-1)} \quad (5.22)$$

$$\begin{aligned} \frac{\partial K(i)}{\partial \theta_j} &= \frac{\partial P(i|i-1)}{\partial \theta_j} H^T(i) B^{-1}(i) + P(i|i-1) \frac{\partial H^T(i)}{\partial \theta_j} B^{-1}(i) \\ &- P(i|i-1) H^T(i) B^{-1}(i) \frac{\partial B(i)}{\partial \theta_j} B^{-1}(i) \end{aligned} \quad (5.23)$$

$$\frac{\partial \hat{x}(i|i)}{\partial \theta_j} = \frac{\partial \hat{x}(i|i-1)}{\partial \theta_j} + \frac{\partial K(i)}{\partial \theta_j} v(i) + K(i) \frac{\partial v(i)}{\partial \theta_j} \quad (5.24)$$

$$\begin{aligned} \frac{\partial P(i|i)}{\partial \theta_j} &= I - K(i) H(i) \frac{\partial P(i|i-1)}{\partial \theta_j} - \frac{K(i)}{\partial \theta_j} H(i) P(i|i-1) \\ &- K(i) \frac{\partial H(i)}{\partial \theta_j} P(i|i-1) \end{aligned} \quad (5.25)$$

$$j = 1, 2, 3, \dots, p$$

The negative of the matrix of second partials of the log-likelihood function is called the information matrix  $M$ . The step size  $\Delta\theta$  for parameter estimates is given by

$$\Delta\theta = p(M + \alpha I)^{-1} \frac{\partial \log(\mathcal{L}(\theta|z))}{\partial \theta} \quad (5.26)$$

where  $\alpha$  is the Marquardt parameter and  $p$  is a scaling term. Observe that as  $\alpha \rightarrow 0$  the step approaches that of the Gauss-Newton procedure. As  $\alpha \rightarrow \infty$  (with  $p/\alpha$  finite) the step approaches that for the steepest descent algorithm. During the optimization, it is desirable to change the Marquardt parameter to promote rapid convergence. If it is found that the step is too large (i.e., the log-likelihood cost increases), the step is cut by increasing the Marquardt parameter by a given factor and another step is taken. If the cost decreases, the Marquardt parameter is decreased by the given factor so that the following step is larger. This is to prevent the slow convergence that results from taking a small step — as is often characteristic of steepest gradient algorithms.

Linear systems.— In a linear system, the functions  $f$  and  $h$  are defined as

$$f(x,u,\theta,t) \triangleq F(\theta,t)x + G(\theta,t)u$$

$$\text{and } h(x,u,\theta,t) \triangleq H(\theta,t)x + D(\theta,t)u$$

The basic algorithm is the same. However, some of the equations can now be simplified. Equations (5.4) and (5.9) now become

$$\frac{d}{dt} \hat{x}(t|t_{i-1}) = F(\theta,t) \hat{x}(t|t_{i-1}) + G(\theta,t) u(t) \quad (5.27)$$

and

$$v(i) = y(i) - H(\theta,t_i) \hat{x}(i|i-1) - D(\theta,t_i) u(t_i) \quad (5.28)$$

Equations (5.17) and (5.19) can be written as

$$\begin{aligned} \frac{\partial v(i)}{\partial \theta_j} = & - H(\theta,t_i) \frac{\partial \hat{x}(i|i-1)}{\partial \theta_j} - \frac{H(\theta,t_i)}{\partial \theta_j} \hat{x}(i|i-1) \\ & - \frac{\partial D(\theta,t_i)}{\partial \theta_j} u(t_i) \end{aligned} \quad (5.29)$$

and

$$\begin{aligned} \frac{d}{dt} \frac{\partial x(t|t_{i-1})}{\partial \theta_j} = & F(\theta,t) \frac{\partial \hat{x}(t|t_{i-1})}{\partial \theta_j} + \frac{\partial F(\theta,t)}{\partial \theta_j} \hat{x}(t|t_{i-1}) \\ & + \frac{\partial G(\theta,t)}{\partial \theta_j} u(t) \end{aligned} \quad (5.30)$$

All other equations remain the same.

There is considerable reduction in computation requirement for time-invariant linear system. In this case, matrices  $F$ ,  $G$ ,  $H$ ,  $D$ ,  $\Gamma$ ,  $Q$  and  $R$  and their derivatives with respect to parameters are constant.

For many cases, the Kalman filter is in steady state for the duration of the experiment. This occurs when the Kalman filter is in operation for a sufficiently long time and the process and measurement noise covariances do not change. The Kalman gain and the innovations and the state covariances approach constant values. The time update and measurement update equations for the covariances are

$$\frac{d}{dt} P(t|t_{i-1}) = FP(t|t_{i-1}) + P(t|t_{i-1})F^T + \Gamma Q \Gamma^T \quad (5.31)$$

$$K = P(i|i-1)H^T B^{-1} \quad (5.32)$$

$$B = HP(i|i-1)H^T + R \quad (5.33)$$

$$P(i|i) = (I-KH) P(i|i-1) \quad (5.34)$$

By definition of the steady state

$$P(i-1|i-1) = P(i|i)$$

Therefore, from (5.31)

$$\begin{aligned} P(i|i-1) &= e^{F\Delta t} P(i-1|i-1) e^{F^T\Delta t} + \int_{t_{i-1}}^{t_i} e^{F(t_i-\tau)} \Gamma Q \Gamma^T e^{F^T(t_i-\tau)} d\tau \\ &= e^{F\Delta t} (I-KH) P(i|i-1) e^{F^T\Delta t} + \int_{t_{i-1}}^{t_i} e^{F(t_i-\tau)} \Gamma Q \Gamma^T e^{F^T(t_i-\tau)} d\tau \\ &\triangleq \phi(\Delta t) (I-KH) P(i|i-1) \phi(\Delta t) + Q' \\ &= \phi(\Delta t) (P(i|i-1) - KBK^T) \phi(\Delta t) + Q' \end{aligned} \quad (5.35)$$

Using (5.32), (5.33) and (5.34), we can solve for  $P(i|i-1)$  and then find  $K$  and  $B$ . Also, it can be shown that

$$\frac{\partial P}{\partial \theta_j} = A_1 \frac{\partial P}{\partial \theta} A_1^T + A_2 - \phi P A_3 P \phi^T \quad (5.36)$$

$$\frac{\partial K}{\partial \theta_j} = (I-KH) \frac{\partial P}{\partial \theta_j} H^T (HPH^T + R)^{-1} + A_2 \quad (5.32)$$

$$\frac{\partial B}{\partial \theta_j} = \frac{\partial H}{\partial \theta_j} PH^T + H \frac{\partial P}{\partial \theta_j} H^T + HP \frac{\partial H^T}{\partial \theta_j} + \frac{\partial R}{\partial \theta_j} \quad (5.38)$$

where

$$A_1 = \phi(I-KH)$$

$$A_2 = \frac{\partial \phi}{\partial \theta_j} (I-KH) P \phi^T + \phi(I-KH) P \frac{\partial \phi^T}{\partial \theta_j} - \phi K \frac{\partial H}{\partial \theta_j} P \phi^T + \frac{\partial Q}{\partial \theta_j}$$

$$A_3 = \frac{\partial H^T}{\partial \theta_j} B^{-1} H + H^T B^{-1} \frac{\partial H}{\partial \theta_j} PH^T + HP \frac{\partial H^T}{\partial \theta_j} + \frac{\partial R}{\partial \theta_j} B^{-1} H$$

$$P \triangleq P(i|i-1)$$

Thus, it is possible to solve for  $\frac{\partial P}{\partial \theta_j}$  using (5.36) and then find  $\frac{\partial K}{\partial \theta_j}$  and  $\frac{\partial B}{\partial \theta_j}$  from (5.37) and (5.38). Equation (5.36) is a linear equation in  $\frac{\partial P}{\partial \theta_j}$  and the coefficient of the unknown matrix does not depend on the parameter  $\theta_j$ . Thus, the sensitivity of state covariance matrix can be determined very quickly for all parameters. Once the sensitivity of P, K and B for unknown parameters is determined, only state sensitivity equations need to be updated.

An approximation simplifies the problem further. The unknown parameters are defined to include elements in K and B matrices instead of Q and R. Optimizing the log-likelihood function for parameters in B gives

$$\hat{B} = \frac{1}{N} \sum_{i=1}^N v(i) v^T(i) \quad (5.39)$$

The gradient of the log-likelihood function with respect to other unknown parameters is

$$\frac{\partial \text{Log} (\mathcal{L}(\theta|z))}{\partial \theta_j} = - \sum_{i=1}^N v^T(i) \hat{B}^{-1} \frac{\partial v(i)}{\partial \theta_j} \quad (5.40)$$

The sensitivity of innovations to parameters is determined using the following recursive equations

$$\frac{d}{dt} \hat{x}(t|t_{i-1}) = F\hat{x}(t|t_{i-1}) + Gu(t) \quad (5.41)$$

$$\frac{d}{dt} \frac{\partial \hat{x}(t|t_{i-1})}{\partial \theta_j} = \frac{\partial F}{\partial \theta_j} \hat{x}(t|t_{i-1}) + F \frac{\partial \hat{x}(t|t_{i-1})}{\partial \theta_j} + \frac{\partial G}{\partial \theta_j} u(t) \quad (5.42)$$

$$j = 1, 2, \dots, p \quad t_{i-1} \leq t \leq t_i$$

$$v(i) = y(i) - H\hat{x}(i|i-1) - Du(t_i) \quad (5.43)$$

$$\hat{x}(i|i) = \hat{x}(i|i-1) + Kv(i) \quad (5.44)$$

$$\frac{\partial v(i)}{\partial \theta_j} = - \frac{\partial H}{\partial \theta_j} \hat{x}(i|i-1) - H \frac{\partial \hat{x}(i|i-1)}{\partial \theta_j} - \frac{\partial D}{\partial \theta_j} u(t_i) \quad (5.45)$$

$$\frac{\partial \hat{x}(i|i)}{\partial \theta_j} = \frac{\partial \hat{x}(i|i-1)}{\partial \theta_j} + \frac{\partial K}{\partial \theta_j} v(i) + K \frac{\partial v(i)}{\partial \theta_j} \quad (5.46)$$

$$j = 1, 2, \dots, p$$

Note that

$$\frac{\partial K}{\partial \theta_j} = 0 \quad \text{if } \theta_j \text{ is not an element of } K \text{ matrix}$$

$$= I_{j',k'} \quad \text{if } \theta_j \triangleq K_{j',k'}$$

where  $I_{j',k'}$  is a matrix of all zeroes except a 1 at the  $j',k'$  position.



## CHAPTER VI

### INPUT DESIGN

In previous sections, we have considered aspects of rotorcraft system identification methodology which address the post flight data processing phase. Data are presented to the procedure, and some level of model and coefficient estimation achieved. One does not have to perform this task many times before it is evident that no post-flight data procedure can identify coefficients if the information on these parameters is not in even the uncorrupted measurement response. An input design requirement, therefore, has arisen because of the need to improve the efficiency of flight testing by obtaining more accurate estimates from response data in less time.

#### Requirements for Input Design

There are several factors that must be considered when choosing inputs for flight tests. These include:

(1) Efficiency: The inputs should improve the efficiency of stability and control flight testing by maximizing coefficient identifiability in fewer maneuvers.

(2) Structural and Safety Constraints: The inputs should excite the modes of interest without violating rotorcraft safety and structural constraints.

(3) Identifiability: The inputs selected must improve parameter estimation accuracy and avoid identifiability problems in the post-flight data analysis stages.

(4) Pilot Acceptability: If the flight test is to be carried out with a pilot onboard the rotorcraft, it is necessary that the control inputs be acceptable to the pilot. The inputs should not maneuver the aircraft into a flight regime from which a pilot cannot recover. In addition, the inputs should be reproducible by the pilot.

(5) Instrumentation: The inputs must consider specific instruments available, and their dynamic range and accuracy. The primary impact of the instruments on input design is on the signal/noise ratios which the response must have for sufficiently accurate data.

(6) Modeling Assumptions: The inputs that are designed must also consider the model that is assumed. For example, inputs chosen for a linear mode should not cause such large rotorcraft motions that the assumption of constant stability and control derivatives is invalid.

## Input Design Methods

Since the first efforts of applying parameter extraction technology to aircraft flight test data, many different control inputs have been used. In one approach, the flight vehicle is excited by sinusoidal inputs over a range of frequencies, usually around the natural frequency of the specific mode, until a steady state is reached at each frequency. The parameters of a suitable linear model are selected to obtain the best fit to the variation with input frequency of the output/input amplitude ratio and phase difference. These inputs work satisfactorily but require much flight test time. Pulse inputs have been used to identify simple low order linear systems. Doublets, steps and finite duration pulse inputs have also been used to identify aircraft parameters. However, the estimates of certain parameters may be quite poor and, in some cases, a set of parameters may not be identifiable at all.

The definition of information matrix,  $M$ , which provides a quantitative meaning to the knowledge about a certain set of parameters, is the starting point for a systematic study of the input design problem. The inverse of the information matrix, referred to as dispersion matrix, is a bound on parameter error covariances, i.e.,

$$\text{cov} \{(\theta - \hat{\theta})(\theta - \hat{\theta})^T\} \geq M^{-1} \Delta D$$

where  $\theta$  is the actual value of a parameter and  $\hat{\theta}$  is the estimate. Most of the analytical methods in input design use a function of information or dispersion matrix as the extremizing criterion.

Optimal input design for dynamic systems.— In this section, we describe a method consisting of two different techniques for design of input signals which provides estimates of unknown parameters in linear systems. The first technique used the time domain representation of system dynamics and develops methods to compute the time history of control input sequence for any duration of the experiment. In the second technique, the system is assumed to be in oscillatory steady state and a frequency domain representation is utilized. This gives the optimal control input spectrum. The corresponding time history is "optimal" only for long experiments. The time domain approach is computationally much more complicated than the frequency domain approach. The two approaches are, therefore, complementary. The frequency domain approach is suitable for long experiments and the time domain approach should be used for short and medium duration experiments.

Consider a linear, time-invariant, dynamic system described by the following differential equation:

$$\begin{aligned}\dot{x} &= Ax + Bu \\ x(0) &= 0 \quad 0 \leq t \leq 1\end{aligned}\tag{6.1}$$

where  $x$  is a  $n \times 1$  state vector,  $u$  is a  $q \times 1$  input vector, and  $A$  and  $B$  are appropriate matrices which depend on  $m$  unknown parameters  $\theta$ . Let there be noisy measurements of  $p$  linear combinations of the state vector

$$y = Cx + v\tag{6.2}$$

where  $v$  is assumed to be a Gaussian white noise vector with intensity  $R$ , and matrix  $C$  is a function of  $\theta$ . Since we are mostly concerned here with finite time problems, we may assume without loss of generality that the final time is one. For practical reasons, we impose a constraint on a quadratic function of the input and the states

$$J = \int_0^1 (x^T Q x + U^T U) dt \leq E\tag{6.3}$$

For linear systems, the inequality sign can be replaced by an equality sign. The information matrix,  $M$ , for parameters  $\theta$  is

$$M = \int_0^1 \left( \frac{\partial y}{\partial \theta} \right)^T R^{-1}(t) \frac{\partial y}{\partial \theta} dt\tag{6.4}$$

The input  $u(t)$  is chosen to minimize parameter estimation errors (in terms of the weighted trace or the determinant of the dispersion matrix) subject to the constraint (6.3). This problem can be reformulated [53] as a two-point boundary value problem.

$$\frac{d}{dt} \begin{bmatrix} \tilde{x} \\ \lambda \end{bmatrix} = \begin{bmatrix} \tilde{A} & -\mu \tilde{B} \tilde{B}^T \\ \tilde{C}^T & \tilde{R}^{-1} \tilde{C} - \tilde{A}^T \end{bmatrix} \begin{bmatrix} \tilde{x} \\ \lambda \end{bmatrix} = H \begin{bmatrix} \tilde{x} \\ \lambda \end{bmatrix}\tag{6.5}$$

$$\begin{aligned}\tilde{x}(0) &= 0, \quad \lambda(1) = 0 \\ u_{opt} &= -\mu \tilde{B}^T \lambda\end{aligned}\tag{6.6}$$

The smallest value of constant  $\mu$  for a nontrivial solution to the two-point boundary value problem gives the optimal control input. The quantities  $\tilde{x}$ ,  $\tilde{A}$ ,  $\tilde{B}$ ,  $\tilde{C}$  and  $\tilde{R}$  are defined below:

$$\tilde{x}^T = \left[ x^T, \frac{\partial x^T}{\partial \theta_1}, \frac{\partial x^T}{\partial \theta_2}, \dots, \frac{\partial x^T}{\partial \theta_m} \right] \quad (6.7)$$

$$\tilde{A} = \begin{bmatrix} A & 0 & 0 & \dots & 0 \\ \frac{\partial A}{\partial \theta_1} & A & 0 & \dots & 0 \\ \frac{\partial A}{\partial \theta_2} & 0 & A & \dots & 0 \\ \frac{\partial A}{\partial \theta_m} & 0 & 0 & \dots & A \end{bmatrix} \quad (6.8)$$

$$\tilde{B}^T = \left[ B^T, \frac{\partial B^T}{\partial \theta_1}, \frac{\partial B^T}{\partial \theta_2}, \dots, \frac{\partial B^T}{\partial \theta_m} \right] \quad (6.9)$$

$$\underline{T\Delta} = \begin{bmatrix} \frac{\partial C}{\partial \theta_1} & C & 0 & \dots & 0 \\ \frac{\partial C}{\partial \theta_2} & 0 & C & \dots & 0 \\ \frac{\partial C}{\partial \theta_m} & 0 & 0 & \dots & C \end{bmatrix} \underline{\Delta} = \begin{bmatrix} T_1 \\ T_2 \\ \vdots \\ T_m \end{bmatrix} \quad (6.10)$$

$$\tilde{R} = \begin{bmatrix} R & 0 & \dots & 0 \\ 0 & R & & \vdots \\ \vdots & & \ddots & \vdots \\ 0 & & & R \end{bmatrix} \quad (6.11)$$

The solution to this two-point boundary value problem, based on the symplectic properties of the Hamiltonian matrix  $H$ , is discussed in [54].

If the duration of the experiment is much longer than the system characteristic time, it is possible to design inputs based on a variety of criteria quickly by making the assumption of steady

state. In an ingenious approach, Mehra [55] converts a linear time-invariant system into its frequency domain representation. This eliminates the dynamics of the system. The parameter estimation problem becomes a regression problem in which input frequencies and the power in each frequency are the control parameters. These parameters, which define the input design, are chosen by an iterative procedure.

Consider the state space representation of a discrete-time linear system

$$x(k+1) = \phi x(k) + Gu(k) \quad k=1,2,3,\dots,N \quad (6.12)$$

and the noisy measurements

$$y(k) = Cx(k) + v(k) \quad (6.13)$$

$\phi$ ,  $C$ , and  $H$  are appropriate matrices and contain  $m$  unknown parameters  $\theta$ . Fourier transform  $y(k)$  to get

$$\begin{aligned} \tilde{y}(n) &= C(e^{-j\frac{2\pi n}{N}} - \phi)^{-1}G \tilde{u}(n) + \tilde{v}(n) \\ &\underline{\Delta}W(n,\theta)\tilde{u}(n) + \tilde{v}(n) \end{aligned} \quad (6.14)$$

As the number of sample points increases, the information matrix per sample approaches [55]

$$M = \frac{1}{2\pi} \operatorname{Re} \int_{-\pi}^{\pi} \frac{\partial W^*}{\partial \theta} S_{vv}^{-1}(\omega) \frac{\partial W}{\partial \theta} dF_{uu}(\omega) \quad (6.15)$$

where  $F_{uu}$  is the spectral distribution function of  $u$  and  $S_{vv}$  is the spectral density of  $v$  and superscript '\*' denotes the conjugate transpose of a matrix. An algorithm based on this approach is outlined in [54].

Optimal multistep inputs for parameter identification.— Several algorithms have been developed for a solution of the boundary value problem leading to the solution of the optimal input design problem. The application of this theory has been limited to low order time invariant systems due to the complexity of the computation procedure. The optimal input selection algorithms may be considerably simplified, for time variant as well as time invariant systems, if the inputs are restricted to be multistep. In this approach, the state equations are first propagated to obtain the state time histories. A simplifying assumption is then made by approximating the states to be multistep and are represented as sums of Walsh basis functions. They may then be determined by using the

methods developed by Corrington [56] and applied to the linear quadratic feedback control design problem by Chen and Hsiao [57]. This approximation may degrade the quality of the input, particularly if the state variables change significantly over the duration of a step.

We consider the system defined by equations (6.1) and (6.2) subject to the constraint (6.3). Matrices A, B and C may be functions of time.

The information matrix for parameters  $\theta$  is

$$M = \int_0^1 \left\{ \frac{\partial [C(t, \theta) x(t)]}{\partial \theta} \right\}^T R^{-1} \left\{ \frac{\partial [C(t, \theta) x(t)]}{\partial \theta} \right\} dt \quad (6.16)$$

The dynamics of the augmented vector  $\tilde{x}$  are defined by the equation

$$\dot{\tilde{x}} = \tilde{A} \tilde{x} + \tilde{B} U \quad (6.17)$$

where  $\tilde{A}$ ,  $\tilde{B}$ ,  $\tilde{x}$  are defined by equations (6.8)-(6.10). Further,

$$\frac{\partial z(t)}{\partial \theta_i} = \frac{C(t, \theta)}{\partial \theta_i} x(t) + C(t, \theta) \frac{\partial x(t)}{\partial \theta_i} . \quad (6.18)$$

A typical element of the information matrix may be written in terms of  $\tilde{x}(t)$

$$M_{ij} = \int_0^1 \tilde{x}^T(t) T_i^T(t) R^{-1} T_j(t) \tilde{x}(t) \cdot dt \quad (6.19)$$

where  $T_i$  and  $T_j$  are defined by equation (6.10).

It is shown that certain mild restrictions on the class of inputs simplifies the input design problem considerably. Two cases are considered in this report.

Case 1: The inputs are restricted to be multistep with  $s$  steps each of duration  $\Delta$ . The state and output sensitivities are obtained by a solution of the differential equations.

Case 2: The inputs are restricted to be multistep with  $s$  steps each of duration  $\Delta$ . The state and outputs are approximated to be multistep.

As the number of steps is increased the multistep inputs approach the general unrestricted input.

The equations for the information matrix and the quadratic constraint are specialized for multistep inputs. These will be used in the derivation of the multi-step input algorithms. The two cases are discussed separately because different techniques are involved in determining the augmented state vector  $\tilde{x}(t)$ .

### Case 1

Under the first approximation, a general representation for input  $u$  is

$$u(t) = Hs(t) \quad (6.20)$$

where  $H$  is a  $q \times s$  matrix and  $s$  is an  $s \times 1$  vector such that

$$\begin{aligned} s_i(t) &= 1, \quad (i-1)\Delta \leq t < i \\ &= 0, \quad \text{elsewhere.} \end{aligned} \quad (6.21)$$

Let  $\tilde{x}_{ij}(t)$  be the response of the augmented sensitivity system (6.17) when a single element  $H_{ij}$  of  $H$  equals one and the remaining elements are zero. In the general time-varying case  $\tilde{x}_{ij}(t)$  may be obtained by a direct solution of the differential equation for each  $i$  and  $j$ . Then because of the linearity of the sensitivity system, it is clear that

$$\begin{aligned} \tilde{x}(t) &= \sum_{i=1}^q \sum_{j=1}^s H_{ij} \tilde{x}_{ij}(t) \\ &\triangleq \sum_{i=1}^{qs} h_i \tilde{x}_i^m(t) \end{aligned} \quad (6.22)$$

where

$$(\cdot)_{(j-1)q+i} = (\cdot)_{ij}$$

Using Equations (6.19) and (6.22), a specific element of the information matrix is

$$\begin{aligned} M_{k\ell} &= \int_0^1 \left\{ T_k \sum_{i=1}^{qs} h_i \tilde{x}_i(t) \right\}^T R^{-1} \left\{ T_\ell \sum_{i=1}^{qs} h_i \tilde{x}_i(t) \right\} dt \\ &= h^T V(k, \ell) h \end{aligned} \quad (6.23)$$

where  $V(k, \ell)$  is a  $q_s \times q_s$  square matrix such that

$$V_{ij}(k, \ell) = \int_0^1 \tilde{x}_i^T(t) T_k R^{-1} T_\ell \tilde{x}_j(t) dt \quad (6.24)$$

Matrices  $V(k, \ell)$  do not depend upon the input  $u$  and therefore they need not be computed again and again in the iterative procedure described in the next section. Notice that a considerable simplification results if the measurement distribution matrix,  $C$ , is time invariant. Then

$$V_{ij}(k, \ell) = \left\{ \text{TR} \quad T_k^T R^{-1} T_\ell \int_0^1 \tilde{x}_j(t) \tilde{x}_i^T(t) \right\} dt \quad (6.25)$$

$$\triangleq \text{Tr} \left\{ T_k^T R^{-1} T_\ell R_{xx}(i, j) \right\}$$

The quadratic constraint on the input and states may also be written in terms of  $h$

$$\int_0^1 \left\{ (T_0 \tilde{x}(t))^T Q (T_0 \tilde{x}(t)) + u^T(t) u(t) \right\} dt = E \quad (6.26)$$

or

$$H^T \tilde{Q} h = 1 \quad (6.27)$$

where

$$\tilde{Q}_{ij} = \frac{1}{E} \left\{ \int_0^1 \tilde{x}_i^T(t) T_0^T R^{-1} T_0 \tilde{x}_j(t) dt + \Delta \delta_{ij} \right\} \quad (6.28)$$

$$\delta_{ij} = \begin{cases} 1 & j=i \\ 0 & i \neq j \end{cases}$$

### Case 2

When the state and outputs are assumed multistep, the Walsh functions prove useful. Details of the properties of the Walsh functions are covered in References [56], [57], and [58]. The important properties for the purpose of the present application are summarized in Appendix B. To simplify the various derivations it is assumed that  $s = 2^\Omega$ , where  $\Omega$  is an integer. Let  $\phi_i$ ,  $i=0,1,\dots,s-1$  be the  $i$ th Walsh function in the dyadic order and let the input be assumed to be



$$u(t) = H \Phi(t) \quad (6.29)$$

$\Phi(t)$  is a vector of Walsh functions from 0 to  $s-1$ . It is shown in Appendix [C] that equations similar to (6.23) and (6.27) can be obtained for information matrix and quadratic constraint respectively.

In the next section, we use the expressions for the information matrix and the quadratic constraints together with some theorems on certain properties of the optimal input leading to a computationally attractive algorithm for the selection of optimal multistep inputs.

Algorithm description: Criteria for input design have been discussed in previous literature [59]. Here, we consider two of the many criteria which are useful. They are: (1) A-optimality (minimize weighted trace of the dispersion matrix, i.e., minimize  $\text{Tr}(wM^{-1})$  where  $w$  is positive semidefinite) and (2) D-optimality (minimize the determinant of the dispersion matrix). Extensions of the theorem and algorithms to other criteria is straightforward.

In deriving the algorithms we consider only nonrandomized inputs. Such an input is completely described by a vector  $h$ . An input  $h$  which satisfied the quadratic constraint on states and input is called a feasible input. It is known that the information matrix is always semidefinite. The following algorithms may be used for detection of inputs.

#### Algorithm 1

(1) Set  $i=0$  and select a feasible input  $h^{(i)}$  such that the corresponding information matrix  $M^{(i)}$  is nonsingular.

(2) Compute  $\tilde{V}$

$$\tilde{V} = \begin{cases} \sum_{k,\ell=1}^m (M^{(i)^{-1}} W M^{(i)^{-1}})_{k\ell} V(k,\ell) \text{ to min } \text{Tr}(WM^{-1}) \\ \sum_{k,\ell=1}^m (M^{(i)^{-1}})_{k\ell} V(k,\ell) \text{ to min } |M^{-1}| \end{cases} \quad (6.34)$$

(3) Find the maximum eigenvalue  $\lambda$  and the corresponding eigenvector  $h$  of the equation

$$\tilde{V} h = \tilde{Q} h \quad (6.35)$$

If the eigenvalue  $\lambda$  is close to its minimum value  $(\text{Tr}(WM^{(i)})^{-1})$  to  $\min \text{Tr}(WM^{-1})$ ; and  $m$  to  $\min |M^{-1}|$ , stop. Otherwise, proceed to (4).

(4) Find an input

$$h^{(i+1)} = \sqrt{\alpha h^{(i)}} + \sqrt{\beta h} \quad (6.36)$$

by choosing  $\alpha$  and  $\beta$  such that it is feasible and minimizes the corresponding cost function.

(5) Change  $i$  to  $i+1$  and return to (2).

The above algorithm converges to the global optimum.

NOTE: What these theorems have achieved for us is an algorithm which converts a complex nonlinear problem into a succession of linear eigenvalue problems. Though the matrix  $V$  may be of relatively high order, it is positive semidefinite and we are only interested in its maximum eigenvalue – a problem much simpler than finding all eigenvalues of a matrix.

Extension to nonlinear systems: For rotorcraft application, we have to extend the multistep input algorithm developed for linear systems to nonlinear systems.

Selection of parameter identifying inputs in nonlinear systems is extremely complex. One major problem is that the inequality constraint on the quadratic function of the input and response, Equation (6.3) cannot be converted into an equality constraint. In fact, it is shown in Reference [60] that to best identify parameters associated with a local instability observed at high angle-of-attack flight of airplanes, a lower amplitude input is better than a high amplitude input. In addition, the theorems corresponding to theorems 1 and 2 on the properties of optimal inputs for linear systems cannot be proven for nonlinear systems. Here we describe an approximate method for input selection for the following system.

$$\begin{aligned} \dot{x} &= f(x, u, t, \theta) \\ y &= h(x, u, t, \theta) + v \end{aligned} \quad (6.37)$$

where  $v$  is white Gaussian noise with power spectral density  $R$ .

#### Algorithm 2

(1) Select an input  $u_0(t)$  which satisfied the constraint of Equation (6.3) and gives a nonsingular information matrix  $M_0$ . Let the corresponding state trajectory be  $x_0(t)$ .

(2) Linearize the system around  $x_0(t)$ ,  $u_0(t)$  to get

$$\begin{aligned}\Delta \dot{x} &= A(t, \theta) \Delta x + B(t, \theta) \Delta u \\ \Delta y &= C(t, \theta) \Delta x + v\end{aligned}\tag{6.38}$$

where

$$\begin{aligned}\Delta x(t) &= x(t) - x_0(t) \\ \Delta u(t) &= u(t) - u_0(t)\end{aligned}\tag{6.39}$$

(3) Design an optimal input  $\Delta u(t)$  for the system of Equation (6.38) under the constraint

$$\int_0^1 \left\{ \Delta x(t) + x_0(t)^T Q \Delta x(t) + x_0(t) + \Delta u(t) + u_0(t)^T \Delta u(t) + u_0(t) \right\} dt \leq 1\tag{6.40}$$

$\Delta u(t)$  may be obtained by a modification of Algorithm 1.

(4) If  $\Delta u(t)$  is small, stop. Otherwise, update  $u(t)$  and  $x(t)$ .

(5) Return to (2).

Figure [6.1] is a flow chart of the rotorcraft nonlinear model input design algorithm. The algorithm is made up of Algorithm 1 and Algorithm 2. First, a trajectory from a previously estimated nonlinear model is generated and linearized. A perturbation input is synthesized for this linear model based on Algorithm 1. The perturbation input is then added to the original nominal input and relinearization of the nonlinear model response to the total input computed. The iteration is continued until a minimum variance solution has been obtained.

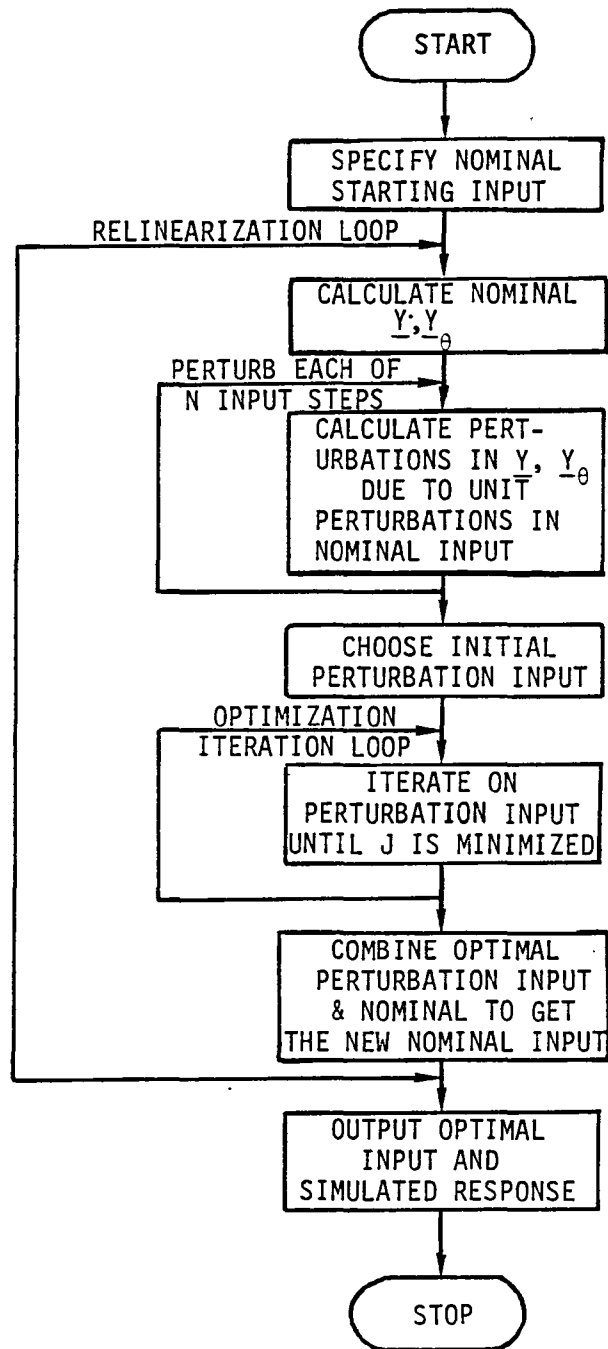


FIGURE 6.1. FLOW CHART OF INPUT DESIGN PROGRAM

CHAPTER VII  
DATA PROCESSING RESULTS  
CH-53 Results

The CH-53A data processing results fall into two categories: simulation data processing and flight data processing. For the simulation data processing phase, a mathematical model was simulated and the outputs contaminated with random measurement noise. These noisy outputs were then used for validation of various computer programs. The flight data processing phase uses actual flight data when executing the computer programs.

CH-53A simulation data processing. - Simulation data processing for the CH-53A consisted of: simulating the CH-53A and contaminating the outputs with random measurement noise, and processing this data through the SCIDNT, NLSCIDNT and DEKFIS computer programs.

CH-53A simulation: A nine degree of freedom linear model for the CH-53A at 100 kts. was used for the simulation data base. This was a 14 state model with the body states:  $u, v, w, p, q, r, \phi$  and  $\theta$ ; and the rotor states:  $\beta_0, \dot{\beta}_0, \beta_{1c}, \dot{\beta}_{1c}, \beta_{1s}$  and  $\dot{\beta}_{1s}$ . There were 4 control inputs:  $B_{1s}, A_{1s}, \theta_{\text{Tail Rotor}}$  and  $\theta_{\text{Main Rotor}}$ , and 14 outputs:  $a_x, a_y, a_z, \dot{p}, \dot{q}, \dot{r}, p, q, r, \phi, \theta, \beta_0, \beta_{1c}$  and  $\beta_{1s}$ . The linear model is shown in Table 7.1. This model was simulated to the input shown in Figure 7.1, which is superior to the more common step or doublet input [Refs. 61 and 62]. The outputs were contaminated with a zero mean white Gaussian measurement noise with variances: (units - ft., rad., sec.)

$$R = \text{diag} [3*0.25, 3*0.0003, 3*0.000076, 2*0.000003, 3*0.000012]$$

The data record was 5 seconds long and sampled at 100 samples per second for a total of 500 data points.

SCIDNT runs on CH-53A simulation data: The linear identification program was used to identify 60 of the parameters in the model. The start-up values of the SCIDNT run were arbitrarily chosen as the simulation values +25 percent.

Table 7.2 shows a comparison of several parameters. (The quantities  $\dot{\beta}_{1s}/\beta_{1s}, \dot{\beta}_{1c}/\beta_{1s}$  and  $\dot{\beta}_{1c}/\dot{\beta}_{1s}$

---

\* Because of the extensive data processing done under this contract, only a portion of the overall results have been presented. An attempt has been made to present the more interesting and potentially useful information.

TABLE 7.1  
NINE DEGREE OF FREEDOM LINEAR MODEL FOR CH-53A - 100 KTS - NO SAS

STATE DERIVATIVE OF STATE	u (FT/SEC)	v (FT/SEC)	w (FT/SEC)	p (RAD/SEC)	q (RAD/SEC)	r (RAD/SEC)	$\phi$ (RAD)	$\theta$ (RAD)	$\delta_o$ (RAD)	$\dot{\delta}_o$ (RAD/SEC)	$\delta_{1c}$ (RAD)	$\dot{\delta}_{1c}$ (RAD/SEC)	$\delta_{1s}$ (RAD)	$\dot{\delta}_{1s}$ (RAD/SEC)	$B_{1s}$ (RAD)	$A_{1s}$ (RAD)	$U_{1R}$ (RAD)	$C_C$ (RAD)
$\ddot{u}$ (ft/sec <sup>2</sup> )	-.0048	.00042	.0942	-.126	-9.97	.865	0	-37.2	25.1	.0416	-24.0	-2.51	-1.91	-.49	-4.92	-4.92	-.48	26.5
$\ddot{v}$ (ft/sec <sup>2</sup> )	.0156	-.0567	-.00216	6.63	-.659	-167.	32.2	0.054	-10.1	-.376	4.32	-.210	25.8	.923	12.0	11.9	6.67	-.708
$\ddot{w}$ (ft/sec <sup>2</sup> )	-.124	-.0071	-.744	-6.12	193.	4.40	0.89	-1.44	-218.	.799	-11.1	3.78	11.7	-4.49	124.	17.1	.534	-269.
$\ddot{p}$ (rad/sec <sup>2</sup> )	-.0011	-.0158	-.0099	-.172	.0170	.443	0	0	-.520	-.01	-4.56	-.472	17.8	1.07	.913	3.33	3.85	-3.45
$\ddot{q}$ (rad/sec <sup>2</sup> )	-.0005	.0023	.0016	-.0055	-5.0	.0045	0	0	-.064	-.0421	3.84	.30	1.00	.104	-.352	-.0795	.0078	.66
$\ddot{r}$ (rad/sec <sup>2</sup> )	-.0016	.0001	-.0002	.111	.0594	-.728	0	0	-1.4	-.0152	-.83	-.0532	1.84	.08	-.0905	-.543	-5.17	4.7
$\ddot{\phi}$ (rad/sec)	0	0	0	1.0	0	.0447	0	0	0	0	0	0	0	0	0	0	0	0
$\ddot{\theta}$ (rad/sec)	0	0	0	0	1.0	0	0	0	0	0	0	0	0	0	0	0	0	0
$\ddot{\delta}_o$ (rad/sec)	0	0	0	0	0	0	0	0	0	1.0	0	0	0	0	0	0	0	0
$\ddot{\delta}_{1c}$ (rad/sec <sup>2</sup> )	.0294	.0005	.432	.495	-3.97	-3.96	0	0	-168.	-13.7	19.0	.999	-16.8	-.59	-64.2	9.82	-1.94	231.
$\ddot{\delta}_{1c}$ (rad/sec)	0	0	0	0	0	0	0	0	0	0	1.0	0	0	0	0	0	0	0
$\ddot{\delta}_{1c}$ (rad/sec <sup>2</sup> )	.0891	-.0707	.0379	-8.46	-18.8	.156	0	0	89.5	3.32	-47.	-19.4	-161.	-23.7	-117.	163.	-.53	30.7
$\ddot{\delta}_{1s}$ (rad/sec)	0	0	0	0	0	0	0	0	0	0	0	0	0	1.0	0	0	0	0
$\dot{\delta}_{1s}$ (rad/sec)	-.0644	-.0506	-.0945	-15.2	12.1	-.72	0	0	-8.31	1.56	154.	22.8	-48.7	-17.6	163.	110.	.29	-84.

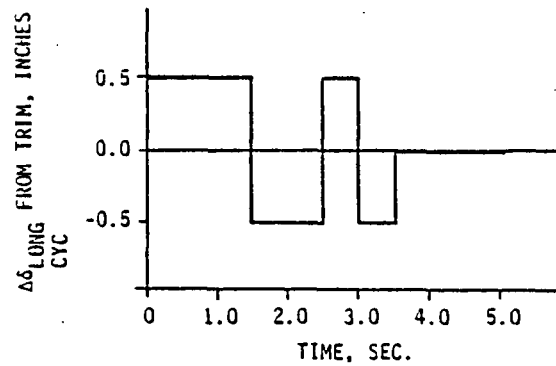


FIGURE 7.1 CONTROL INPUT FOR CH-53A SIMULATION

TABLE 7.2 -- TYPICAL CH-53 PARAMETER ESTIMATES  
AFTER TWO ITERATIONS

	SIMULATION VALUE	IDENTIFIED VALUE	F-RATIO
$X_u$	-0.0048	-0.00075	0.33
$M_u$	-0.0005	-0.0017	248.9
$Y_v$	-0.0567	-0.069	60.8
$Y_w$	0.00216	0.046	0.008
$Z_w$	-0.744	-0.37	414.5
$M_w$	0.0016	-0.0066	150.1
$M_p$	-0.0055	0.057	0.08
$N_p$	0.111	0.099	68.2
$L_q$	0.017	0.47	0.05
$M_q$	-5.00	-5.40	64018.8
$M_r$	0.0045	-0.0349	0.02
$N_r$	-0.728	-1.19	781.6
$\beta_0/\beta_0$	-168.0	-138.15	1747.5
$\beta_{1c}/\beta_0$	89.5	42.80	609.3
$\beta_0/\beta_0$	-13.7	-9.59	494.3
$\beta_{1c}/\beta_0$	3.32	5.89	8.6
$Z_{\beta_0}$	0.78	-2.29	23.8
$\beta_0/\beta_{1c}$	19.0	24.65	375.5
$\beta_{1c}/\beta_{1c}$	-47.0	-51.14	523.5
$\beta_{1s}/\beta_{1c}$	154.0	175.13	168157.0
$M_{\beta_{1c}}$	0.30	0.28	2675.7
$\beta_0/\beta_{1c}$	1.00	1.24	97.95
$\beta_{1c}/\beta_{1s}$	-161.0	-172.84	3750.6
$\beta_{1s}/\beta_{1s}$	-48.7	-29.25	761.3
$\beta_0/\beta_{1s}$	-0.59	-3.17	431.5
$\beta_{1c}/\beta_{1s}$	-23.7	-19.92	12022.3
$\beta_{1s}/\beta_{1s}$	-17.6	-22.22	14004.9
$X_{\beta_{1s}}$	-4.92	-5.39	115.4
$Y_{\beta_{1s}}$	12.0	16.59	1185.0
$Z_{\beta_{1s}}$	124.0	101.71	19243.9
$L_{\beta_{1s}}$	0.913	1.29	968.9
$M_{\beta_{1s}}$	-0.352	-0.387	486.6
$N_{\beta_{1s}}$	-0.091	-0.0075	27.7
$\beta_0/\beta_{1s}$	-64.2	-49.67	8558.6
$\beta_{1c}/\beta_{1s}$	-117.0	-149.7	55842.1

are rotor stability derivatives, e.g.,  $\ddot{\beta}_{1s}/\beta_{1s} = \partial\ddot{\beta}_{1s}/\partial\beta_{1s}$ ). Only two iterations on each of the 60 parameters were made. Correspondence is reasonable, with the exception of those with low F-ratios signifying poor identifyability.

Table 7.3 shows a comparison of the starting and final poles of the transfer function of the vehicle response. The simulation values are also given.

CH-53A flight data processing. - Flight data processing for the CH-53A consisted of: reading the flight data tape and preprocessing the data, and processing this data through the DEKFIS, OSR and SCIDNT computer programs.

CH-53A flight data: The CH-53A flight data was provided by the Sikorsky Aircraft Division of UTC under contract by NASA. The maneuver processed was specifically flown at 100 kts for system identification purposes. The control input sequence for this maneuver is shown in Figure 7.2. The data record was 27.5 seconds long and sampled at 100 samples per second. The following measurements were available:  $a_x, a_y, a_z, \dot{p}, \dot{q}, \dot{r}, V, \beta, \alpha, p, q, r, \phi, \theta, \psi, \delta_{LONG}, \delta_{LAT}, \delta_{PED}, \delta_{COLL}$  (pilot control deflections),  $\delta_{LONG}, \delta_{LAT}, \delta_{PED}, \delta_{COLL}$  (aux servo deflections in equivalent stick deflections - sum of pilot + SAS),  $\beta_i, i=1,6$  (blade flapping angle for all blades) and  $\cos \psi_R$  (rotor azimuth).

DEKFIS runs on CH-53A flight data: The CH-53A flight data was processed through the fuselage/gust estimator and the rotor state estimator options of DEKFIS.

The primary purpose of the fuselage gust estimator is to provide data consistency between the measurements by correcting for bias and scale factor errors and eliminating random noise effects. A secondary purpose is to provide estimates of  $u, v, w$  and their derivatives since the measurements are  $V, \beta, \alpha, a_x, a_y$  and  $a_z$ .

Figures 7.3a and 7.3b show the actual measured and estimated time histories of the normal accelerometer and the angle-of-attack vane. In both cases, the estimated measurements track the actual measurements well. There is a well defined oscillation on the  $\alpha$ -vane measurement (attributed later to boom natural frequency which was not included in



TABLE 7.3. — COMPARISON OF IDENTIFIED CH-53A POLE LOCATIONS

STARTING POLES	CONVERGED POLES	SIMULATION VALUES
$-10.1 \pm 1.17j$	$-13.9 \pm 20.1bj$	$-11.46 \pm 21.7j$
$-8.4 \pm 19.9j$	$-6.48 \pm 3.54j$	$-6.81 \pm 2.88j$
$-4.39 \pm 10.2j$	$-4.68 \pm 10.5j$	$-6.26 \pm 10.9j$
$-0.246 \pm 1.33j$	$-0.334 \pm 1.25j$	$-0.210 \pm 1.23j$
$-0.0123 \pm 0.0874j$	$-0.0120 \pm 0.0920$	$-0.0145 \pm 0.110j$
-5.59	-4.75	-4.41
-1.48	-2.29	-2.34
-1.21	-0.959	-0.955
-0.219	-0.285	-0.167

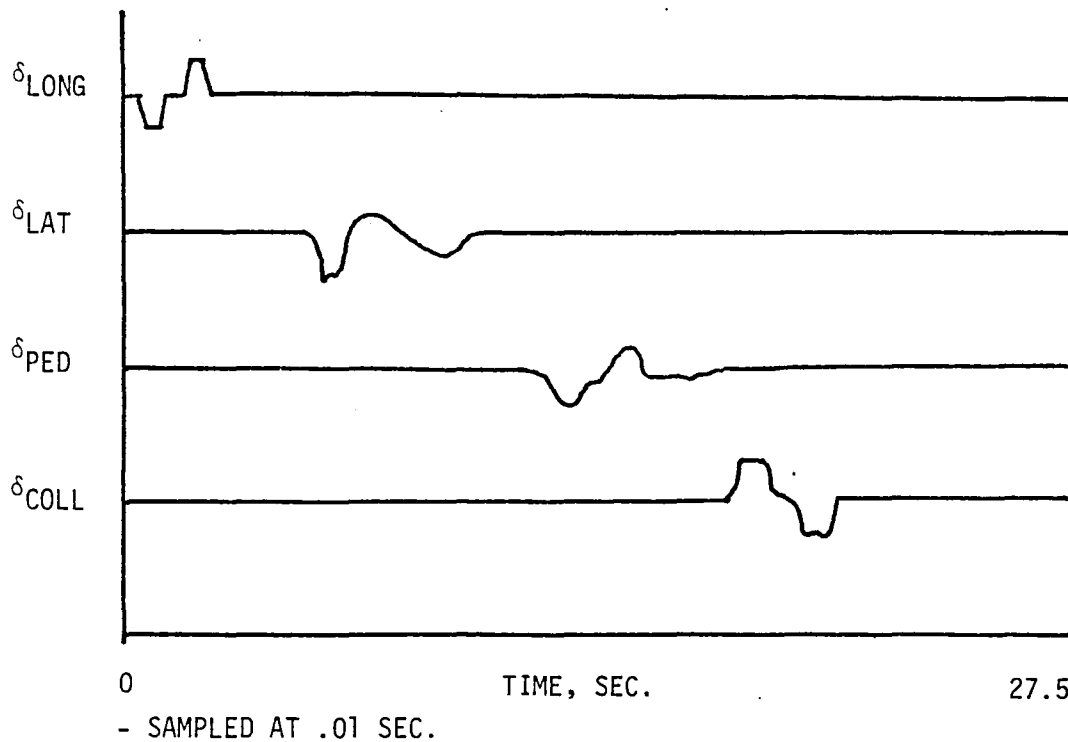


FIGURE 7.2 CH-53A FLIGHT DATA PROCESSING - SI MANEUVER INPUT SEQUENCES

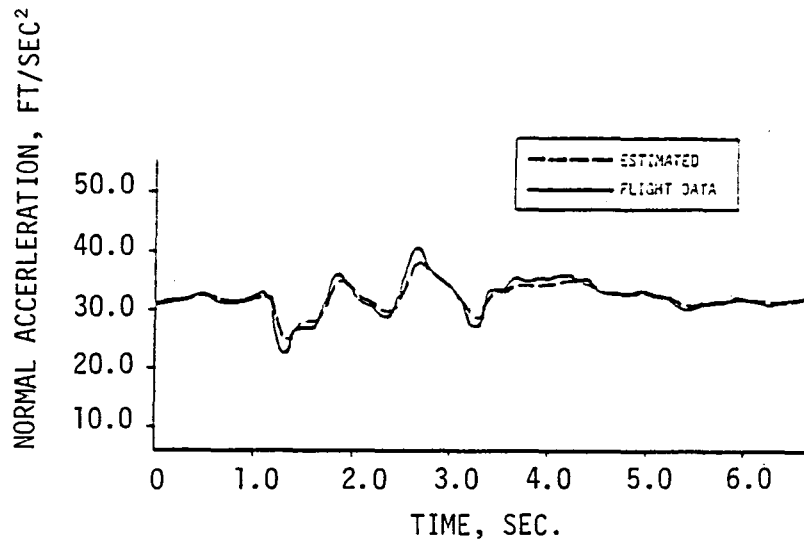


FIGURE 7.3a — COMPARISON OF STATE ESTIMATE AND CH-53A FLIGHT DATA (100 KTS) — NORMAL ACCELERATION

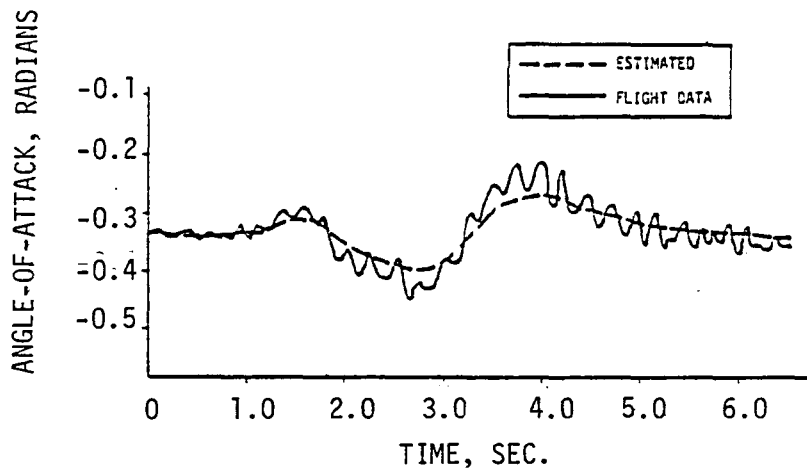


FIGURE 7.3b — COMPARISON OF STATE ESTIMATE AND CH-53A FLIGHT DATA (100 KTS) — ANGLE-OF-ATTACK

the filter model). Figure 7.4 shows the scale factor error calibration on the accelerometers and gyros for this test. The comparison is based on the value of scale factor assumed prior to the filtering, indicating the change in scale factor error concluded by the additional information provided by the flight data. Table 7.4 shows the bias error estimates obtained from this data processing.

The rotor state estimator was used to process the six main rotor blade flapping measurements and the rotor azimuth measurement and estimate the fixed system states  $\beta_0$  (coning angle),  $\beta_{1c}$  (longitudinal flapping) and  $\beta_{1s}$  (lateral flapping). Initially, the trim portion of the maneuver (first second of data) was processed to obtain any biases on the blade flapping measurements. Coning, longitudinal and lateral flapping were approximated as constants in trim. Then, the entire maneuver was processed holding these biases fixed, and allowing  $\beta_0$ ,  $\beta_{1c}$  and  $\beta_{1s}$  estimates to vary in time. The rotor state estimator also provided first and second derivatives of  $\beta_0$ ,  $\beta_{1c}$ , and  $\beta_{1s}$  for subsequent use in OSR processing.

An example of the estimation of flapping angles with the rotor state estimator option of DEKFIS is shown in Figure 7.5 for blade 5.

OSR runs on CH-53A flight data: One of the key issues in rotorcraft modeling is the degree to which an explicit rotor model should be included in a stability and control simplified linear model. The objective is, of course, to work with the minimum order model which predicts stability or control requirements adequately. The model structure estimation was applied to CH-53 flight test data to determine the significance of the rotor in explaining the vehicle response. Three generic models were formulated:

(1) A six degree of freedom (6 dof) model with fuselage states ( $u, v, w, p, q, r, \phi, \theta$ ). This is a quasi-static model in that the rotor dynamics are assumed much faster than the fuselage/body dynamics and are lumped in with the fuselage/body dynamics.

(2) A nine degree of freedom (9 dof) with a first order rotor model with the nine fuselage states and three rotor tip-path-plane states ( $\beta_0, \beta_{1c}, \beta_{1s}$ ). The first order rotor assumes a tip-path-plane but assumes only first order

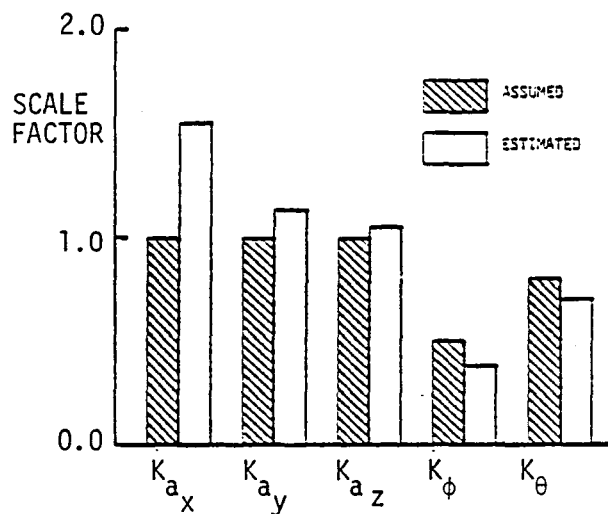


FIGURE 7.4.— SCALE FACTOR ERRORS IN ACCELEROMETER AND GYRO MEASUREMENTS (FROM CH-53A FLIGHT TEST DATA, 100 KTS)

TABLE 7.4.— BIAS CALIBRATION FOR CH-53A FLIGHT DATA (100 KTS)

$\phi$	$\theta$	$q$	$a_x$	$a_y$	$a_z$
0.0089 RAD	0.0165 RAD	-0.0013 RAD/SEC	0.73 FT/SEC <sup>2</sup>	-0.11 FT/SEC <sup>2</sup>	-0.25 FT/SEC <sup>2</sup>

dynamics for each rotor degree of freedom. (They do couple, however). This model corresponds to a rotor precession model.

(3) A nine degree of freedom with a second order rotor model. Now, second order dynamics are assumed for each tip-path-plane degree of freedom. The additional states are the tip-path-plane rates ( $\dot{\beta}_0, \dot{\beta}_{1c}, \dot{\beta}_{1s}$ ).

Each of these three rotorcraft models was identified for the augmented and unaugmented CH-53A. Referring to Figure 7.6, it is clear that closed loop parameters (with the SAS lumped in) may be identified by formulating the identification with  $\delta_{\text{PILOT}}$  as the control input, and  $y$  as the measured output. It is also possible to identify the unaugmented helicopter by using  $\delta_{\text{AUX SERVO}}$  as the control inputs. As long as there is sufficient control excitation, the  $\delta_{\text{AUX SERVO}}$  channel will be independent of the states being fed back. One might expect the identification of the unaugmented vehicle to provide better results since the SAS dynamics and nonlinearities (e.g., saturation) are inherent in the  $\delta_{\text{AUX SERVO}}$  input and are not being lumped into the model. In addition, problems due to stick slop and hysteresis that occur between the pilot station and the auxiliary (SAS summing) servo are avoided, so that the  $\delta_{\text{AUX SERVO}}$  input also provides a cleaner control input for identification.

OSR identified models for each of the six cases are presented in Tables 7.5 through 7.10. It is possible to assess the quality of the results by observing the statistics in the tables. Any given run generates one column in the tables. The  $R^2$  (multiple correlation coefficient squared) at the bottom of any given column is indicative of the fit error, being the ratio of the regression sum of squares, to the observation sum of squares. The F-ratio at the bottom of any given column gives the total F-ratio for that regression. The F-to-remove number provides F-ratio for that regression. The F-to-remove number provides a measure of the relative identifiability within a given column. A high F-to-remove indicates a well identified parameter (e.g.,  $M_{\beta_{1c}}$  in Table 7.7). A low F-to-remove indicates poor identifiability. Note that it is not advisable to compare F-to-remove values between column, unless the columns have a similar overall fit.

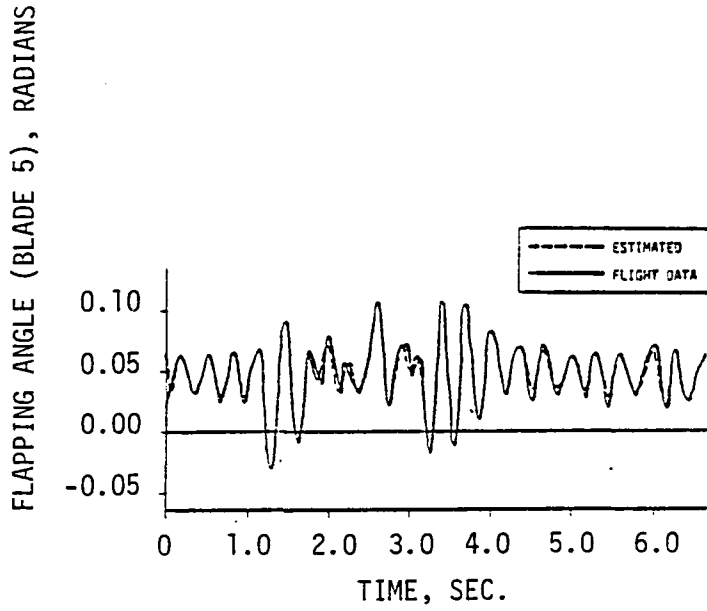


FIGURE 7.5 COMPARISON OF STATE ESTIMATE AND CH-53A FLIGHT DATA (100 KTS) - BLADE FLAPPING ANGLE

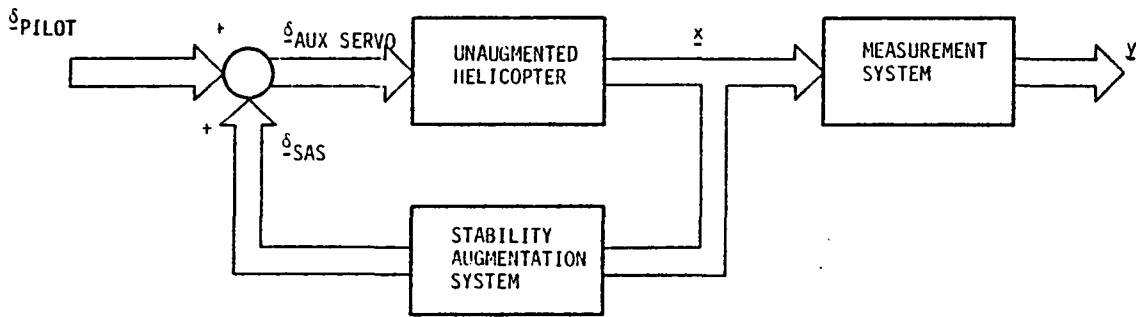


FIGURE 7.6 BLOCK DIAGRAM FOR CH53A SYSTEM

Results for three of these models are cross tabulated in Table 7.11 for the  $\dot{q}$  dependent variable regressions. The corresponding regression fits are presented in Figure 7.7. Based on these, the model structure estimation program analyzed the relative significance of the three models with two criteria, the  $R^2$  multiple correlation coefficient and the F-ratio. Figure 7.8 illustrates the relative significance of explicit rotor modeling. By both criteria, the increase in model accuracy is notable by including at least the rotor precession. Further, but less significant, improvement is obtained by the complete tip path plane model. Note, however, that in Table 7.11 the first order rotor model tended to enter the controls into the regression; whereas, one would expect most of the control effects to come through the rotor flapping terms. The second order rotor model does not enter these controls into the regression; rather, the tip-path-plane rates are entered giving an improved fit! On the other hand, inclusion of the rotor dynamics does not always lead to an improved fit. One can observe this in the X-force ( $\dot{u}$ ) and Y-force ( $\dot{v}$ ) equations. Although the  $R^2$  multiple correlation coefficient increases, (which is generally expected since the number of terms in the regression has been increased), the total F-ratio decreases. This can be attributed to the independent regression variables fitting the noise and not the process. This is generally the case whenever there is a low signal-to-noise ratio resulting from insufficient signal excitation.

Table 7.12 shows a comparison between the SAS on quasi-static model and the SAS off quasi-static model. It is interesting to note that the SAS off  $M_q$  stability derivative is positive (but with a very low F-ratio) and it becomes negative with the inclusion of SAS. ( $M_q$  may well be positive for the SAS off case since we are dealing with a reduced order (quasi-static) model that has the rotor dynamics lumped in. It is difficult to be certain in this case since  $M_q$  is basically unidentifiable.) For the higher order models, the SAS on effect manifests itself in the  $M_q$  and  $\beta_{1c}/q$  stability derivatives.

SCIDNT runs on Ch-53A flight data: a limited number of SCIDNT runs were attempted on Ch-53A flight data. Because of the high order of the model (14 states), the large number of parameters involved (>100) and the number of data points being processed (2750 time points for 19 channels) it was determined to be infeasible to run SCIDNT on the fully coupled 9 dof helicopter. (A problem of this magnitude, whereas possible with the SCIDNT software, would be extremely costly in terms of computer time, and would require a large number of iterations to insure proper convergence\*.) Hence, a high order identification model was abandoned and a simple 3rd order model (states  $\theta$ ,  $q$ ,  $\beta_{1c}$ ) was adopted, using only the longitudinal stick input portion of the maneuver. The modeling errors were compensated by including process noise in the model. Unfortunately, the converged parameter values were not reasonable, and proved to be very dependent.

---

\* The numerical efficiency of the current version of SCIDNT (1980) has been improved 20:1 relative to the version used for this study.

TABLE 7.5. - CH-53A FLIGHT DATA - OPTIMAL SUBSET REGRESSION RESULTS

142

- 100 kts, with SAS
- Aerodynamic terms only
- SI Maneuver
- 6 dof quasistatic model

	$\ddot{u}$ ft/sec <sup>2</sup>	$\ddot{r}$ ft/sec <sup>2</sup>	$\ddot{w}$ ft/sec <sup>2</sup>	$\ddot{p}$ RAD/sec <sup>2</sup>	$\ddot{q}$ RAD/sec <sup>2</sup>	$\ddot{r}$ RAD/sec <sup>2</sup>
u, ft/sec		-.1722/29.24	-.07939/3.812	.008592/2.413		-.006343/20.30
v, ft/sec		-.08335/126.9	-.03447/14.78		.001572/32.05	.003533/117.5
w, ft/sec		-.03696/3.937	-.05283/5.826	.01017/11.28	-.01339/327.7	
p, RAD/sec	-1.737/9.040	-2.325/13.13	1.542/6.084	-1.075/123.0		-.1045/13.36
q, RAD/sec	5.100/6.292	3.467/3.846	18.98/71.32		-.6639/92.09	.5666/56.02
r, RAD/sec	2.881/2.400	-3.387/2.983		1.854/29.01	-.3331/17.80	-.6182/57.32
$\delta_{long}$ , inches	2.318/69.69	.8789/14.36	4.555/236.5		-.1435/231.7	.03488/11.96
$\delta_{lat}$ , inches		.3150/4.691		.3841/233.5	-.02354/24.06	.04597/48.00
$\delta_{coll}$ , inches		-.5512/7.278	-7.295/780.4	.06481/3.838	.03535/18.91	
$\delta_{ped}$ , inches		-2.597/22.15		.2188/5.555	-.08264/14.19	-.3877/247.0
F-RATIO	23.27	30.83	154.0	54.64	134.87	76.62
R <sup>2</sup>	.1459	.3639	.6655	.4137	.6660	.5312



TABLE 7.6. - CH-53A FLIGHT DATA - OPTIMAL SUBSET REGRESSION RESULTS

- 100 kts., with SAS
- Aerodynamic terms only
- SI Maneuver
- 9 dof model - 1st order rotor

KEY:  
 Parameter value  
 xxxx/xxxx  
 F to Remove

	$\dot{u}$ ft/sec <sup>2</sup>	$\dot{v}$ ft/sec <sup>2</sup>	$\dot{w}$ ft/sec <sup>2</sup>	$\dot{p}$ RAD/sec <sup>2</sup>	$\dot{q}$ RAD/sec <sup>2</sup>	$\dot{r}$ RAD/sec <sup>2</sup>	$\dot{\beta}_0$ RAD/sec	$\dot{\beta}_{1c}$ RAD/sec	$\dot{\beta}_{1s}$ RAD/sec
u, ft/sec		-.1730/30.37	-.06570/5.219	.005569/4.989	-.002059/6.290	-.005380/16.62		.001944/5.195	
v, ft/sec	.01374/2.660		-.02101/11.73	-.001422/6.045		.004069/173.7			-.0009028/15.92
w, ft/sec		-.05269/7.931		-.04706/3.349	-.001211/3.737	-.006328/37.31		-.002832/19.78	
p, ft/sec	-1.521/5.960	-1.140/4.902		.3336/31.26	-.1356/52.34	.1015/21.09	-.09729/28.47	-.1103/50.93	-.3032/153.0
q, ft/sec	3.644/2.754	3.495/4.032	4.654/8.728		.2000/14.50	.2030/6.214	-.4021/64.94	-1.425/687.5	-.1587/8.388
r, ft/sec	3.058/2.114	-4.283/4.878	-4.266/6.527	.9565/41.03		-.8988/111.5			-.1351/6.725
$\beta_0$ , RAD			-308.4/302.0	-6.155/27.81			1.099/6.032	3.533/132.4	2.544/28.24
$\beta_{1c}$ , RAD	-12.44/2.755		-50.16/50.67		6.334/898.6	-2.718/61.01	-.6362/17.41	-2.489/114.7	
$\beta_{1s}$ , RAD	-16.86/4.749	28.10/20.83	25.34/19.22	29.61/1939.	-1.113/25.64	3.572/170.4	-.9623/20.67		-.9873/12.79
$\delta_{long}$ , Inches	1.838/23.66	.9946/18.70			.04000/22.70	-.3280/5.820	-.04142/24.55	-.1280/227.6	
$\delta_{lat}$ , Inches				-.03842/6.392	-.008685/3.152		.01654/11.65	.01268/11.17	.04978/63.57
$\delta_{coll}$ , Inches		-.6403/10.10	-2.079/45.84	.07251/10.24	.01421/7.221		.01907/5.053		-.02514/6.898
$\delta_{ped}$ , Inches		-2.516/21.38	-.9547/4.065	.2806/41.46		-.4212/326.9		-.01899/2.629	
F-RATIO	14.99	33.35	281.0	422.9	395.7	87.72	13.93	88.27	28.01
R <sup>2</sup>	.1622	.3822	.8390	.8758	.8683	.6194	.1708	.5953	.2929

TABLE 7.7. - CH-53A FLIGHT DATA - OPTIMAL SUBSET REGRESSION RESULTS

144

- 100 kts., with SAS
- Aerodynamic terms only
- SI Maneuver
- 9 dof model - w/ 2nd order rotor

KEY:  
 Parameter value  
 xxxx/xxxx  
 F to Remove

	$\dot{u}$ ft/sec <sup>2</sup>	$\dot{v}$ ft/sec <sup>2</sup>	$\dot{w}$ ft/sec <sup>2</sup>	$\dot{p}$ RAD/sec <sup>2</sup>	$\dot{q}$ RAD/sec <sup>2</sup>	$\dot{r}$ RAD/sec <sup>2</sup>	$\ddot{\beta}_0$ RAD/sec <sup>2</sup>	$\ddot{\beta}_{1c}$ RAD/sec <sup>2</sup>	$\ddot{\beta}_{1s}$ RAD/sec <sup>2</sup>
u, ft/sec		-.1746/32.95	-.06034/5.002	.005909/7.374	-.001306/3.117	-.005953/21.56	-.01913/7.310		
v, ft/sec		-.07649/114.6	-.01818/10.23	-.002701/28.68		.004191/192.9			
w, ft/sec		-.07854/17.21	-.06330/7.707		-.002838/26.48	-.005714/31.26	.08361/154.1		.04008/24.41
p, RAD/sec	-2.798/21.27	2.051/5.795		-.08598/2.264	-.1805/272.8	.1724/26.89	-.7654/39.09	-.7521/14.88	-1.729/38.01
q, RAD/sec	-13.16/25.43	11.50/23.62		-.5186/15.05	-.2470/22.92	.6857/58.83	3.018/19.14	-3.675/41.26	6.122/51.76
r, RAD/sec		-3.627/3.657	-5.294/11.07	.8932/48.06		-.9109/127.4	-1.287/8.091	-3.113/29.10	1.266/4.809
$\dot{\beta}_0$ , RAD/sec	6.861/8.872		-10.78/67.29		-.2493/31.14	-.1671/4.685	-.7367/2.993		
$\dot{\beta}_{1c}$ , RAD/sec	-13.23/45.56	5.765/16.37		-.4539/25.86	-.2372/40.64	.3968/37.25	2.496/36.42		4.248/74.02
$\dot{\beta}_{1s}$ , RAD/sec	-2.988/4.027	5.188/18.00		-1.148/165.0			-1.369/25.20	-2.928/65.06	-.6940/2.548
$\dot{\beta}_0$ , RAD	30.63/5.021		-288.3/292.0		2.187/60.72	-1.623/10.89	-128.0/663.6	-49.60/113.3	
$\beta_{1c}$ , RAD	-41.12/54.86		-62.75/95.74		5.279/1143.	-2.030/53.41	21.75/79.20	-21.86/135.0	24.52/25.00
$\beta_{1s}$ , RAD		39.14/25.75	21.36/14.92	27.79/2612.	-1.444/93.95	3.897/120.6	4.291/8.274		-46.11/234.9
$\delta_{Long}$ , Inches		1.706/42.87	-.4456/3.508				-.3986/21.11	-1.025/117.5	.5862/22.7
$\delta_{Lat}$ , Inches		-.5313/7.947		.03299/6.041		-.01542/3.885		.1366/10.17	.5628/69.
$\delta_{coll}$ , Inches		-1.015/23.77	-2.041/46.09				1.843/470.7	.9106/99.79	
$\delta_{Ped}$ , Inches		-2.392/20.58	-1.297/8.347	.2951/60.80		-.4193/359.4	-.3290/7.714	-.6093/15.83	
F-RATIO	19.40	30.34	288.6	526.5	497.6	74.36	60.50	42.56	31.67
R <sup>2</sup>	.2003	.4239	.8551	.9071	.8924	.6433	.6129	.4412	.3701

TABLE 7.8. — CH-53A FLIGHT DATA - OPTIMAL SUBSET REGRESSION RESULTS

- 100 kts, without SAS
- Aerodynamic Terms Only
- SI Maneuver
- 6 dof quasistatic

	$\dot{u}$ ft/sec <sup>2</sup>	$\dot{v}$ ft/sec <sup>2</sup>	$\dot{w}$ ft/sec <sup>2</sup>	$\dot{p}$ RAD/sec <sup>2</sup>	$\dot{q}$ RAD/sec <sup>2</sup>	$\dot{r}$ RAD/sec <sup>2</sup>
u, ft/sec		-.1569/25.94				
v, ft/sec	.01573/3.175	-.09861/198.5		-.005183/26.05	.001326/22.99	.003600/136.0
w, ft/sec	-.09037/10.77	-.1203/30.61	-.3201/177.7		-.004692/31.34	-.001968/3.465
p, RAD/sec	-1.209/3.916	-2.774/34.11	2.696/29.37	-.5123/51.96	-.05173/7.385	
q, RAD/sec	-5.861/7.084		-7.306/15.20	.6538/8.639	.1569/6.085	.3786/24.46
r, RAD/sec				1.049/25.25		-.2050/7.749
$\delta_{\text{long aux}}$ , inches	2.971/66.62	1.416/27.58	7.103/522.1		-.2282/468.7	.06784/27.16
$\delta_{\text{lat aux}}$ , inches		.6672/45.70		.3803/755.8	.02145/34.72	.05630/149.2
$\delta_{\text{coll aux}}$ , inches	-.6170/6.007	-.5674/8.529	-8.220/1435.	.09366/11.97	.05507/54.00	-.04522/26.03
$\delta_{\text{ped aux}}$ , inches			-2.481/13.86	.3927/20.93	-.05997/6.232	-.4620/262.7
F-RATIO	16.35	47.56	291.48	148.3	191.1	82.74
R <sup>2</sup>	.1530	.3805	.7631	.6570	.7387	.5503

TABLE 7.9. - CH-53A FLIGHT DATA - OPTIMAL SUBSET REGRESSION RESULTS

146

- 100 kts., without SAS
- Aerodynamic terms only
- SI Maneuver
- 9 dof model - 1st order rotor

	$\dot{u}$ ft/sec <sup>2</sup>	$\dot{v}$ ft/sec <sup>2</sup>	$\dot{w}$ ft/sec <sup>2</sup>	$\dot{p}$ RAD/sec <sup>2</sup>	$\dot{q}$ RAD/sec <sup>2</sup>	$\dot{r}$ RAD/sec <sup>2</sup>	$\dot{\beta}_0$ RAD/sec	$\dot{\beta}_{1c}$ RAD/sec	$\dot{\beta}_{1s}$ RAD/sec
u, ft/sec		-.1769/34.09			-.001906			.001526/3.902	
v, ft/sec		-.1106/234.2		-.001137/3.267	.0005303/9.281	.004441/184.9	-0004905/7.606	-.0006978/12.79	-.001370/31.89
w, ft/sec	-.1134/10.33	-.08100/13.06	-.09912/14.06		-.003352/37.12	-.003908/14.18	.003404/39.73	.002154/7.307	
p, RAD/sec	-2.532/13.95	-4.367/50.95	2.669/24.76	.3134/38.12	-.1179/94.72	.1394/32.95	-.09999/44.22	-.1397/62.95	-.2638/181.7
q, RAD/sec	-5.832/6.324		2.528/2.842		-.09554/4.715	.3622/21.72		-.6268/189.7	
r, RAD/sec			-4.006/7.383	.5212/16.30		-.2898/15.56		.1008/6.210	-.1513/9.245
$\beta_0$ , RAD	63.62/5.676		-261.4/170.9	-6.227/26.33				3.824/46.05	-2.712/33.60
$\beta_{1c}$ , RAD		63.25/29.76	-72.89/84.08		7.035/836.7	-2.813/31.36	-1.920/45.79	-4.114/159.6	
$\beta_{1s}$ , RAD	-62.06/16.33	-45.12/12.18	59.69/29.80	31.33/920.7		4.125/206.5	-1.972/38.20	-1.952/35.99	-3.590/81.29
$\delta_{\text{long aux}}$ , inches	3.632/46.56	4.030/53.10			.09085/55.23	-.04166/2.654	-.1453/114.1	-.2386/264.8	
$\delta_{\text{lat aux}}$ , inches	.8477/12.23	1.259/37.70	-.5632/10.81	-.05912/12.62	-.02750/128.0		.03080/37.06	.04059/63.64	.07513/137.0
$\delta_{\text{coll aux}}$ , inches	-1.465/7.778	-.9610/20.11	-3.181/87.30	.08012/11.61		-.03909/15.89	.05904/125.1	.03114/8.744	-.02269/6.264
$\delta_{\text{ped aux}}$ , inches			-3.085/31.07	.2820/29.11		-.4829/271.3		.03795/5.355	-.02905/2.077
F-RATIO	14.48	42.46	304.47	462.5	513.1	76.79	30.53	91.08	38.44
R <sup>2</sup>	.1764	.4144	.8496	.8724	.8835	.5876	.3110	.6884	.3624

TABLE 7.10. - CH-53A FLIGHT DATA - OPTIMAL SUBSET REGRESSION RESULTS

- 100 kts., without SAS
- Aerodynamic terms only
- S1 Maneuver
- 9 dof model - 2nd.order rotor

	$\dot{u}$ ft/sec <sup>2</sup>	$\dot{v}$ ft/sec <sup>2</sup>	$\dot{w}$ ft/sec <sup>2</sup>	$\dot{p}$ RAD/sec <sup>2</sup>	$\dot{q}$ RAD/sec <sup>2</sup>	$\dot{r}$ RAD/sec <sup>2</sup>	$\ddot{\beta}_0$ RAD/sec <sup>2</sup>	$\ddot{\beta}_{1c}$ RAD/sec <sup>2</sup>	$\ddot{\beta}_{1s}$ RAD/sec <sup>2</sup>
u, ft/sec		-.1817/37.35		.004233/3.545	-.001295/3.115		-.01118/2.823	.02233/7.334	
v, ft/sec		-.09508/195.2	-.009164/2.127	-.003159/30.86	.0005216/9.925	.004771/205.4			-.01333/30.08
w, ft/sec	-.09864/7.880	-.1606/47.91	-.08390/10.75		-.003514/40.37	-.004621/12.63	.1186/310.1	.04956/35.28	.02797/13.76
p, RAD/sec	-5.465/46.24	-1.454/6.977	.8080/2.453	-.1301/5.128	-.1265/114.9	.2042/43.32	-.7297/24.86	-.9488/27.40	-2.521/107.7
q, RAD/sec	-16.75/41.36	2.997/2.441		-.6353/19.19	-.2358/21.15	.7388/71.55	5.486/139.0	1.778/9.521	2.826/17.52
r, RAD/sec			-4.029/8.039	.4729/15.32		-.3446/24.23	-.7296/4.214	-1.471/11.17	.8181/2.494
$\dot{\beta}_0$ , RAD/sec	5.011/4.799		-11.23/59.66		-.2222/25.85		-1.137/7.904	-1.736/12.01	
$\dot{\beta}_{1c}$ , RAD/sec	-16.70/71.39	9.542/36.58			-.1825/23.59	.5920/81.97	1.961/23.92	-1.223/6.067	2.442/19.41
$\dot{\beta}_{1s}$ , RAD/sec	-7.351/22.44	3.421/8.511	-1.727/2.861				-1.200/18.90	-3.440/101.2	-2.294/29.92
$\beta_0$ , RAD	143.8/23.87		-241.4/160.1		1.7323/39.09	-2.873/10.69	-142.7/752.9	-48.33/56.35	7.777/2.560
$\beta_{1c}$ , RAD	-66.48/38.14	89.94/55.01	-87.31/57.51	-3.429/12.86	5.139/1115.		9.844/9.475	-50.99/165.7	22.93/23.33
$\beta_{1s}$ , RAD	-99.64/37.03		25.33/20.31	25.53/678.0		4.935/75.37	10.07/11.97	-14.20/15.53	-90.04/383.2
$\delta_{long}$ aux, inches		6.583/88.21	-.9083/2.976	-.1977/15.65		.1073/31.97	-1.415/81.32	-2.911/224.5	.9066/17.54
$\delta_{lat}$ aux, inches	1.732/42.64	.3774/13.89		.06482/15.10	-.02470/108.7	-.01776/3.699	-.07459/2.509	.3473/35.46	1.129/217.1
$\delta_{coll}$ aux, inches	-1.389/8.648	-1.885/5716	-2.822/61.07	.08207/19.52		-.04923/7.590	2.198/587.0	1.357/145.8	
$\delta_{ped}$ aux, inches			-2.975/27.84	.2844/34.41		-.5070/327.7	-.2679/3.969	-.5812/12.18	
F-RATIO	18.37	40.36	281.5	404.9	460.0	76.04	68.90	45.98	43.40
R <sup>2</sup>	.2730	.4521	.8628	.9076	.8951	.6295	.6593	.5636	.4923

TABLE 7.11.- OSR RESULTS FOR THREE LINEAR MODELS

DERIVATIVE \ MODEL	6 DOF	9 DOF 1st ORDER ROTOR	9 DOF 2nd ORDER ROTOR
$M_u$ , 1/(ft*sec)	-	-.00206/6.290	-.00131/3.117
$M_v$ , 1/(ft*sec)	.00157/32.05	-	
$M_w$ , 1/(ft*sec)	-.01339/327.7	-.00121/3.737	-.00284/26.48
$M_p$ , 1/sec	-	-.13561/52.34	-.18051/272.8
$M_q$ , 1/sec	-.66386/92.09	.20003/14.50	-.24699/22.92
$M_r$ , 1/sec	-.33308/17.80	-	-
$M_{\beta 0}$ , 1/sec <sup>2</sup>	-	-	2.18694/60.72
$M_{\beta 1c}$ , 1/sec <sup>2</sup>	-	6.33428/898.6	5.27916/1143.
$M_{\beta 1s}$ , 1/sec <sup>2</sup>	-	-1.11285/25.64	-1.44412/93.95
$M_{\beta 0}$ , 1/sec	-	-	-.249272
$M_{\beta 1c}$ , 1/sec	-	-	-.23720/40.64
$M_{\beta 1s}$ , 1/sec	-	-	-
$M_{\delta LONG}$ , 1/(sec <sup>2</sup> *in)	-.14347	.03999/22.70	
$M_{\delta LAT}$ , 1/(sec <sup>2</sup> *in)	-.02354/24.06	-.008685/3.152	-
$M_{\delta COLL}$ , 1/(sec <sup>2</sup> *in)	.03535/18.91	.01421/7.221	-
$M_{\delta PED}$ , 1/(sec <sup>2</sup> *in)	-.08264/14.19	-	-
$R^2$	.666037	.868342	.892402
F-Ratio	134.87	395.73	497.63

- CH-53A Flight Data, 100 KTS
- SAS On

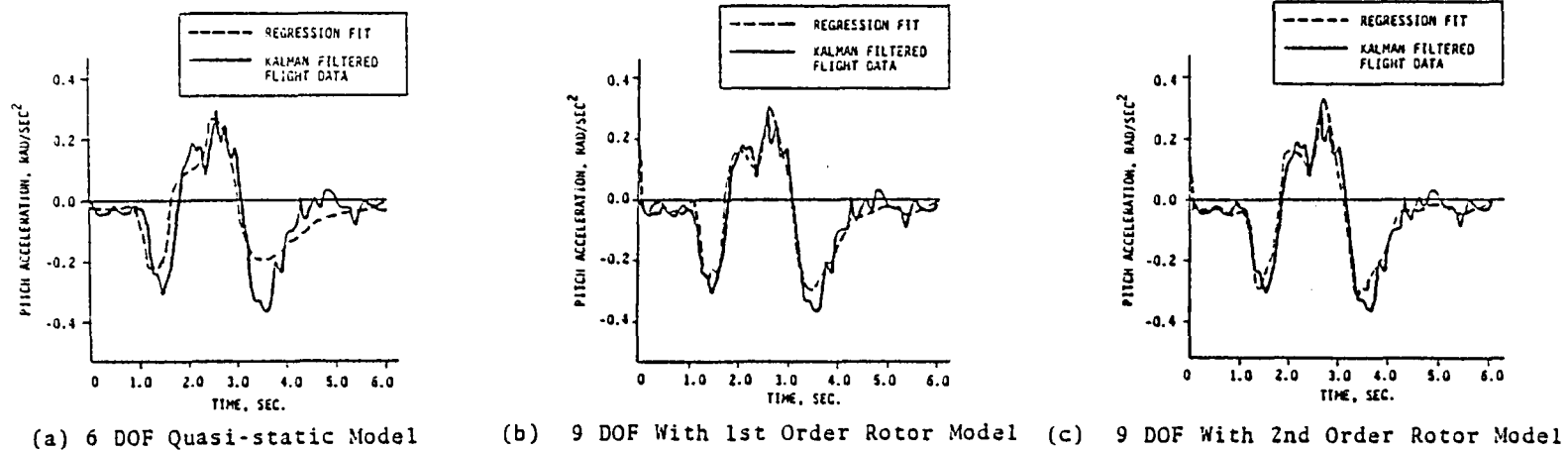


FIGURE 7. 7.- COMPARISON OF KALMAN FILTERED FLIGHT DATA WITH THE REGRESSION FIT ON PITCH ACCELERATION FOR A CH-53A AT 100 KTS, SAS ON

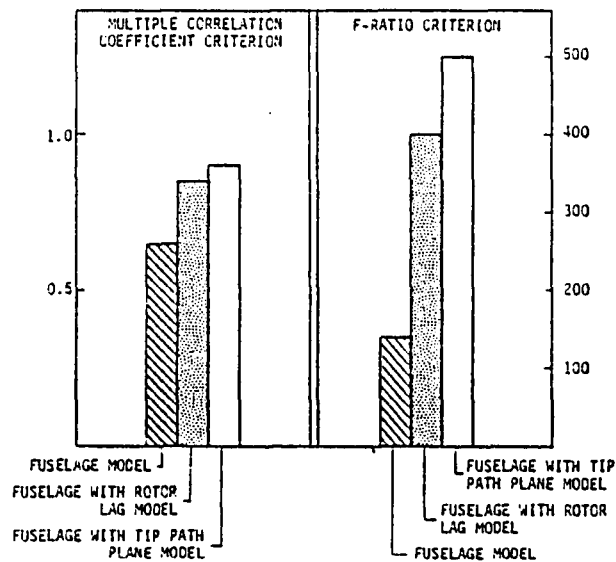


FIGURE 7. 8.- FLIGHT DATA IDENTIFIED CONTRIBUTIONS OF ROTOR MODEL TO OVERALL "FIT"

TABLE 7.12.— OSR RESULTS WITH AND WITHOUT SAS

DERIVATIVE \ MODEL	SAS ON	SAS OFF
$M_u$ , 1/(ft*sec)	-	-
$M_v$ , 1/(ft*sec)	.00157/32.05	.00133/22.99
$M_w$ , 1/(ft*sec)	-.0134/327.7	-.00469/31.34
$M_p$ , 1/sec	-	-.0517/7.39
$M_q$ , 1/sec	-.664/92.09	.1569/6.09
$M_r$ , 1/sec	-.3331/17.80	-
$M_{\beta 0}$ , 1/sec <sup>2</sup>	-	-
$M_{\beta 1c}$ , 1/sec <sup>2</sup>	-	-
$M_{\beta 1s}$ , 1/sec <sup>2</sup>	-	-
$\dot{M}_{\beta 0}$ , 1/sec	-	-
$\dot{M}_{\beta 1c}$ , 1/sec	-	-
$\dot{M}_{\beta 1s}$ , 1/sec	-	-
$M_{\delta LONG}$ , 1/(sec <sup>2</sup> *in)	-.143/231.7	-.2282/468.7
$M_{\delta LAT}$ , 1/(sec <sup>2</sup> *in)	-.0235/24.06	.0215/34.72
$M_{\delta COLL}$ , 1/(sec <sup>2</sup> *in)	.0354/18.91	.0551/54.00
$M_{\delta PED}$ , 1/(sec <sup>2</sup> *in)	-.0826/14.9	-.05997.6.23
$R^2$	.666037	.73865
F-Ratio	134.87	191.13

- CH-53A Flight Data, 100 KTS
- 6 DOF Linear Model

PARAMETER VALUE

XXXXX/XXXXX

F TO REMOVE



on the level of process noise chosen. Further attempts to identify the process noise power spectral density were inconclusive. The moral of this effort is that it is dangerous to rely on low order models when significant higher order dynamics are present.

### Bell 609 Rotorcraft Results

Parameter identification results were generated with linear SCIDNT for the Bell 609 rotorcraft, using actual in-flight data as input. This flight data was acquired from Bell Helicopter (Textron) on a magnetic tape which contained control and measurement time history records of longitudinal maneuvers performed on May 23, 1973. The particular maneuver data used in this identification example was #4158, which consisted of a 1 second aft pulse on the stick (longitudinal cyclic input). This particular maneuver was chosen because there was very little lateral stick motion.

A fourth-order linear model was used in the parameter identification program. This model is

$$\frac{d}{dt} x(t) = Fx(t) + Gu(t)$$

$$y(t) = Hx(t) + v(t)$$

$$E[v(t)v^T(\tau)] = R\delta(t-\tau)$$

Assigning the states  $u(t)$ ,  $w(t)$ ,  $q(t)$ , and  $\theta(t)$ , longitudinal velocity, vertical velocity, pitch rate, and pitch attitude to  $x$  and  $y$ , and assigning the controls  $B_{1c}(t)$  and  $l$  to  $u$ , the model can be written as follows:

$$\frac{d}{dt} \begin{bmatrix} u(t) \\ w(t) \\ q(t) \\ \theta(t) \end{bmatrix} = \begin{bmatrix} X_u & X_w & X_q - W_o & -g \cos\theta_o \\ Z_u & Z_w & Z_q + U_o & -g \sin\theta_o \\ M_u & M_w & M_q & 0 \\ 0 & 0 & 1 & 0 \end{bmatrix} \begin{bmatrix} u(t) \\ w(t) \\ q(t) \\ \theta(t) \end{bmatrix} + \begin{bmatrix} X_B & X_o \\ Z_B & Z_o \\ M_B & M_o \\ 0 & 0 \end{bmatrix} \begin{bmatrix} B_{1c}(t) \\ l \end{bmatrix}$$

$$\begin{bmatrix} u_m(t) \\ w_m(t) \\ q_m(t) \\ \theta_m(t) \end{bmatrix} = \begin{bmatrix} 1. & 0. & 0. & 0. \\ 0. & 1. & 0. & 0. \\ 0. & 0. & 1. & 0. \\ 0. & 0. & 0. & 1. \end{bmatrix} \begin{bmatrix} u(t) \\ w(t) \\ q(t) \\ \theta(t) \end{bmatrix} + \begin{bmatrix} n_u(t) \\ n_w(t) \\ n_q(t) \\ n_\theta(t) \end{bmatrix}$$

The time history measurements used were:  $V_m$ , total velocity,  $\alpha_m$ , angle-of-attack,  $q_m$ , pitch rate, and  $\theta_m$ , pitch attitude.  $V_m$  and  $\alpha_m$  were resolved into  $u_m$  and  $w_m$ , and after proper units conversion, the tape was read by SCIDNT. A total of 287 points, spaced at a .125 second sample interval, were used (every 64th point was used). The nominal airspeed of the maneuver was 60 kts (100 ft/sec).

The SCIDNT run was started with most of the unknown parameters in F and G as zero. The F and G matrices were initially input as follows (with parameters to be identified starred).

$$F = \begin{bmatrix} 0.* & 0.* & 0.* & -32.17 \\ 0.* & 0.* & 100.* & .337 \\ 0.* & 0.* & 0.* & 0. \\ 0. & 0. & 1. & 0. \end{bmatrix}$$

$$G = \begin{bmatrix} 0.* & 0.* \\ 0.* & 0.* \\ 0.* & 0.* \\ 0. & 0. \end{bmatrix}$$

After 27 iterations, linear SCIDNT calculated the following F and G matrices:

Final F =

$$\begin{bmatrix} 3.59 \times 10^{-6*} & -1.83 \times 10^{-6*} & -31.7* & -32.17 \\ -.157* & 4.93 \times 10^{-7*} & 66.9* & .337 \\ .00567* & -9.0 \times 10^{-9*} & -3.83* & 0 \\ 0 & 0 & 1. & 0 \end{bmatrix}$$

Final G =

$$\begin{bmatrix} .116* & -5.41* \\ .837* & -40.3* \\ -.0244* & 1.16* \\ 0. & 0. \end{bmatrix}$$

The final F matrix had the following eigenvalues:

$$-3.8, 0.0, \text{ and } -1.73 \pm j0.22.$$

The particular estimates from these matrixes, as well as the standard deviations and F-ratios are presented in Figure 7.9.

It can be seen from the F-statistics that the pitching moment coefficients should be regarded as the most accurate parameter estimates. This is to be expected, as longitudinal stick motion primarily excites pitch dynamics. Other parameters, such as  $X_u$ ,  $X_w$ ,  $Z_w$  and  $M_w$  are basically unidentifiable as is indicated by the low F-ratios.

Since the initial value of the control was not subtracted out of the data, and bias terms  $X_o$ ,  $Z_o$ , and  $M_o$  are estimated, an approximate value of the control bias can be calculated as

$$\begin{aligned} B_{1c_o} &= -(X_o^2 + Z_o^2 + M_o^2) / (X_{B_{1c}} X_o + Z_{B_{1c}} Z_o + M_{B_{1c}} M_o) \\ &\approx 48.2\% \end{aligned}$$

The estimate of the control bias is fairly good, that is, 48 percent, compared to an actual value of 50 percent.

In conclusion, careful preliminary analysis of the flight data and the modeling should be made prior to any SCIDNT run. In particular, it is recommended that DEKFIS be used to verify flight data consistency and OSR be used to assure proper modeling. In this case, it was attempted to bypass these steps with obvious consequences.

### RSRA Results

Results for the rotor systems research aircraft (RSRA) consist of simulation data processed through the optimal subset regression (OSR) computer program

The simulation data was provided by NASA Langley Research Center and was generated by the Nonlinear RSRA simulation mathematical model [Ref. 63]. This model was simulated to the control inputs shown in Figure 7.10. These inputs are superior to the more common step and doublet inputs usually used for identification [Refs. 61 and 62]. Unfortunately, the magnitude of these control inputs was exceedingly large, and the unstable simulation model diverged over the length of the 25.5 second maneuver. Nevertheless, the data were processed through OSR to show its flexibility in breaking out the rotor force and moment contributions. Whereas the results alone are of questionable value, the techniques investigated should prove to be quite useful when processing actual RSRA flight data.

Three different models were identified from this data. These were:

(1) 12 dof with 2nd order rotor; (2) rotor hub force/moment breakdown; (3) 6 dof with rotor hub force/moment contributions.

The first model is a 12 degree of freedom (dof) model with 6 body dof's, 3 rotor flapping dof's and 3 motor lagging dof's. Each rotor flapping and lagging degree of freedom is of second order. The resulting OSR identified model is shown in Table 7.13. Because of the large nonzero mean excursions in the independent variables (i.e.,  $u, w, q$ ), the parameters identified in the linear model are not physically realistic. An attempt was made to identify some nonlinear (polynomial type) parameters. This is shown in Table 7.14.

The second model is a rotor hub force and moment breakdown model where the hub forces and moments were treated as dependent variables and the 12 dof rotor (only) model was identified. Table 7.15 shows this breakdown.

The third model identified is a 6 dof body/fuseage model where the rotor hub forces and moments are treated as control inputs (i.e., independent variables). The results are shown in Table 7.16

Note that in many cases quite reasonable regression fits and F-ratios were achieved. These results can be deceiving, however. Since the sum of squares of the signal was large, the residual error will be proportionately large for a given multiple correlation coefficient ( $R^2$ ). These residual errors are

Parameter	Estimated Value	Standard Deviation	F-Value
$X_U$	$3.59 \times 10^{-6}$	$1.62 \times 10^{-3}$	$4.93 \times 10^{-6}^*$
$Z_U$	-.157	.0482	10.5
$M_U$	.0057	.0005	126.
$X_W$	$-1.83 \times 10^{-6}$	$7.78 \times 10^{-3}$	$5.56 \times 10^{-8}^*$
$Z_W$	$4.93 \times 10^{-7}$	$6.73 \times 10^{-3}$	$5.36 \times 10^{-9}^*$
$M_W$	$-9.0 \times 10^{-9}$	$1.48 \times 10^{-4}$	$3.69 \times 10^{-9}^*$
$X_Q$	-31.65	1.84	29.4
$Z_Q$	-33.08	33.06	4.09
$M_Q$	-3.83	.336	130.0
$X_{B1c}$	.115	.023	25.2
$Z_{B1c}$	.837	.160	27.26
$M_{B1c}$	-.0244	.00171	20.3
$X_O$	-5.42	1.14	22.6
$Z_O$	-40.4	7.63	27.9
$M_O$	1.16	.0818	201.1

\* Not Identifiable

FIGURE 7.9 - PARAMETER ESTIMATES AND STANDARD DEVIATIONS FOR BELL MODEL 609 AT 60 KTS.

not negligible, and substantially more nonlinear modeling is required to yield reasonable numbers. On the other hand, if too many additional independent variables are added, the number of independent variables can equal or exceed the number of data points in the regression. For the supplied sampling period ( $T=0.2$  sec), it is neither reasonable to substantially increase the number of independent variables to model the nonlinearities nor to reduce the length of the data segment to maintain the linearity of the data.

### UH-1H Results

The UH-1H results consist of control input design and flight data processing through the SCIDNT computer program. Initially, a series of stepwise control inputs were designed for implementation in the UH-1H flight test program based on a UH-1H linear model. These inputs were subsequently duplicated by the pilot during the flight testing. The conventional doublet inputs were also used in the flight tests. The final step was to process the data through the SCIDNT parameter identification program and get improved linear models.

Input design for UH-1H flight testing. - To illustrate the sequence of computations and type of inputs, the application of the input design algorithm to a low order simulated linear model of a UH-1H helicopter (no stabilizer bar) at 60 kts was computed. Only the longitudinal dynamics were considered, and thus the quasi-static rotor assumption is evoked. The assumed model, based on C-81 [Ref. 64] computations, is shown in Figure 7.11, where five measurements are assumed ( $u, w, q, \theta, a_z$ ) and with measurement random noise power spectral density (units ft, rad, sec)

$$R = \text{diag} [4., 4., 10^{-4}, 10^{-4}, 4.]$$

The two controls, collective stick  $\delta_{\text{COLL}}$  and longitudinal cyclic stick  $\delta_{\text{LONG}}$  are assumed applied individually. It is desired to design inputs which maximize the accuracy of the parameters underlined in the matrices (10 parameters). For this input, 8 seconds of total input time are specified, with only 1 second steps allowed. For both inputs,  $\delta_{\text{COLL}}$  and  $\delta_{\text{LONG}}$ , mean square control excursions are limited:

$$\int_0^8 100 \delta^2 dt = 1.0.$$

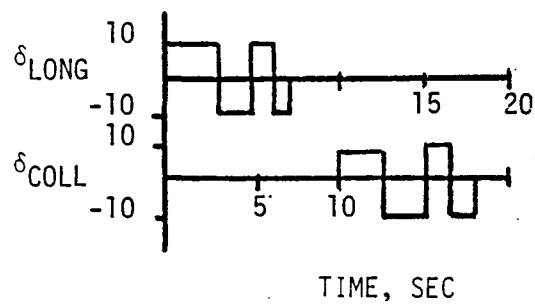
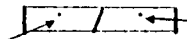


FIGURE 7.10.— RSRA SIMULATION CONTROL INPUTS  
 (STICK DEFLECTION IS IN PERCENT  
 OF TOTAL TRAVEL RELATIVE TO THE  
 TRIM STICK POSITION)

TABLE 7.13. - RSRA SIMULATION DATA - OSR RUNS - LINEAR - 12 DOF WITH  
2ND ORDER ROTOR


F to Remove  
Coefficient Value

	$\ddot{u}$ FT/SEC <sup>2</sup>	$\ddot{v}$ FT/SEC <sup>2</sup>	$\ddot{w}$ FT/SEC <sup>2</sup>	$\ddot{p}$ RAD/SEC <sup>2</sup>	$\ddot{q}$ RAD/SEC <sup>2</sup>	$\ddot{r}$ RAD/SEC <sup>2</sup>
u, ft/sec	-.108938/659.7	-	-.0982755/55.82	-	-	-.0001866/42.16
v, ft/sec	-	.780321/582.7	.527098/36.42	.0040090/11.15	-	.0025545/61.72
w, ft/sec	-	-1.32923/134.1	-	-	-	-.00131511/36.62
p, rad/sec	.792670/17.20	-	-	-	-	-.0424003/45.91
q, rad/sec	-	-10.7371/5.915	136.726/266.3	-	-	-
r, rad/sec	-38.5933/456.2	-154.652/403.9	78.9239/17.53	-	-.500467/161.4	-.309070/23.53
$\phi$ , radians	-2.75896/660.8	-	-	-	.0292561/119.6	-
$\psi$ , radians	-35.8445/1623.	-	-	-	-.0613266/15.35	-
$\beta$ , rad/sec	-	-38.0693/23.41	-	2.33184/35.98	.253363/14.37	-.154603/6.503
$\beta_{1c}$ , rad/sec	-6.37844/75.98	44.5946/23.29	16.9444/19.89	-1.64247/180.6	-.15317/45.97	.137973/38.46
$\beta_{1s}$ , rad/sec	27.5079/72.46	-207.816/376.6	-190.027/133.4	10.2840/439.9	1.66507/265.4	-.351517/20.73
$\beta_0$ , rad	-	495.536/69.57	-	-	-2.02214/170.9	-
$\beta_{1c}$ , rad	-	135.652/149.2	125.448/23.94	-	-	-
$\beta_{1s}$ , rad	-	-	-	-	-	.430655/181.5
$\zeta_0$ , rad/sec	-	-	-	-	-	-
$\zeta_{1c}$ , rad/sec	-	-	-	-	-	-
$\zeta_{1s}$ , rad/sec	-	-	-	-	-	-
$\zeta_0$ , rad	25.5739/98.12	-	-149.185/69.88	-	.631489/52.49	-.662435/105.6
$\zeta_{1c}$ , rad	-	-	-	-	-	-
$\zeta_{1s}$ , rad	.0849889/30.03	-	-	-	-	.0014917/17.53
$\delta_{LONG}$ , inches	-	-	-	-	-	-
$\delta_{LAT}$ , inches	-	-1.66441/85.07	-.569339/33.32	-	.0092254/232.6	-
$\delta_{COLL}$ , inches	-	-	-	-	-	-
$\delta_{PED}$ , inches	-	-	-	-	-	-
F-Ratio	4631.7	179.25	46.271	181.12	96.594	82.9
R <sup>2</sup>	.997177	.938729	.798175	.854863	.891961	.887149



TABLE 7.13. -- CONCLUDED

	$\ddot{\beta}_0$ RAD/SEC <sup>2</sup>	$\ddot{\beta}_{1c}$ RAD/SEC <sup>2</sup>	$\ddot{\beta}_{1s}$ RAD/SEC <sup>2</sup>	$\ddot{\zeta}_0$ RAD/SEC <sup>2</sup>	$\ddot{\zeta}_{1c}$ RAD/SEC <sup>2</sup>	$\ddot{\zeta}_{1s}$ RAD/SEC <sup>2</sup>
u, ft/sec	-	-	-	-.00135146/93.50	-	.0005515/83.09
v, ft/sec	-	-	-	-	-	-
w, ft/sec	-	-	-	-	-	-
p, rad/sec	-	-	-	-	-	-
q, rad/sec	-	-	-	.487964/12.41	-	-.161654/19.65
r, rad/sec	-	-	-	-	-.111215/7.750	-
$\phi$ , rad	-	-	-	-	-	-
$\theta$ , rad	-	-	-	-	-	-
$\dot{\beta}_0$ , rad/sec	1.24137/14.70	-3.70532/50.43	-1.1000/61.52	-	-	-
$\dot{\beta}_{1c}$ , rad/sec	.615372/35.19	-2.49783/255.3	-.506508/120.4	-	-.479954/1009.	.215715/163.4
$\dot{\beta}_{1s}$ , rad/sec	1.66034/21.50	-3.05377/27.76	-	-	-	-
$\beta_0$ , rad	-	-	-.532184/28.29	-	-	.658497/46.39
$\beta_{1c}$ , rad	-	-	-1.1689/56.93	-	-	-
$\beta_{1s}$ , rad	-	-	-.458404/33.76	-	.331959/53.39	-
$\dot{\zeta}_0$ , rad/sec	-	-	-	-3.89073/20.94	-	-
$\dot{\zeta}_{1c}$ , rad/sec	3.36914/11.45	-	-	-	3.03866/134.7	-
$\dot{\zeta}_{1s}$ , rad/sec	-	-	-	-	-	-
$\zeta_0$ , rad	-	-	-	-3.92671/125.2	-	-
$\zeta_{1c}$ , rad	-	-	-	-	-	-
$\zeta_{1s}$ , rad	-	-	-	-	-	-10.5956/145.4
$\delta_{LONG}$ , inches	-	-.022818/44.47	-	-	-	-
$\delta_{LAT}$ , inches	-.0165573/60.87	-	-	-	-.002584/19.59	-
$\delta_{COLL}$ , inches	-	-	-	-	-	-
$\delta_{PED}$ , inches	-	-	-	-	-	-
F-Ratio	84.373	255.34	87.987	47.629	276.40	84.357
R <sup>2</sup>	.775680	.8925	.78289	.607678	.918883	.775646

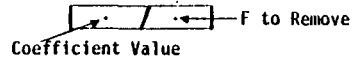
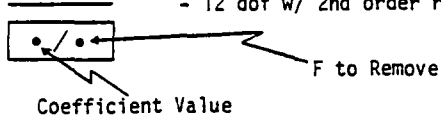
 F to Remove  
Coefficient Value

TABLE 7.14. - RSRA SIMULATION DATA - OSR RUNS

- Longitudinal
- Transgenerated  $u^2, w^2, q^2, uw, u, q, wq$  terms
- 12 dof w/ 2nd order rotor



	$\dot{u}$ ft/sec <sup>2</sup>	$\dot{w}$ ft/sec <sup>2</sup>	$\dot{q}$ ft/sec <sup>2</sup>
u, ft/sec	.0462094/45.23		
v, ft/sec	-.150251/328.7		
w, ft/sec			-.00222258/7.712
p, rad/sec		-51.4330/169.9	
q, rad/sec	-12.0530/54.60	50.3129/38.40	.287329/45.96
r, rad/sec		90.4102/72.66	-.479089/103.5
$u^2, ft^2/sec^2$	-.000282046/709.7		
$w^2, ft^2/sec^2$			
$q^2, rad^2/sec^2$		-331.375/56.42	-1.90977/72.51
$u \cdot w, ft^2/sec^2$		.00720504/153.0	-.000014654/20.38
$u \cdot q, ft \cdot rad/sec^2$	-.172689/132.4	.976432/139.4	
$w \cdot q, ft \cdot rad/sec^2$	-1.16709/213.7		.0187846/43.95
$\phi, radians$	-.733555/43.35		.0260525/153.6
$\phi, radians$	-27.2399/1544.		
$\dot{\beta}_O, rad/sec$			
$\dot{\beta}_{1C}, rad/sec$			-.220495/112.3
$\dot{\beta}_{1S}, rad/sec$			1.30155/398.3
$\beta_O, radians$		199.449/39.26	-1.48749/12.30
$\beta_{1C}, radians$	8.79354/47.60		-1.01747/119.4
$\beta_{1S}, radians$		840.703/189.9	
$\dot{\zeta}_O, rad/sec$			
$\dot{\zeta}_{1C}, rad/sec$			
$\dot{\zeta}_{1S}, rad/sec$			
$\zeta_O, radians$		-153.125/74.72	.591002/97.90
$\zeta_{1C}, radians$			
$\zeta_{1S}, radians$			
$\delta_{LONG}, inches$		-.595814/49.57	
$\delta_{LAT}, inches$			.00750275/42.01
$\delta_{COLL}, inches$			.00750275/42.01
$\delta_{PED}, inches$			
F-Ratio	10210.	49.731	129.75
R <sup>2</sup>	.998718	.809541	.936692

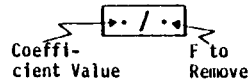
TABLE 7.15. - RSRA SIMULATION DATA - OSR RUNS - LINEAR, 12 DOF,  
2ND ORDER ROTOR - ROTOR FORCE/MOMENT BREAKDOWN

Coefficient Value →  $\cdot / \cdot$  ← F to Re-move

	$X_R$ ft/sec <sup>2</sup>	$Y_R$ ft/sec <sup>2</sup>	$Z_R$ ft/sec <sup>2</sup>	$L_R$ rad/sec <sup>2</sup>	$M_R$ rad/sec <sup>2</sup>	$N_R$ rad/sec <sup>2</sup>
u, ft/sec	-.00652639/45.39		-.155099/539.8	-.00120664/28.57	.000663154/71.47	.000338245/610.3
v, ft/sec		.02646/51.93				-.00416582/493.7
w, ft/sec			-.679121/195.0	.00728603/46.09		
p, rad/sec		1.84322/615.0				
q, rad/sec	-2.1530/62.34				.298756/158.4	
r, rad/sec		1.28644/3.263		.687865/16.19		.876033/563.6
$\psi$ , rad	-.192164/79.05		-3.43178/451.5	-.0975959/56.85	.0346858/309.8	
$\theta$ , rad	2.39862/155.0		-27.7042/324.0		-.0990877/41.31	
$\delta_{LONG}$ , inches	.030524/66.35					
$\delta_{LAT}$ , inches						
$\delta_{COLL}$ , inches		-.0240146/24.90	-1.17629/284.3			.00346815/110.7
$\delta_{PED}$ , inches						
$\beta_0$ , rad			267.937/111.6			-.393753/55.19
$\beta_{1C}$ , rad			83.0572/166.7	-1.10282/23.61	-.763121/404.2	
$\beta_{1S}$ , rad			27.9802/32.99			-1.03361/284.2
$\dot{\beta}_0$ , rad/sec				1.40552/22.46		
$\dot{\beta}_{1C}$ , rad/sec	-1.39531/131.1	-1.95725/122.8		-1.75356/268.9		
$\dot{\beta}_{1S}$ , rad/sec		7.19282/92.32	-20.4926/44.39	8.89439/478.3	.391089/111.1	
$\zeta_0$ , rad						-.780316/375.8
$\zeta_{1C}$ , rad						
$\zeta_{1S}$ , rad						
$\dot{\zeta}_0$ , rad/sec		-2.51541/56.39	-24.0639/157.0	-.838172/29.75		.334434/454.2
$\dot{\zeta}_{1C}$ , rad/sec						
$\dot{\zeta}_{1S}$ , rad/sec						
F-Ratio	2089.3	383.57	501.07	159.66	1094.0	924.32
R <sup>2</sup>	.990440	.957219	.977183	.924115	.981900	.984162

TABLE 7.16. - RSRA SIMULATION DATA - OSR RUNS - LINEAR - 6 DOF WITH ROTOR FORCE/MOMENT CONTRIBUTIONS

162



	$\ddot{u}$ ft/sec <sup>2</sup>	$\ddot{v}$ ft/sec <sup>2</sup>	$\ddot{w}$ ft/sec <sup>2</sup>	$\ddot{p}$ rad/sec <sup>2</sup>	$\ddot{q}$ rad/sec <sup>2</sup>	$\ddot{r}$ rad/sec <sup>2</sup>
u, ft/sec	-.106146/360.9					-.000151235/2.313
v, ft/sec						.00917058/507.2
w, ft/sec			.627368/50.99		-.00851137/341.4	-.00211978/66.10
p, rad/sec		-33.2212/144.4			-.0302990/10.27	.110442/52.49
q, rad/sec	14.3666/48.48		110.979/132.9			
rad, rad/sec	-22.1317/112.2	-49.6356/27.72	96.4448/90.56			-1.14855/209.1
$\phi$ , rad	-2.68670/286.5	-3.38161/42.00	4.87067/115.7	.0320097/231.5		
$\theta$ , rad	-41.5172/1474.	13.9795/73.52				.0991914/16.96
$\delta_{LONG}$ , inches					-.00149956/8.895	
$\delta_{LAT}$ , inches						
$\delta_{COLL}$ , inches		.493362/44.62	576395/23.85			-.00557196/176.6
$\delta_{PED}$ , inches						
$X_R$ , ft/sec <sup>2</sup>	3.51784/74.48				.0743372/30.05	.0102781/6.407
$Y_R$ , ft/sec <sup>2</sup>		15.1571/68.35				-.0367486/17.04
$Z_R$ , ft/sec <sup>2</sup>		.357942/28.54	1.40466/105.1		-.00617716/40.11	
$L_R$ , rad/sec <sup>2</sup>		-40.0115/259.8		1.10766/12460.	.0958124/145.0	-.0538265/32.54
$M_R$ , rad/sec <sup>2</sup>	12.3210/12.26		32.6719/17.82		1.27048/38.70	
$N_R$ , rad/sec <sup>2</sup>				.522857/84.28	-.572691/74.12	.994565/613.1
F-Ratio	3840.6	111.87	33.763	4596.4	94.979	139.06
R <sup>2</sup>	.995556	.882638	.663244	.991088	.864593	.929513

STATE EQUATIONS:

$$\frac{d}{dt} \begin{bmatrix} u \\ w \\ q \\ \theta \end{bmatrix} = \begin{bmatrix} \underline{-.0227} & .0587 & -5.645 & -32.09 \\ .0013 & \underline{-.7542} & 101.71 & -2.314 \\ \underline{.00373} & \underline{-.0032} & \underline{-.5305} & 0 \\ 0 & 0 & 1.0 & 0 \end{bmatrix} \begin{bmatrix} u \\ w \\ q \\ \theta \end{bmatrix} + \begin{bmatrix} \underline{.7115} & \underline{.862} \\ \underline{-9.818} & \underline{2.46} \\ \underline{.0064} & \underline{-.180} \\ 0 & 0 \end{bmatrix} \begin{bmatrix} \delta_{\text{COLL}} \\ \delta_{\text{LONG}} \end{bmatrix}$$

MEASUREMENT EQUATIONS:

$$\begin{bmatrix} u_M \\ w_M \\ q_M \\ \theta_M \\ a_{z_M} \end{bmatrix} = \begin{bmatrix} 1.0 & 0 & 0 & 0 \\ 0 & 1.0 & 0 & 0 \\ 0 & 0 & 1.0 & 0 \\ 0 & 0 & 0 & 1.0 \\ .0013 & \underline{-.7542} & 0 & 0 \end{bmatrix} \begin{bmatrix} u \\ w \\ q \\ \theta \end{bmatrix} + \begin{bmatrix} 0 & 0 \\ 0 & 0 \\ 0 & 0 \\ 0 & 0 \\ \underline{-9.818} & \underline{2.460} \end{bmatrix} \begin{bmatrix} \delta_{\text{COLL}} \\ \delta_{\text{LONG}} \end{bmatrix}$$

FIGURE 7.11. — THREE DEGREE OF FREEDOM LINEAR STATE AND MEASUREMENT EQUATIONS FOR THE UH-1H HELICOPTER

- No Stabilizer Bar
- 60 Kts

Figures 7.12 and 7.13 show the iteration outputs as the algorithm minimizes the sum of the estimated variances of the parameter error covariance matrix (J). In both cases, a conventional pulse input is used to start the iteration. The cyclic input is seen to reduce the cost J by 60 percent. The collective input reduces J by 68 percent.

A considerably more complex input design approach was taken for flight test. The linear math model used in this design was derived from C-81 simulation. It is an eight degree-of-freedom, 10-state model with four inputs. It is assumed that we have measurements of 10 independent quantities. The states, controls and measurements are as follows:

States (x): u, w, q,  $\theta$ , v, p, r,  $\phi$ ,  $a_1$ ,  $b_1$

Inputs (u):  $\delta_{LONG}$ ,  $\delta_{LAT}$ ,  $\delta_{PED}$ ,  $\delta_{COLL}$

Measurements (y): u, w, q,  $\theta$ , v, p, r,  $\phi$ ,  $a_1$ ,  $a_z$

The state and measurement equations are

$$\dot{x} = Fx + Gu$$

$$y(k) = Hx(k) + Du(k) + v(k)$$

Nominal values of F, G, and H matrices used in input design are shown in Table 7.17. Note that we have continuous state equations with discrete measurements. v(k) is a noise term which is assumed zero mean white Gaussian with covariance (units ft., sec., rad).

$$R = \text{diag}[4.0, 4.0, 0.0001, 0.0004, 4.0, 0.0001, 0.0001, 0.0004, 0.0004, 4.0]$$

There are about 80 parameters of interest. Since a single input could not possibly excite the system to identify all the parameters simultaneously, 10 individual sequences were designed. Each input sequence was designed to maximize estimation accuracy of only 10 parameters. Some important parameters are included in two or more sequences. Table 7.18 lists the parameters for which each of the 10 inputs is designed. The inputs are shown in Figure 7.14. Each input consists of a sequence of eight steps each of 1 sec. duration and has been designed to minimize total input energy (which in turn also restricts output energy).

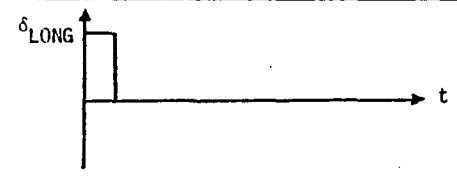
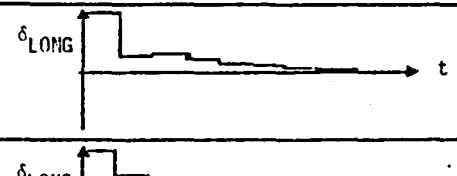
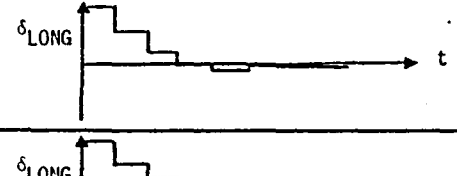
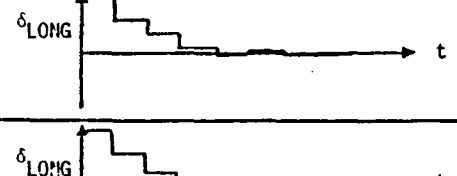
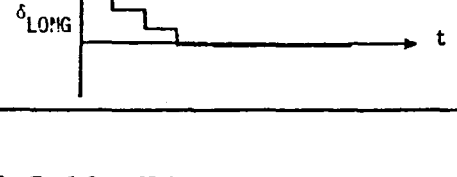
ITERATION	8 STEP INPUT	J	LARGEST EIGENVALUE	Y
1		416.47	962.19	.37263
2		323.60	483.04	.67249
3		261.85	290.01	.81753
4		255.92	269.58	.93784
5		251.27		

FIGURE 7.12 UH-1H INPUT DESIGN - LONGITUDINAL STICK CONTROL,  $\delta_{LONG}$

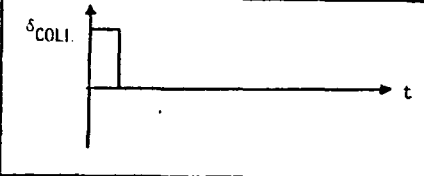
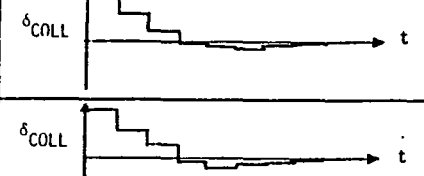
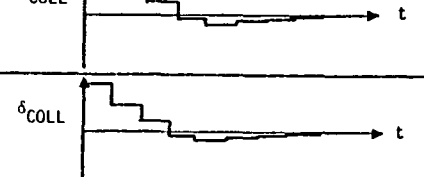
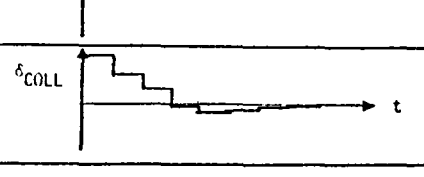
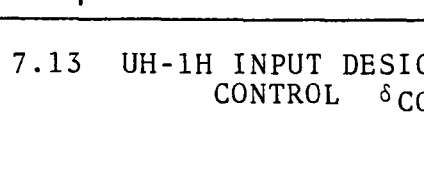
ITERATION	8 STEP INPUT	J	LARGEST EIGENVALUE	Y
1		68051.	104385.	.77643
2		46599.	47168.3	.99022
3		46209.	46229.6	.99973
4		46195.	46196.5	.99998
5		46194.		

FIGURE 7.13 UH-1H INPUT DESIGN - COLLECTIVE STICK CONTROL  $\delta_{COLL}$

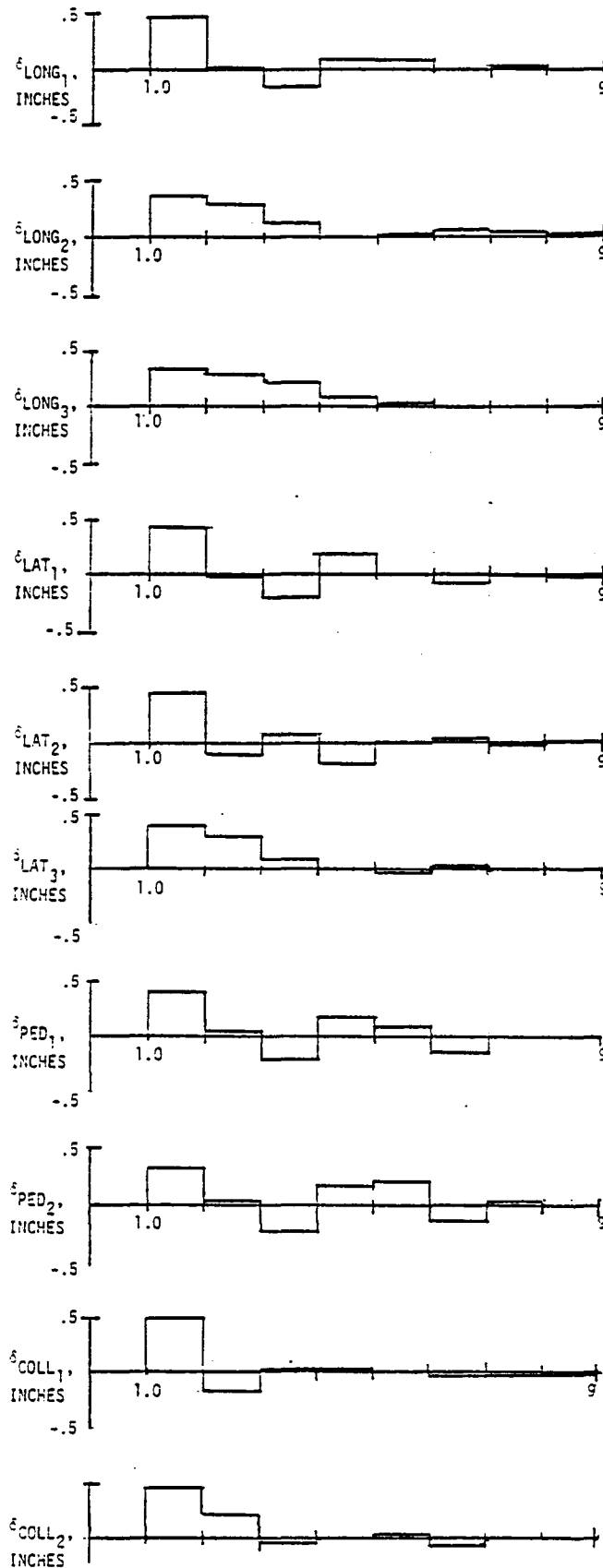


FIGURE 7.14 OPTIMAL INPUTS



Table 7.17

Eight Degree of Freedom Linear State And Measurement  
For the UH-1H Helicopter

• No Stabilizer Bar

• 60 Kts

F	1	2	3	4	5	6	7	8	9	10
1	-1.3400E-02	6.3300E-02	-7.0660E+00	-3.2090E+01	1.2800E-02	5.2150E-01	-1.8530E-01	0.	-3.1800E+01	8.5700E+00
2	4.4000E-04	-7.5860E-01	1.0226E+02	-2.3140E+00	-2.3900E-02	-1.5840E+00	1.8531E+00	0.	1.0187E+01	2.1310E+00
3	2.2150E-03	-3.9700E-03	-3.0910E-01	0.	-9.1000E-04	-7.6100E-02	-1.4200E-02	0.	5.1870E+00	-1.4633E+00
4	0.	0.	1.0000E+00	0.	0.	0.	0.	0.	0.	0.
5	1.5240E-03	-2.2790E-02	2.6910E-01	0.	-1.0570E-01	6.0126E+00	-1.0131E+02	9.2090E+01	1.1457E+01	2.0717E+01
6	1.9530E-03	-3.1700E-03	1.0050E-01	0.	-5.5800E-02	-7.4630E-01	1.7054E+00	0.	1.3573E+01	1.5361E+01
7	-2.3500E-03	-1.6670E-02	1.2120E-01	0.	4.0190E-02	3.3600E-01	-1.3770E+00	0.	-6.2740E+00	-2.7390E-01
8	0.	0.	0.	0.	0.	1.0000E+00	7.2130E-02	0.	0.	0.
9	2.4000E-03	7.8500E-03	-1.0170E+00	0.	1.7400E-03	1.2360E-02	3.0400E-02	0.	-1.3450E+01	-6.0650E+00
10	-4.1200E-03	5.0300E-03	3.9300E-02	0.	-5.4900E-03	-1.0330E+00	-1.1050E-01	0.	6.5670E+00	-1.4036E+01

G	1	2	3	4
1	1.2630E+00	-1.4670E-01	-3.2860E-01	-4.0800E-02
2	-1.3238E+01	3.5830E+00	-2.9700E-02	-4.5800E-02
3	-1.1060E-01	-7.9000E-03	1.5310E-02	-1.8400E-02
4	0.	0.	0.	0.
5	-3.2210E-01	4.3690E-01	2.1500E-01	1.6781E+00
6	-3.9400E-01	2.5380E-01	2.7860E-01	2.0870E+00
7	1.9130E-01	3.1300E-02	-1.4660E-01	-1.6010E+00
8	0.	0.	0.	0.
9	1.2500E-01	-4.4930E-01	1.8890E-01	2.2900E-02
10	-6.2600E-02	2.3170E-01	3.7090E-01	-1.1500E-02

H	1	2	3	4	5	6	7	8	9	10
1	1.0000E+00	0.	0.	0.	0.	0.	0.	0.	0.	0.
2	0.	1.0000E+00	0.	0.	0.	0.	0.	0.	0.	0.
3	0.	0.	1.0000E+00	0.	0.	0.	0.	0.	0.	0.
4	0.	0.	0.	1.0000E+00	0.	0.	0.	0.	0.	0.
5	0.	0.	0.	0.	1.0000E+00	0.	0.	0.	0.	0.
6	0.	0.	0.	0.	0.	1.0000E+00	0.	0.	0.	0.
7	0.	0.	0.	0.	0.	0.	1.0000E+00	0.	0.	0.
8	0.	0.	0.	0.	0.	0.	0.	1.0000E+00	0.	0.
9	0.	0.	0.	0.	0.	0.	0.	0.	1.0000E+00	0.
10	0.	0.	0.	0.	0.	0.	0.	0.	0.	1.0000E+00

	1	2	3	4	5	6	7	8	9	10
1	4.4000E-01	-7.5560E-01	9.2900E-01	0.	-2.3900E-02	-1.5841E+00	1.5531E+00	0.	1.0187E+01	2.1310E+00

TABLE 7.18. — INPUTS AND THE CORRESPONDING PARAMETERS FOR WHICH THEY ARE OPTIMIZED

INPUT #1	INPUT #2	INPUT #3	INPUT #4	INPUT #5	INPUT #6	INPUT #7	INPUT #8	INPUT #9	INPUT #10
$\delta_{\text{LONG } 1}$	$\delta_{\text{LONG } 2}$	$\delta_{\text{LONG } 3}$	$\delta_{\text{LAT } 1}$	$\delta_{\text{LAT } 2}$	$\delta_{\text{LAT } 3}$	$\delta_{\text{PEDAL } 1}$	$\delta_{\text{PEDAL } 2}$	$\delta_{\text{COLL } 1}$	$\delta_{\text{COLL } 2}$
$M_u$	$Y_u$	$X_u$	$L_v$	$M_p$	$X_v$	$Y_v$	$X_v$	$Z_w$	$Y_w$
$M_u$	$L_w$	$Z_u$	$L_v$	$N_p$	$Z_v$	$N_v$	$Z$	$M_w$	$L_w$
$M_w$	$L_q$	$L_u$	$L_p$	$M_p$	$Y_v$	$L_v$	$M_v$	$M_w$	$N_w$
$M_q$	$L_q$	$N_u$	$L_p$	$M_r$	$N_v$	$L_r$	$M_v$	$Z_{a1}$	$L_w$
$M_q$	$Y_{a1}$	$L_u$	$L_r$	$L_{a1}$	$M_v$	$N_r$	$M_r$	$M_{a1}$	$L_q$
$X_{a1}$	$L_{a1}$	$N_q$	$Y_{b1}$	$X_{b1}$	$L_v$	$L_r$	$M_r$	$M_{a1}$	$L_{a1}$
$Z_{a1}$	$N_{a1}$	$X_{a1}$	$L_{b1}$	$Z_{b1}$	$Y_{b1}$	$Y_{\delta\text{PED}}$	$X_{\delta\text{PED}}$	$X_{\delta\text{COLL}}$	$Y_{\delta\text{COLL}}$
$M_{a1}$	$L_{a1}$	$X_{\delta\text{LONG}}$	$N_{b1}$	$M_{b1}$	$Y_{\delta\text{LAT}}$	$L_{\delta\text{PED}}$	$Z_{\delta\text{PED}}$	$Z_{\delta\text{COLL}}$	$L_{\delta\text{COLL}}$
$M_{a1}$	$M_{b1}$	$Z_{\delta\text{LONG}}$	$L_{b1}$	$M_{b1}$	$L_{\delta\text{LAT}}$	$N_{\delta\text{PED}}$	$M_{\delta\text{PED}}$	$M_{\delta\text{COLL}}$	$N_{\delta\text{COLL}}$
$M_{\delta\text{LONG}}$	$L_{\delta\text{LONG}}$	$M_{\delta\text{LONG}}$	$L_{\delta\text{LAT}}$	$M_{\delta\text{LAT}}$	$N_{\delta\text{LAT}}$	$L_{\delta\text{PED}}$	$M_{\delta\text{PED}}$	$M_{\delta\text{COLL}}$	$L_{\delta\text{COLL}}$

UH-1H Flight Data Processing.— Flight data processing for the UH-1H consisted of: reading the flight data tape, editing and preprocessing the data, and processing the data through the SCIDNT computer program. (Due to the limit imposed on computer resources, it was not feasible to run DEKFIS and OSR on this data.)

UH-1H flight data: Flight data for the UH-1H V/STOLAND helicopter was provided by NASA Ames Research Center. This data was from Flight 68 and dated February, 1978. The maneuvers processed were specifically flown at 60 kts for system identification purposes using the optimally designed inputs discussed previously. Conventional doublet inputs were also flown for comparison. The pilot's rendition of the optimal longitudinal stick input ( $\delta_{LONG_3}$ ) is shown in Figure 7.15. The optimal input sequence is repeated three times in succession. Figure 7.15 also shows the collective stick motion during this period. The optimal collective stick input analyzed is likewise presented in Figure 7.16. Optimal collective stick input  $\delta_{COLL_2}$  is repeated three times at the beginning of the maneuver and once towards the end. Longitudinal and collective doublet inputs are shown in Figures 7.17 and 7.18 respectively. The four data records processed (each corresponding to the inputs of Figures 7.15 to 7.18 were 50 seconds long with a sample period of 0.0504 second (for a total of 990 data points). The following measurements were utilized:  $V_{TOTAL}$ ,  $\dot{h}$ ,  $q$ ,  $\theta$ ,  $a_x$ ,  $a_z$ ,  $\delta_{LONG}$  and  $\delta_{COLL}$ .

SCIDNT runs on UH-1H data: The UH-1H flight data was processed using a linear 3 dof, 4th order longitudinal model. (A simple longitudinal model was chosen in order to conserve computer time.) Since all the maneuvers were flown at the same flight condition, it was decided to process a longitudinal stick input and a collective stick simultaneously to obtain a single identified linear model. Three separate longitudinal-collective stick maneuver combinations were considered. These cases are shown in Table 7.19. These cases produced three separate final estimated parameter models: a model identified using only optimal inputs, a model identified using only doublet inputs, and a model using the combination shown for Case 3 (to be discussed further below).

The initial parameter estimates were based on C-81 computations for a 3 dof longitudinal model without stabilizer bar stability augmentation. The F,G,H and D matrixes for this model are shown in Figure 7.19, with states, controls and outputs as follows:

States:  $u, w, q, \theta$

Control Inputs:  $\delta_{LONG}, \delta_{COLL}$

Outputs:  $V_{TOTAL}, \dot{h}, q, \theta, a_x, a_z$

This initial parameter model is shown simulated to the pilot's optimal longitudinal stick inputs (of Figure 7.15 in Figures 7.20(a) - (f)). This simulation ("B" trace) is shown compared to the actual UH-1H response time history ("A" trace). Large discrepancies can be noted. The same model is likewise simulated to the pilot's optimal collective stick input (of Figure 7.16 in Figures 7.21(a) - (f)).

For Case 1, a new set of parameters was obtained by running SCIDNT. These parameters, along with the associated standard deviations and F-ratios, (which in this case is  $(\text{Parameter}/\sigma)^2$ ), are shown in Table 7.20. Simulations of these parameters for each of the optimal longitudinal stick input and the optimal collective stick input are shown in Figures 7.22(a)-(f) and 7.23(a)-(f), respectively. These time histories are a marked improvement over the simulations of the initial parameters, although many discrepancies still exist. There are several possible reasons for this poor agreement. First, it is possible that there are unmodeled bias, scale factor and other measurement error effects in the  $\delta_{\text{COLL}}$  maneuver. Also, there may be substantial lateral coupling and unmodeled rotor effects present. Another possibility is that key  $\delta_{\text{COLL}}$  parameters had not converged resulting in the poor matches. This would be the case if the  $\delta_{\text{COLL}}$  and the  $\delta_{\text{LONG}}$  were at slightly different flight conditions, and the SCIDNT program converged to the  $\delta_{\text{LONG}}$  parameters because of the higher signal level.

The SCIDNT results for Case 2 (doublet inputs) are presented in Table 7.21. Final parameter simulations to the longitudinal stick doublet input (Figure 7.17) and the collective stick doublet (Figure 7.18) are shown in Figures 7.24 and 7.25 respectively. In this case, improved results were observed for the  $\delta_{\text{COLL}}$  maneuver. Note that this does not necessarily mean that doublet inputs are "better" than optimum inputs. In order to properly compare doublet and optimal inputs, there must be a low level of external disturbances (i.e., gusts) and all other factors must be the same (particularly the energy of the input signals). In addition, the pilot must be able to adequately duplicate the optimal stick input. Even then, the doublet inputs may give better results. The optimally designed stick input may not really be optimal because of the procedure used for designing that input. It is possible that modeling errors (coming about from higher degrees of freedom, nonlinearities and/or erroneous parameter values) can cause large differences in the "optimal" inputs. In addition, there are inherent limitations in the multi-step input approach that can lead to differences. These limitations come about due to the size and number of steps in the designed input. Large steps (i.e., large  $\Delta T$ ) can make identification of shorter period characteristics difficult. Increasing the

number of steps (to make the step size smaller) increases the computer time, core storage and accuracy requirements. Hence, there is also a limitation on the length of the maneuver.

In order to obtain the best results at this flight condition, an additional run was set up using the optimal  $\delta_{LONG}$  control input and the doublet  $\delta_{COLL}$  control input for simultaneous processing. The results of this Case 3 are presented in Table 7.22 and the corresponding simulations in Figures 7.26 and 7.27. These results are somewhat better but not completely converged. A comparison of the parameters estimated for all three cases are presented in Table 7.23. There are notable differences in these results which warrant further study.

One of the principal benefits of a complete state variable model is that many transfer functions can be rapidly obtained. For the Case 3 model identified from the flight data, the following stick to pitch attitude transfer function is derived:

$$\frac{\theta(s)}{\delta_{LONG}} = \frac{.17s^2 + .100s + .0017}{s^4 + 1.18s^3 + 1.39s^2 + .10s + .0044}$$

the poles of which are  $s_{1,2} = -.565 \pm j.99$ ,  $s_{3,4} = -.024 + j.182$  and the zeroes of which are  $-.560$  and  $-.017$ . (Here  $\delta_{LONG}$  is positive inches of aft stick.) The corresponding Bode plot is shown in Figure 7.28.

Table 7.19  
Makeup of the Three Cases

	MANEUVER 1	MANEUVER 2
Case 1	Optimal Longitudinal Stick Input	Optimal Collective Stick Input
Case 2	Longitudinal Stick Doublet	Collective Stick Doublet
Case 3	Optimal Longitudinal Stick Input	Collective Stick Doublet

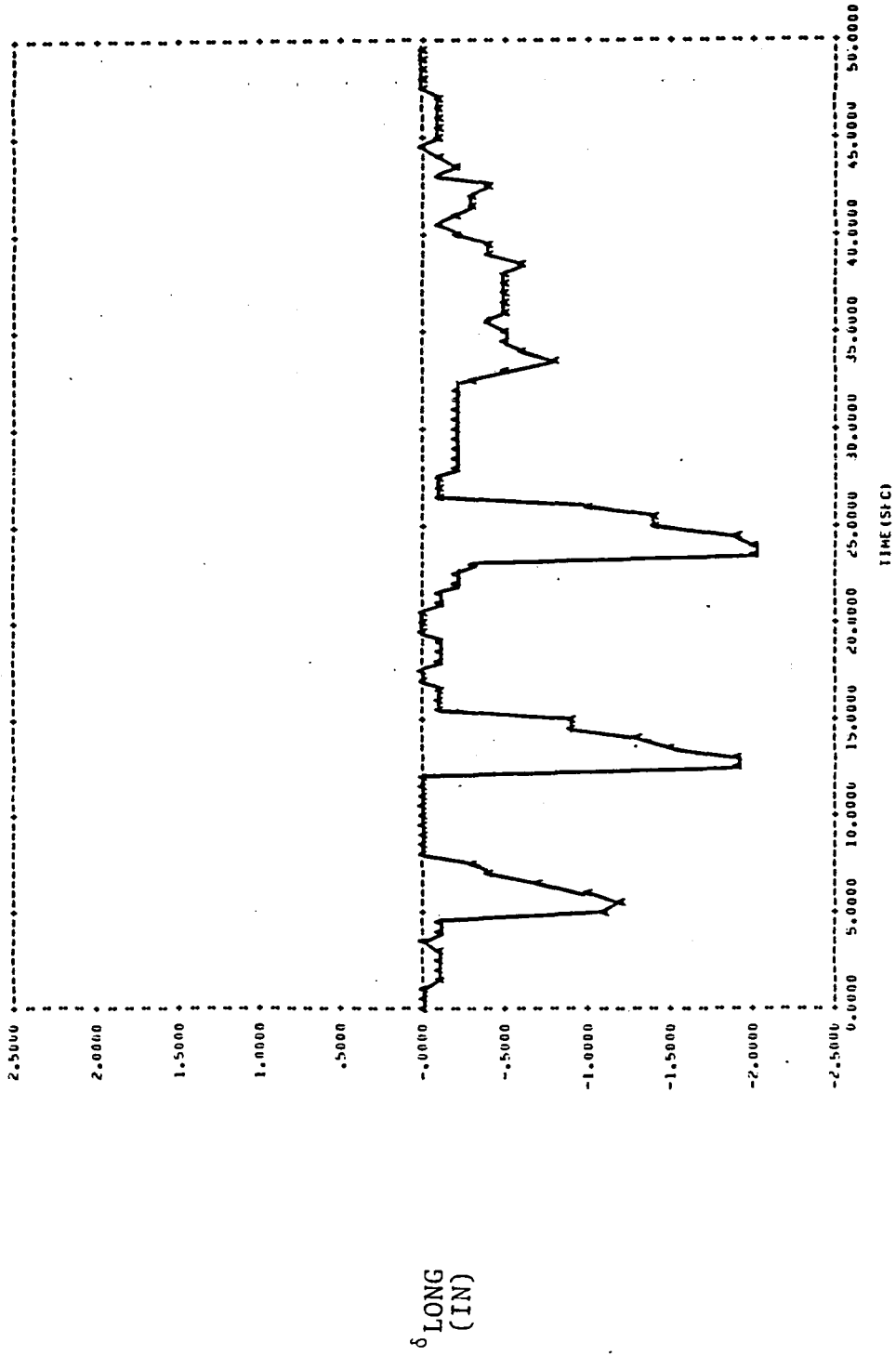


FIGURE 7.15(a).- OPTIMAL LONGITUDINAL STICK INPUT  
MANEUVER

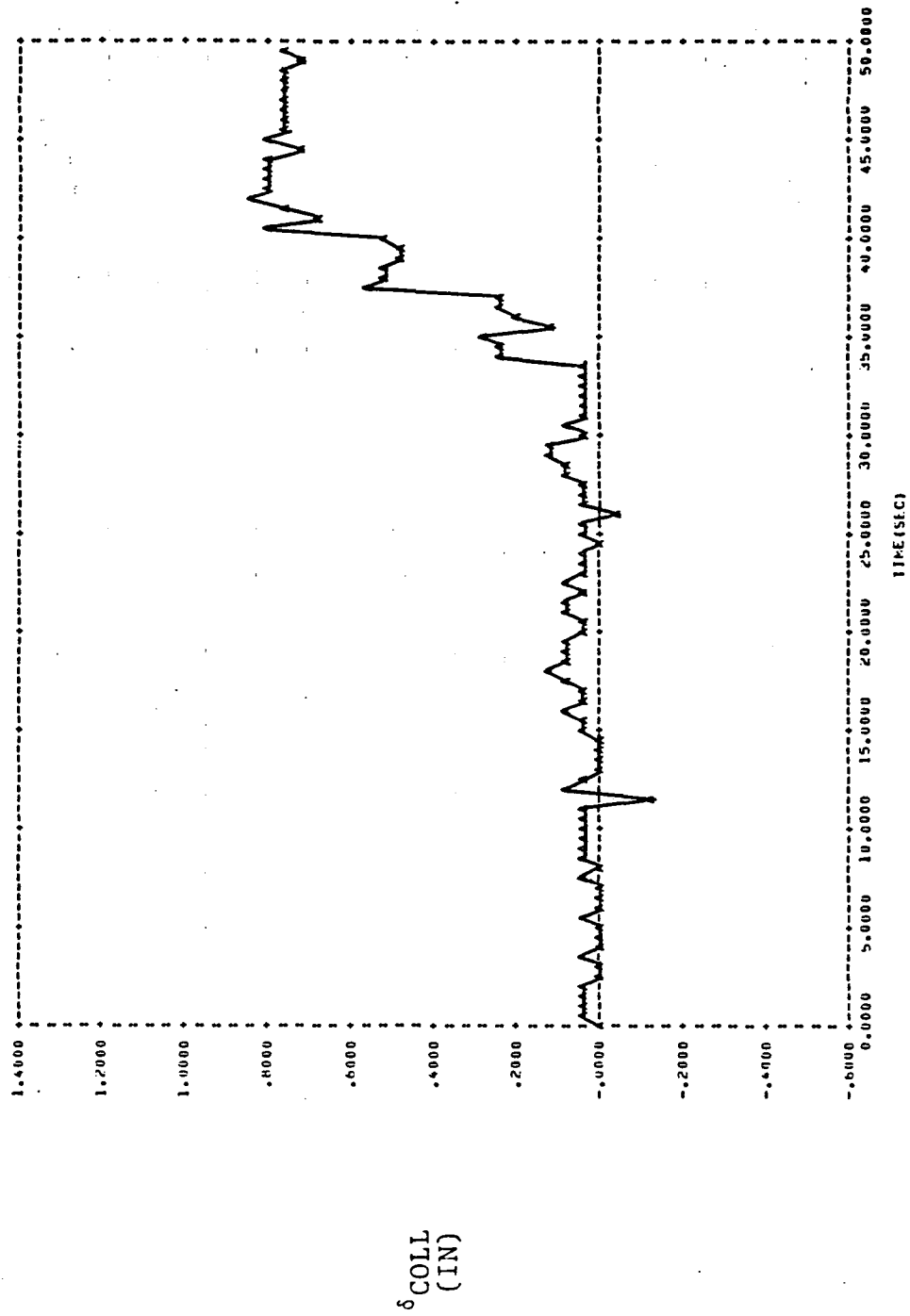


FIGURE 7.15(b). - (CONTINUED)

●  $\delta_{\text{COLL}}$  EXCITATION

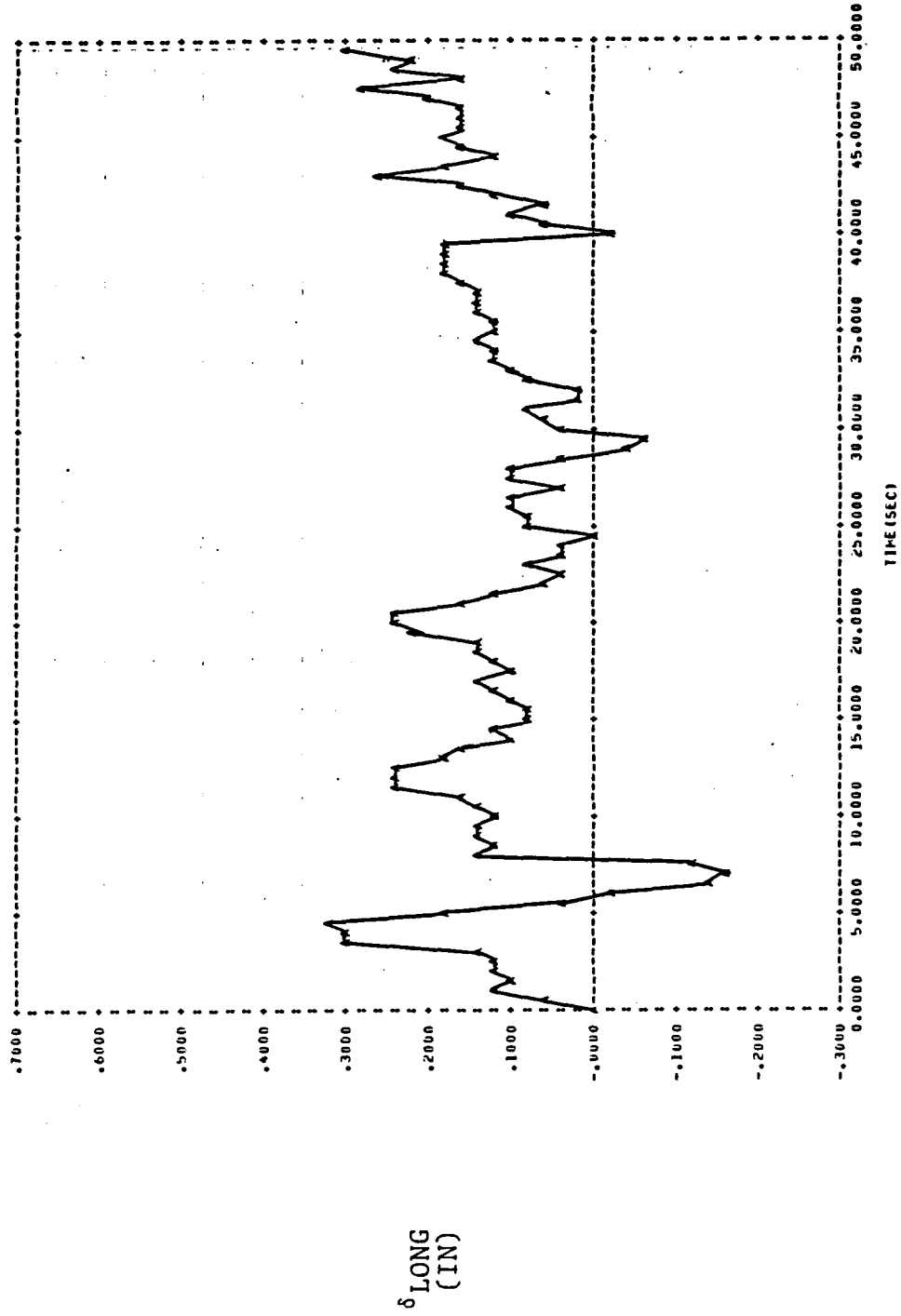


FIGURE 7.16(a). — OPTIMAL COLLECTIVE STICK INPUT MANEUVER



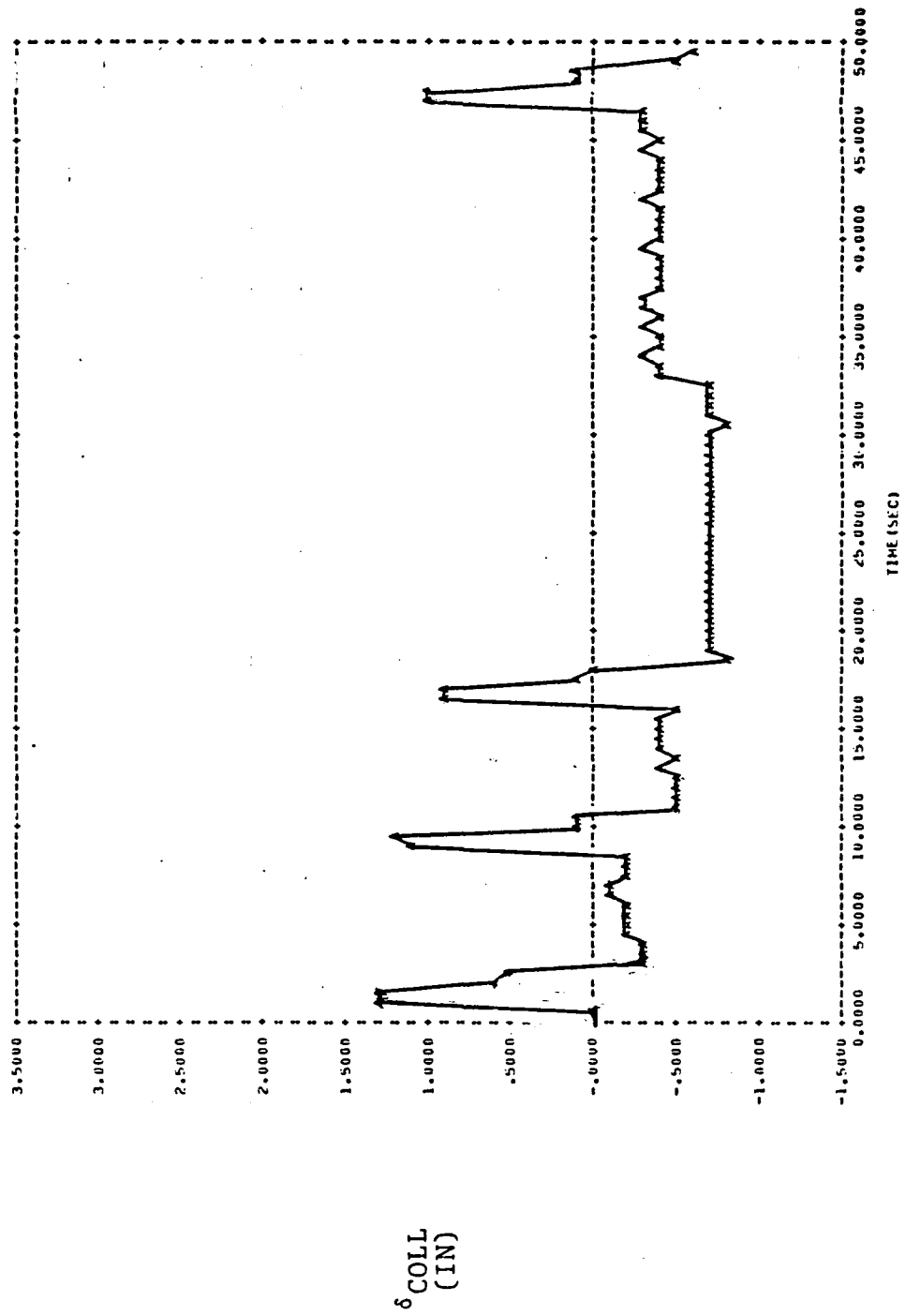


FIGURE 7.16 (b).— (CONTINUED)

●  $\delta_{\text{COLL}}$  EXCITATION

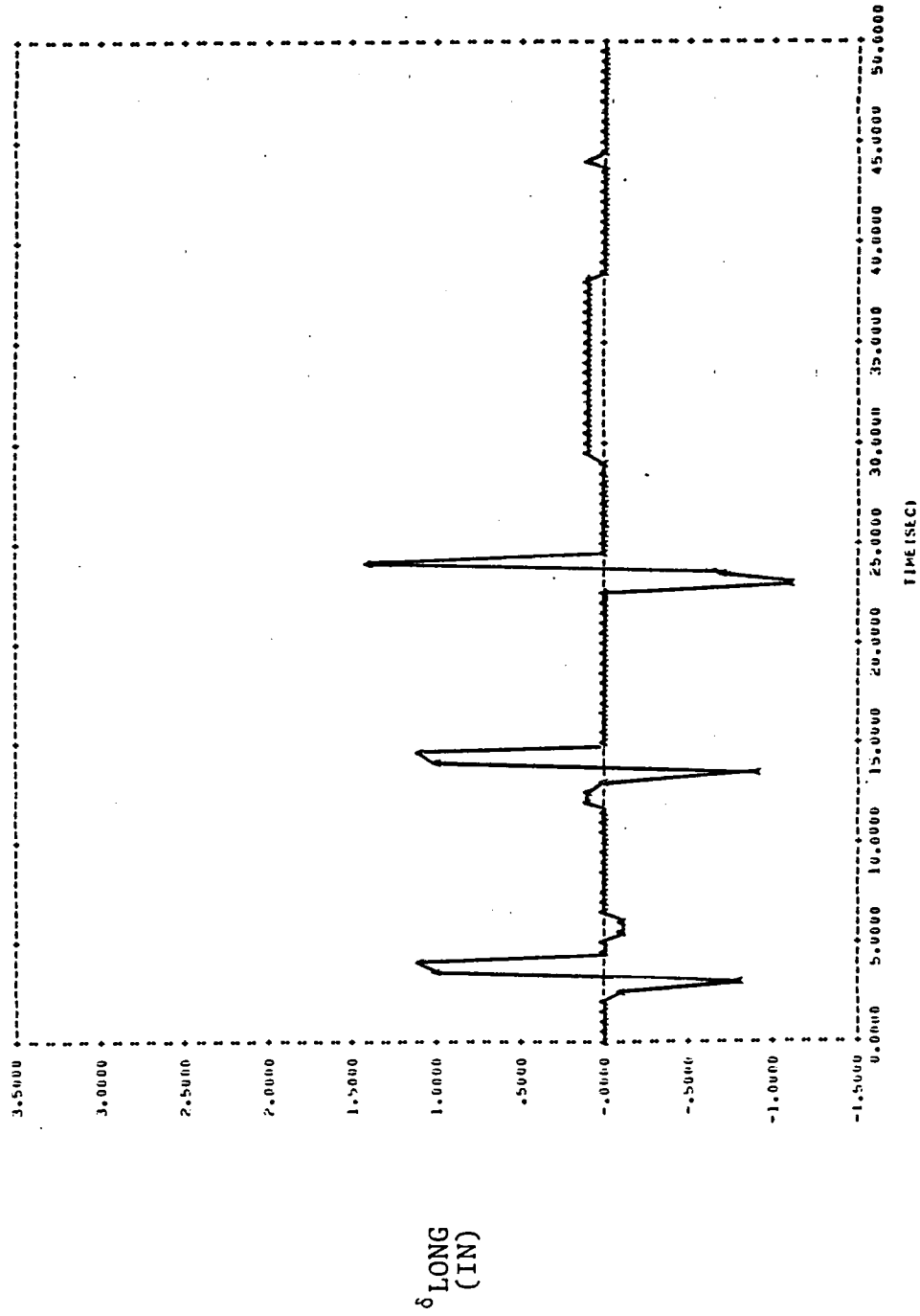


FIGURE 7.17(a).— LONGITUDINAL STICK DOUBLET INPUT  
MANEUVER

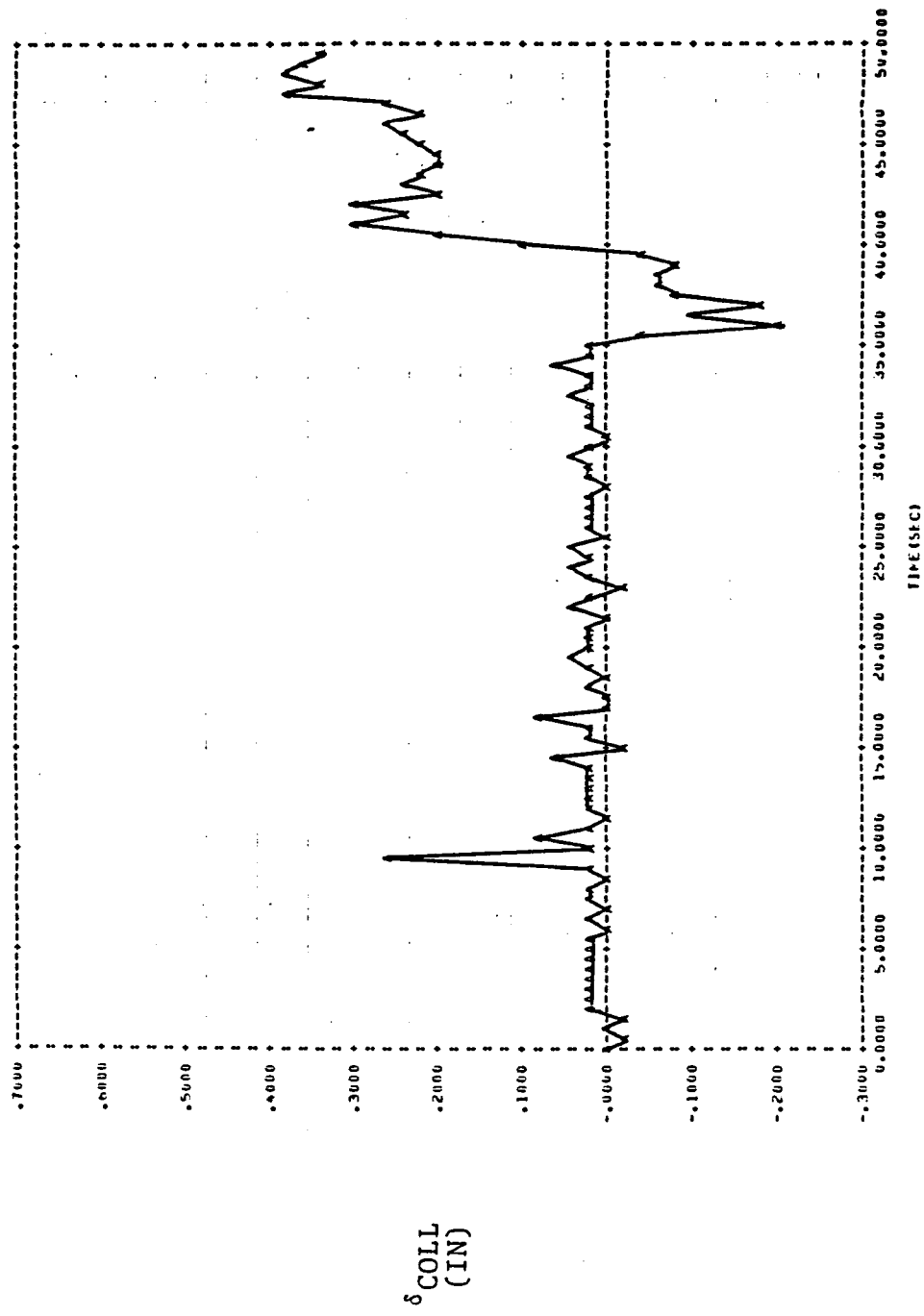


FIGURE 7.17(b). - (CONTINUED)

●  $\delta_{\text{COLL}}$  EXCITATION

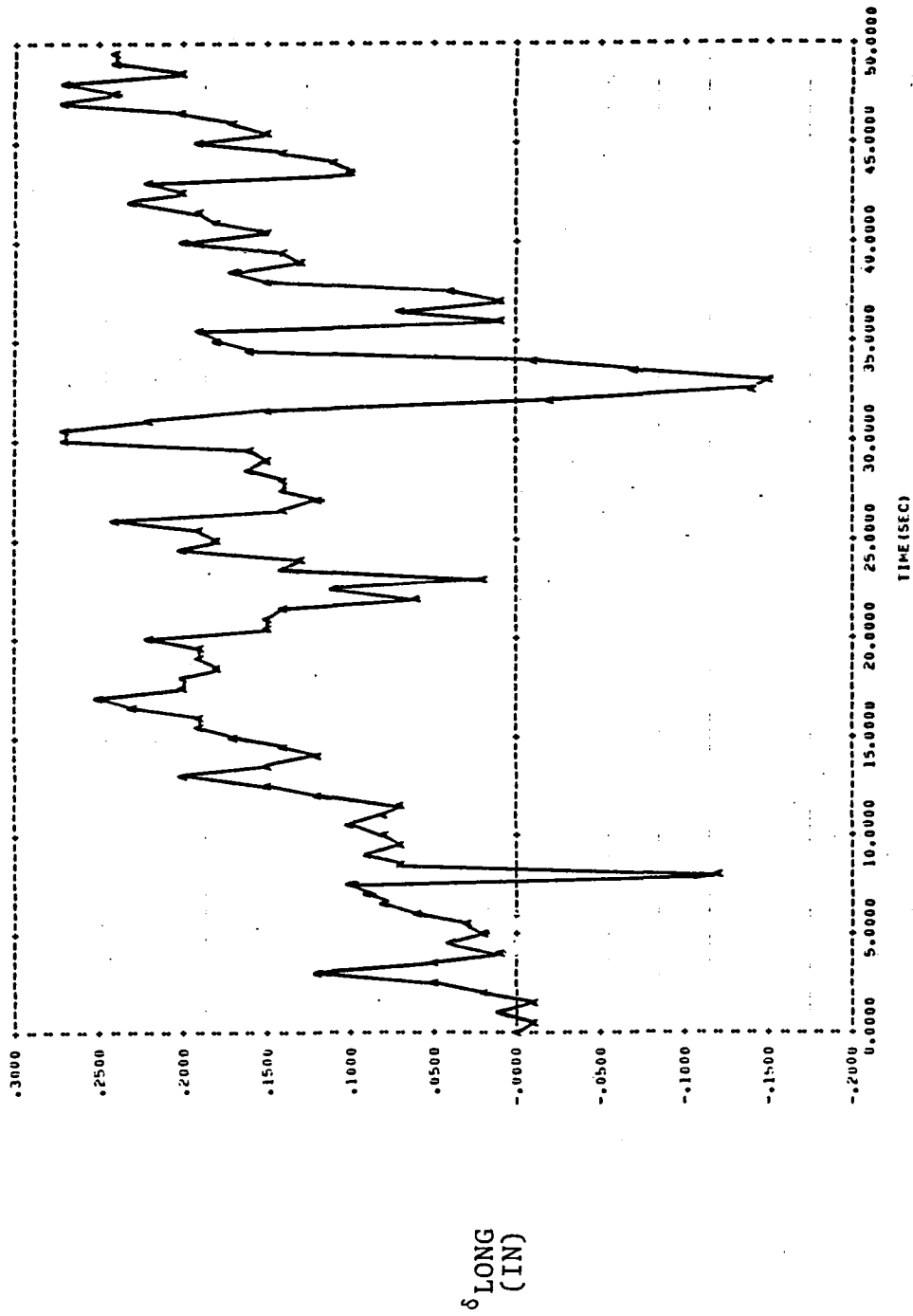


FIGURE 7.18 (a). - COLLECTIVE STICK DOUBLET INPUT  
MANEUVER

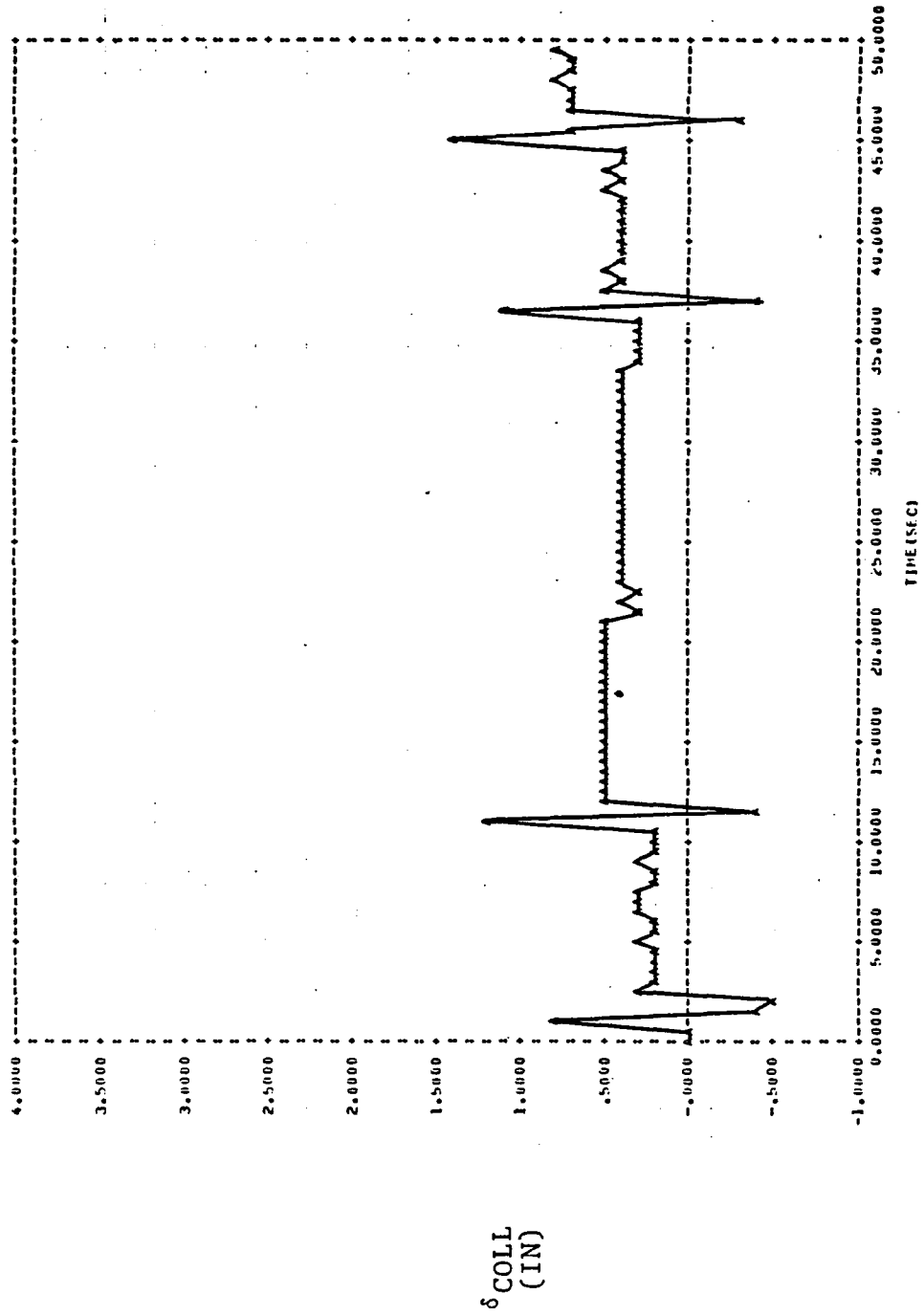


FIGURE 7.18(b).- (CONTINUED)

●  $\delta_{\text{COLL}}$  EXCITATION

	1	2	3	4
F 1	-2.2700E-02	5.8700E-02	-3.0300E+00	-3.2161E+01
F 2	1.3000E-03	-7.5420E-01	1.0591E+02	-9.2080E-01
F 3	3.7300E-03	-3.2000E-03	-5.3050E-01	0.
F 4	0.	0.	1.0000E+00	0.

## EIGENVALUES OF F -- REAL PARTS

	1
1	-6.8550E-01
2	-6.8550E-01
3	3.1796E-02
4	3.1796E-02

	1	2
G 1	8.6200E-01	7.1150E-01
G 2	2.4600E+00	-9.8180E+00
G 3	-1.8000E-01	6.4000E-03
G 4	0.	0.

## EIGENVALUES OF F -- IMAGINARY PARTS

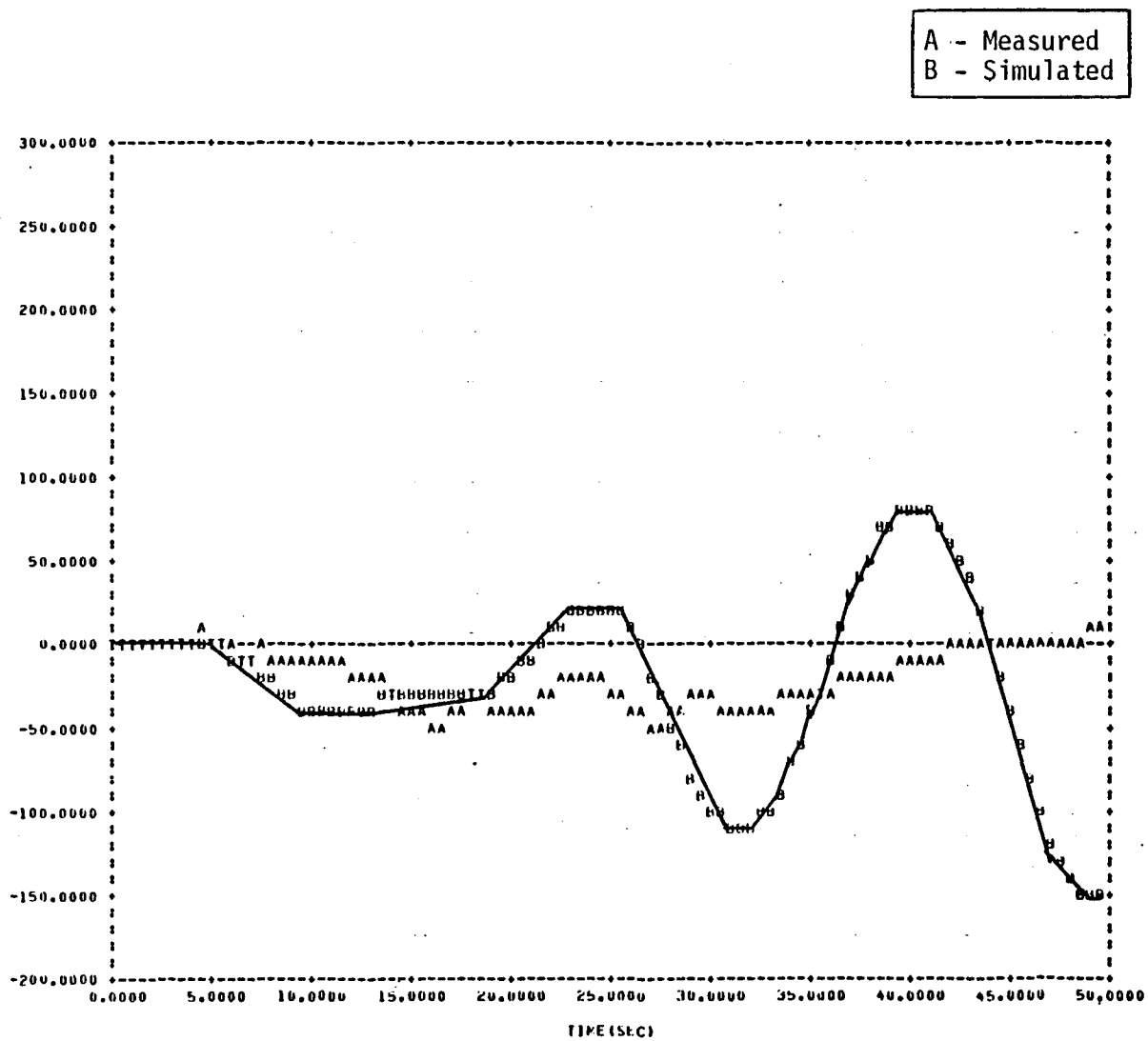
	1
1	5.2466E-01
2	-5.2466E-01
3	3.4699E-01
4	-3.4699E-01

	1	2	3	4
H 1	9.9959E-01	2.8619E-02	0.	0.
H 2	2.8619E-02	-9.9959E-01	0.	1.0595E+02
H 3	0.	0.	1.0000E+00	0.
H 4	0.	0.	0.	1.0000E+00
H 5	-2.2700E-02	5.8700E-02	0.	0.
H 6	1.3000E-03	-7.5420E-01	0.	0.

	1	2
D 1	0.	0.
D 2	0.	0.
D 3	0.	0.
D 4	0.	0.
D 5	8.6200E-01	7.1150E-01
D 6	2.4600E+00	-9.8180E+00

FIGURE 7.19.- INITIAL PARAMETER MODEL USED FOR UH-1H IDENTIFICATION  
(BASED ON C-81 MODEL)

V<sub>TOTAL</sub>  
(FPS)



181

FIGURE 7.20(a).— SIMULATION OF INITIAL PARAMETER MODEL TO THE OPTIMAL LONGITUDINAL STICK INPUT COMPARED TO THE ACTUAL UH-1H RESPONSE

● V<sub>TOTAL</sub> MEASUREMENT

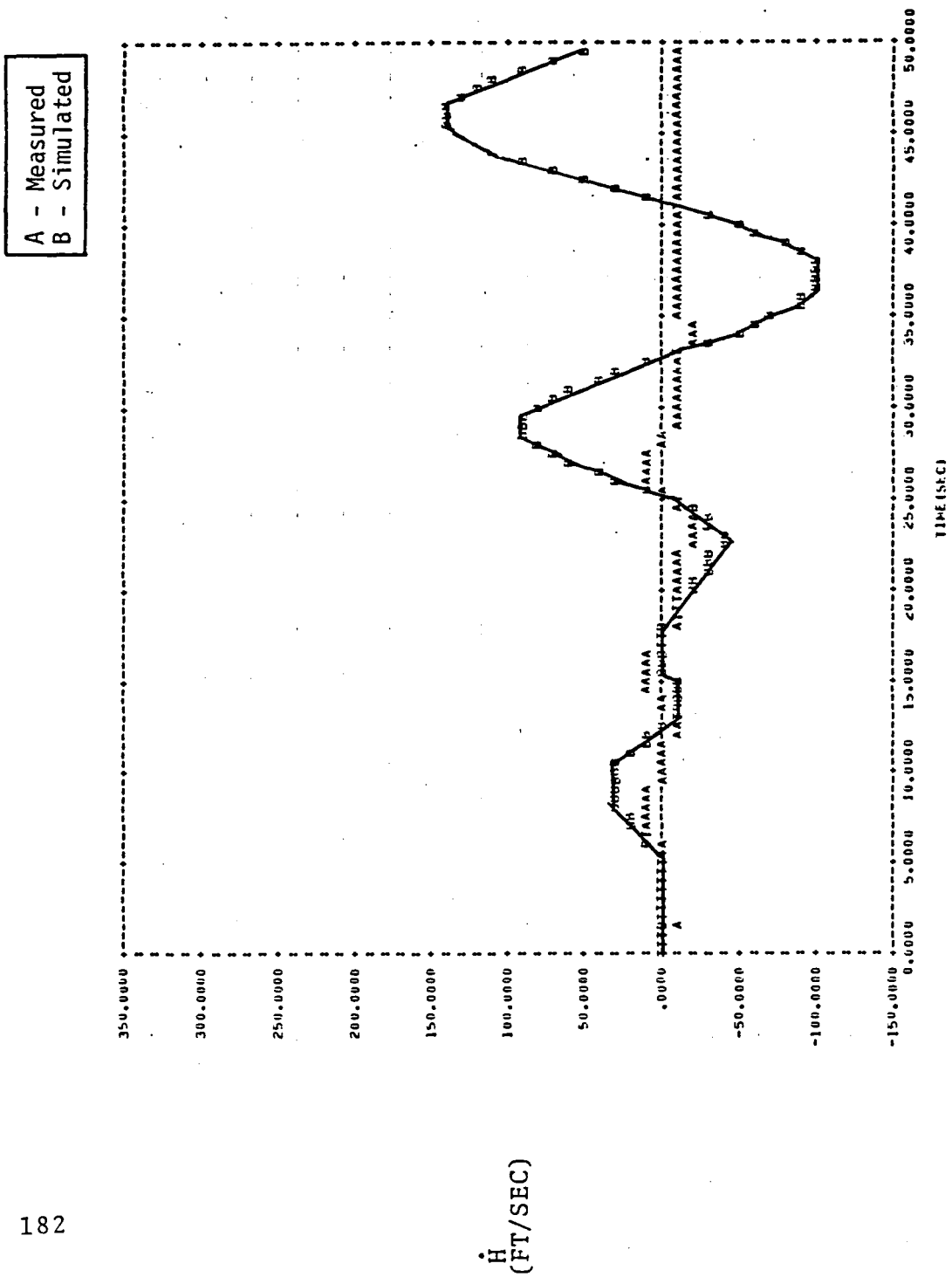


FIGURE 7.20 (b)  $\dot{h}$  (CONTINUED)

●  $\dot{h}$  MEASUREMENT



A - Measured  
B - Simulation

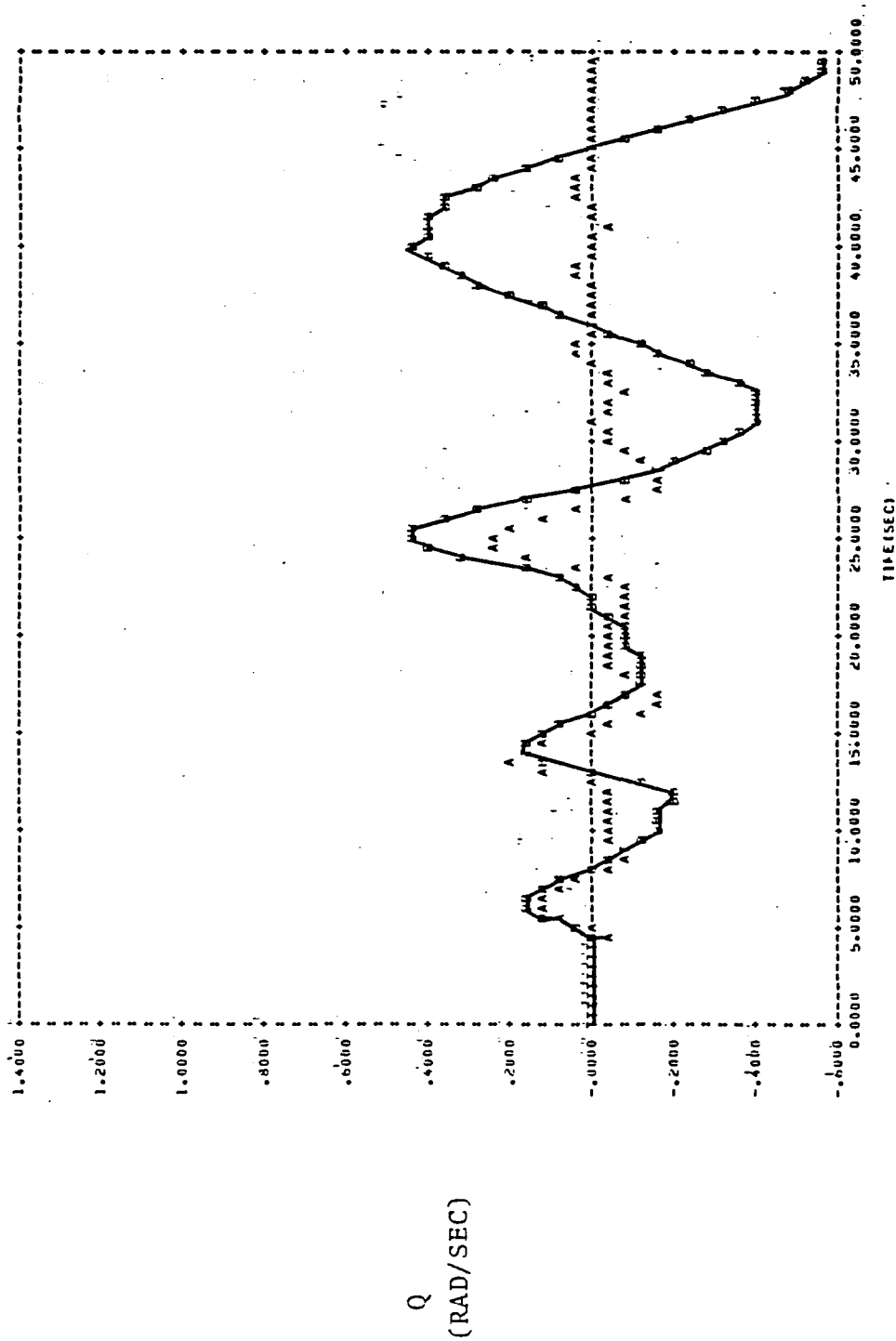


FIGURE 7.20(c). - (CONTINUED)  
● q MEASUREMENT

A - Measured  
B - Simulated

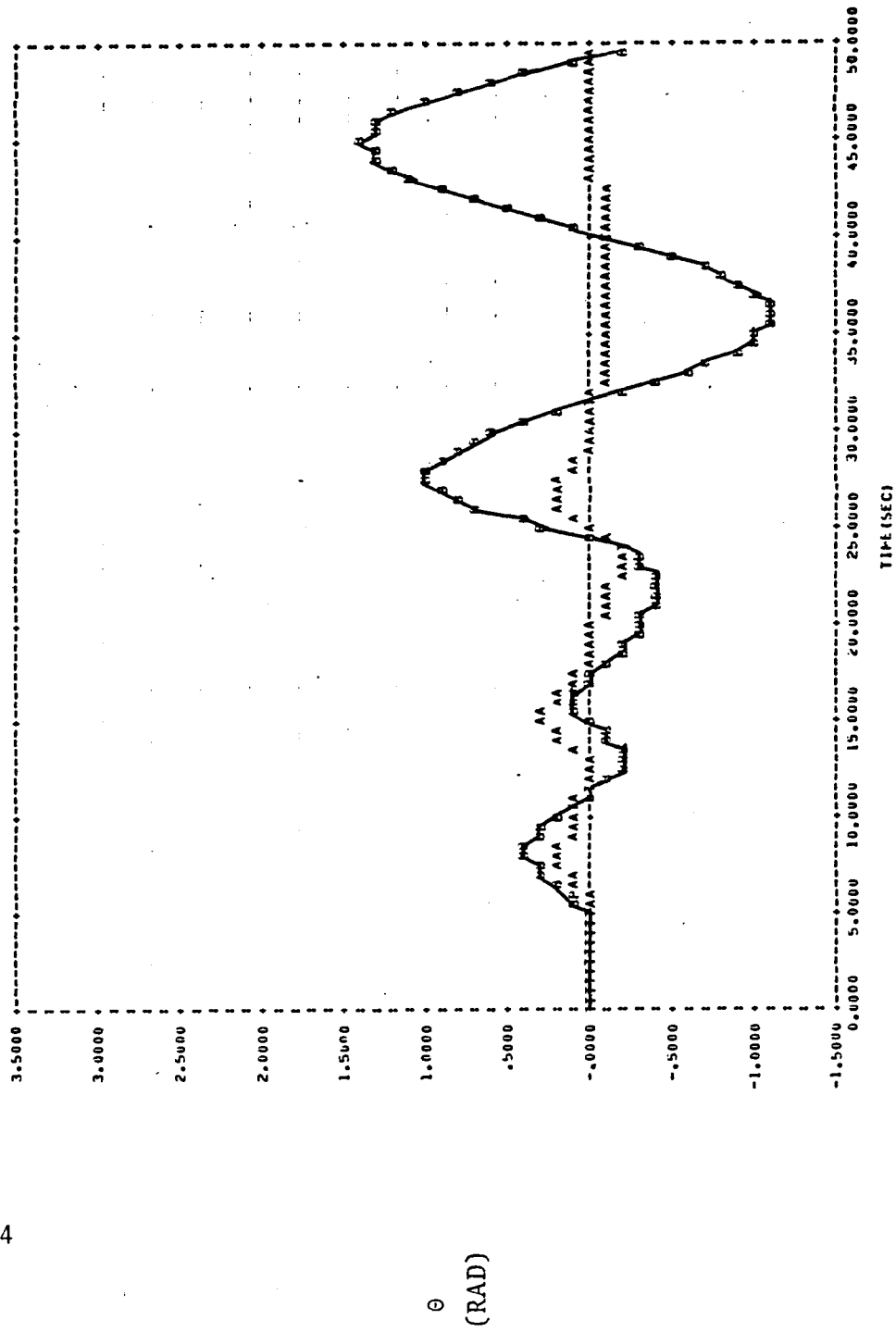


FIGURE 7.20 (d). - (CONTINUED)

●  $\theta$  MEASUREMENT

A - Measured  
B - Simulated

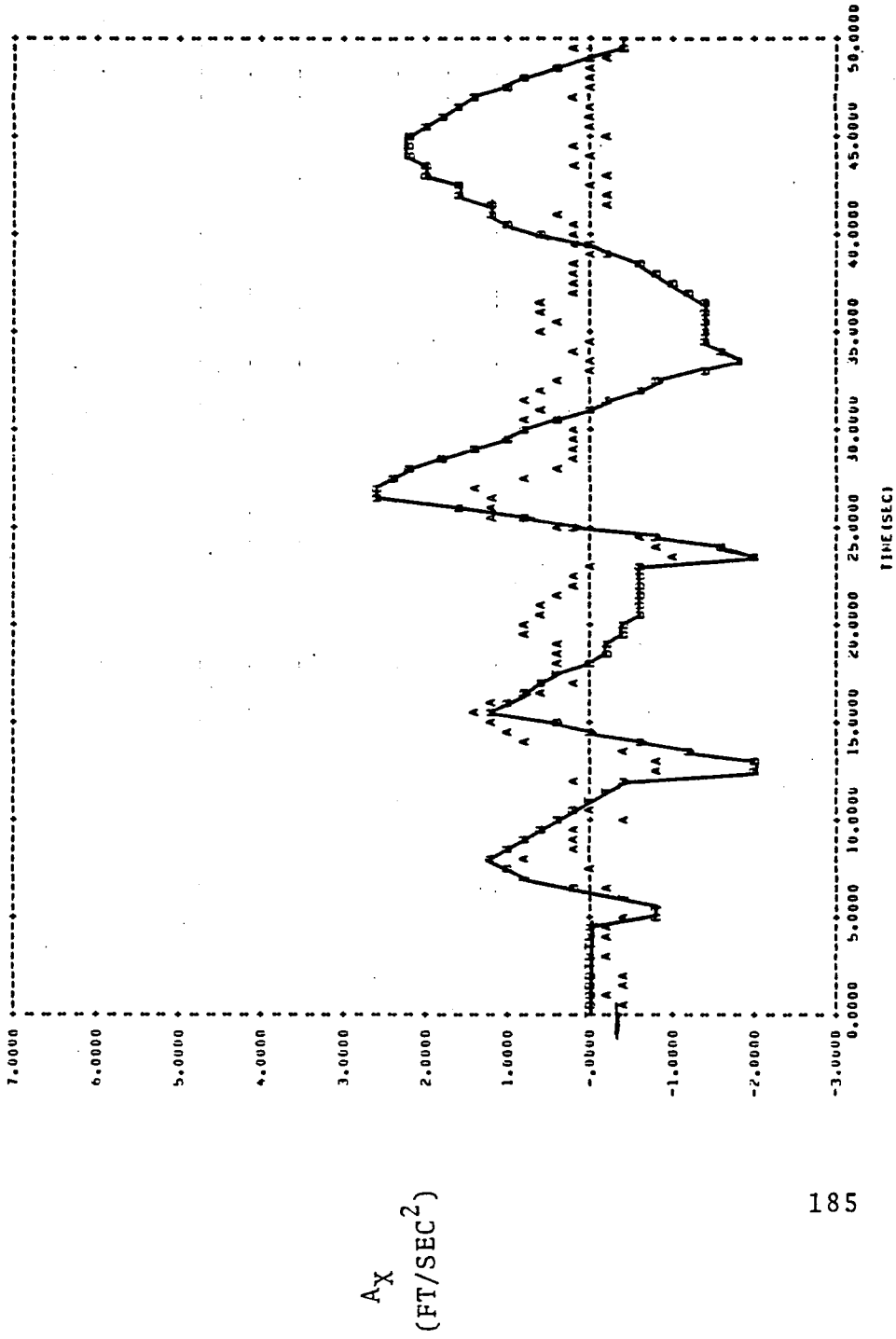


FIGURE 7.20 (e). - (CONTINUED)

●  $a_x$  MEASUREMENT

A - Measured  
B - Simulated

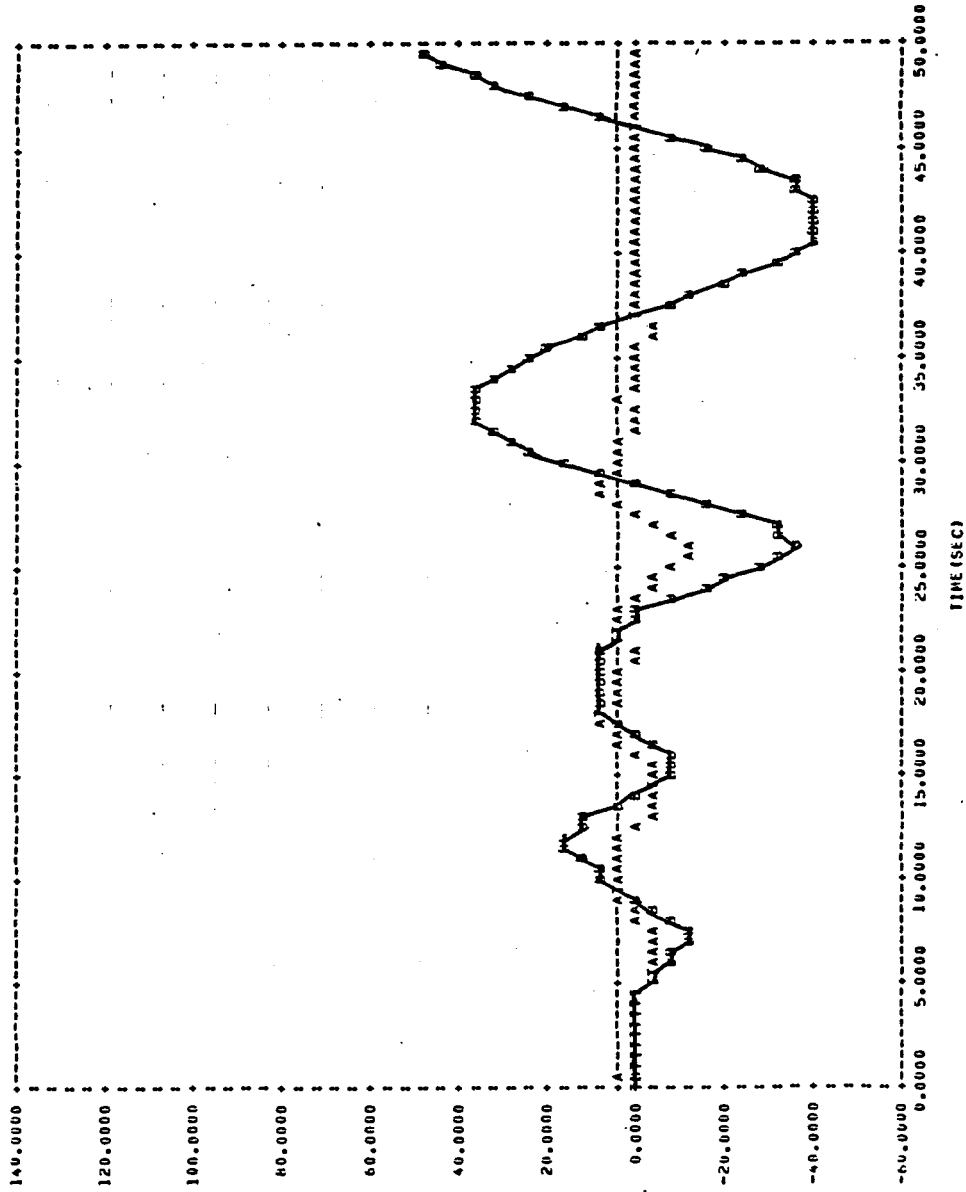


FIGURE 7.20 (f). - (CONTINUED)

●  $a_z$  MEASUREMENT

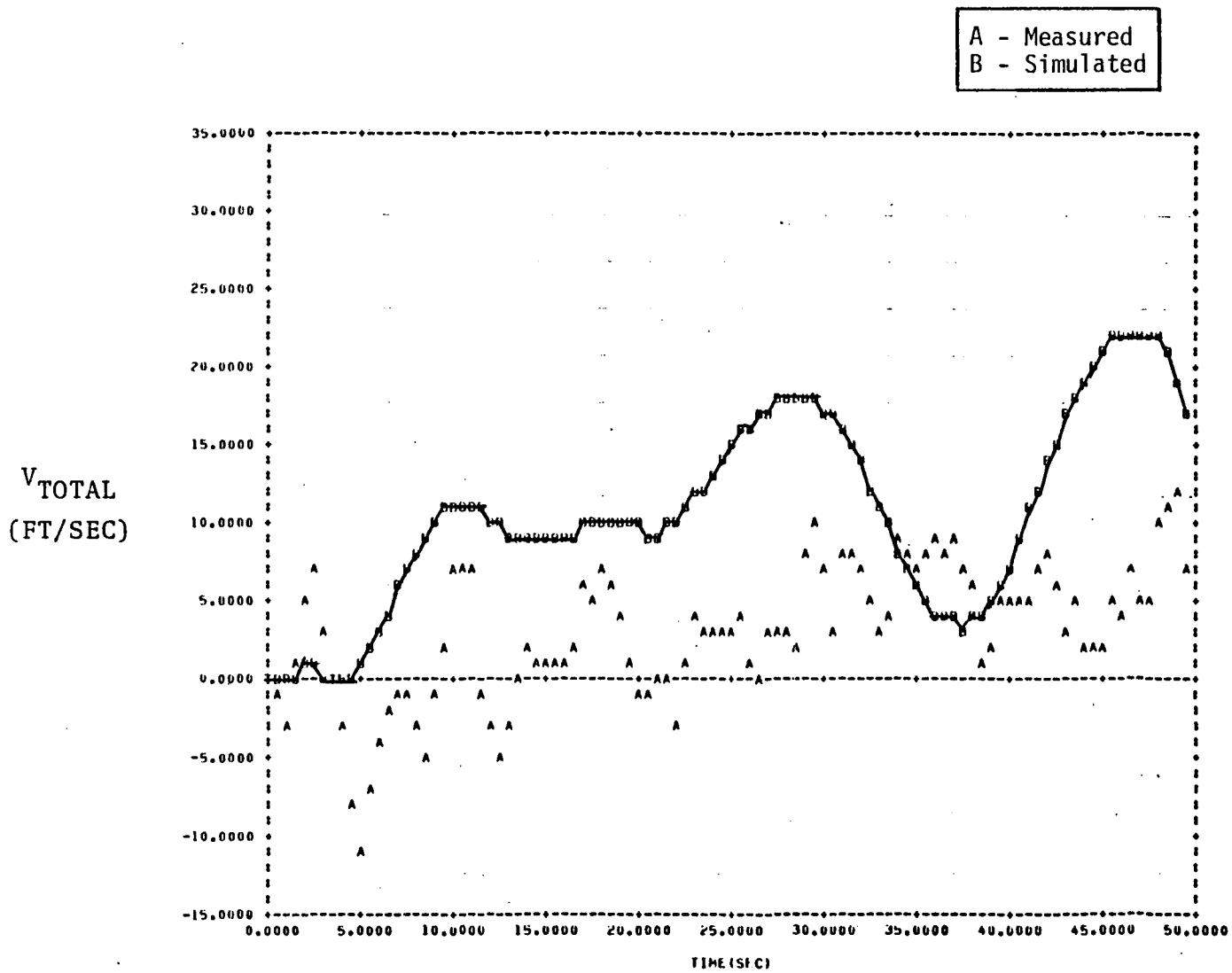


FIGURE 7.21 (a).— SIMULATION OF INITIAL PARAMETER MODEL TO THE OPTIMAL COLLECTIVE STICK INPUT. COMPARED TO ACTUAL UH-1H RESPONSE

●  $V_{TOTAL}$  MEASUREMENT

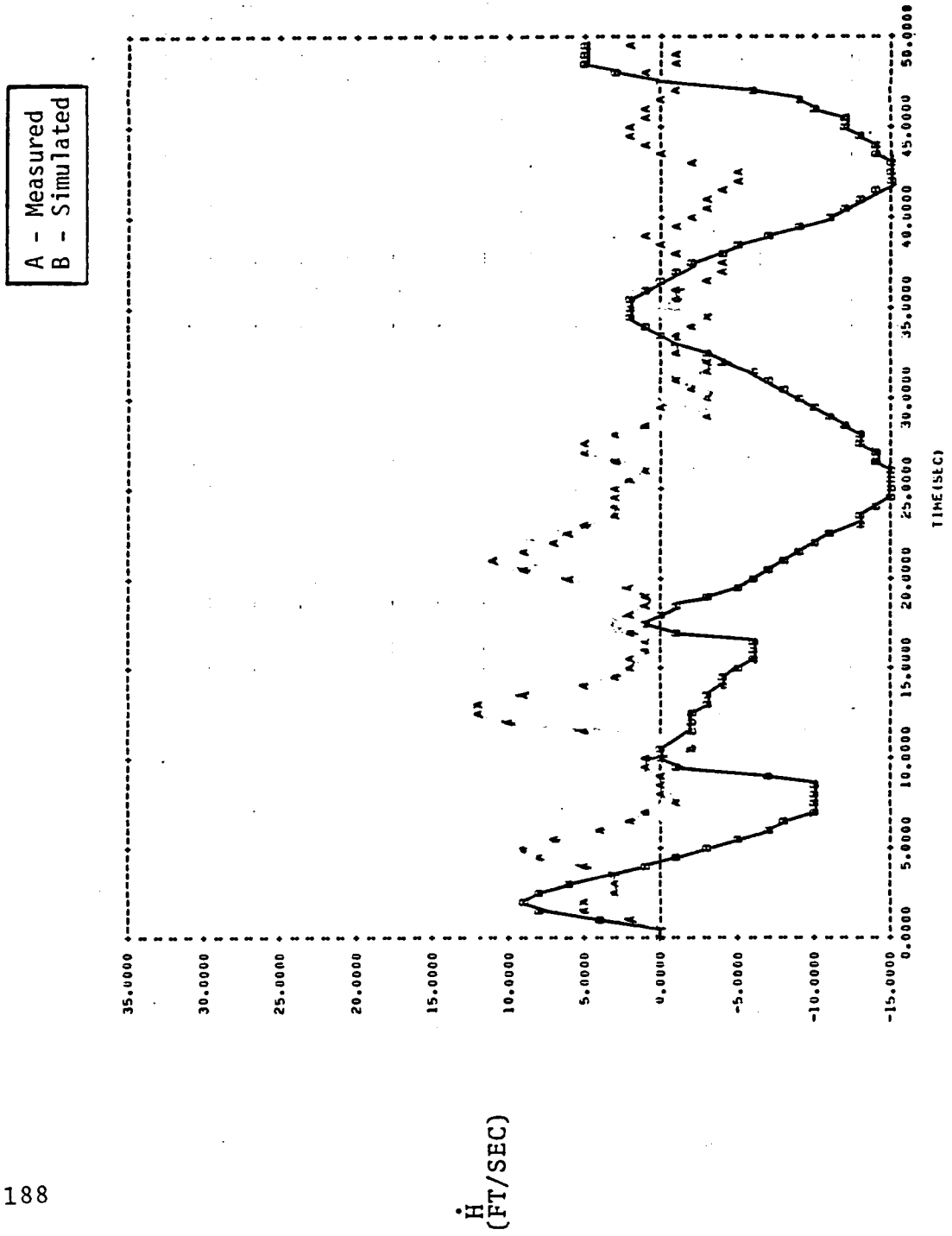
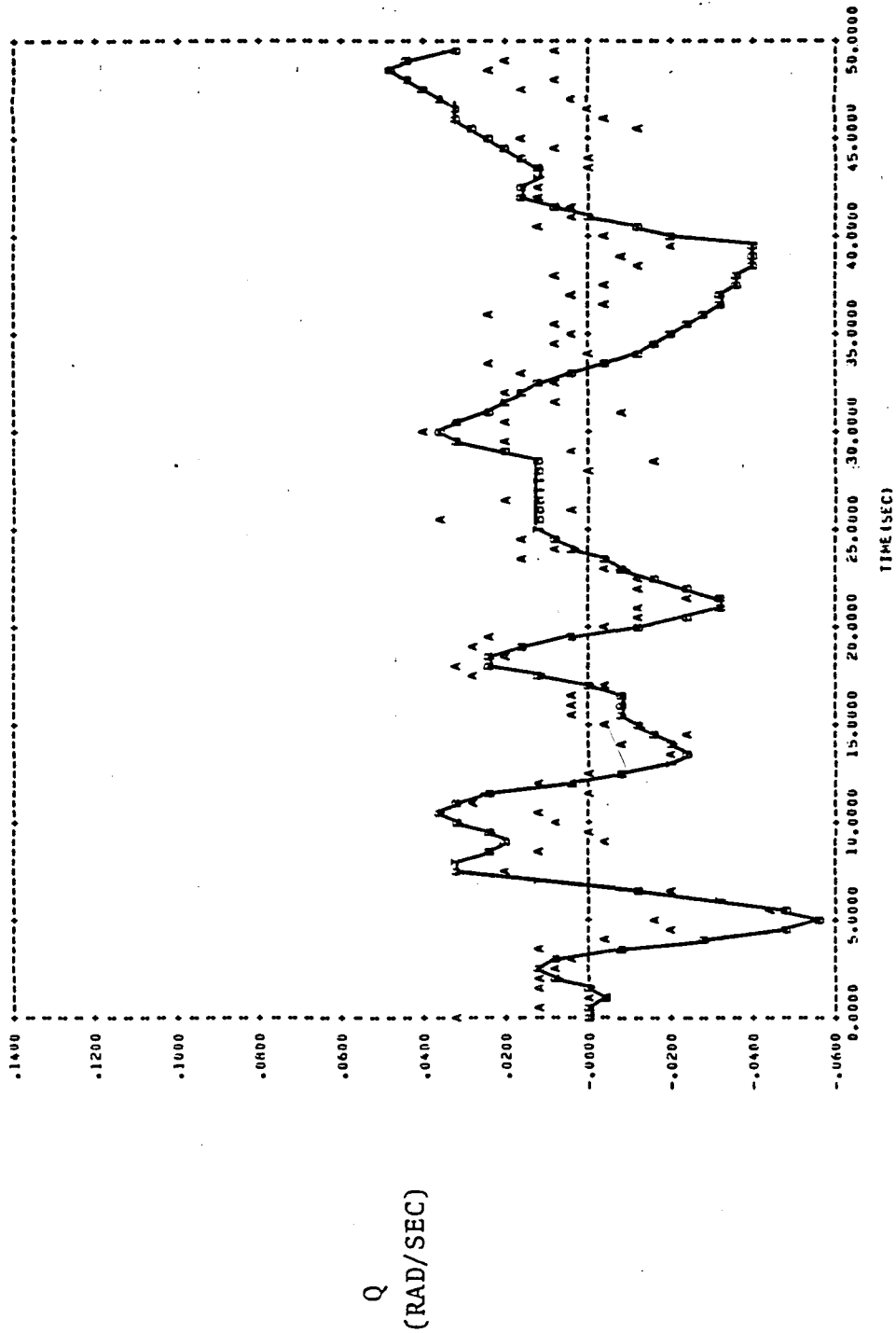


FIGURE 7.21(b). - (CONTINUED)

●  $\dot{h}$  MEASUREMENT

A - Measured  
B - Simulated



7.21 (c) - (CONTINUED)

● q MEASUREMENT

A - Measured  
B - Simulated

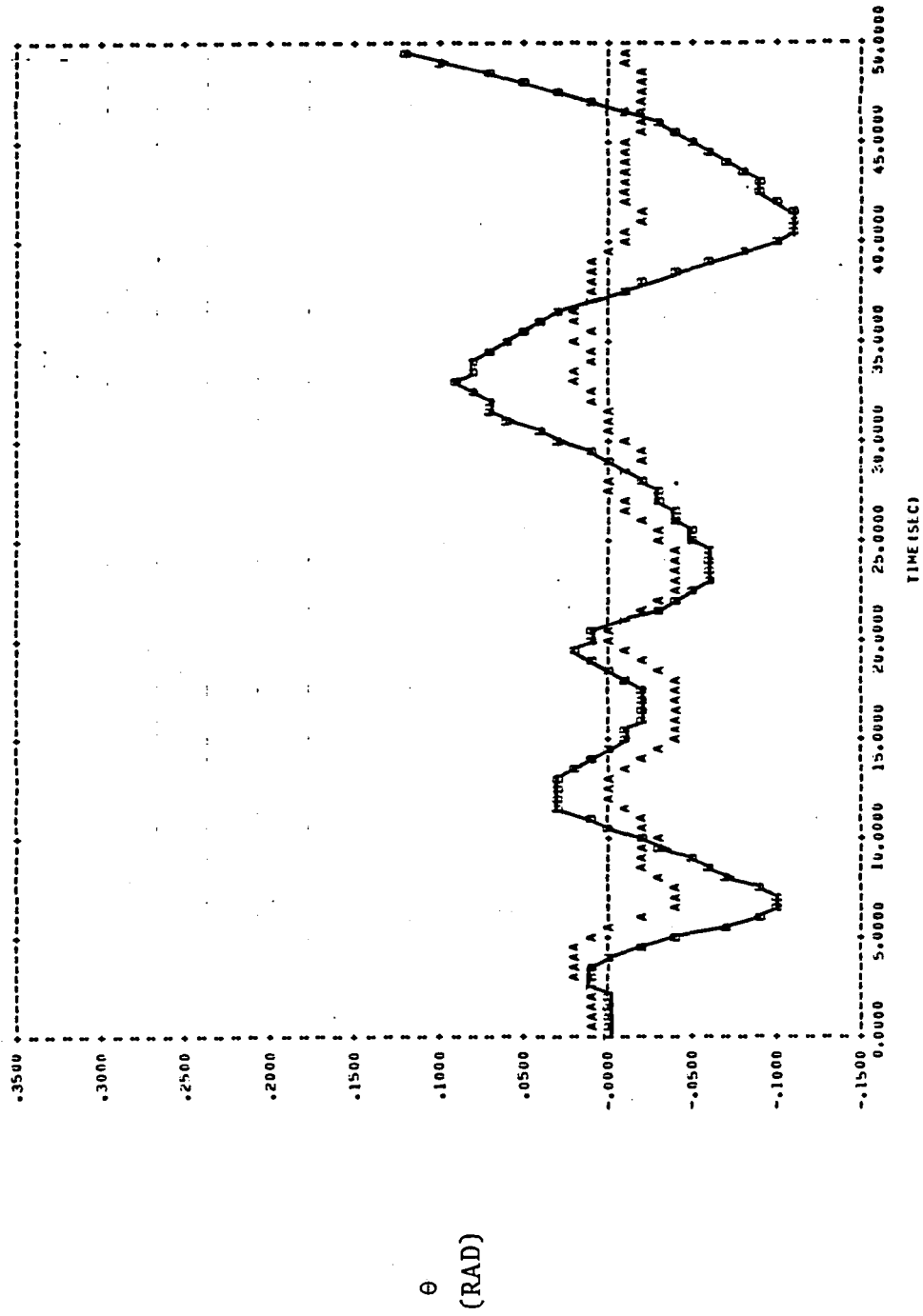


FIGURE 7.21 (d). - (CONTINUED)

o  $\theta$  MEASUREMENT



$A_x$   
(FT/SEC<sup>2</sup>)

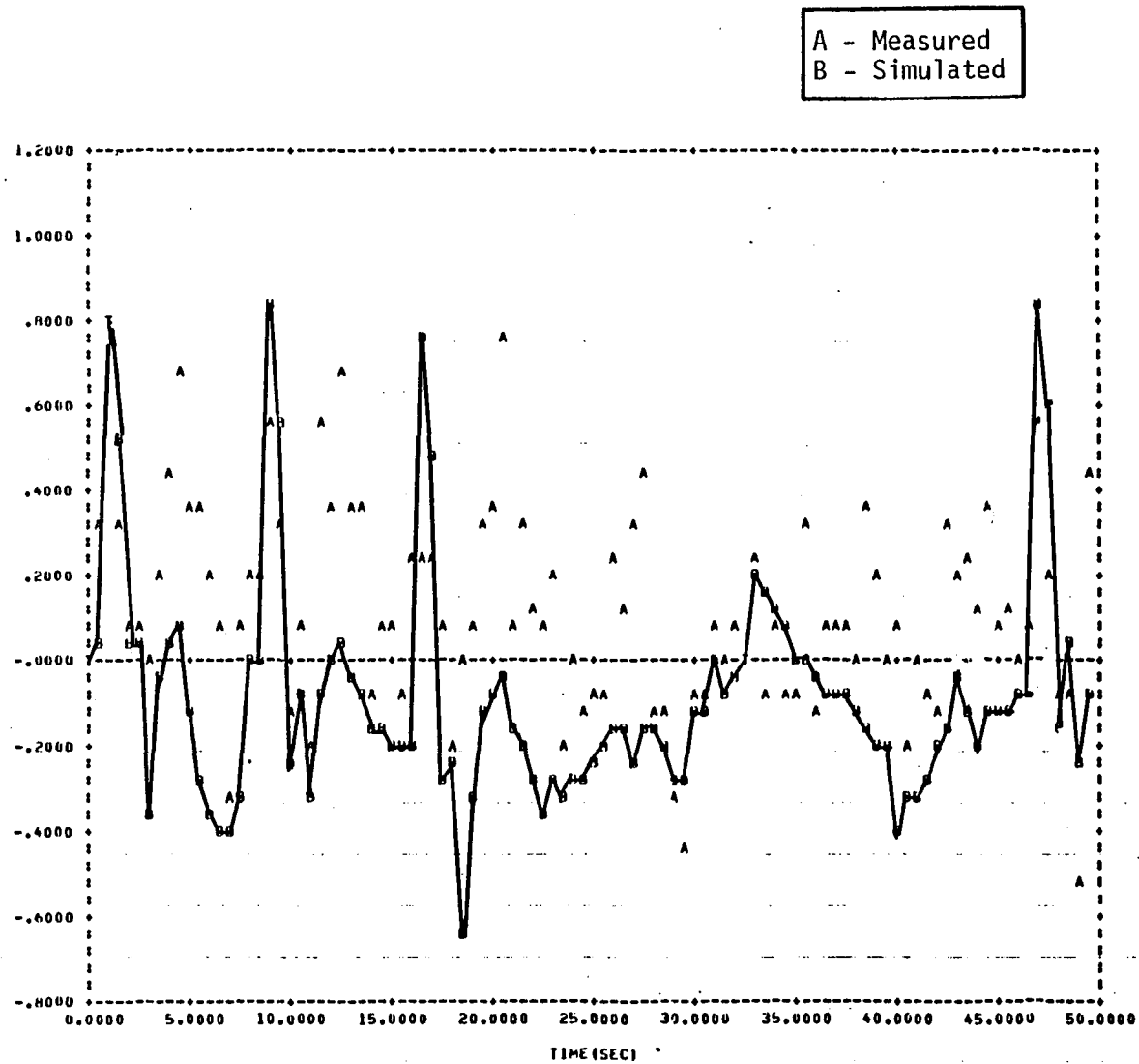


FIGURE 7.21 (e).— (CONTINUED)

●  $a_x$  MEASUREMENT

A - Measured  
B - Simulated

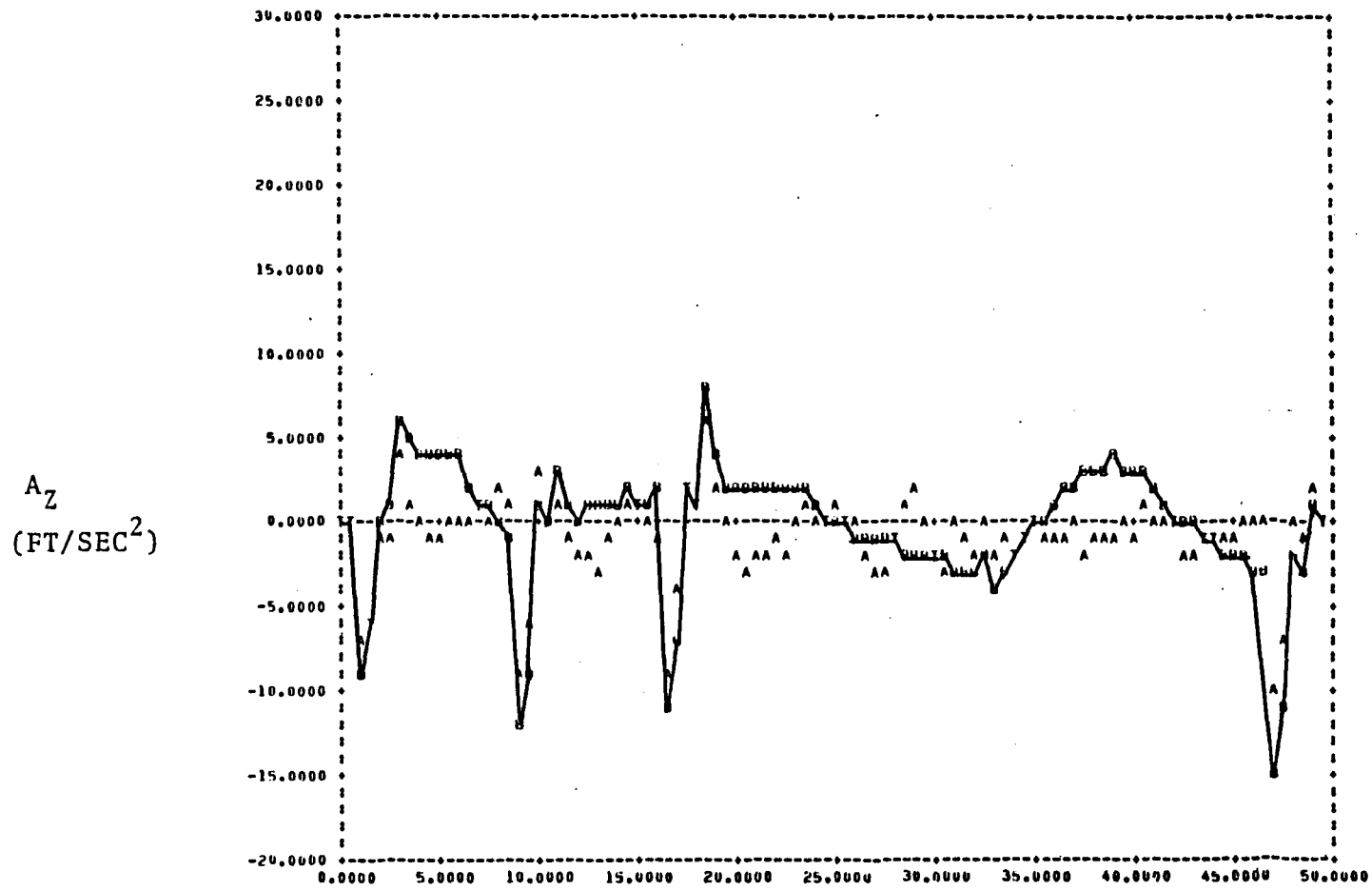


FIGURE 7.21(f).- (CONCLUDED)

●  $a_z$  MEASUREMENT

Table 7.20  
Parameter Estimates and Standard Deviations for UH-1H

• Case 1

	INITIAL PARAMETER ESTIMATE	FINAL PARAMETER ESTIMATE	STANDARD DEVIATION	F-RATIO
$X_u$ , 1/sec	-0.0227	-0.0264	0.00024	12296.49
$Z_u$ , 1/sec	0.0013	-0.0255	0.00128	394.00
$M_u$ , 1/ft-sec	0.0037	0.0025	0.00002	11664.90
$X_w$ , 1/sec	0.0587	0.0429	0.00070	3757.95
$Z_w$ , 1/sec	-0.7542	-0.4258	0.00312	18572.47
$M_w$ , 1/ft-sec	-0.0032	-0.0093	0.00005	31510.22
$M_q$ , 1/sec	-0.5305	-0.7509	0.00775	9396.00
$X_{\delta_{LONG}}$ , ft/sec <sup>2</sup> -in	0.8620	0.5947	0.0115	2677.86
$Z_{\delta_{LONG}}$ , ft/sec <sup>2</sup> -in	2.4600	2.1250	0.0602	1246.41
$M_{\delta_{LONG}}$ , 1/sec <sup>2</sup> -in	-0.1800	-0.1709	0.0011	25094.51
$X_{\delta_{COLL}}$ , ft/sec <sup>2</sup> -in	0.7115	0.2051	0.0094	472.72
$Z_{\delta_{COLL}}$ , ft/sec <sup>2</sup> -in	-9.8180	-2.9867	0.0573	2717.62
$M_{\delta_{COLL}}$ , 1/sec <sup>2</sup> -in	0.0064	-0.0332	0.0010	1096.91

$V_{TOTAL}$   
(FT/SEC)

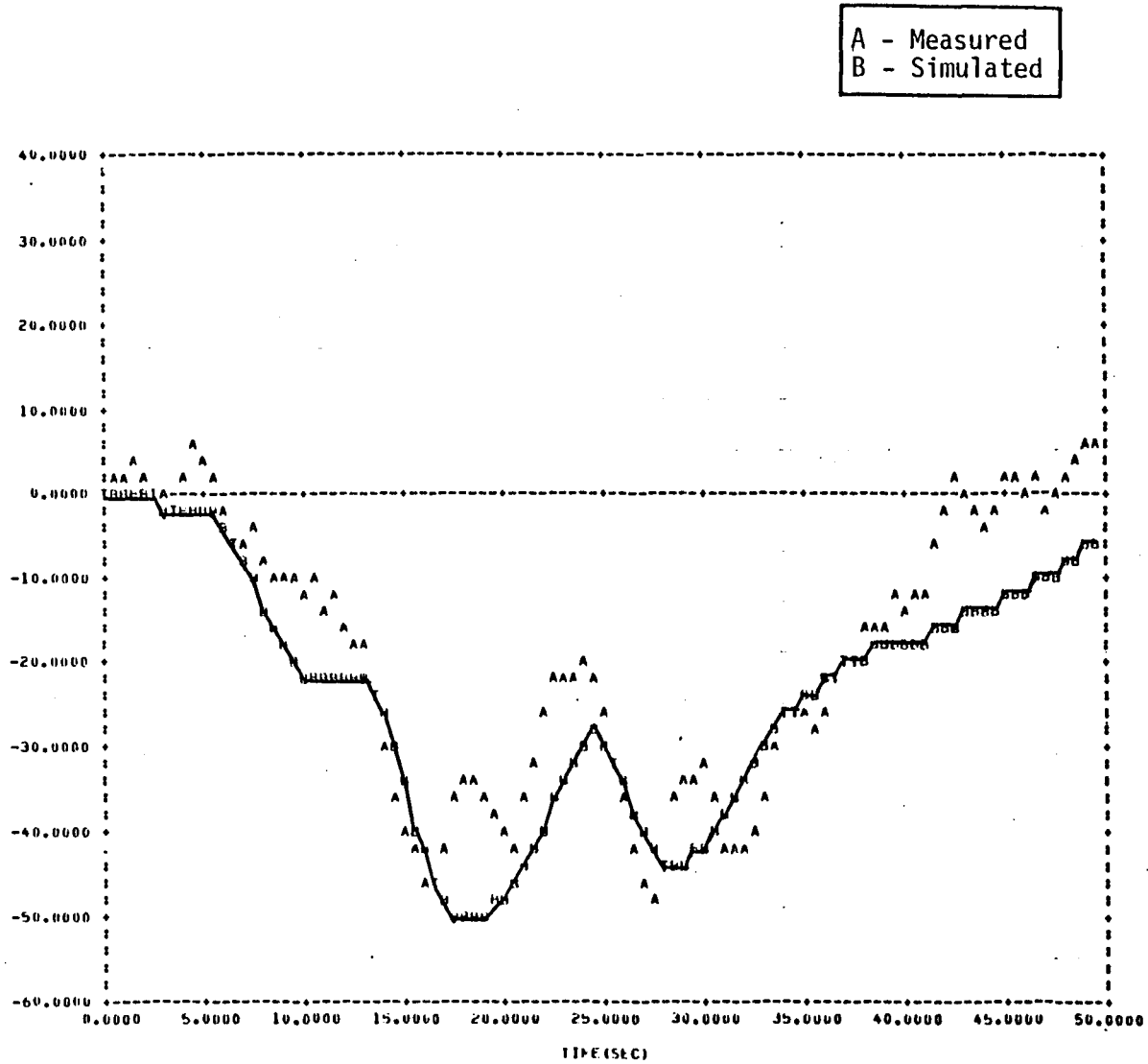
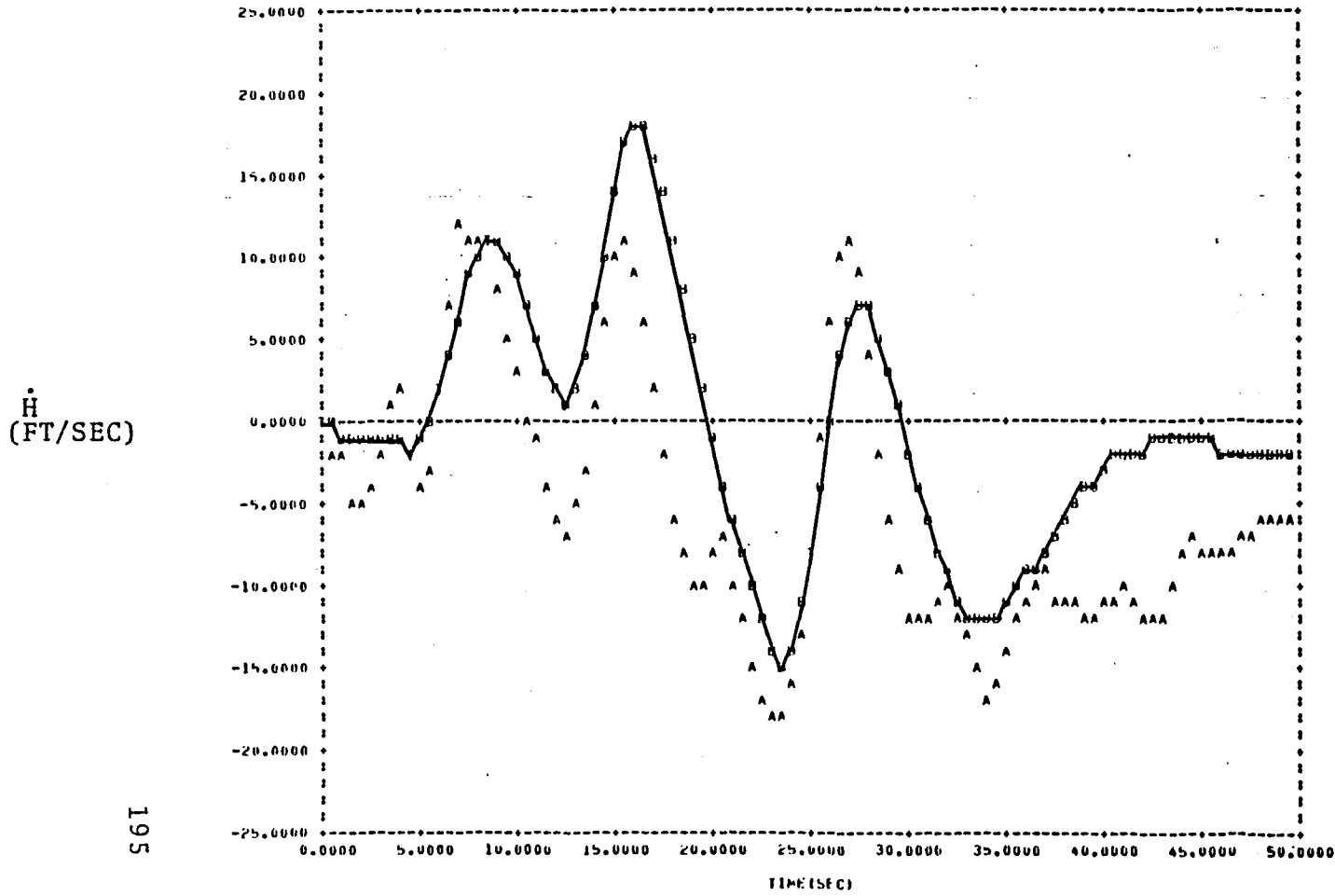


FIGURE 7. 22(a).- SIMULATION OF CASE 1 FINAL PARAMETER MODEL TO THE OPTIMAL LONGITUDINAL STICK INPUT. COMPARED TO ACTUAL UH-1H RESPONSE

•  $V_{TOTAL}$  MEASUREMENT

A - Measured  
B - Simulated



195

FIGURE 7.22 (b).- (CONTINUED)

●  $\dot{h}$  MEASUREMENT

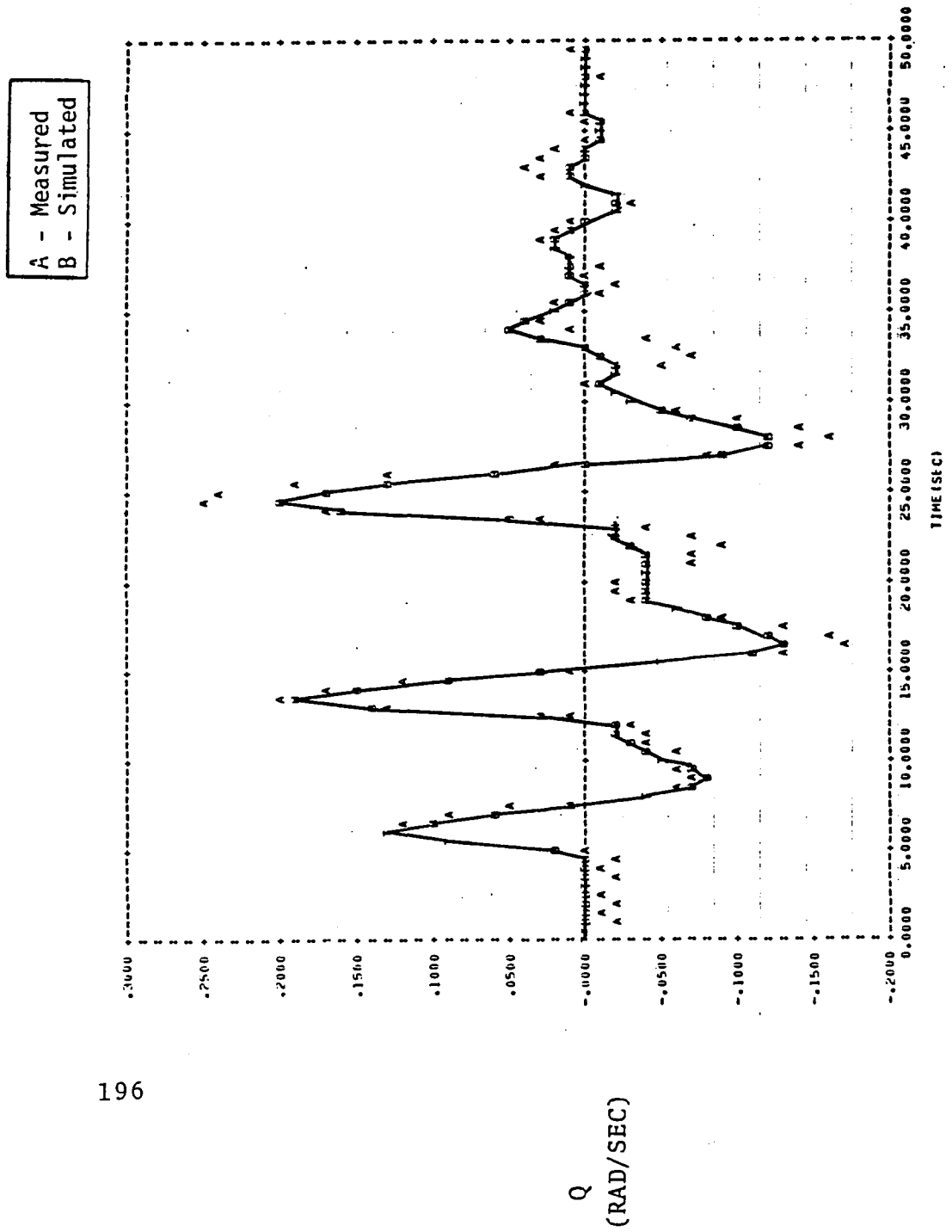


FIGURE 7.22(c). - (CONTINUED)  
● q MEASUREMENT

A - Measured  
 B - Simulated

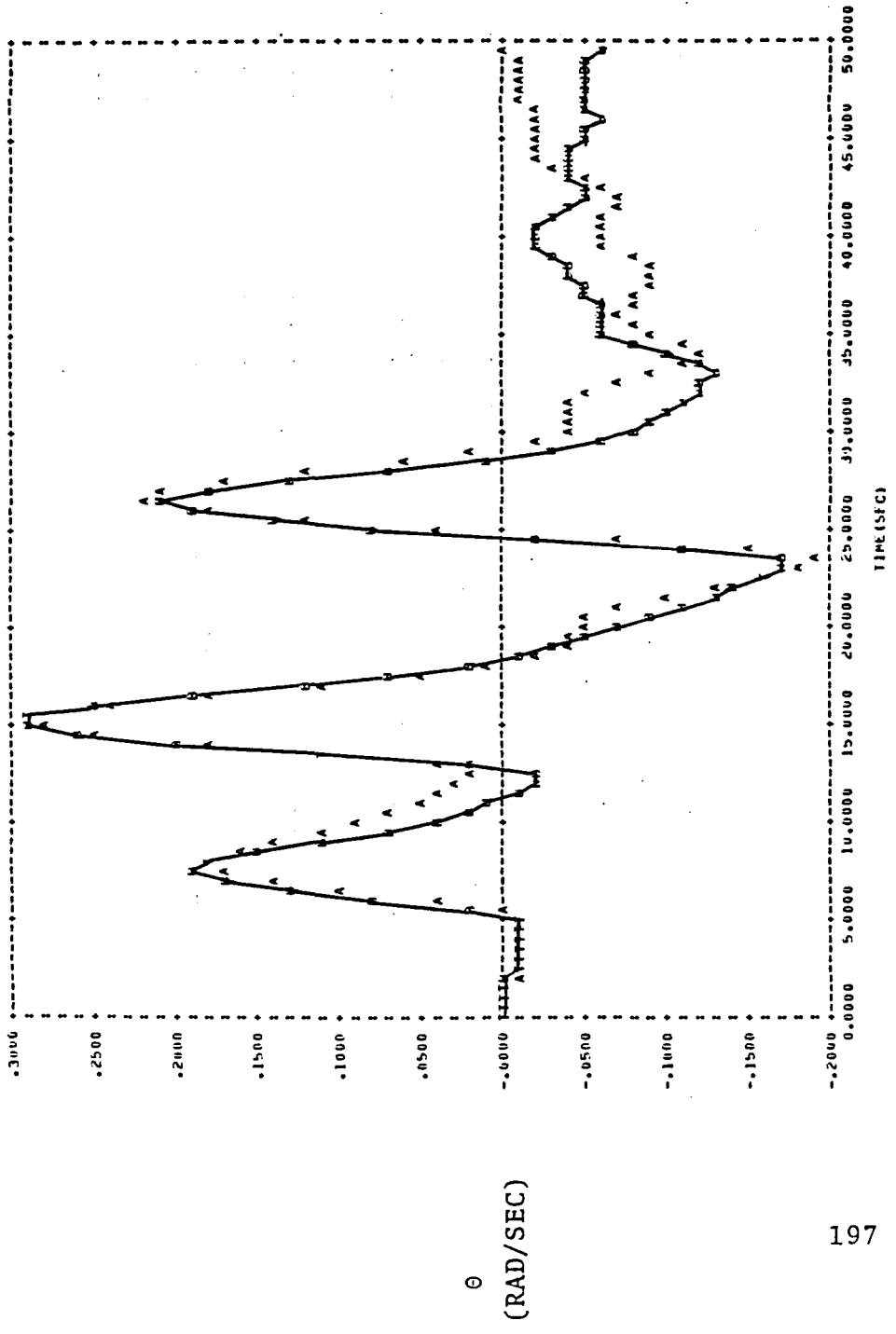


FIGURE 7.22(d). - (CONTINUED)

●  $\theta$  MEASUREMENT

A - Measured  
B - Simulated

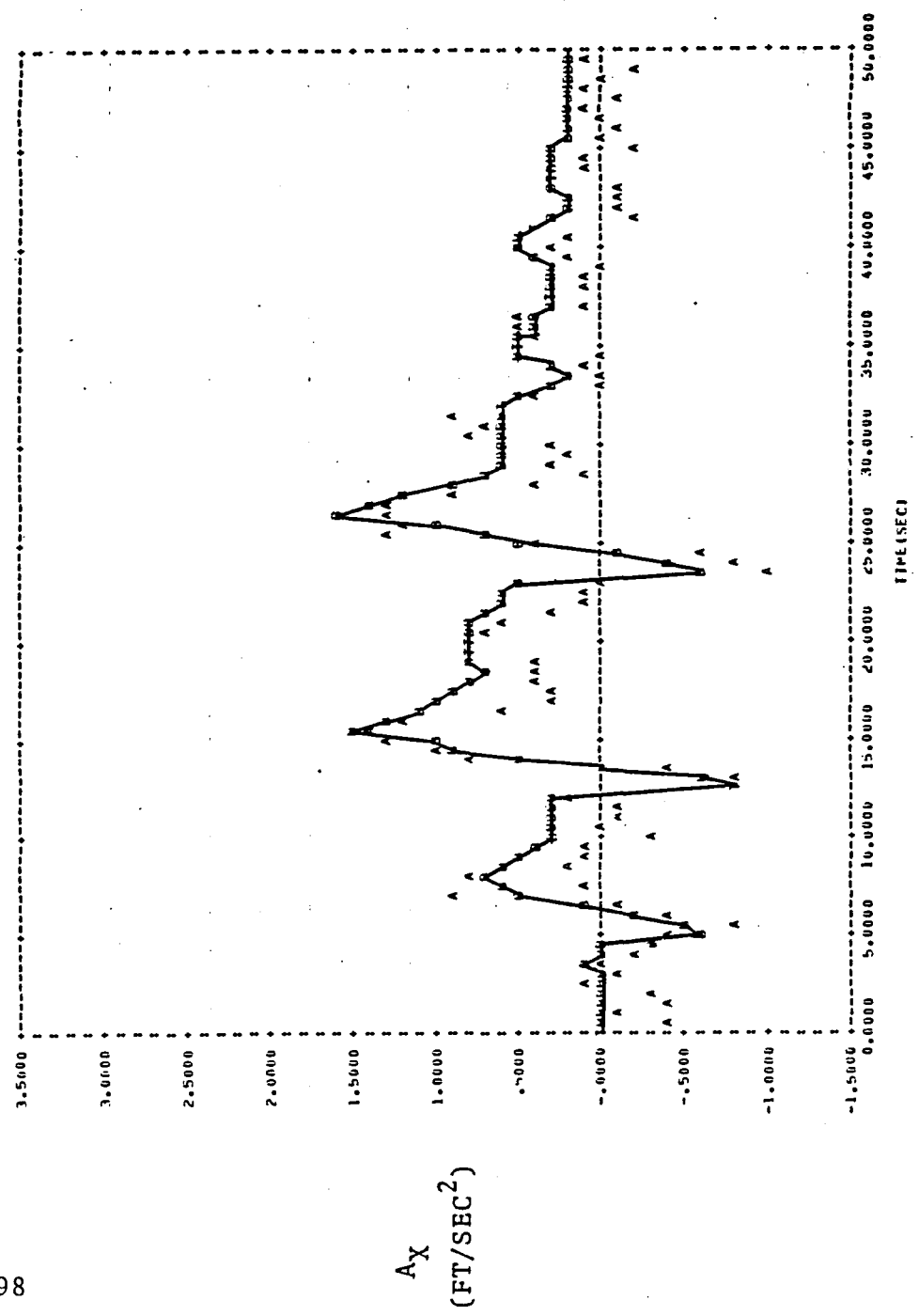
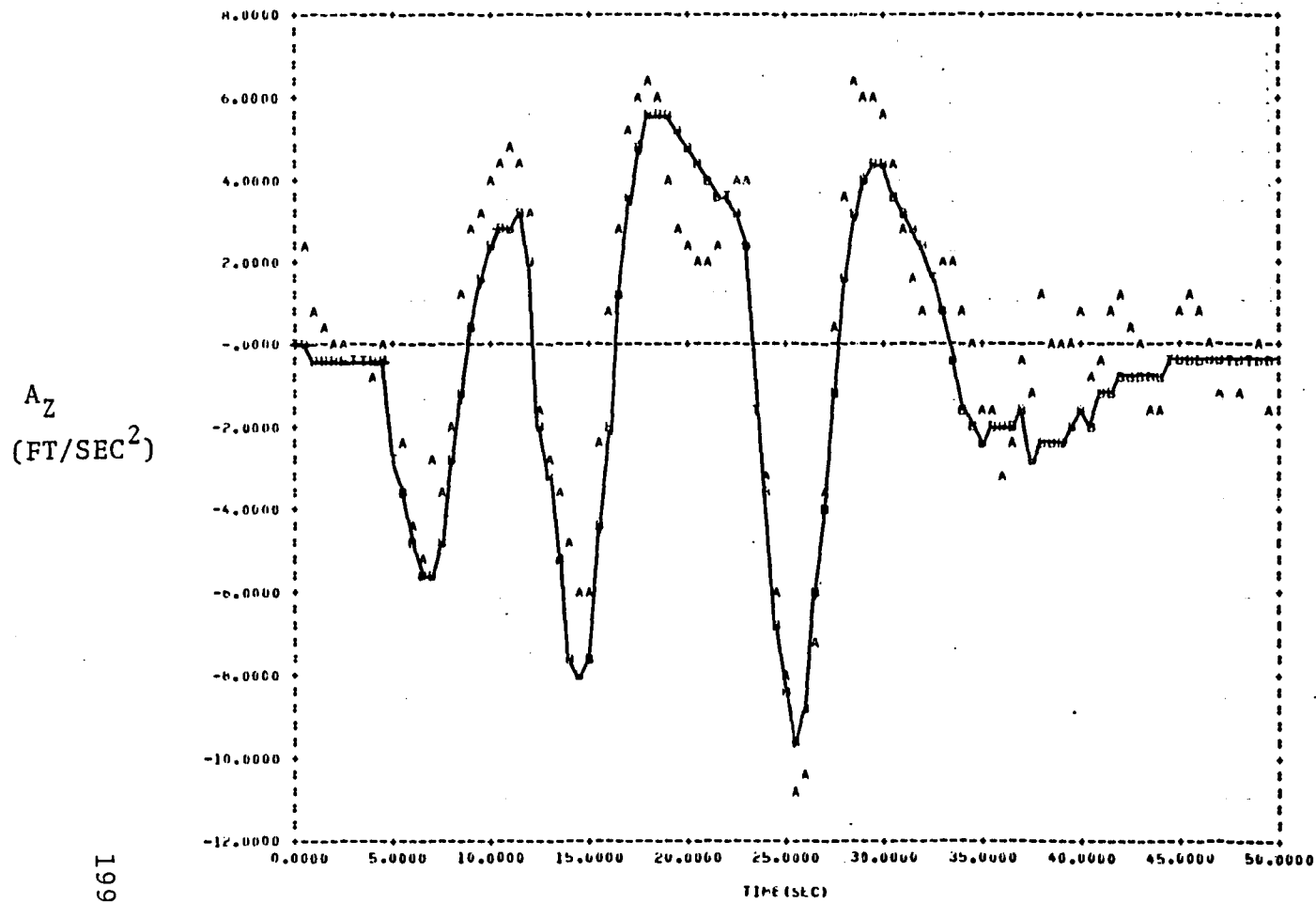


FIGURE 7.22(e).- (CONTINUED)

•  $a_x$  MEASUREMENT



A - Measured  
B - Simulated



$A_z$   
( $\text{FT/SEC}^2$ )

199

FIGURE 7.22(f).- (CONTINUED)

●  $a_z$  MEASUREMENT

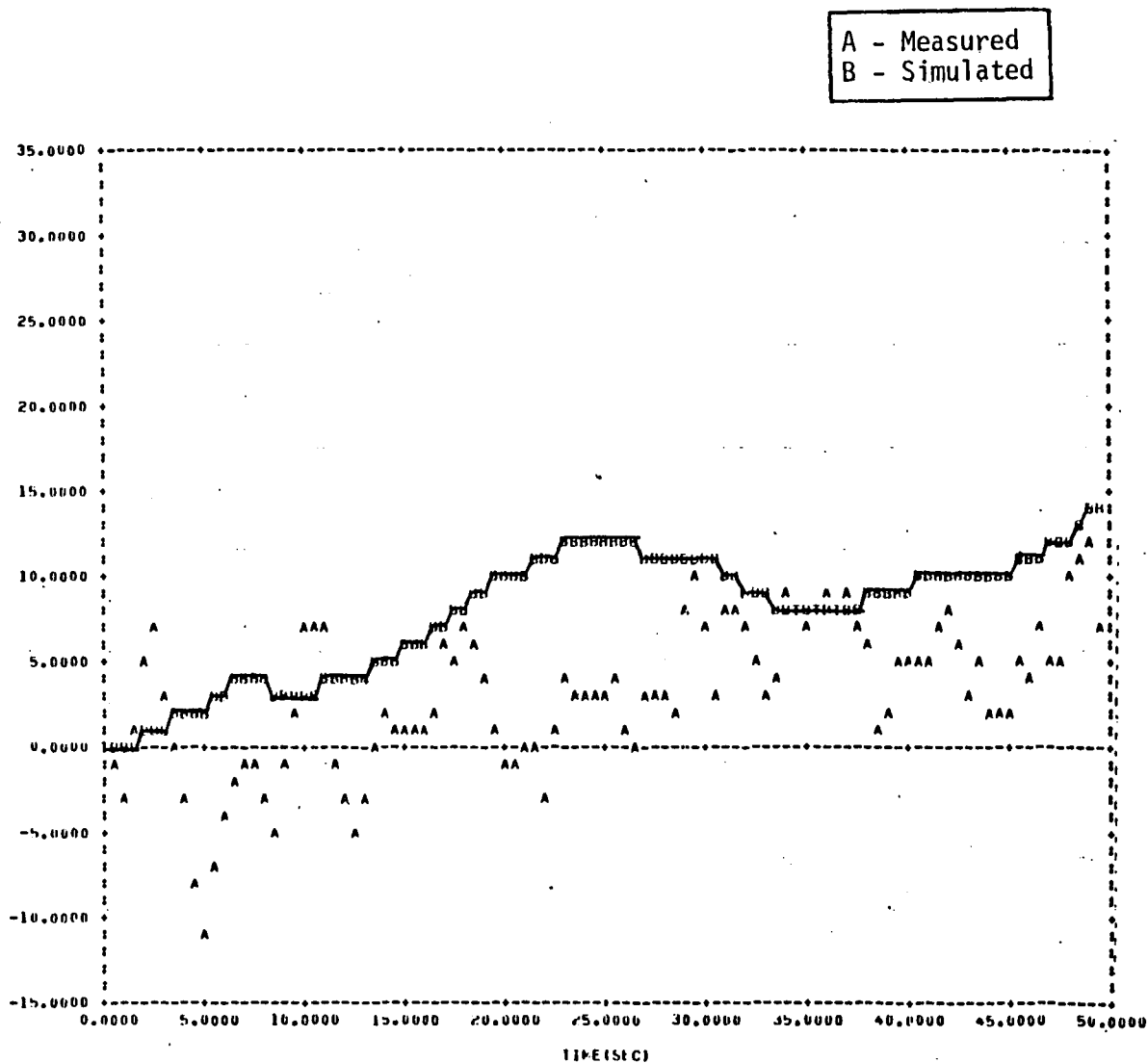
$V_{TOTAL}$   
 (FT/SEC)


FIGURE 7.23(a).— SIMULATION OF CASE 1 FINAL PARAMETER MODEL TO THE OPTIMAL COLLECTIVE STICK INPUT. COMPARED TO ACTUAL UH-1H RESPONSE

●  $V_{TOTAL}$  MEASUREMENT

A - Measured  
B - Simulated

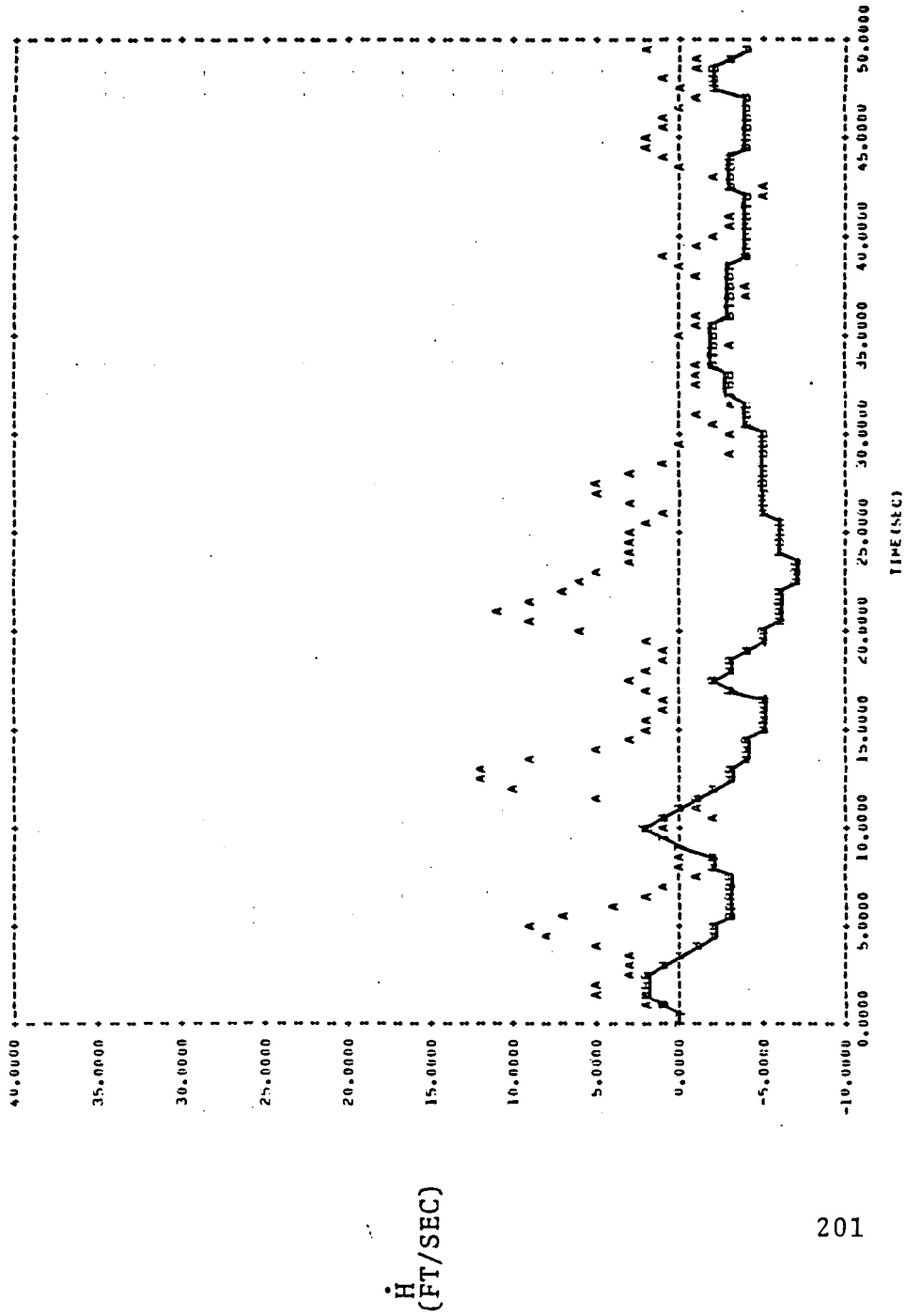


FIGURE 7.23 (b). - (CONTINUED)

●  $\dot{h}$  MEASUREMENT

Q  
(RAD/SEC)

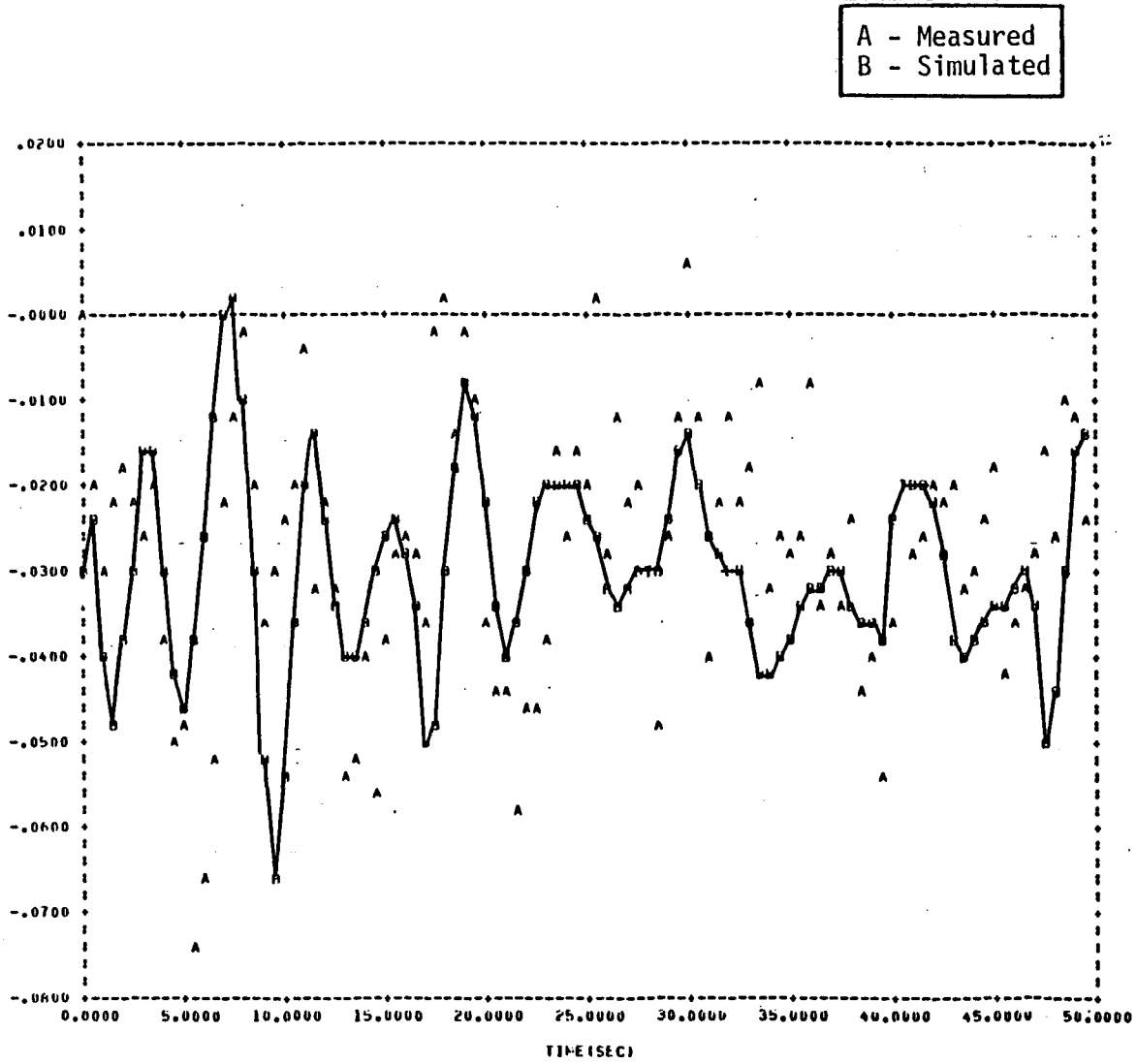
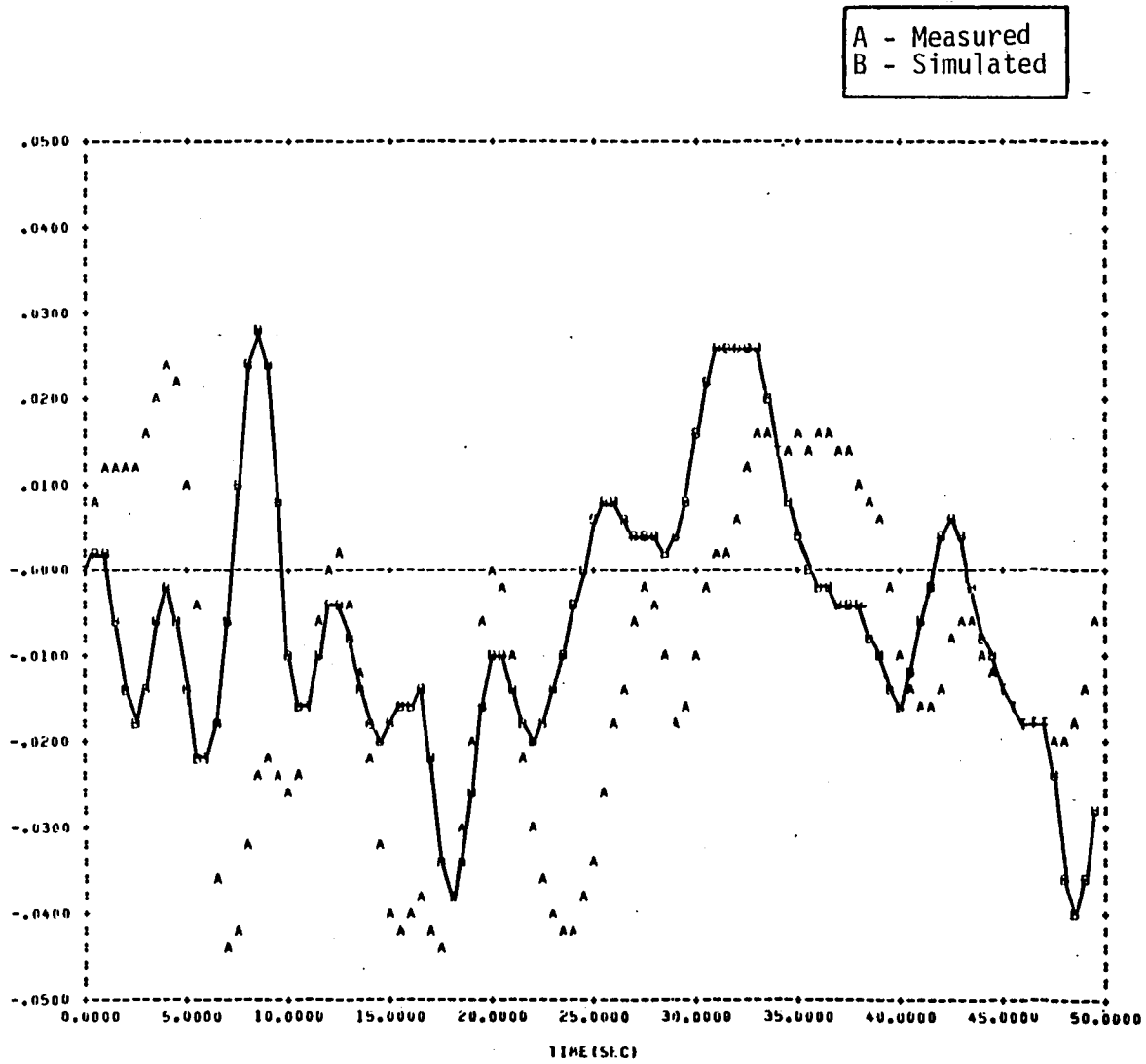


FIGURE 7.23(c).- (CONTINUED)

● q MEASUREMENT

$\theta$   
(RAD)



203

FIGURE 7.23(d).— (CONTINUED)

●  $\theta$  MEASUREMENT

$A_x$   
(FT/SEC<sup>2</sup>)

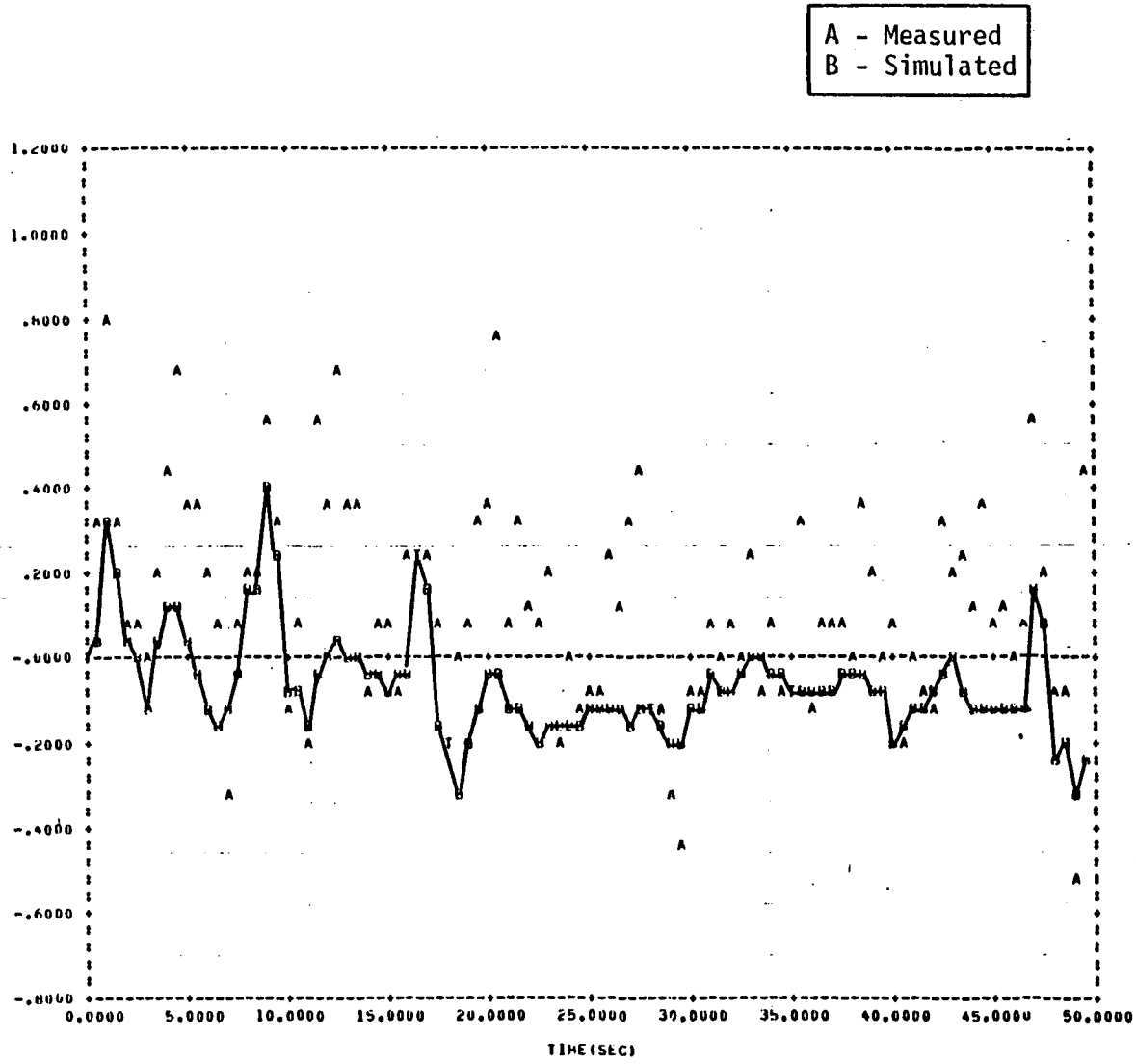


FIGURE 7.23 (e).— (CONTINUED)

●  $a_x$  MEASUREMENT

A - Measured  
B - Simulated

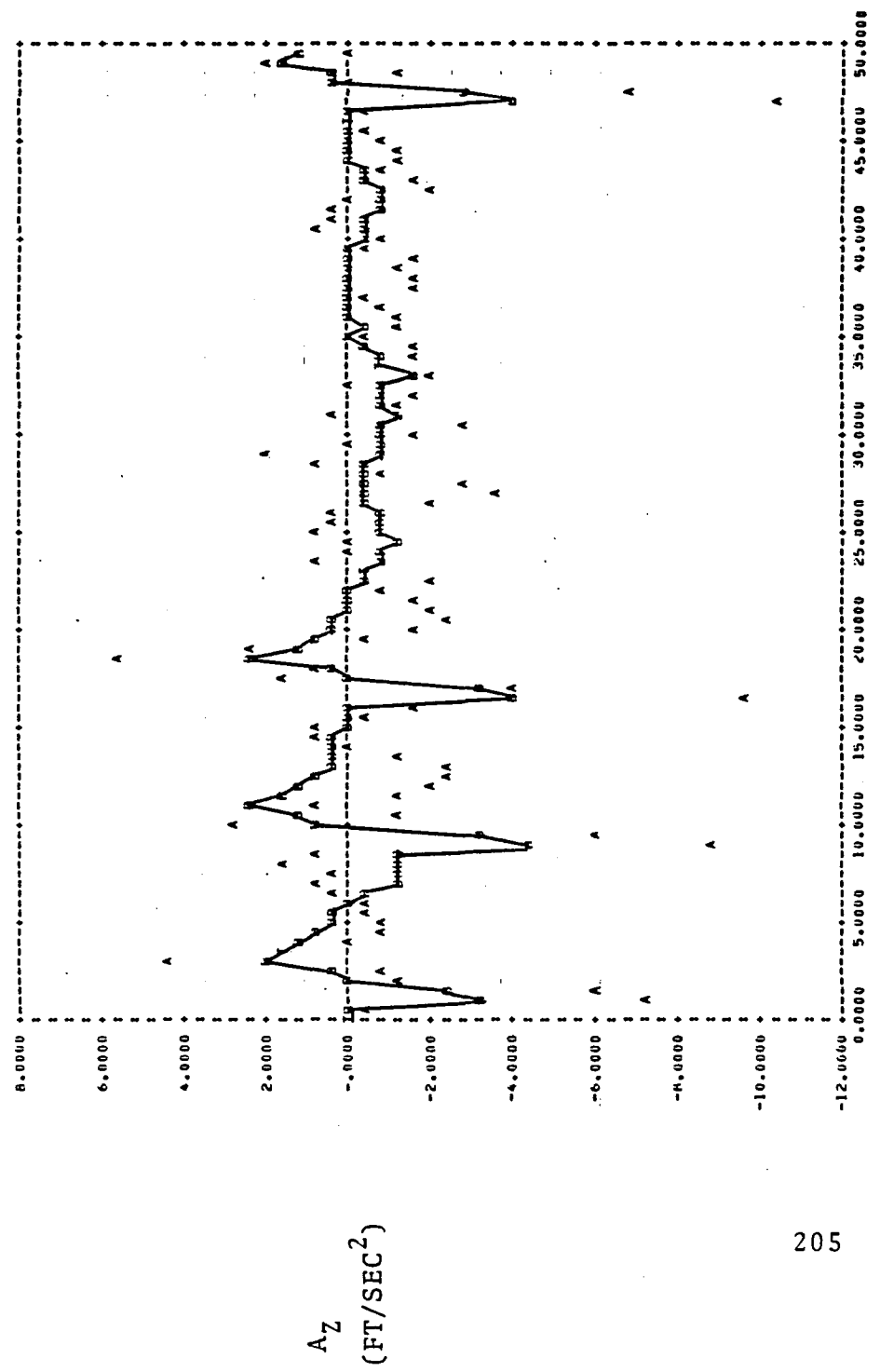


FIGURE 7.23 (f). - (CONCLUDED)

●  $a_z$  MEASUREMENT

Table 7.21  
Parameter Estimates and Standard Deviations for UH-1H

• Case 2

	INITIAL PARAMETER ESTIMATE	FINAL PARAMETER ESTIMATE	STANDARD DEVIATION	F-RATIO
$X_u$ , 1/sec	-0.0227	-0.0328	0.00063	2713.21
$Z_u$ , 1/sec	0.0013	-0.0221	0.00478	21.27
$M_u$ , 1/ft-sec	0.0037	0.0040	0.00007	3430.32
$X_w$ , 1/sec	0.0587	0.0257	0.00201	162.97
$Z_w$ , 1/sec	-0.7542	-0.5268	0.00601	7681.96
$M_w$ , 1/ft-sec	-0.0032	-0.0075	0.00008	8471.64
$M_q$ , 1/sec	-0.5305	-0.5170	0.01405	1354.68
$X_{\delta_{LONG}}$ , ft/sec <sup>2</sup> -in	0.8620	0.4725	0.01556	921.96
$Z_{\delta_{LONG}}$ , ft/sec <sup>2</sup> -in	2.4600	2.7983	0.09074	951.04
$M_{\delta_{LONG}}$ , 1/sec <sup>2</sup> -in	-0.1800	-0.1103	0.00151	5356.71
$X_{\delta_{COLL}}$ , ft/sec <sup>2</sup> -in	0.7115	0.2907	0.01036	788.00
$Z_{\delta_{COLL}}$ , ft/sec <sup>2</sup> -in	-9.8180	-5.1817	0.07954	4243.93
$M_{\delta_{COLL}}$ , 1/sec <sup>2</sup> -in	0.0064	-0.0583	0.00130	2001.03



$V_{TOTAL}$   
(FT/SEC)

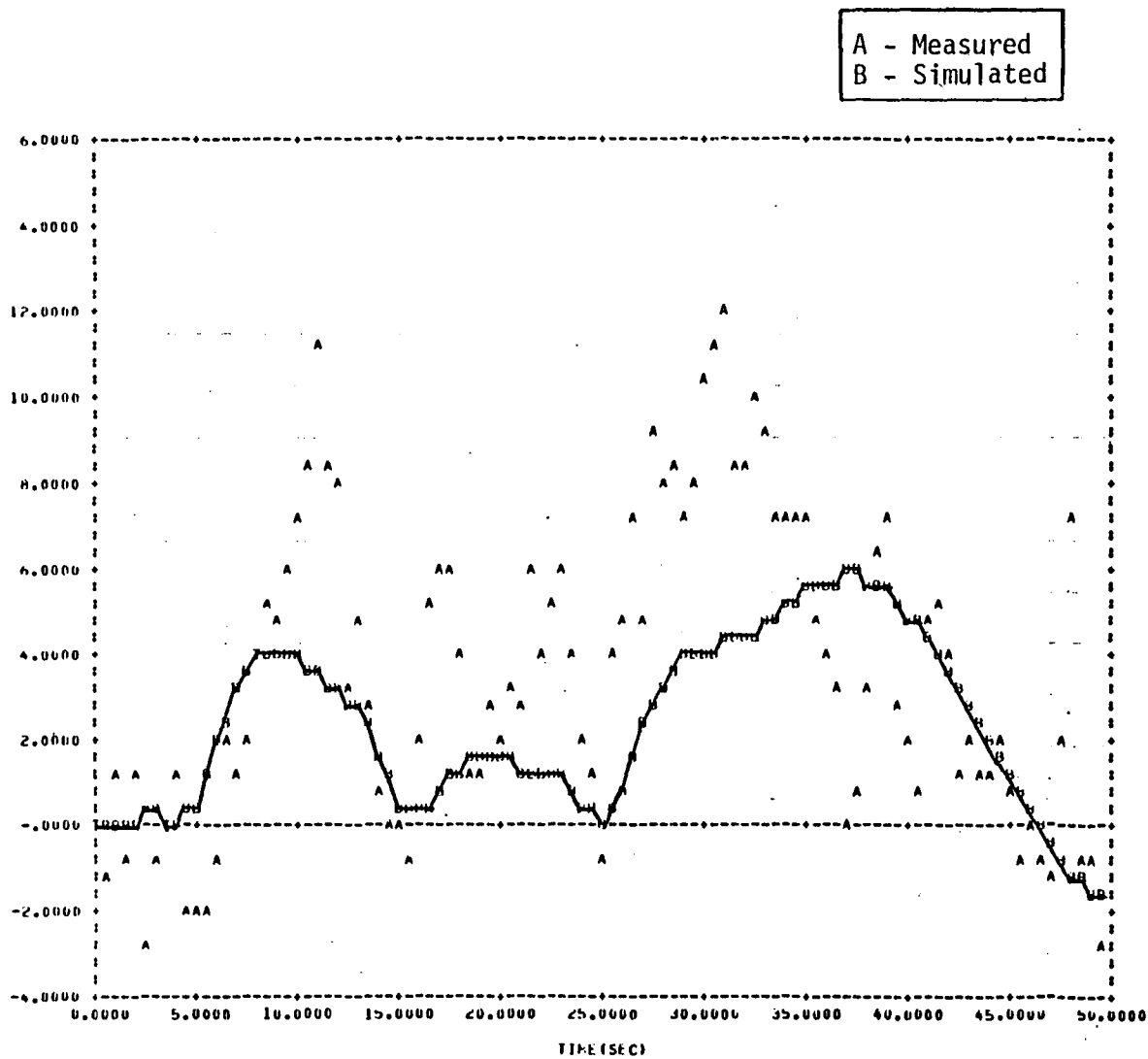


FIGURE 7.24(a).— SIMULATION OF CASE 2 FINAL PARAMETER MODEL TO THE LONGITUDINAL STICK DOUBLET INPUT. COMPARED TO ACTUAL UH-1H RESPONSE

●  $V_{TOTAL}$  MEASUREMENT

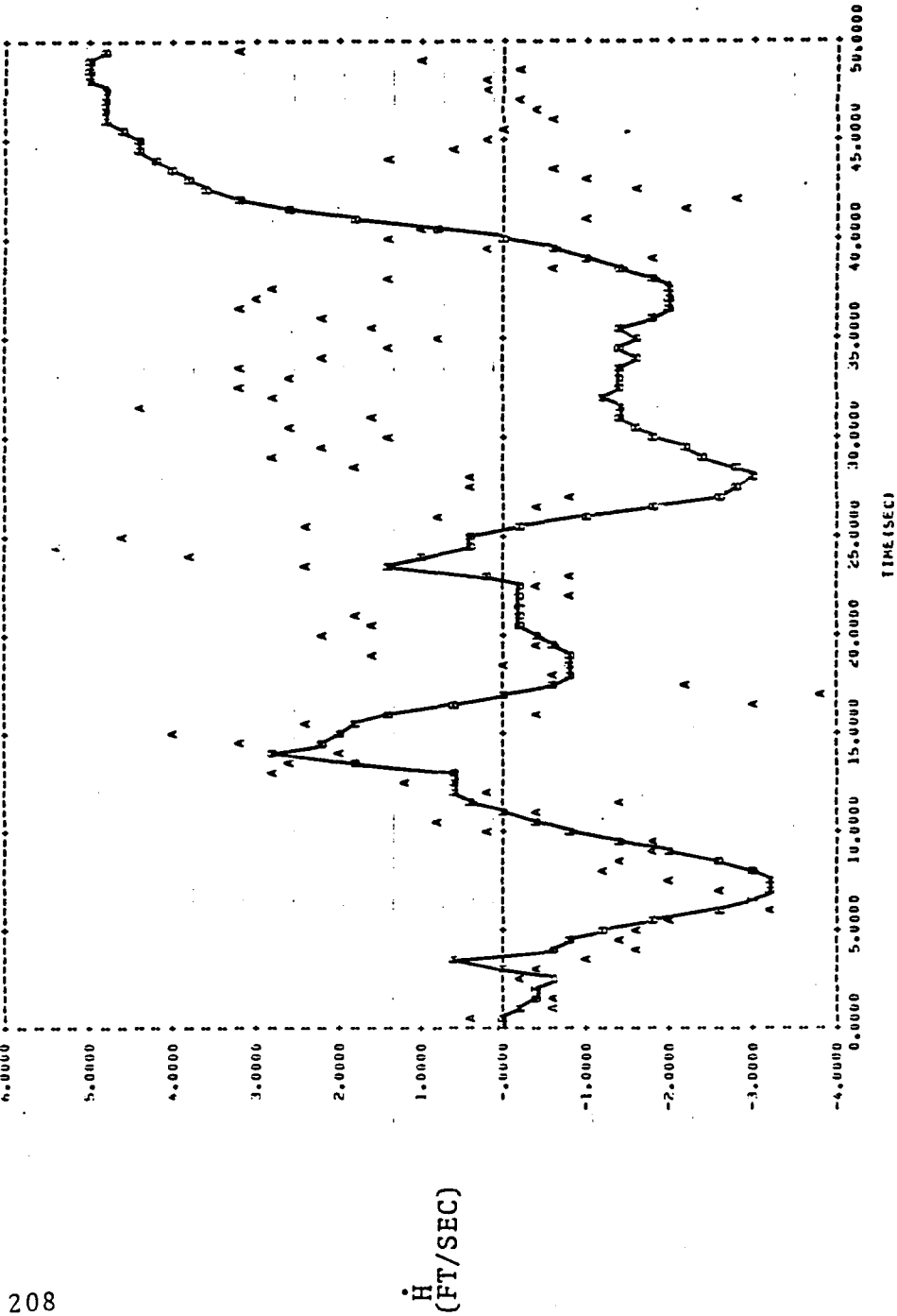


FIGURE 7.24 (b).— (CONTINUED)

●  $\dot{h}$  MEASUREMENT

A - Measured  
B - Simulated

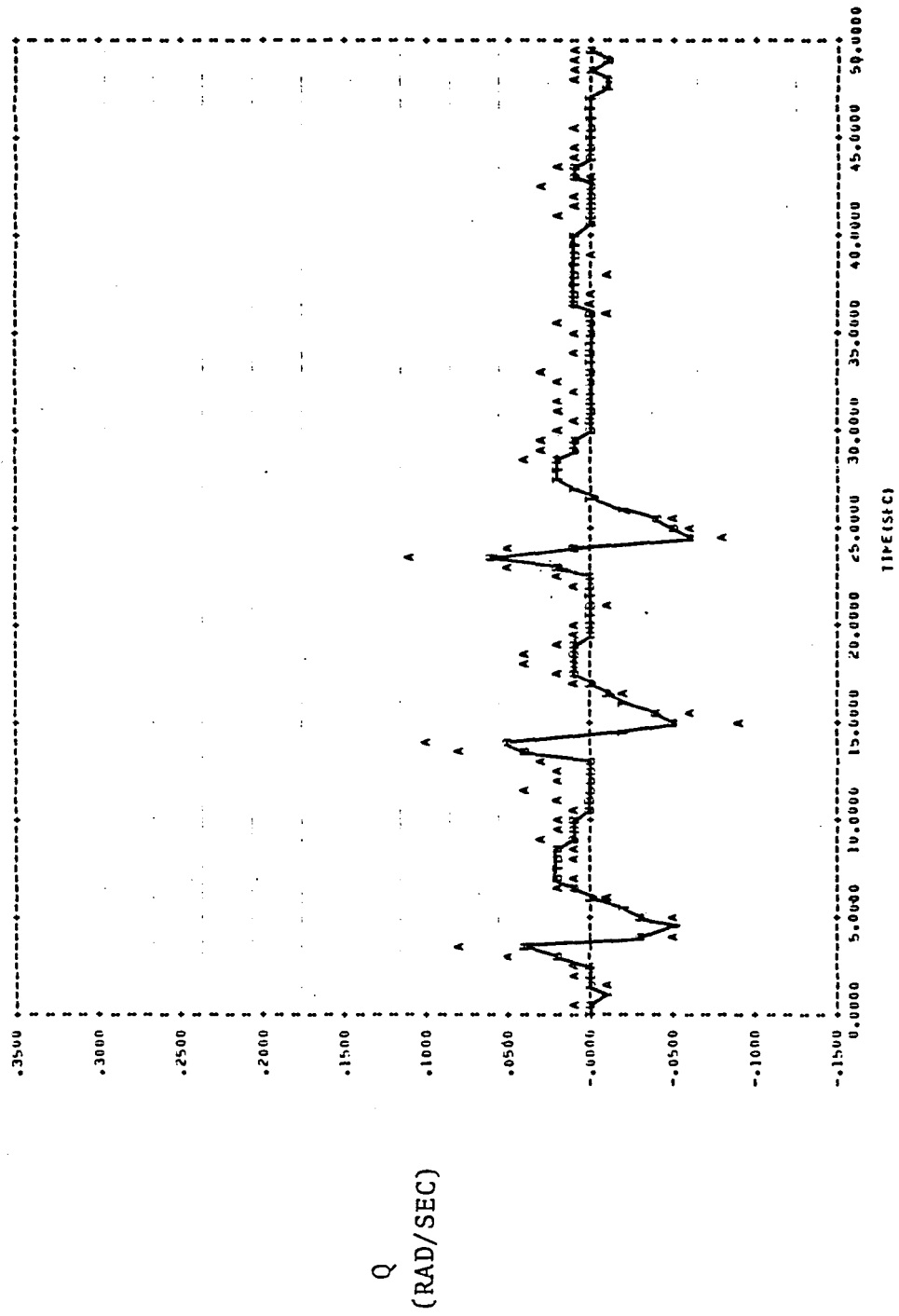


FIGURE 7.24 (c). - (CONTINUED)

● q MEASUREMENT

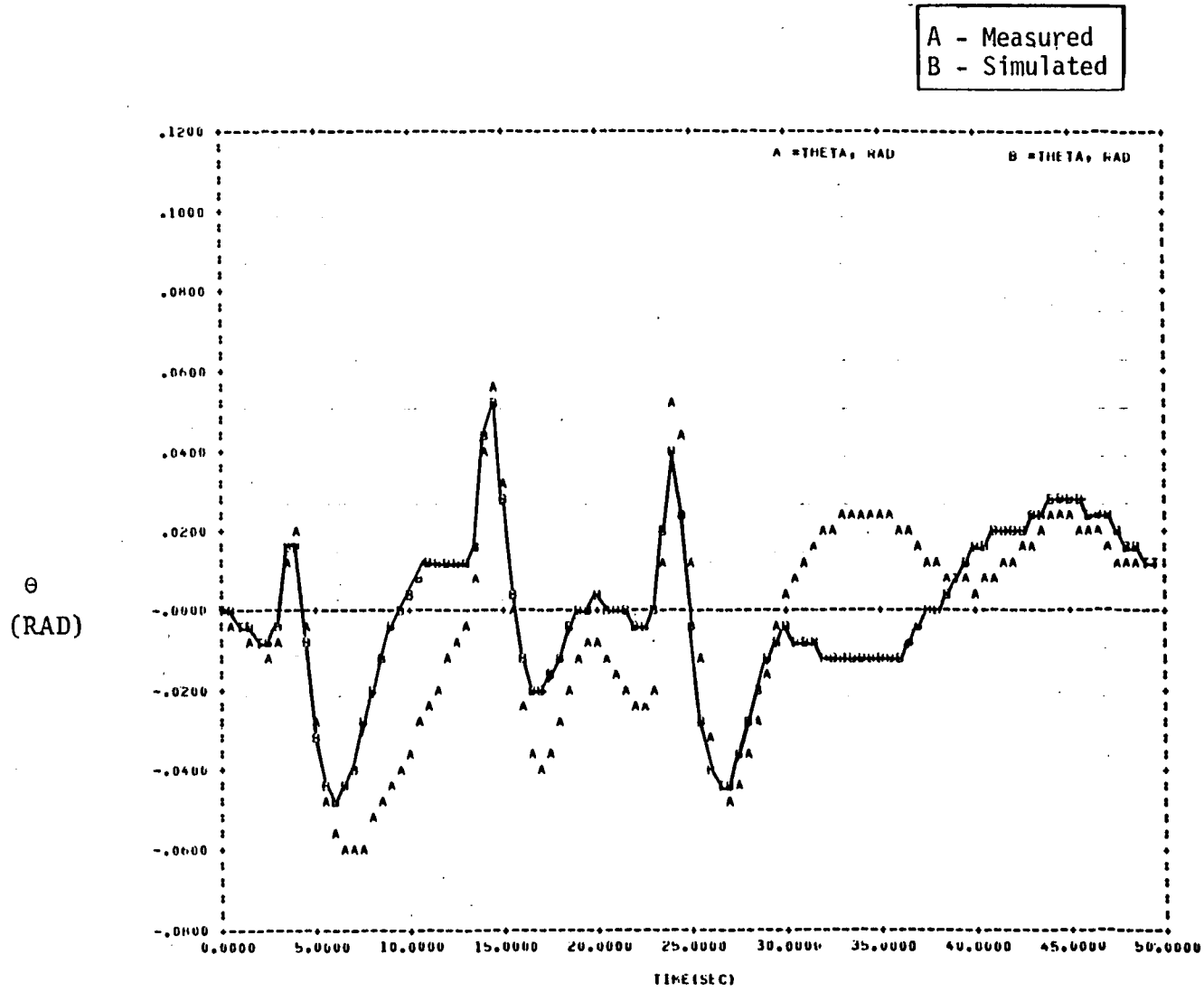


FIGURE 7.24 (d).— (CONTINUED)

●  $\theta$  MEASUREMENT

$A_x$   
(FT/SEC<sup>2</sup>)

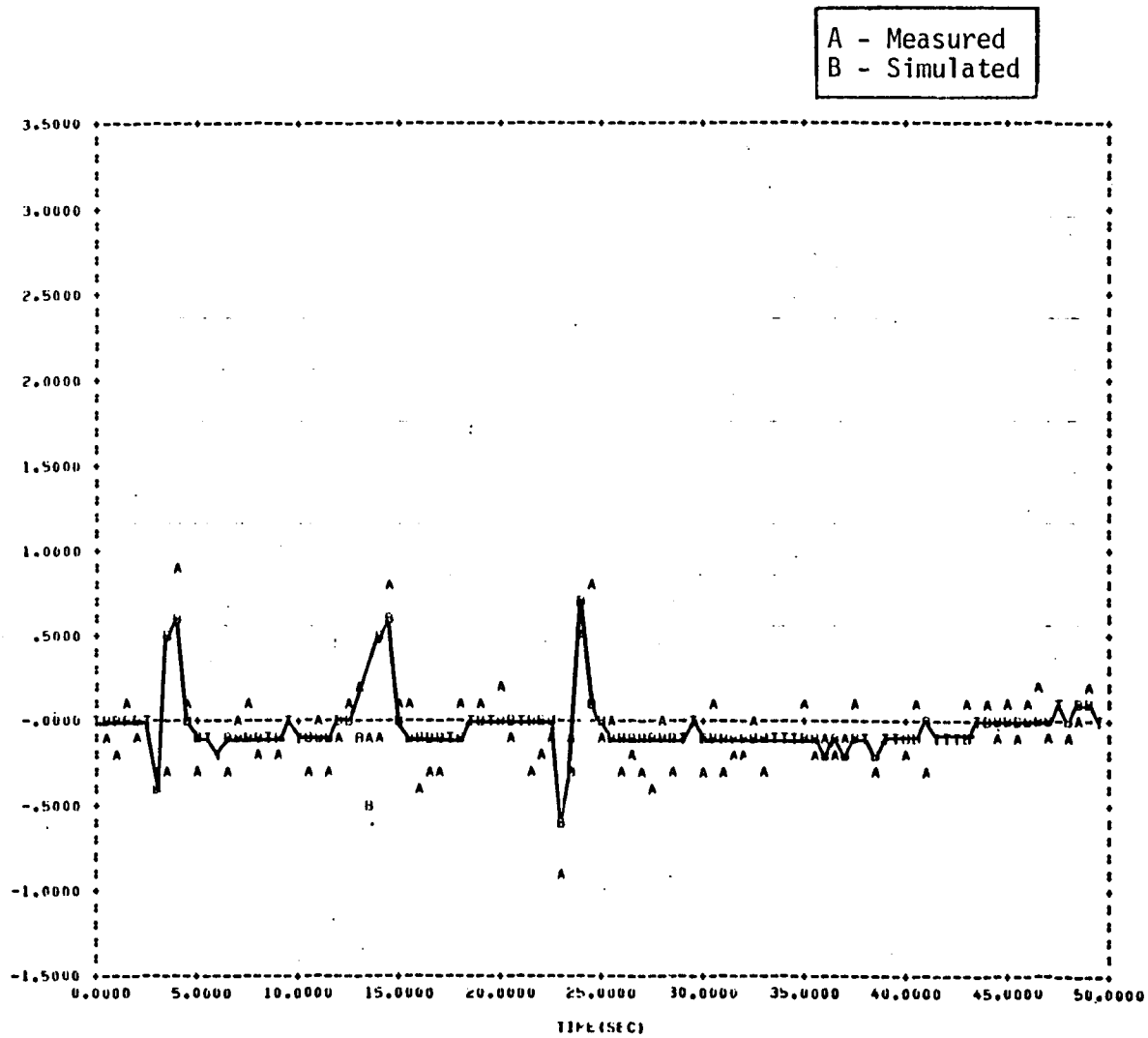


FIGURE 7.24(e).- (CONTINUED)

●  $a_x$  MEASUREMENT

A - Measured  
B - Simulated

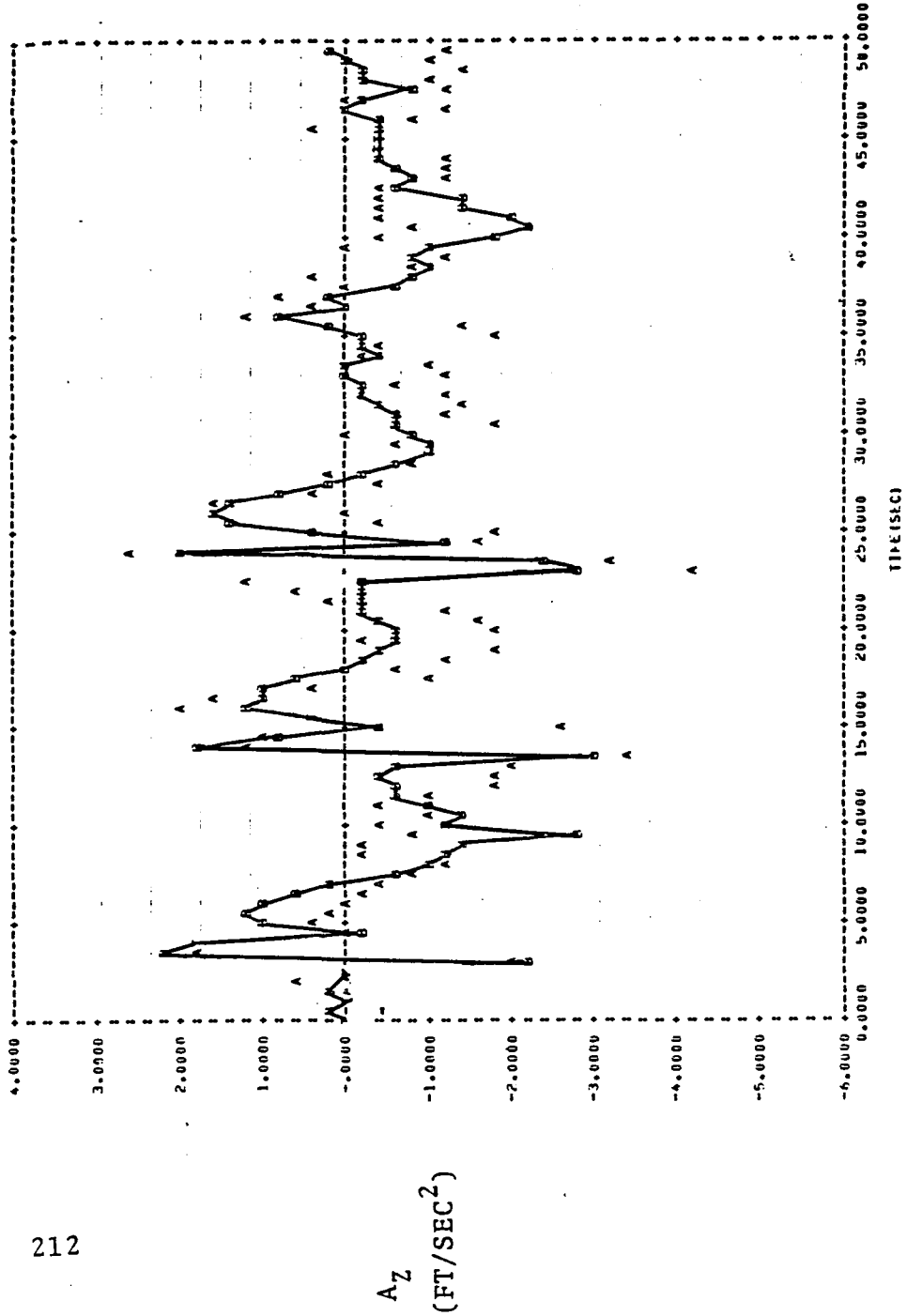
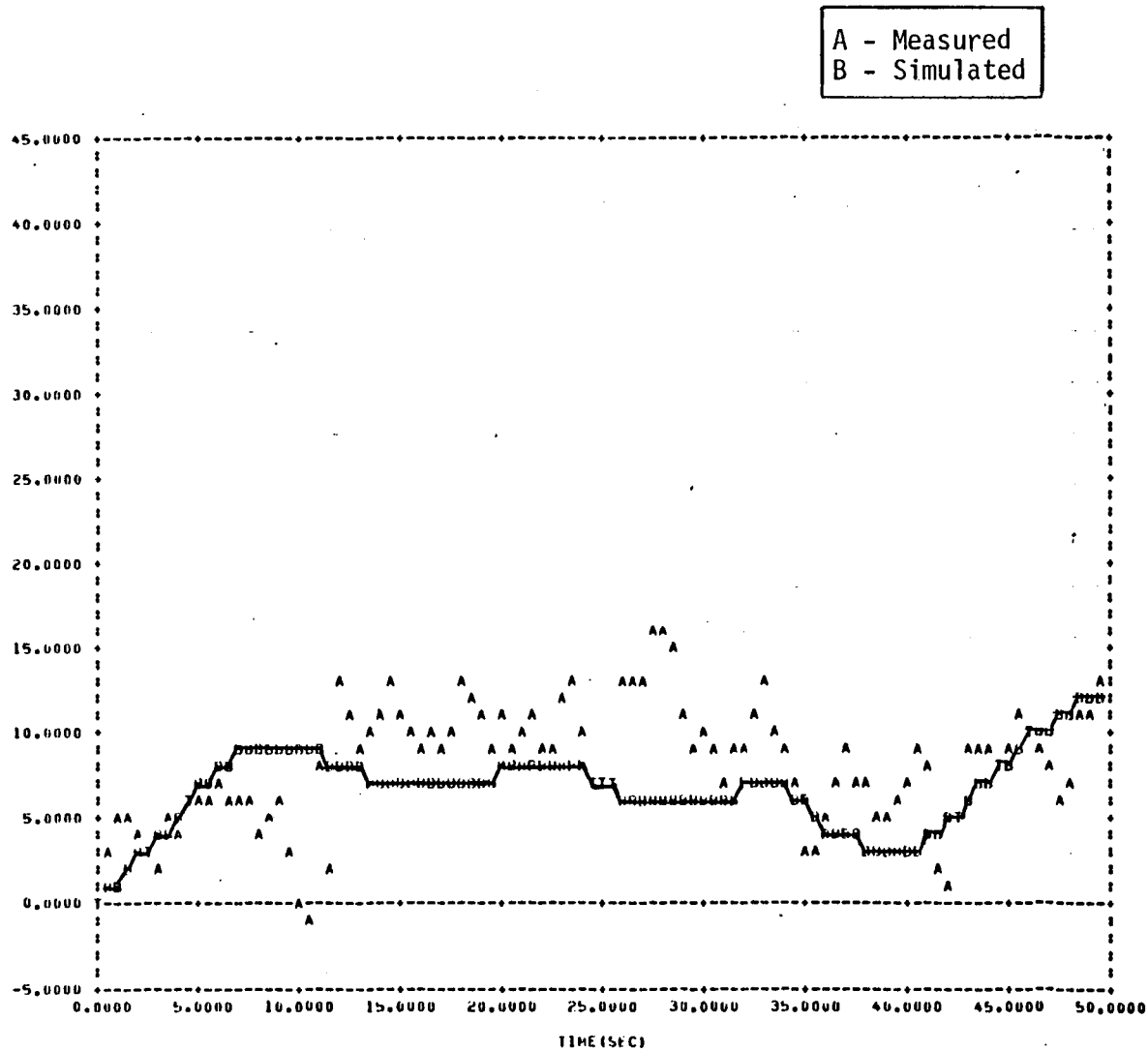


FIGURE 7.24 (f). - (CONTINUED)

●  $a_z$  MEASUREMENT

$V_{TOTAL}$   
(FT/SEC)



213

FIGURE 7.25 (a).— SIMULATION OF CASE 2 FINAL PARAMETER MODEL TO THE COLLECTIVE STICK DOUBLET INPUT. COMPARED TO ACTUAL UH-1H RESPONSE

●  $V_{TOTAL}$  MEASUREMENT

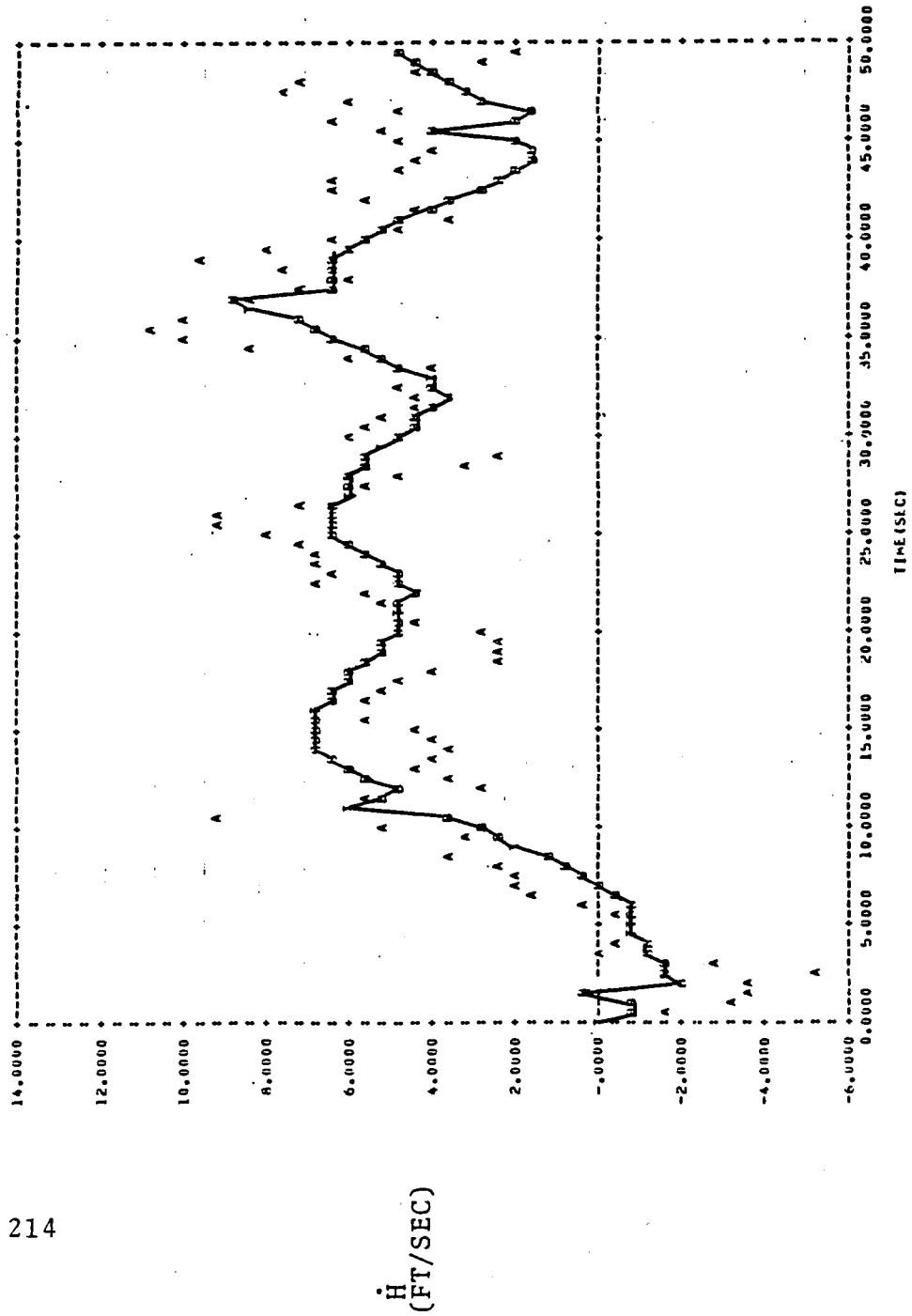


FIGURE 7.25 (b). - (CONTINUED)

●  $\dot{h}$  MEASUREMENT



A - Measured  
B - Simulated

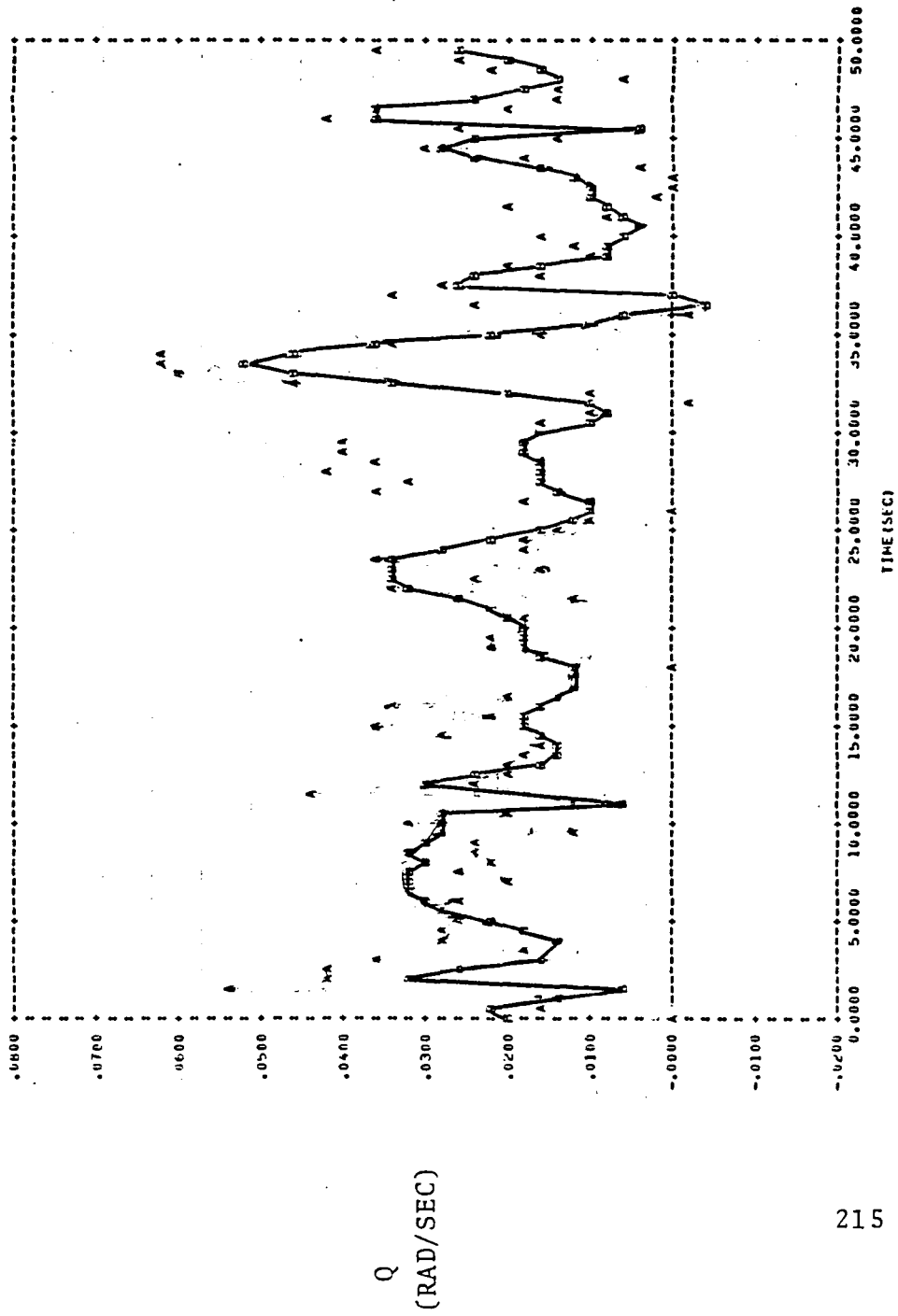


FIGURE 7.25(c). - (CONTINUED)

● q MEASUREMENT

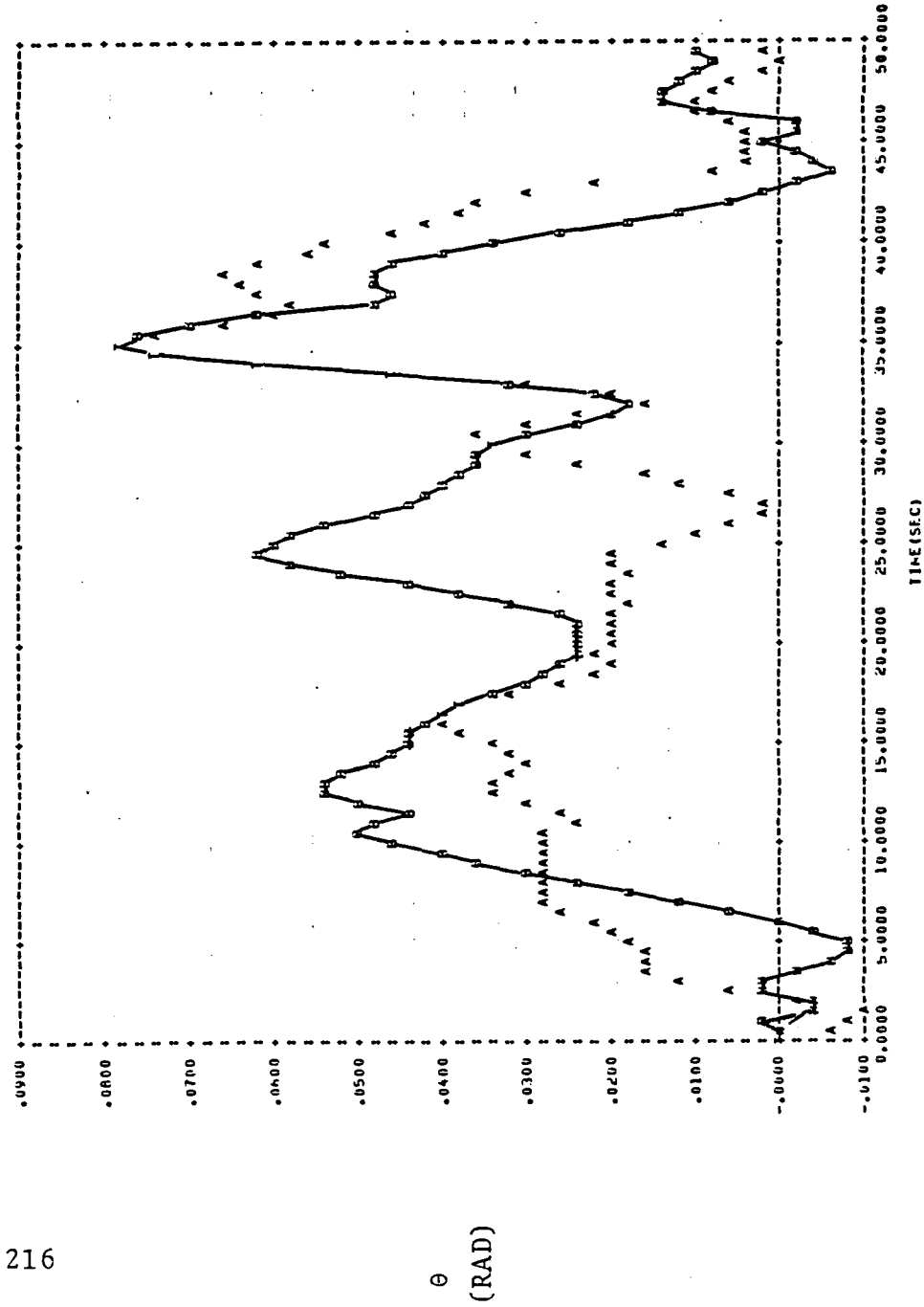


FIGURE 7.25(d). - (CONTINUED)

●  $\theta$  MEASUREMENT

A - Measured  
B - Simulated

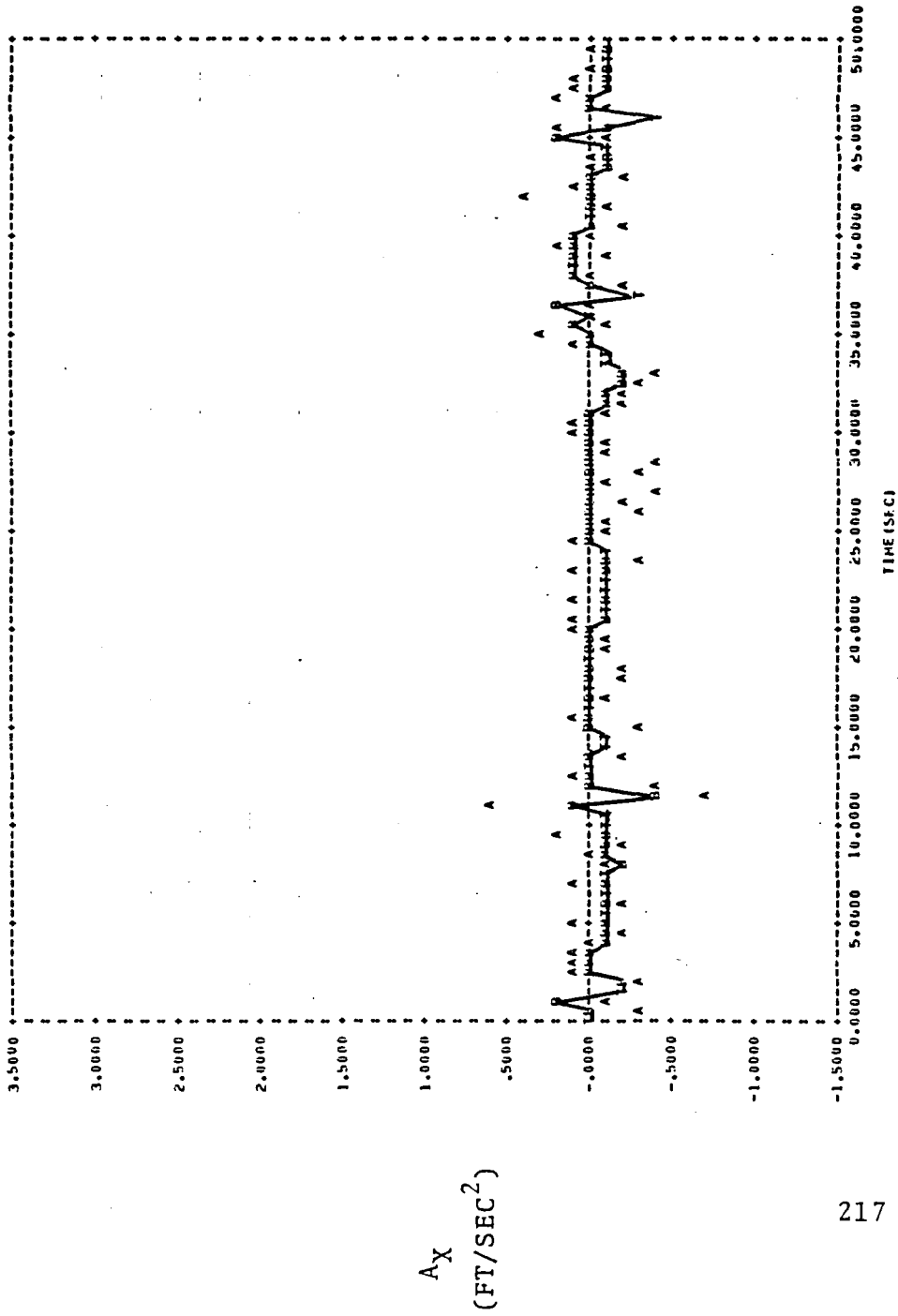


FIGURE 7.25 (e). - (CONTINUED)

●  $a_x$  MEASUREMENT

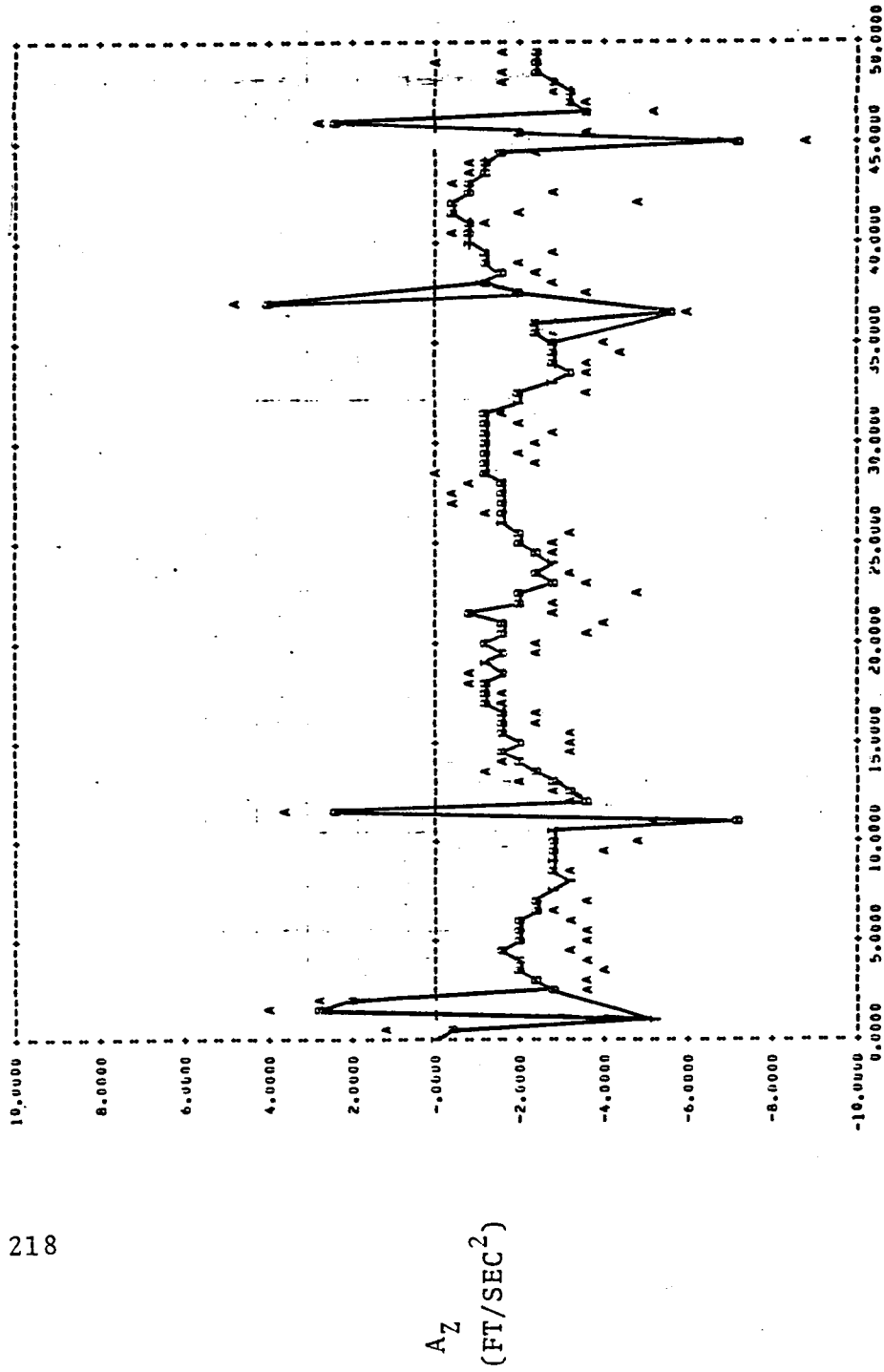


FIGURE 7.25(F). - (CONCLUDED)  
 ● a<sub>z</sub> MEASUREMENT

TABLE 7.22.— PARAMETER ESTIMATES AND STANDARD DEVIATIONS FOR UH-1H

• Case 3

	INITIAL PARAMETER ESTIMATES	FINAL PARAMETER ESTIMATES	STANDARD DEVIATION	F-RATIO
$X_u$ , 1/sec	-0.0227	-0.0271	0.00026	11092.39
$Z_u$ , 1/sec	0.0013	-0.0226	0.00144	244.79
$M_u$ , 1/ft-sec	0.0037	0.0027	0.00003	9694.58
$X_w$ , 1/sec	0.0587	0.0391	0.00075	2701.15
$Z_w$ , 1/sec	-0.7542	-0.4573	0.00337	18361.13
$M_w$ , 1/ft-sec	-0.0032	-0.0095	0.00006	28760.19
$M_q$ , 1/sec	-0.5305	-0.7017	0.00697	10141.01
$X_{\delta\text{LONG}}$ , ft/sec <sup>2</sup> -in	0.8620	0.5871	0.01119	2754.05
$Z_{\delta\text{LONG}}$ , ft/sec <sup>2</sup> -in	2.4600	1.9616	0.06012	1064.63
$M_{\delta\text{LONG}}$ , 1/sec <sup>2</sup> -in	-0.1800	-0.1685	0.00106	25282.50
$X_{\delta\text{COLL}}$ , ft/sec <sup>2</sup> -in	0.715	0.1691	0.01151	215.80
$Z_{\delta\text{COLL}}$ , ft/sec <sup>2</sup> -in	-9.8180	-3.9439	0.08663	2072.84
$M_{\delta\text{COLL}}$ , 1/sec <sup>2</sup> -in	0.0064	-0.0535	0.00163	1072.94

$V_{TOTAL}$   
(FT/SEC)

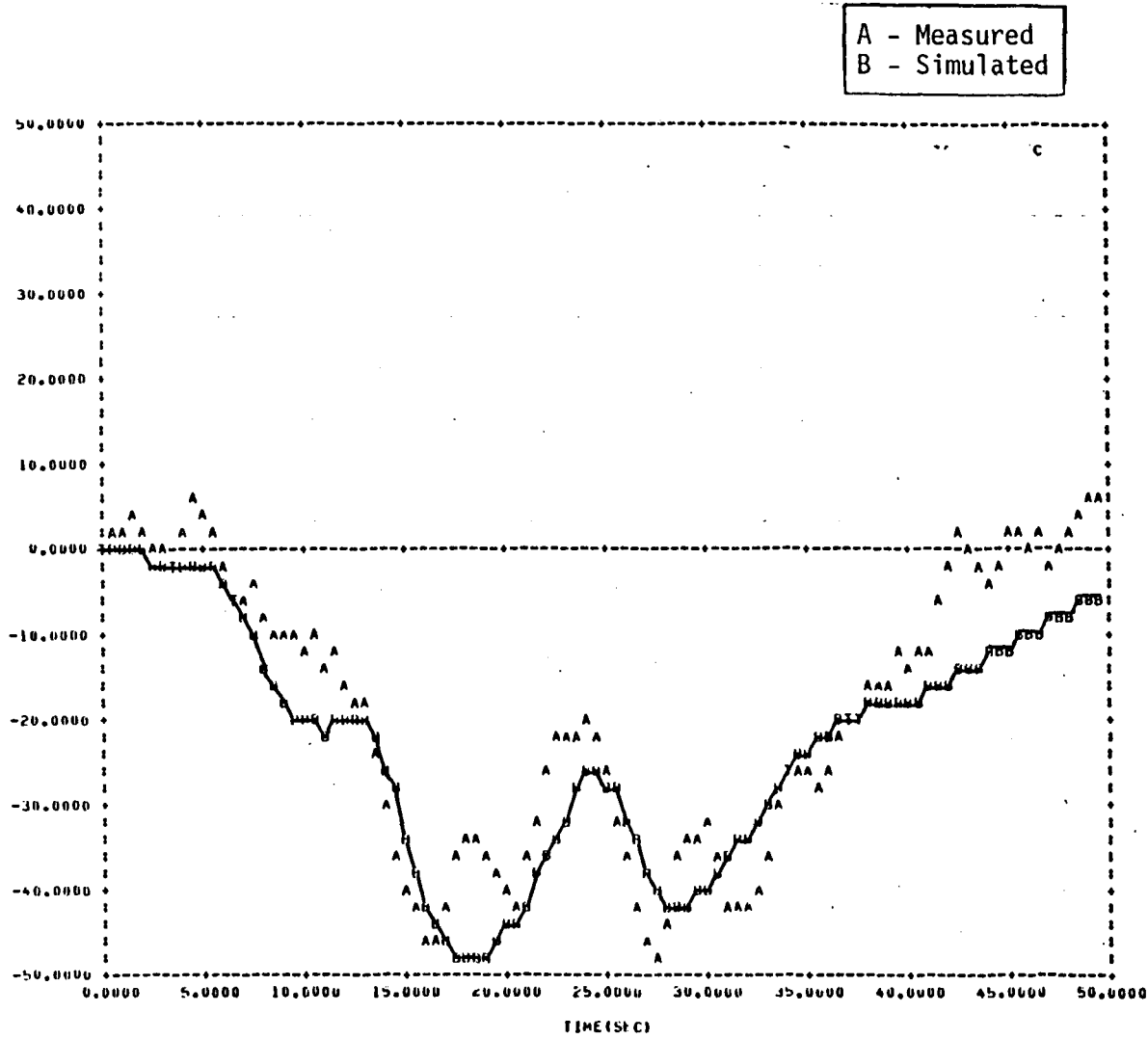
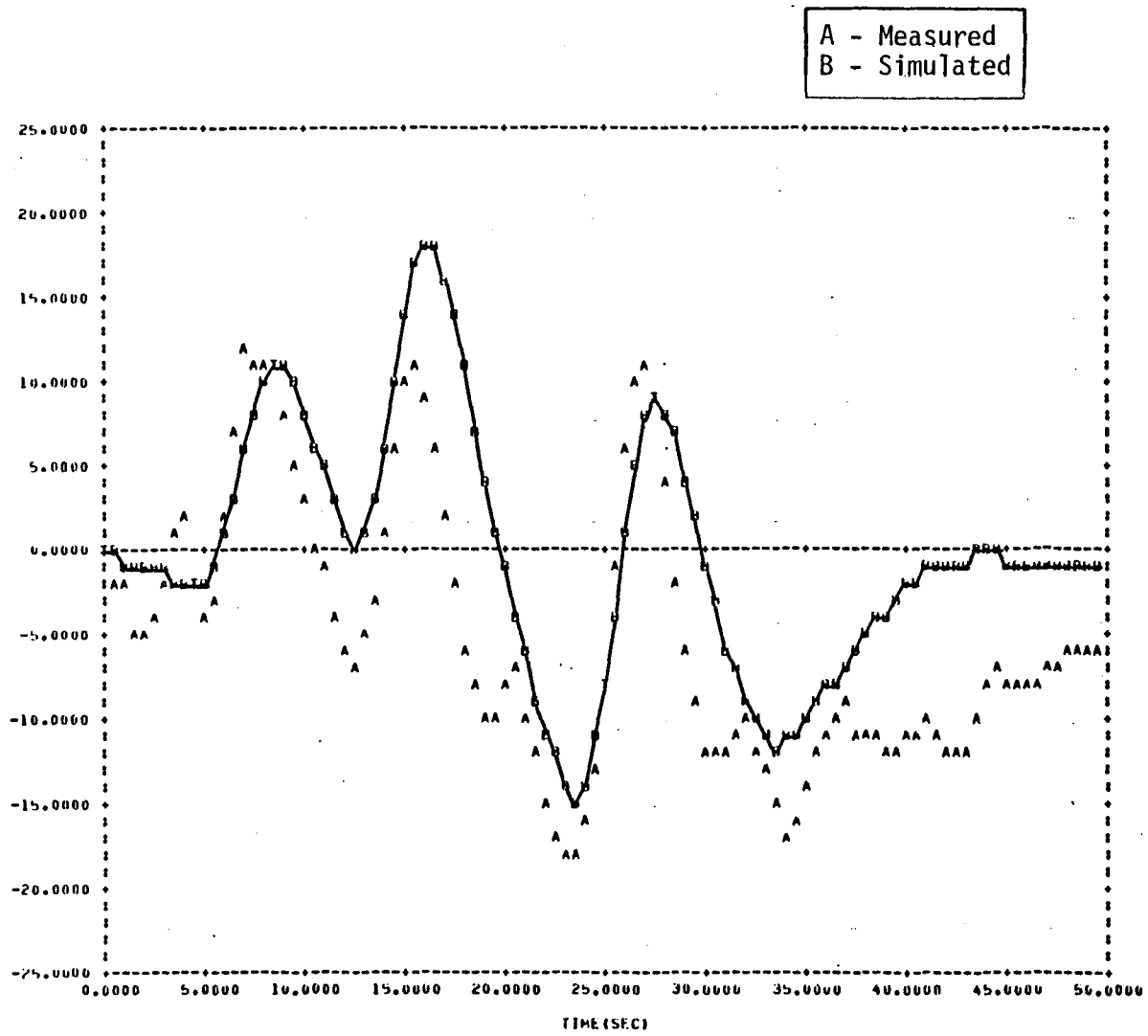


FIGURE 7.26(a).— SIMULATION OF CASE 3 FINAL PARAMETER MODEL TO THE OPTIMAL LONGITUDINAL STICK INPUT. COMPARED TO ACTUAL UH-1H RESPONSE

●  $V_{TOTAL}$  MEASUREMENT

$\dot{H}$   
(FT/SEC)



221

FIGURE 7.26(b).- (CONTINUED)

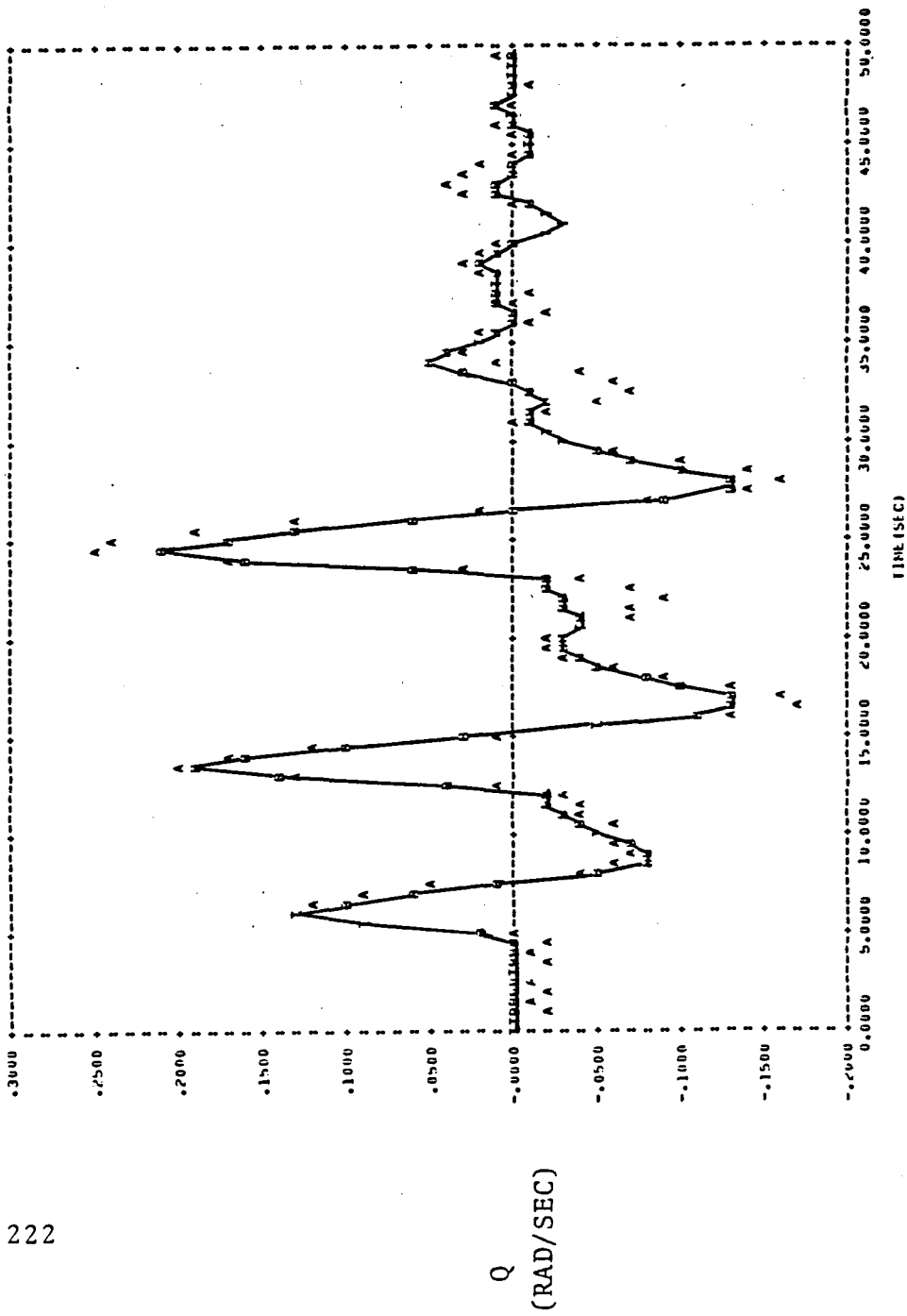


FIGURE 7.26 (c).-- (CONTINUED)

● q MEASUREMENT



A - Measured  
 B - Simulated

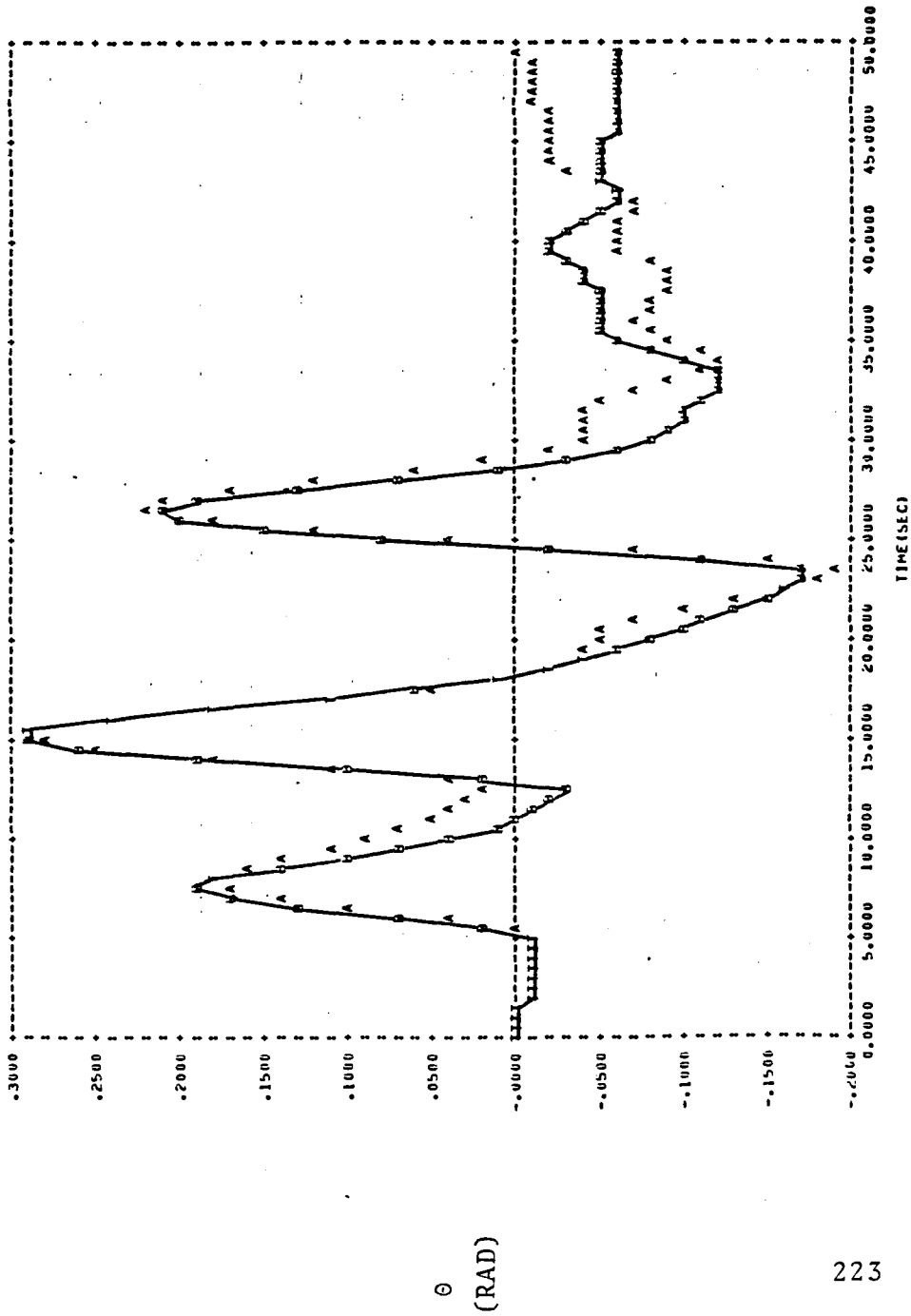


FIGURE 7.26(d). - (CONTINUED)

●  $\theta$  MEASUREMENT

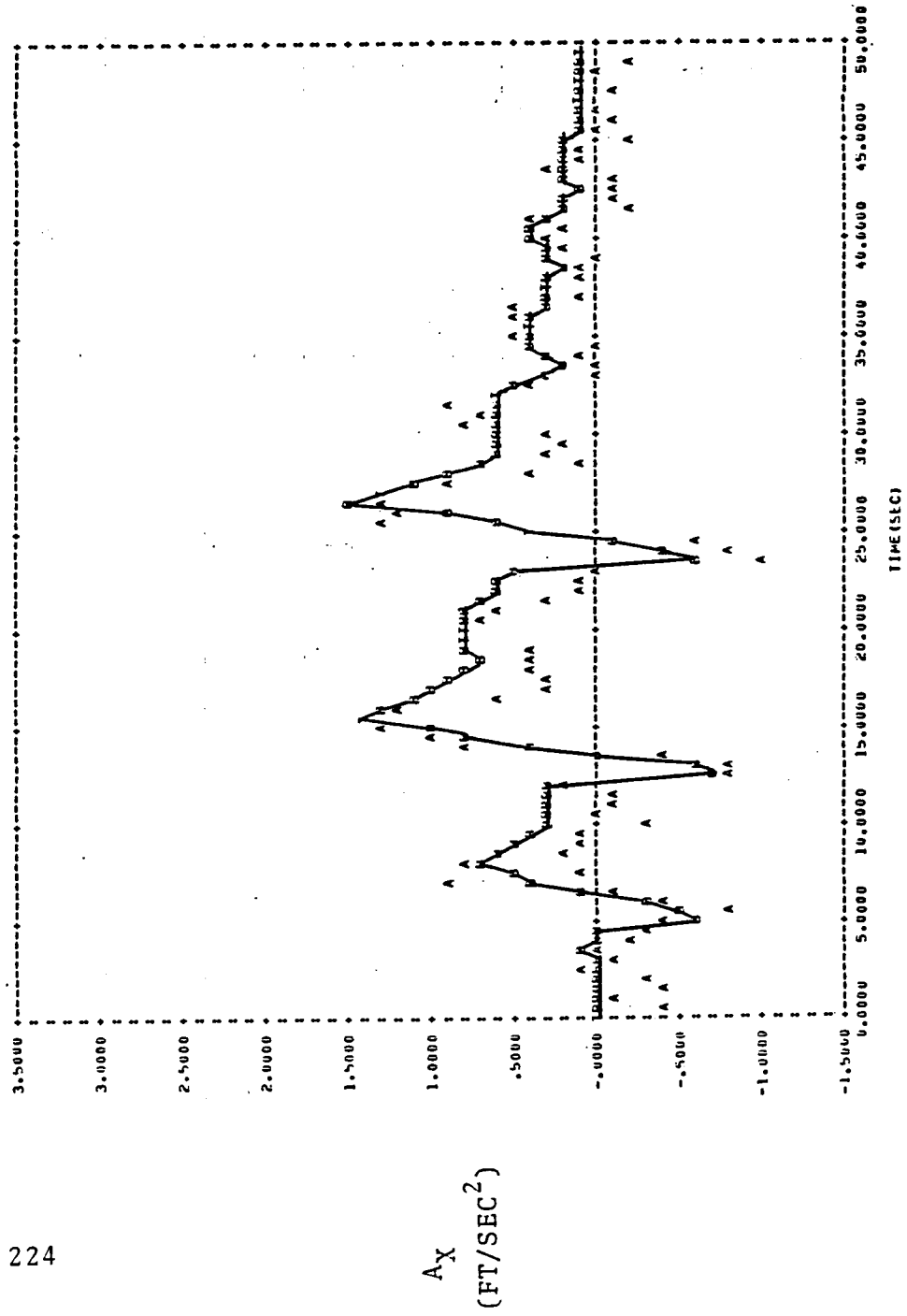


FIGURE 7.26 (e). - (CONTINUED)

●  $a_x$  MEASUREMENT

$A_z$   
(FT/SEC<sup>2</sup>)

225

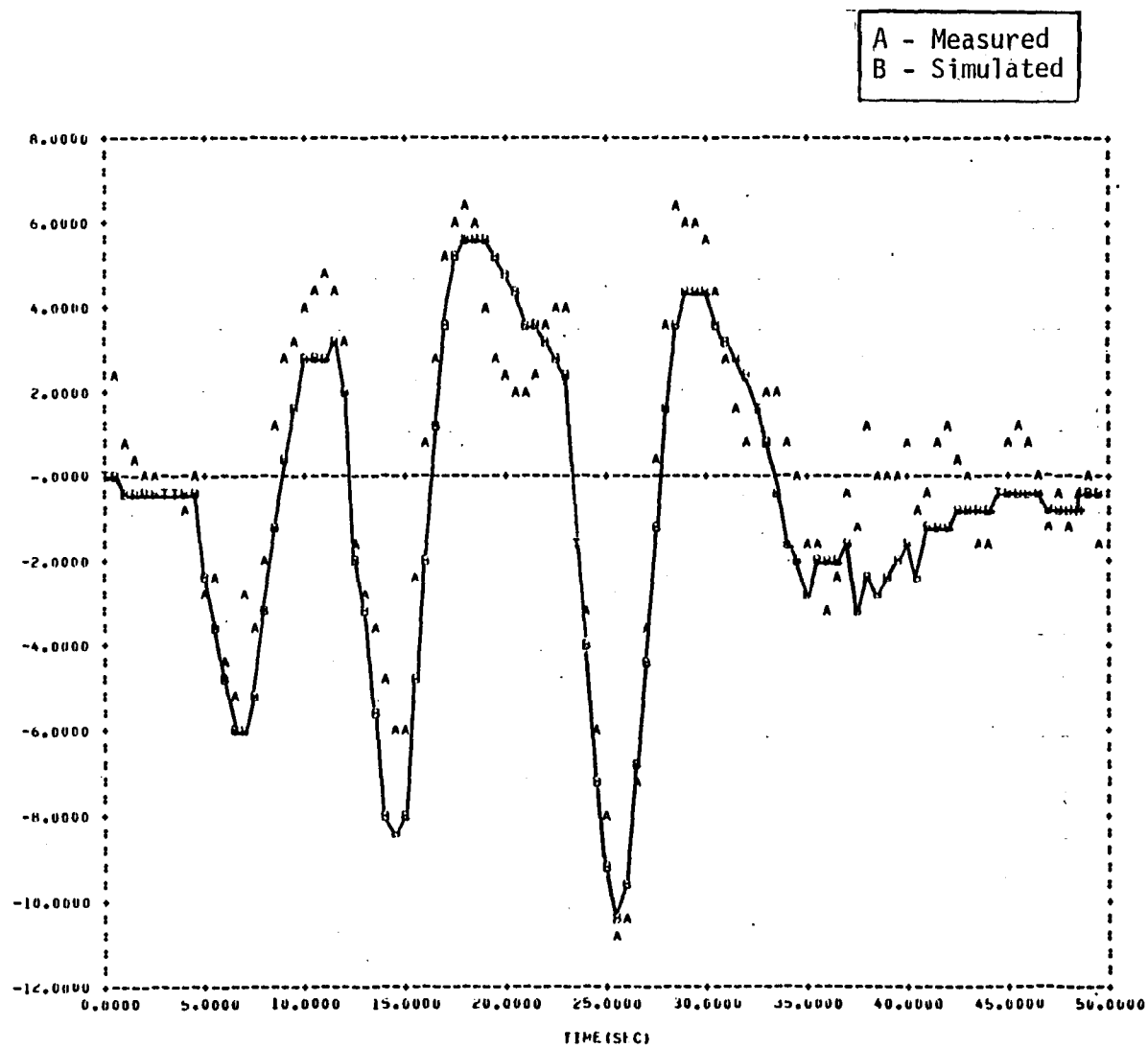


FIGURE 7.26(f).- (CONTINUED)

●  $a_z$  MEASUREMENT

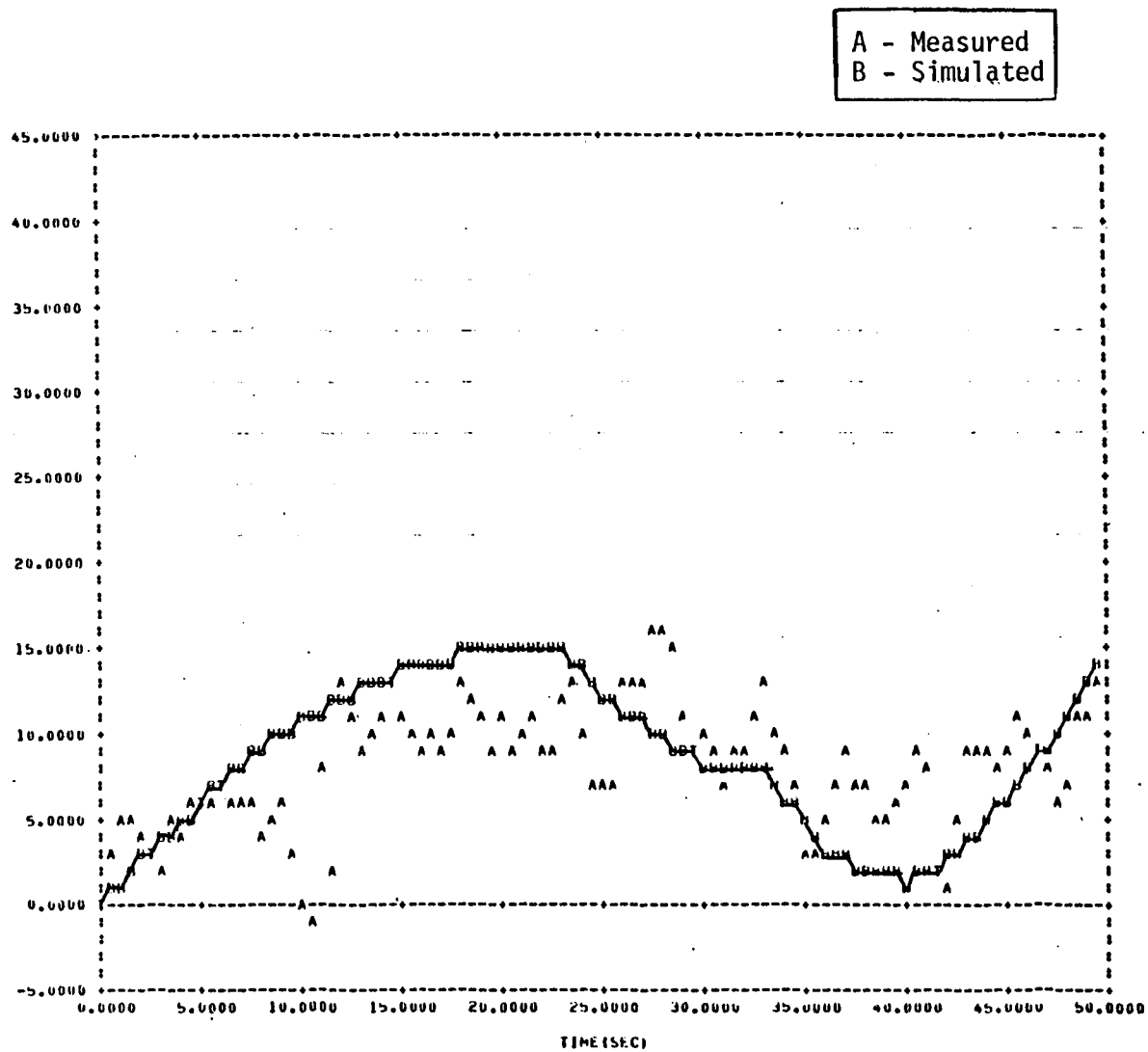
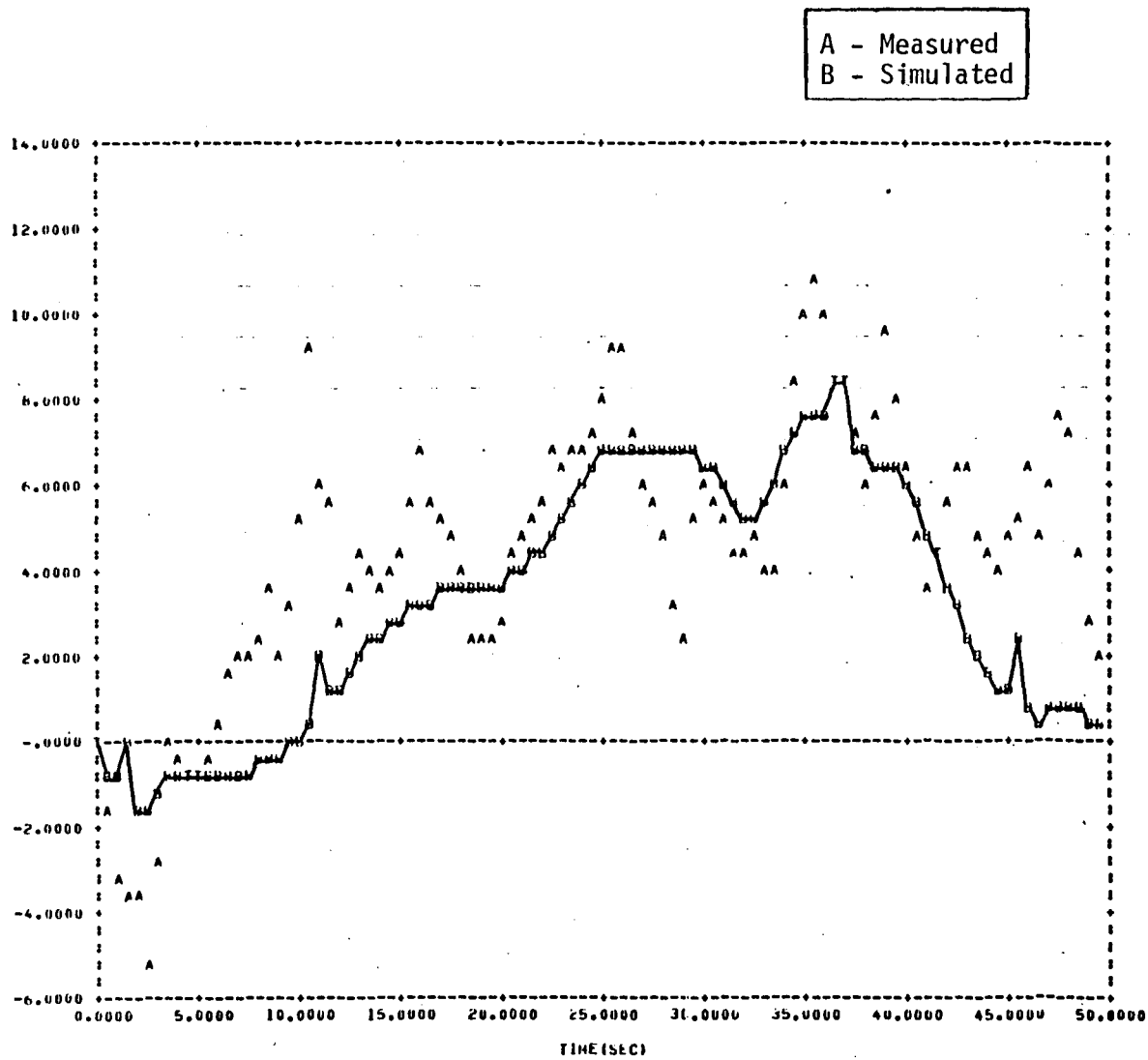
$V_{TOTAL}$   
 (FT/SEC)


FIGURE 7.27(a).— SIMULATION OF CASE 3 FINAL PARAMETER MODEL TO THE COLLECTIVE STICK DOUBLET INPUT. COMPARED TO ACTUAL UH-1H RESPONSE

●  $V_{TOTAL}$  MEASUREMENT

$\dot{h}$   
(FT/SEC)



227

FIGURE 7.27(b). - (CONTINUED)

●  $\dot{h}$  MEASUREMENT

Q  
(RAD/SEC)

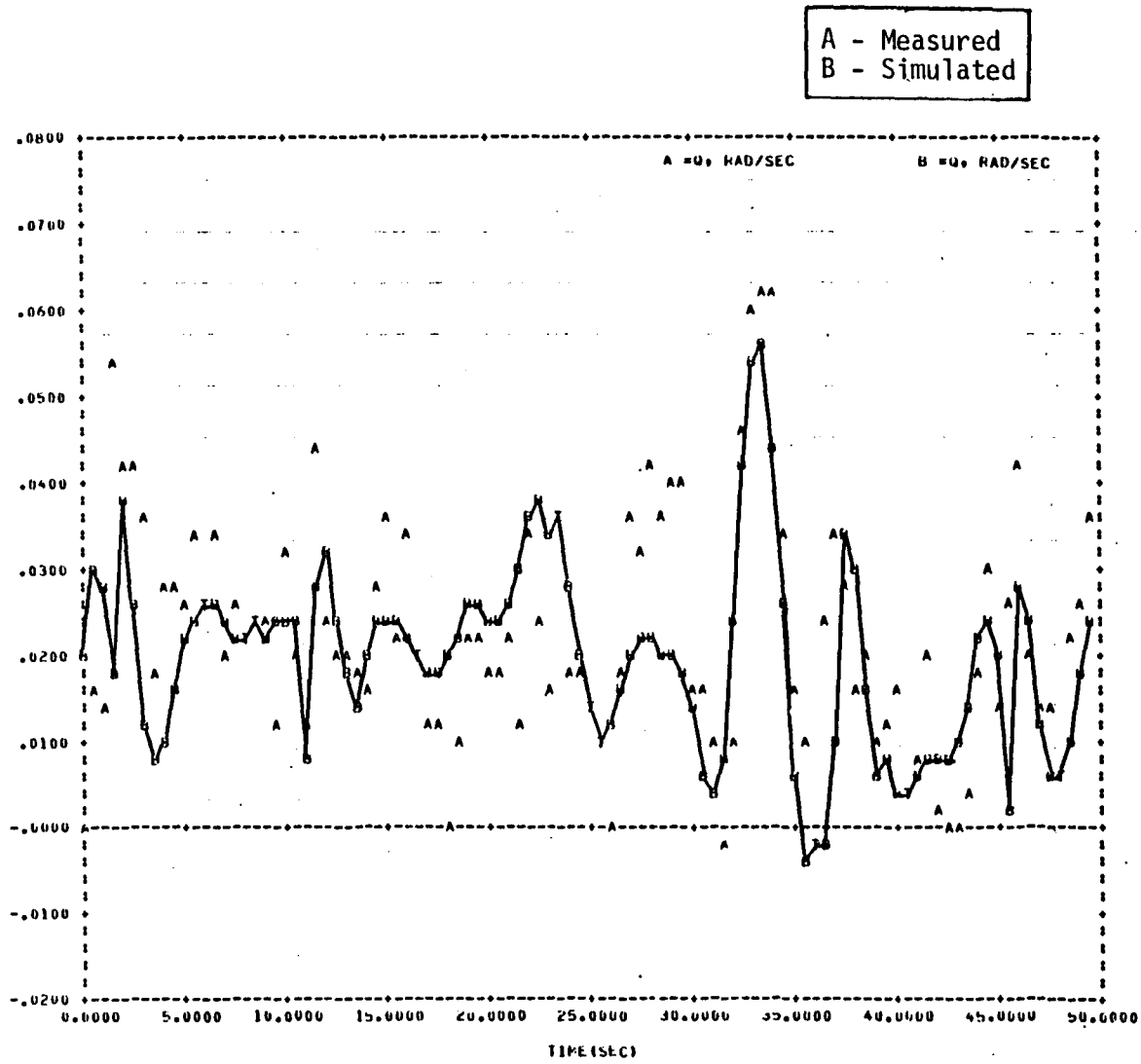
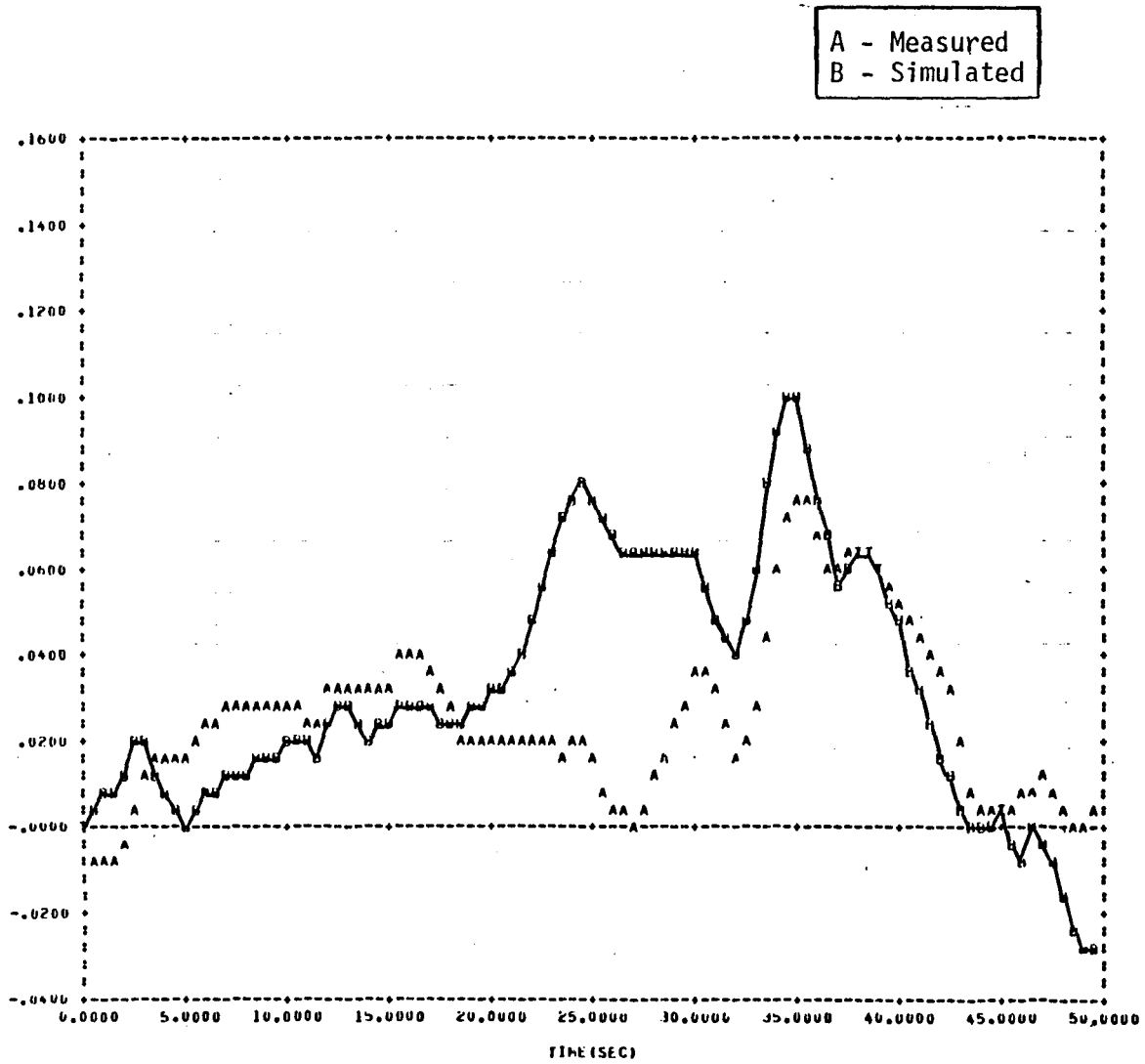


FIGURE 7.27(c).— (CONTINUED)

● q MEASUREMENT

$\theta$   
(RAD)



229

FIGURE 7.27(d).- (CONTINUED)

●  $\theta$  MEASUREMENT

230

$A_x$   
(FT/SEC<sup>2</sup>)

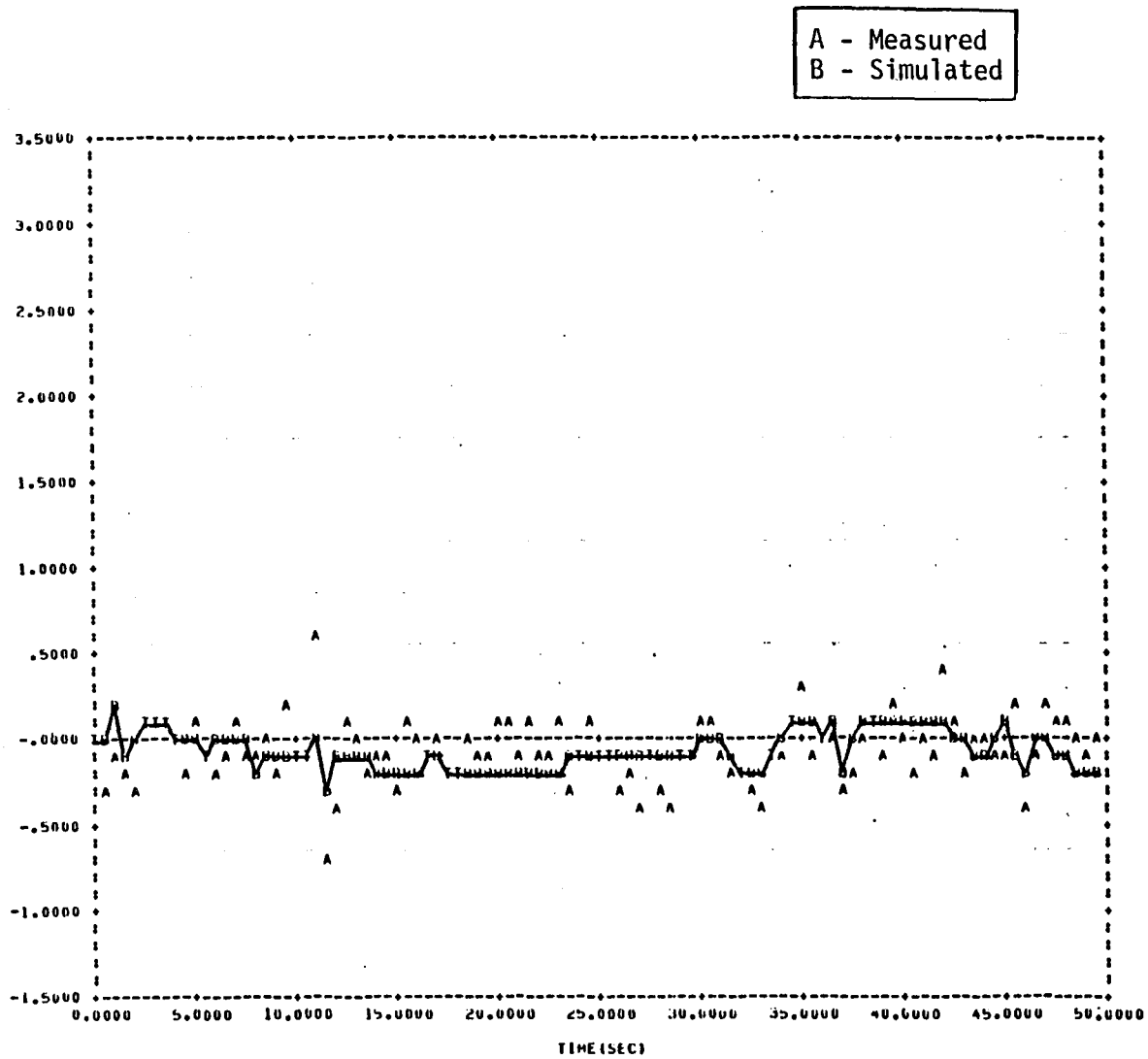


FIGURE 7.27(e). - (CONTINUED)

●  $a_x$  MEASUREMENT



$A_z$   
(FT/SEC<sup>2</sup>)

231

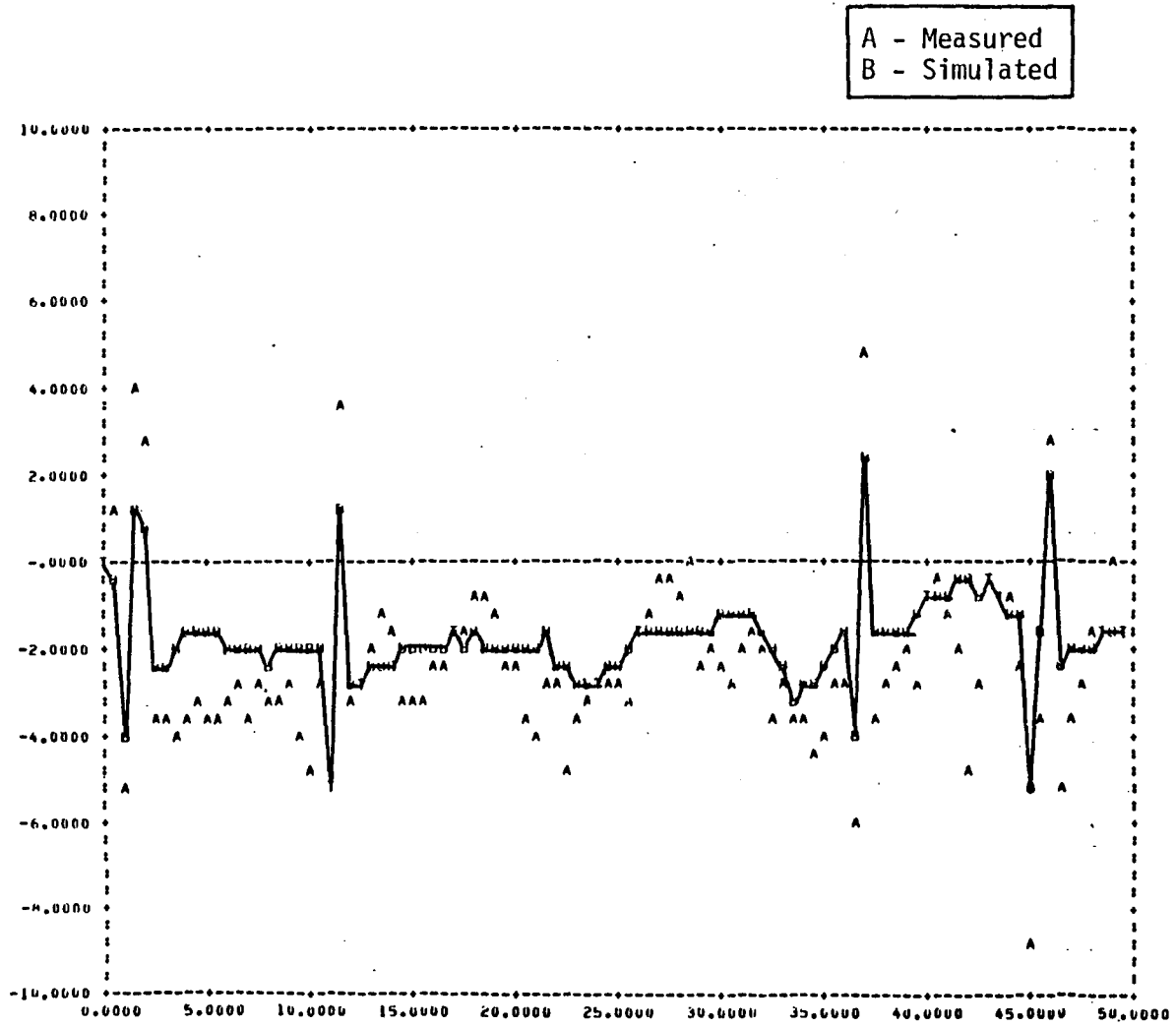


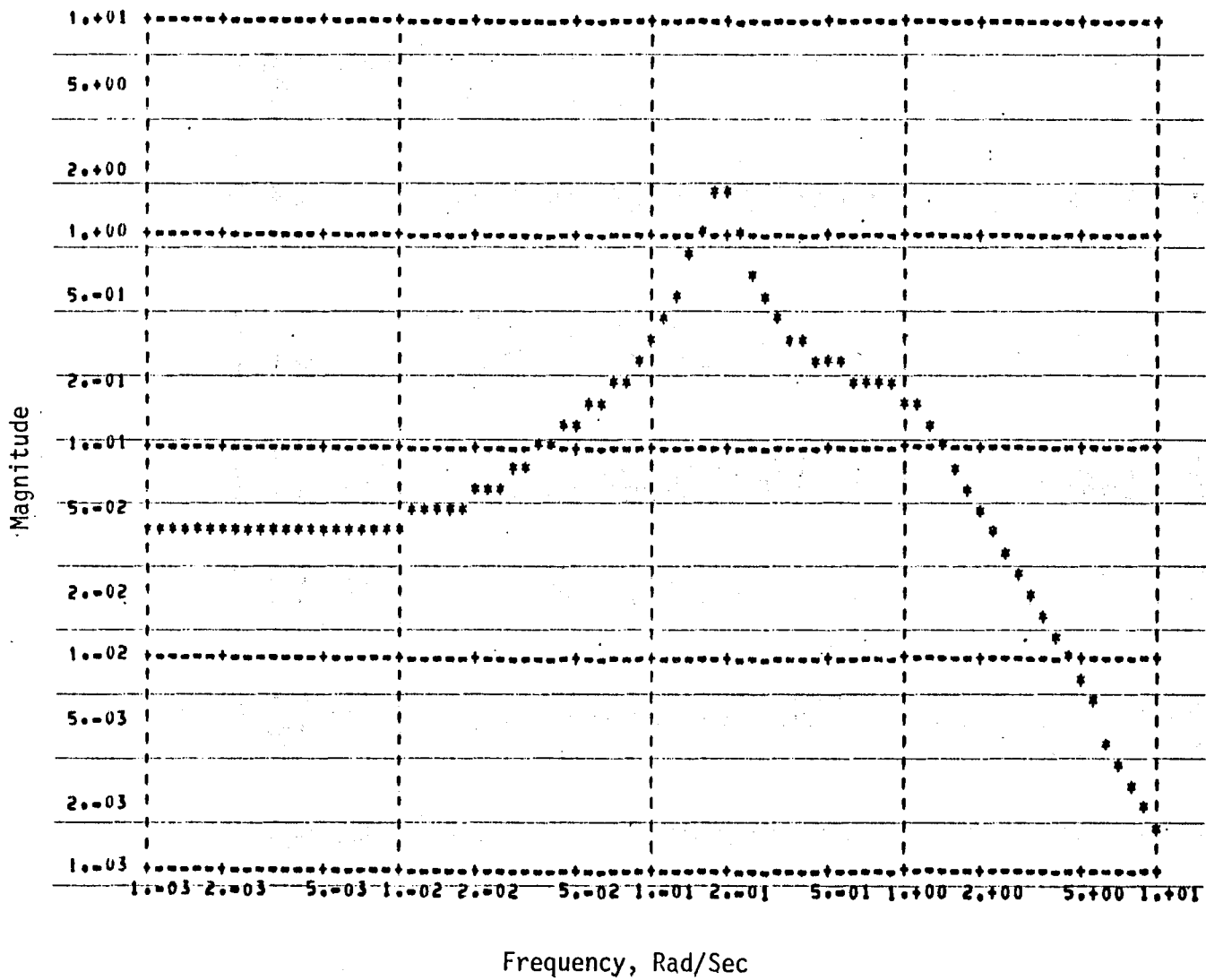
FIGURE 7.27 (f) .- (CONCLUDED)

●  $a_z$  MEASUREMENT

TABLE 7.23.— UH-1H FLIGHT IDENTIFIED PARAMETERS — COMPARISON OF THE THREE CASES

- 60 Knots
- 2 Maneuver Runs

	INITIAL PARAMETER ESTIMATES	CASE 1 FINAL PARAMETER ESTIMATES	CASE 2 FINAL PARAMETER ESTIMATES	CASE 3 FINAL PARAMETER ESTIMATES
$X_u$ , 1/sec	-0.0227	-0.0264	-0.0328	-0.0271
$Z_u$ , 1/sec	0.0013	-0.0255	-0.0221	-0.0226
$M_u$ , 1/ft-sec	0.0037	0.0025	0.0040	0.0027
$X_w$ , 1/sec	0.0587	0.0429	0.0257	0.0391
$Z_w$ , 1/sec	-0.7542	-0.4258	-0.5268	-0.4573
$M_w$ , 1/ft-sec	-0.0032	-0.0093	-0.0075	-0.0095
$M_q$ , 1/sec	-0.5305	-0.7509	-0.5170	-0.7017
$X_{\delta LONG}$ , ft/sec <sup>2</sup> -in	0.8620	0.5947	0.4725	0.5871
$Z_{\delta LONG}$ , ft/sec <sup>2</sup> -in	2.4600	2.1250	2.7983	1.9616
$M_{\delta LONG}$ , 1/sec <sup>2</sup> -in	-0.1800	-0.1709	-0.1103	-0.1685
$X_{\delta COLL}$ , ft/sec <sup>2</sup> -in	0.7115	0.2051	0.2907	0.1691
$Z_{\delta COLL}$ , ft/sec <sup>2</sup> -in	-9.8180	-2.9867	-5.1817	-3.9439
$M_{\delta COLL}$ , 1/sec <sup>2</sup> -in	0.0064	-0.0332	-0.0583	-0.0535



233

FIGURE 7.28 (a), - BODE PLOT OF  $\theta(s)/\delta(s)$  TRANSFER FUNCTION EXTRACTED FROM UH-1H FLIGHT DATA (60 KTS), MAGNITUDE

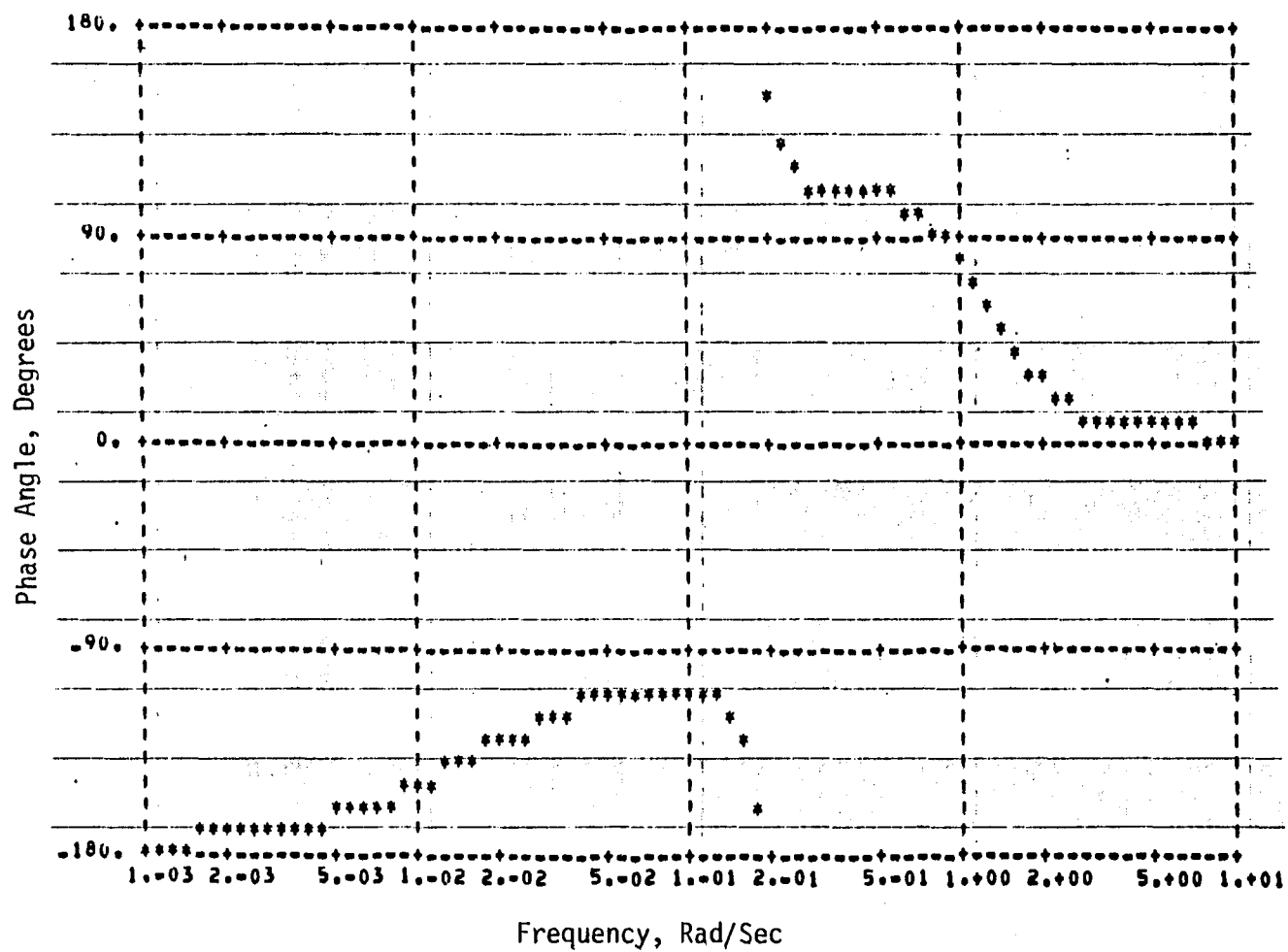


FIGURE 7.28(b).— BODE PLOT OF  $\theta(s)/\delta(s)$  TRANSFER FUNCTION EXTRACTED FROM UH-1H FLIGHT DATA (60 KTS), PHASE ANGLE

## CHAPTER VIII

### CONCLUSIONS

An integrated methodology for rotorcraft system identification has been described. This methodology consists of three distinct data processing steps and a technique for designing inputs to improve the identifiability of the data. These elements are as follows:

- (1) A Kalman Filter/Smoother Algorithm which estimates states and sensor errors from error-corrupted data. Gust time histories and statistics may also be estimated.
- (2) A Model Structure Estimation Algorithm for isolating a model which adequately explains the data.
- (3) A Maximum Likelihood Algorithm for estimating the parameters and estimates for the variance of these estimates.
- (4) An Input Design Algorithm, based on a maximum likelihood approach, which provides inputs to improve the accuracy of parameter estimates.

A discussion of each step is presented, with examples to both flight and simulated data cases.

Simulated data examples indicate that the software is valid for the idealized errors of such synthetic tests. Such simulation data processing provides intuitive insight into the manner in which various errors affect the identification performance. One unexpected benefit of applying the algorithms presented as part of the methodology is that simulation bugs were rapidly found and, in some cases, corrected.

The following principal conclusions are made from the experience gained on the flight data processing.

- (1) Any set of flight data poses unique problems for estimation of the data errors, model structure estimation, and parameter identification. Maximum flexibility on the part of software is needed to quantify the numerous possibilities of errors.
- (2) Rotorcraft can pose a particularly severe instrumentation problem. For the data

provided to us for this effort, no rotorcraft, as expected, had a complete set of perfect sensors. Sensors were either completely absent, failed, or badly degraded on the data. This stresses the importance of the state estimation aspect of the methodology, which can be used to reconstruct very poor data channels.

- (3) Use of a sequential processing scheme provides valuable engineering judgement to be applied at key points in the processing. The three basic software algorithms can be used to actually check and double-check some estimates of each other. For example, sensor bias can be estimated by all the algorithms independently.

## REFERENCES

1. "Parameter Estimation Techniques and Applications in Aircraft Flight Testing," NASA TND-7647, April 1974.
2. "Methods for Aircraft State and Parameter Identification," AGARD-CP-172, May 1975.
3. Molusis, J. A., "Helicopter Stability Derivative Extraction and Data Processing Using Kalman Filter Techniques," preprint no. 641, presented at the 28th Annual AHS Forum, May 1972.
4. Gould, D. G. and Hindson, W. S., "Estimates of the Lateral-Directional Stability Derivatives of a Helicopter From Flight Measurements," National Research Council, Canada, Aero Report LR-572, December 1973.
5. Johnson, W. and Gupta, N. K., "Transfer Function and Parameter Identification Methods for Dynamic Stability Measurement," preprint no. 77.3-35, 33rd Annual AHS Forum, May 1977.
6. Hall, W. E. and Gupta, N. K., "System Identification for Nonlinear Aerodynamic Flight Regimes," Journal of Spacecraft and Rockets, Special Issue on Guidance, Control, and Dynamics, Vol. 14, No. 2, February 1977, pp. 73-80.
7. Seckel, E., Stability and Control of Airplanes and Helicopters, John Wiley, New York, 1964.
8. Johnson, W., "Aeroelastic Analysis for Rotorcraft in Flight or in a Wind Tunnel," NASA TND-8515, July 1977.
9. Johnson, W., "Dynamics of Tilting Proprotor Aircraft in Cruise Flight," NASA TND-7677, May 1974.
10. Bryson, A. E. and Ho, Y. C., Applied Optimal Control, Blaisdell Publishing Company, 1969.
11. Condon, G. W., "Rotor Systems Research Aircraft (RSRA) - Requirements for, and Contributions to, Rotorcraft State Estimation and Parameter Identification AGARD-CP-172, November 1974.

12. Hall, W. E., Gupta, N. K., and Tyler, J. S., "Model Structure Determination and Parameter Identification for Nonlinear Aerodynamic Regimes," AGARD Specialist Meeting on Methods for Aircraft State and Parameter Identification, NASA, November 1974.
13. Gupta, N. K., Hall, W. E., and Trankle, T. L., "Advanced Methods of Model Structure Determination from Test Data," AIAA Guidance and Control Journal, May-June 1978.
14. Thiel, H., Principles of Econometrics, Wiley, New York, 1971.
15. Lee, R. C. K., Optimal Estimation, Identification, and Control, MIT Research Monograph 28, MIT Press, Cambridge, Massachusetts, 1964.
16. Akaike, H., "Statistical Predictor Identification," Annals of the Institute of Statistics, Vol. 20, February 1970, pp. 203-217.
17. Kullback, S., Information Theory and Statistics, Wiley, New York, 1959.
18. Gerlach, O. H., "The Determination of Performance and Stability Derivatives from Dynamic Maneuvers," Delft University of Technology, Netherlands, Report VTH-163, March 1971.
19. Hamming, R., Numerical Methods for Engineers and Scientists, McGraw-Hill, New York, 1962, p. 249.
20. Ivakhnenko, A. G., "Polynomial Theory of Complex Systems," IEEE Transactions on Systems, Man, and Cybernetics, Vol. SMC-1, October 1971, pp. 364-378.
21. Gupta, N. K., "Bias and Mean Square Error Properties of General Estimators," Decision and Control Conference, Clearwater Beach, Florida, 1976.
22. Parzen, E., "A New Look at the Statistical Model Identification," IEEE Transactions on Automation and Control, Vol. AC-19, December 1974, pp. 723-729.
23. Kendall, M. G. and Stuart, A., The Advanced Theory of Statistics, Vol. I and II, 2nd Edition, Charles Griffin & Company, Ltd., London, 1967.



24. Draper, M. R. and Smith, H., Applied Regression Analysis, John Wiley & Sons, Inc., New York, 1966.
25. DiFranco, Dante, "In-Flight Parameter Identification by the Equation of Motion Technique - Application to the Variable Stability T-33 Airplane," Cornell Aeronautical Laboratory, Report No. TC-1921-F-3, 15 December 1965.
26. Turley, R., Private Communication, U. S. Air Force Flight Test Center, April, 1971.
27. Gerlach, O. H., "Determination of Performance and Stability Parameters from Non-Steady Flight Test Maneuvers," SAE National Business Aircraft Meeting, Wichita, Kansas, March 1970.
28. Denery, D. G., "An Identification Algorithm Which is Insensitive to Initial Parameter Estimates," AIAA Eighth Aerospace Science Conference, January 1970.
29. Young, P. C., "Process Parameter Estimation and Adaptive Control," In Theory of Self-Adaptive Control Systems, P. Hammond, ed., Plenum Press, New York, 1966.
30. Schalow, R. D., "Quasilinearization and Parameter Estimation Accuracy," Ph.D. Thesis, Syracuse University, 1967.
31. Larson, D., "Identification of Parameters by Method of Quasilinearization," CAL Report 164, May 1968.
32. Dolbin, B., "A Differential Correction Method for the Identification of Airplane Parameters from Flight Test Data," University of Buffalo, Masters Thesis, December 1968.
33. Lason, L. S., et. al., "The Conjugate Gradient Method for Optimal Control Problems," IEEE Transactions, G-AL, Vol. 12, No. 2, April 1967.
34. J. A. Eney, et. al., "Flight Evaluation of Various Short Period Dynamics in the Variable Stability F-8D," NATC TR FT-13R-TO.
35. Rediess, H., Private Communication, NASA Flight Test Center, October 1971.

36. Wingrove, R., Private Communication, NASA Ames Research Center, October 1971.
37. Queijo, J., Private Communication, NASA Langley Research Center, October 1971.
38. Tyler, J. S., Powell, J. D., Mehra, R. K., "The Use of Smoothing and Other Advanced Techniques for VTOL Aircraft Parameter Identification," Final Report to Cornell Aeronautical Laboratory under Naval Air Systems Command Contract No. N0019-69-C-0534, June 1970.
39. Molusis, J. A., "Helicopter Stability Derivative Extraction from Flight Data Using the Bayesian Approach to Estimation," Journal American Helicopter Society, July 1973.
40. Molusis, J. A., Analytical Study to Define a Helicopter Stability Derivative Extraction Method, Final Report of NASA Contract NAS1-11613, April 1973.
41. Chen, R. T. N., Eulrich, B. J., and Lebacqz, J. V., "Development of Advanced Techniques for the Identification of V/STOL Aircraft Stability and Control Derivatives," Cornell Aeronautical Laboratory Report No. BM-2820-F-1, August 1971.
42. Stepner, D. S. and Mehra, R. K., "Maximum Likelihood Identification and Optimal Input Design for Identifying Aircraft Stability and Control Derivatives," NASA CR-2200, March, 1973.
43. Mehra, R. K., "Maximum Likelihood Identification of Aircraft Parameters," 1970 Joint Automatic Control Conference, Atlanta, Georgia.
44. Aoki, M. and Staley, R. M., "On Input Signal Synthesis in Parameter Identification," Automatica, Vol. 6, 1970.
45. Nahi, N. E. and Wallis, D. E., Jr., "Optimal Inputs for Parameter Estimation in Dynamic Systems with White Noise Observation Noise," preprints, JACC, Boulder, Colorado. August 1969.
46. Levine, M. J., "Estimation of a System Pulse Transfer Function in the Presence of Noise," IEEE AC, 1964, pp. 229-235.
47. Levadi, V. C., "Design of Input Signal for Parameter Estimation," IEEE G-AC, Vol. AC-11, No. 2, April 1966.

48. Fisher, R. A., Statistical Methods and Scientific Inference, Oliver and Boyd, Edinburg, 1956.
49. Fisher, R. A., "Two New Properties of the Mathematical Likelihood," Proceedings, Royal Society. London, 144, 285; 1934.
50. Barnard, G. A., "Statistical Inference," Journal Royal Statistical Society, B11, 116, 1949.
51. Levenberg, K., "A Method for the Solution of Certain Nonlinear Problems in Least Squares," Quarterly Applied Mathematics, 2 (1944), pp. 164-168.
52. Marquardt, D. W., "An Algorithm for Least-Squares Estimation of Nonlinear Parameters," Journal SIAM, Vol. 11, No. 2, June 1963.
53. Mehra, R. K., "Optimal Inputs for Linear System Identification, Part I - Theory," JACC, Stanford, California, 1972.
54. Gupta, N. K. and Hall, W. E., "Input Design for Identification of Aircraft Stability and Control Derivatives," NASA CR-2493, February 1975.
55. Mehra, R. K., "Frequency Domain Synthesis of Optimal Inputs for Linear System Parameter Estimation," Technical Report No. 645, Division of Engineering and Applied Physics, Harvard University, Cambridge, 1973.
56. Corrington, M. S., "Solutions of Differential and Integral Equations Via Walsh Functions," IEEE Transactions Circuit Theory, CT-20, 470-476, September 1973.
57. Chen, C. F. and Hsiao, C. H., "Design of Piecewise Constant Gains for Optimal Control Via Walsh Functions," IEEE Transactions Automatic Control, AC-20, 596-602, October 1975.
58. Beachamp, K. G., "Walsh Functions and Their Applications, Techniques of Physics," No. 3, pp. 236, Academic Press, 1976.
59. Mehra, R. K. "Optimal Input Signals for Parameter Estimation in Dynamic Systems - Survey and New Results," IEEE Transactions Automatic Control, Vol. AC-19, pp. 753-768, December 1974.
60. Hall, W. E., Jr., Gupta, N. K., and Smith R. G., "Identification of Aircraft Stability and Control Derivatives for the High Angle-of-Attack Regime," SCI Technical Report No. 2, prepared for the Office of Naval Research, 1974.

61. Marchand, M. and Koehler, R., "Determination of Aircraft Derivatives by Automatic Parameter Adjustment and Frequency Response Methods," AGARD CP-172, May 1975.
62. Rix, O., Huber, H. and Kaletka, J., "Parameter Identification of a Hingeless Rotor Helicopter," Presented at the 33rd Annual AHS Forum, May 1977.
63. Houck, J.A., et al., "Rotor Systems Research Aircraft-Simulation Mathematical Model," NASA TM-78629, Nov. 1977.
64. Davis, J.M., "Rotorcraft Flight Simulation with Aeroelastic Rotor and Improved Aerodynamic Representation," USAAMRDL-TR-74-10, June 1974.

APPENDIX A  
 MAXIMUM LIKELIHOOD WITH NO PROCESS OR MEASUREMENT NOISE

The maximum likelihood method can be simplified when either process noise or measurement noise are absent.

No process noise.— If the process noise is zero and initial states are known perfectly, i.e.,  $w(t)$  and  $P(0)$  are zero, the covariance of the error in the predicted state is also zero. It is clear that Kalman gains are zero. The innovations are the output error, i.e.,

$$v(i) = y(i) - h(x(t_i), u(t_i), \theta, t_i) \quad (1)$$

and the innovation covariance is

$$B(i) = R \quad (2)$$

the log-likelihood function is,

$$\text{Log} (\mathcal{L}(\theta|z)) = - \frac{1}{2} \sum_{i=1}^N v^T(i) R^{-1} v(i) + \log |R| \quad (3)$$

which on optimizing for unknown parameters in  $R$  gives

$$\hat{R} = \frac{1}{N} \sum_{i=1}^N v(i) v^T(i) \quad (4)$$

The equality in (4) holds only for those elements of  $R$  which are not known a priori. For instance, even if  $R$  is known to be diagonal, the right hand side matrix will not be diagonal, in general; but, the off-diagonal terms should be ignored before they are equated to  $\hat{R}$ . Using (4) in (3)

$$\text{Log} (\mathcal{L}(\theta|z)) = - \frac{1}{2} \sum_{i=1}^N v^T(i) \hat{R}^{-1} v(i) + \text{constant} \quad (5)$$

The optimizing function is the same as that for the output error method except that the measurement noise covariance matrix is determined using (4) and is used as the weighting matrix in the criterion function. In the output error method, the measurement noise is assumed known and the weighting function is arbitrary.

The first and second derivatives of the log-likelihood function with respect to unknown parameters are

$$\frac{\partial}{\partial \theta_j} \log (\mathcal{L}(\theta|z)) = - \sum_{i=1}^N v^T(i) \hat{R}^{-1} \frac{\partial v(i)}{\partial \theta_j} \quad (6)$$

$$\begin{aligned} \frac{\partial^2 \log (\mathcal{L}(\theta|z))}{\partial \theta_j \partial \theta_k} = & - \sum_{i=1}^N \left\{ \frac{\partial v^T(i)}{\partial \theta_k} \hat{R}^{-1} \frac{\partial v(i)}{\partial \theta_j} \right. \\ & \left. + v^T(i) \hat{R}^{-1} \frac{\partial^2 v(i)}{\partial \theta_j \partial \theta_k} \right\} \quad (7) \end{aligned}$$

The terms in the second derivative are approximated as

$$\frac{\partial^2 \log (\mathcal{L}(\theta|z))}{\partial \theta_j \partial \theta_k} = - \sum_{i=1}^N \left\{ \frac{\partial v^T(i)}{\partial \theta_k} \hat{R}^{-1} \frac{\partial v(i)}{\partial \theta_j} \right\} \quad (8)$$

No measurement noise.— If all states are measured with no noise, the covariance of the error in state estimates is zero at the beginning of any time update,

$$\begin{aligned} P(i-1|i-1) &= 0 \\ \text{and } x(i-1|i-1) &= x(i-1) \end{aligned} \quad (9)$$

It is easy to show in this case that for fast sampling the log-likelihood function is quadratic in the difference between measured values of  $\dot{x}$  and  $f(x,u,\theta,t)$ . The method reduces to the equation error method, the weight  $W$  being chosen as

$$W = \frac{1}{T} \int_0^T (\dot{x} - f(x,u,\theta,t)) (\dot{x} - f(x,u,\theta,t))^T dt \quad (10)$$

Thus, the maximum likelihood method and equation-error methods are equivalent except for the technique for choosing the weighting matrix.

## APPENDIX B

This Appendix gives a brief description of Walsh functions and a short summary of their properties. The Walsh functions  $\phi_0(t)$ ,  $\phi_1(t)$ ,  $\phi_2(t)$ , ...  $\phi_n(t)$  are a set of square waves which are orthonormal. Each Walsh function can be decomposed into more elementary square waves, or Rademacher functions.

Rademacher functions  $r_k(t)$ , are a set of square waves of unit height with periods equal to  $1, 1/2, 1/4, \dots, 2^{(1-k)}$ . In other words, the number of cycles of the square waves of  $r_k(t)$  is  $2^{k-1}$ . A few Rademacher functions are shown in Fig. B.1. The Walsh functions are defined in terms of  $r_k(t)$  as follows:

$$\begin{aligned} \phi_0(t) &= r_0(t) \\ \phi_1(t) &= r_1(t) \\ &\vdots \\ \phi_i(t) &= [r_k(t)]^{b_k} \cdot [r_{k-1}(t)]^{b_{k-1}} [r_{k-2}(t)]^{b_{k-2}} \dots \end{aligned}$$

where

$$k = [\log_2 i] + 1.$$

[.] means taking the integral part "." and  $b_k, b_{k-1}, \dots, b_1$  is the binary number expression of  $i$ . Typical Walsh functions are shown in Fig. B.2.

Next, we consider some of the properties of the Walsh functions.

Integration of Walsh Functions.— Integrals of Walsh functions may be approximated by sums of Walsh functions. It is shown in Reference [4] that for the first four functions

$$\int_0^t \phi(\tau) d\tau = \begin{bmatrix} \frac{1}{2} & -\frac{1}{4} & -\frac{1}{8} & 0 \\ \frac{1}{4} & 0 & 0 & -\frac{1}{8} \\ \frac{1}{8} & 0 & 0 & 0 \\ 0 & \frac{1}{8} & 0 & 0 \end{bmatrix} \phi(t) = P_{4 \times 4} \phi(t) \quad 245$$

Higher dimension P matrices may be obtained straightforwardly.

Evaluation of  $\phi_i(t)\phi(t)$ .— If two Walsh functions are multiplied together the produce is a Walsh function obtained by the mod 2 addition of the binary representation of the original functions. Therefore,  $\phi_i(t)\phi(t)$  may be written in terms of Walsh functions. It is easy to show that

$$\phi_0(t)\phi(t) = \begin{bmatrix} 1 & 0 & 0 & 0 \\ 0 & 1 & 0 & 0 \\ 0 & 0 & 1 & 0 \\ 0 & 0 & 0 & 1 \end{bmatrix} \phi(t)$$

$$\phi_1(t)\phi(t) = \begin{bmatrix} 0 & 1 & 0 & 0 \\ 1 & 0 & 0 & 0 \\ 0 & 0 & 0 & 1 \\ 0 & 0 & 1 & 0 \end{bmatrix} \phi(t)$$

$$\phi_2(t)\phi(t) = \begin{bmatrix} 0 & 0 & 1 & 0 \\ 0 & 0 & 0 & 1 \\ 1 & 0 & 0 & 0 \\ 0 & 1 & 0 & 0 \end{bmatrix} \phi(t)$$

$$\phi_3(t)\phi(t) = \begin{bmatrix} 0 & 0 & 0 & 1 \\ 0 & 0 & 1 & 0 \\ 0 & 1 & 0 & 0 \\ 1 & 0 & 0 & 0 \end{bmatrix} \phi(t)$$

Delay Matrix.— A delayed  $\phi(t)$  may also be written in terms of the Walsh functions. It is easy to verify that for first four Walsh functions

$$\left(t - \frac{1}{4}\right) = \frac{1}{4} \begin{bmatrix} 3 & -1 & -1 & -1 \\ 1 & 1 & 1 & -3 \\ 1 & 1 & -3 & 1 \\ -1 & 3 & -1 & -1 \end{bmatrix} \phi(t) = D_{4 \times 4} \phi(t)$$



It is clear that  $D^2$  will produce two units of delay, e.g.,

$$\phi(t - \frac{1}{2}) = D^2 \phi(t) = \frac{1}{16} \begin{bmatrix} 8 & -8 & 0 & 0 \\ 8 & -8 & 0 & 0 \\ 0 & 0 & 8 & -8 \\ 0 & 0 & 8 & -8 \end{bmatrix} \phi(t)$$

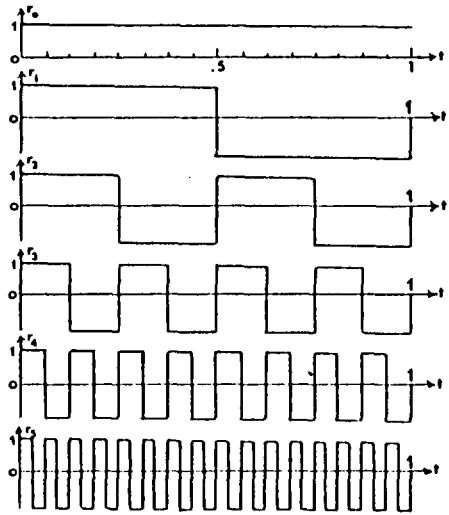


FIGURE B.1— RADEMACHER FUNCTIONS

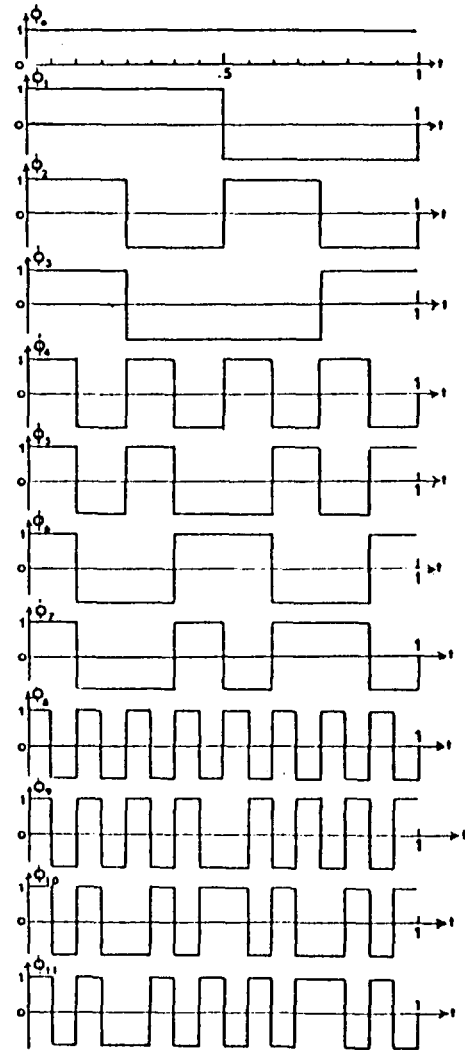


FIGURE B.2— DYADIC ORDERED WALSH FUNCTIONS

## APPENDIX C

In this appendix we derive expressions for the information matrix and the quadratic constraint when the state and outputs are assumed to be multistep. Walsh functions are used in this derivation. Details of the properties of the Walsh functions are covered in References [56], [57], and [58]. The important properties for the purpose of the present application are summarized in Appendix . To simplify the various derivations it is assumed that  $s=2^\Omega$ , where  $\Omega$  is an integer. Let  $\phi_i$ ,  $i=0,1,\dots,s-1$  be the  $i$ th Walsh function in the dyadic order and let the input be assumed to be

$$u(t) = H \phi(t) \quad (1)$$

$\phi(t)$  is a vector of Walsh functions from 0 to  $s-1$ . Also, let

$$\dot{\tilde{x}}(t) = W \phi(t) \quad (2)$$

Since  $\tilde{x}(0)=0$ ,

$$\tilde{x}(t) = W \int_0^t \phi(\tau) d\tau = W P \phi(t) \quad (3)$$

where  $P$  is an  $s \times s$  matrix described in Appendix A. Next, we approximate time varying matrices  $\tilde{A}$ ,  $\tilde{B}$ , and  $\tilde{C}$  by Walsh series

$$\begin{aligned} \tilde{A}(t) &= \sum_{i=0}^{s-1} A(i) \phi_i(t) \\ \tilde{B}(t) &= \sum_{i=0}^{s-1} B(i) \phi_i(t) \end{aligned} \quad (4)$$

$$T_k(t) = \sum_{i=0}^{s-1} T_k(i) \phi_i(t)$$

Using this approximation, Equation (6) becomes

$$W\dot{\phi}(t) = \sum_{i=0}^{s-1} A(i)\phi_i(t) W\phi(t) + \sum_{i=0}^{s-1} B(i)\phi_i(t) H\phi(t) \quad (5)$$

where  $U(i)$  is an  $s \times s$  matrix such that (see Appendix A)

$$\phi_i(t)\phi(t) = U(i)\phi(t)$$

Matrix H can be rearranged into a vector as before and the matrix W may be rearranged into another  $n(m+1)s$  vector  $w$  by substituting its first column into the first  $n(m+1)$  element of  $w$ , the second column into the next  $n(m+1)$  elements and so on. Then Equation (5) becomes

$$\left\{ I - \sum_{i=0}^{s-1} A(i) \otimes (PU(i))^T \right\} w = \sum_{i=0}^{s-1} B(i) \otimes U^T(i) h \quad (6)$$

where

$$A \otimes B = \begin{bmatrix} B_{11}A & B_{12}A & \dots & B_{1n}A \\ B_{21}A & B_{22}A & & B_{2n}A \\ B_{n1}A & B_{n2}A & & B_{nn}A \end{bmatrix} \quad (7)$$

therefore

$$w = I - \left\{ \sum_{i=0}^{s-1} A(i) \otimes (PU(i))^T \right\}^{-1} \sum_{i=0}^{s-1} B(i) \otimes U^T(i) h \quad (8)$$

$\Delta L h$

Similarly, Equation (6.18) may be written as

$$\begin{aligned} \frac{\partial z}{\partial \theta_k} &= \sum_{i=0}^{s-1} T_k(i) \phi_i(t) W \phi(t) \\ &= \sum_{i=0}^{s-1} T_k(i) W P U(i) \phi(t) \end{aligned} \quad (9)$$

A typical element of the information matrix is

$$M_{k\ell} = \sum_{i,j=1}^{s-1} \text{Tr} \left\{ T_k^T(i) R^{-1} T_\ell(j) W P U(j) U^T(i) P^T W^T \right\} \quad (10)$$

Since  $w$  is a linear function of  $h$ ,  $M_{k\ell}$  may be written as

$$M_{k\ell} = h^T V(k,\ell) h \quad (11)$$

An explicit expression for  $V(k, \ell)$  may be obtained by the reader. The quadratic constraint may also be written in terms of the vector  $h$ .

$$\begin{aligned}
 1 &= \frac{1}{E} \int_0^1 \left\{ \left( \sum_{i=0}^{s-1} T_0(i) WPU(i) \phi(t) \right)^T Q \left( \sum_{i=0}^{s-1} T_0(j) WPU(j) \phi(t) \right) \right. \\
 &\quad \left. + u^T(t) u(t) \right\} dt \\
 &= \text{Tr} \left\{ \frac{1}{E} \sum_{i,j=1}^{s-1} T_0^T(i) Q T_0(j) WPU(j) U^T(i) P^T W^T \right. \\
 &\quad \left. + H^T H \right\} = h^T Q h \qquad (12)
 \end{aligned}$$

We note that in both cases (see 6.2.2) similar kinds of relationships are obtained for the information matrix and the state and input quadratic constraint.

**End of Document**